1996

Flow injection chemistries for the in situ monitoring of nutrients in sea water

McCormack, Trevor

FLOW INJECTION CHEMISTRIES FOR THE IN SITU MONITORING OF NUTRIENTS IN SEA WATER

By

TREVOR M^{c}CORMACK, B.Sc.

A thesis submitted to the University of Plymouth in partial fulfilment for the degree of

DOCTOR OF PHILOSOPHY

Department of Environmental Sciences
Faculty of Science

In collaboration with:
The Plymouth Marine Laboratory

May 1996

Signed..T. McComack.....

Date.....06/06/96.....

ABSTRACT

FLOW INJECTION CHEMISTRIES FOR THE IN SITU MONITORING OF NUTRIENTS IN SEA WATER

Trevor McCormack

In order to investigate the biogeochemistry of aquatic ecosystems, a quantitative knowledge of nutrient status i.e. spatial and temporal distribution, and primary production is necessary. This thesis describes chemistries for the determination of the major nutrient species, nitrate (as total oxidised nitrogen minus nitrite) and phosphate (as orthophosphate) using Flow Injection (FI) analysis. Chapter One describes the role of nitrogen and phosphorus in the aquatic environment and overviews laboratory and in situ methods for their determination.

Chapter Two describes the development and optimisation of an FI method for the determination of nitrate in natural waters of varying salinity (0 - 35 ‰). The final manifold can be used for the direct determination of nitrate in riverine, estuarine and sea water without the need for sample pre-treatment or salinity correction. The limit of detection is 0.1 μmol l^{-1} NO_3-N. The method is validated by participation in two interlaboratory exercises (EU Community Bureau of Reference (BCR) and International Council for the Exploration of the Sea) for nitrate in river and sea water respectively.

The analytical performance of reverse FI and FI molybdenum blue methods for the determination of orthophosphate in riverine, coastal and open ocean waters is described in Chapter Three. The high phosphate blank and salt error of the methods using tin(II) chloride and ascorbic acid as the reducing agents are investigated, in order to achieve a lower limit of detection (0.1 μmol l^{-1} PO_4-P) for the determination of environmental levels of orthophosphate.

The shipboard operation and performance of the FI methods for the determination of nitrate and orthophosphate are described in Chapters Four and Five. Field data from the Tamar

Estuary, Sutton Harbour and the coastal waters of the North Sea are presented and related to biogeochemical processes. TON concentration showed an inverse correlation with salinity at all three locations as well as seasonal variation in the Tamar Estuary with levels varying between 0.01 - 0.39 and 1.2 - 3.3 mgl^{-1} N at the high and low salinity endmembers respectively. Buffering of orthophosphate by Fe phase in the sediments was also evident in the Tamar Estuary as well as anthropogenic inputs into the lower 10 km of the estuary. A comparison between FI and the traditional AutoAnalyzer® method is also made in Chapter Five for the shipboard deployment in the North Sea along the NE English coastline and into the high nutrient Humber Plume.

The final chapter investigates the coupling of FI with a charge coupled device detector using fibre optic connections for the spectrophotometric determination of nitrate in water. Comparisons are made with the traditional UV/Visible spectrophotometric detection method as described in Chapter Two in terms of LOD and suitability for shipboard use.

ACKNOWLEDGEMENTS

For his help and guidance over the last three and a half years, I must firstly thank Paul Worsfold, especially for applying the pressure in these last few months in order to make this thesis a reality.

I must thank the Natural Environmental Research Council and the Plymouth Marine Laboratory for their financial support and use of their Research Vessels, *Tamaris, Sea Vigil, Challenger* and of course *Squila*, who's comforts I only enjoyed twice (Shame!).

Thank you to Miguel Valcarcel and Angel Rios for enabling me to spend three months in Cordoba, Spain as part of the ERASMUS scheme. Thanks to the people who made the visit a pleasure and one that was all too short, especially, Chris, Anton, Arty, Tomaz, Pilar, Florrie and The Level Gang.

Thanks to my friends and colleagues at the University of Plymouth, where it was a joy to come into 'work' each day. Thanks to: Slim, Simon L., Anthony, Nick, Wavey and WPL, Foxy, Kevy-Kev, Tony, Hefty, Andy-Mare, Dazzy-Daz, Little Matty, Rob (Ow do!), Tommy-Tom, Ian M., Simoni and Crispy-Cris.

Finally, the deepest gratitude goes to my parents and my sister, Julia, who have always supported and encouraged me in everything I do.

AUTHORS DECLARATION

At no time during the registration for the degree of Doctor of Philosophy has the author been registered for any other university award.

The work was financed with the aid of a studentship from the Natural Environmental Research Council, and with CASE support contributed by the Plymouth Marine Laboratory.

The work described in this thesis has entirely been carried out by the author. Relevant scientific seminars and conferences were regularly attended at which work was often presented; external institutions were visited for consultation purposes, and several papers were prepared for publication.

Publications:

1. T. M^{c}Cormack, A.R.J. David, P.J. Worsfold and R. Howland., *Anal. Proc.*, **31**, (1994), 81.
2. T. M^{c}Cormack, A.R.J. David, P.J. Worsfold., *Frontiers in Analytical Spectroscopy*, D.L. Andrews and A.M.C. Davies (Eds), RSC, Cambridge, 1995, pp 129-135.

Conferences Attended:

1. Perstorp Analytical Environmental Analysis Seminar. The Wildlife and Wetlands Trust Centre, Slimbridge. March 18th 1993
2. R & D Topics Meeting. University of Bradford. July 13-14th July 1993
3. Inland and Coastal Quality 93. Warren Spring Laboratory, Stevenage. September 29th 1993
4. Oceanology International 94. Brighton. March 8-11th 1994
5. R & D Topics Meeting. University of Hertfordshire. July 18-19 July 1994
6. UK Oceanography 94. University of Stirling. August 29th - September 2nd 1994
7. R & D Topics Meeting. University of Hull. July 10-11th July1995
8. SAC 95. University of Hull. July 11th-15th 1995

External Contacts:

Dr. Alan Morris, PML

Mr. Robin Howland, PML

Signed...T. McCormack.....

Date.....06/06/96.....

CONTENTS

LIST OF FIGURES

LIST OF TABLES

Chapter One
Introduction

1. INTRODUCTION

1.1. NUTRIENTS IN NATURAL WATERS

A nutrient element is one which is functionally involved in the process of living organisms [1]. Traditionally, in chemical oceanography the term has been applied almost exclusively to inorganic nitrogen, phosphorus, silicon and carbon, but strictly a number of the major constituents of sea water (e.g. potassium, calcium and sodium), together with a large number of the essential trace metals (e.g. iron, manganese and molybdenum) are also nutrient elements. The primary processes which influence the concentrations of the nutrients and other elements in the sea are the geophysical and biogeochemical processes. The products of rock weathering and of the decay of organic material, together with discarded wastes, are the major sources of most forms of the nutrient elements in the sea, to which they are usually carried by terrestrial drainage. Contributions also arise from submarine weathering, glacial action at the poles, and volcanic and other geothermal activity. There is also the possibility of contributions as a result of transport from the atmosphere; this may occur by direct gaseous uptake by the sea, by addition of rain water and by deposition of solid particles. Table 1.1 shows the concentration of riverine and atmospheric nutrient input to the Western Mediterranean and North Sea.

Table 1.1. Inorganic nutrient input to W. Mediterranean and North Sea (10^3 tonnes y^{-1}) [2].

REGION	RIVERS		ATMOSPHERE	
	N	P	N	P
N.W. MED.	340	115	130*	35*
W. MED.	403	144	350*	90*
NORTH SEA	1073	111	400	200

* input as rainfall

Much of the material mobilised during both natural crustal weathering and anthropogenic activities is dispersed by rivers, which transport the material towards the land/sea margins.

These riverine inputs have a greater potential to stimulate eutrophic events in the coastal region than on open ocean waters, where the majority of chemical species are retained (~3 % of riverine inputs reach the open ocean). Whilst the diffuse atmospheric inputs have a greater impact on the open ocean waters where the natural nutrient levels are lower (<0.1 μM N).

Anthropogenic Sources of Nitrogen

Apart from the natural input of nitrogen from rainfall, the main inputs of nitrogenous matter into freshwater come from farm slurry and sewage and, most significantly, from leaching of fertiliser from agricultural land [3] via wastewater point discharges and diffuse runoff.

On a global scale, it was suggested [4] that the average concentration of nitrogen for world rivers in a pristine state would be 0.015 mg l^{-1} NH_4-N, 0.001 mg l^{-1} NO_2-N and 0.1 mg l^{-1} NO_3-N. A report published by the United Nations Environmental Programme (UNEP) and the World Health Organisation (WHO) [5] found that in some regions of the world, particularly in Europe, less than 10 % of the rivers could be classified as pristine. The median concentration for nitrate in stations outside Europe was 0.25 mg l^{-1} NO_3-N whereas for European rivers the median was 4.5 mg l^{-1} NO_3-N [6]. It is generally accepted that the concentration of nitrate in surface waters has increased in recent decades [7]. However, as nitrogen reaches surface waters primarily from diffuse sources, it is difficult to clearly isolate the assumed link between land use, fertiliser application and stream water quality. This is despite the fact that there is strong evidence that the scale of the nitrate pollution problem is increasing. The EC Nitrate Directive concerning the protection of waters against pollution caused by nitrates from agricultural sources recognises that excessive use of fertilisers constitutes an environmental risk due to enhanced eutrophication, which may ultimately affect drinking water because of toxic algae, and because of the concern over methaemoglobinaemia and stomach cancer. The EC Drink Water Directive states that

nitrate concentrations in all public water supplies must be kept below the maximum admissible concentration of 11.3 mg l^{-1} NO_3-N.

Anthropogenic Sources of Phosphorus

The growing utilisation of synthetic detergents and phosphate fertilisers [8] has resulted in increased concentrations of inorganic phosphorus in aquatic systems. Similarly, increasing organic phosphorus is largely due to sources such as domestic sewage, plant and animal wastes and industrial effluents.

The total phosphorus load of a river may arise from many sources,

1. The leaching and weathering of igneous and sedimentary rocks.
2. The decomposition of organic matter containing phosphorus compounds.
3. Effluents of domestic or industrial origin.
4. Diffuse inputs from agricultural land due to inorganic fertiliser application.
5. Atmospheric deposition and soil/river bank erosion.

The entry of phosphorus into a river may be classified as either point sources, surface runoff, subsurface runoff, groundwater runoff or as direct wet and dry deposition [9]. Point source inputs such as sewage treatment plants are of greater significance during periods of low flow and dry years. In wetter years and during storm events diffuse inputs are the dominant nutrient source. The phosphorus concentration of a typical treated sewage effluent is about 10 mg l^{-1}. The European Communities directive on urban wastewater treatment [10] requires sewage works discharging into 'sensitive areas' and serving populations of between 10,000 and 100,000 to achieve annual average concentrations below 2 mg l^{-1} in their effluents.

Variability in nutrient yield from agricultural catchments is dependent on the soil structure, crop type and the relative importance of surface and subsurface runoff. Although phosphorus is generally retained by most soils, subsurface runoff by field drains may contain

relatively high concentrations of dissolved reactive phosphorus (DRP) because of the diminished contact between the subsoil and percolating water.

1.2. NITROGEN

The most abundant form of nitrogen in sea water is elemental nitrogen, as dinitrogen (N_2). Exchange with the atmosphere maintains the concentration of elemental nitrogen in solution near saturated values (Table 1.2). Sea water also contains much lower concentrations of a wide range of inorganic and organic nitrogen compounds in which the nitrogen occurs in many of the nine different oxidation states from -3 to +5. Nitrate is the most thermodynamically stable form of combined inorganic nitrogen in well oxygenated sea water, and variation in the concentration of this species, and of the more reduced inorganic nitrogenous compounds, is predominantly the result of biologically activated reactions. Inorganic nitrogen in the form of nitrite is usually present in lower concentrations in sea water (Table 1.2) and is the intermediate oxidation state between ammonium and nitrate-nitrogen. As such it can appear as a transient in both the oxidation of ammonium and the reduction of nitrate. Dissolved organic nitrogen in natural sea water is mainly of the form of amino acids, the greatest proportion of which are present as peptides. Also present are urea, soluble nitrogenous excretory products e.g. of animals, and compounds dissolved from nitrogenous detritus. Sea water also contains organic nitrogen in living and detrital particulate matter.

Combined inorganic nitrogen is added to the oceans by terrestrial drainage and most river waters contain substantially greater amounts of combined nitrogen than does sea water. Interconversion of the various forms of nitrogen in sea water and in marine organisms are dependent, directly or indirectly, upon the store of inorganic nitrogen in the sea for the synthesis of many of their essential components [10].

Table 1.2. Concentration of nitrogen species in the hydrosphere [7].

SPECIES	SURFACE OCEANIC 0-100 m ($\mu g\ l^{-1}$ N)	DEEP OCEANIC > 100 m ($\mu g\ l^{-1}$ N)	COASTAL ($\mu g\ l^{-1}$ N)	ESTUARINE ($\mu g\ l^{-1}$ N)
Nitrogen gas (N_2)	800	1150	700 - 1100	700 - 1100
Nitrate (NO_3^-)	0.2	35	0 - 30	0 - 350
Nitrite (NO_2^-)	0.1	< 0.1	0 - 2	0 - 30
Ammonium (NH_4^+)	< 0.5	< 0.1	0 - 25	0 - 600
Dissolved organic N	5	3	3 - 10	5 - 150
Particulate organic N	0.4	< 0.1	0.1 - 2	1 - 100

1.2.1. The Nitrogen Cycle

A schematic of the nitrogen cycle is shown in Figure 1.1. Physical effects such as the sinking of dead organisms and upwelling tend to bring about a redistribution of inorganic and organic nitrogen species in the water column.

Nitrate is considered to control primary production in the euphotic (nutrient rich) surface layer. The concentration of nitrate in these layers is governed by the advective transport of nitrate into the surface layers, microbial oxidation of ammonia and uptake by the primary producers. If light penetration into the water column is sufficient, the uptake rate is usually much faster than the processes transporting the nitrate into the surface layers. Therefore, the nitrate concentration in most oceanic surface waters fall below the limit of detection. In temperate climatic zones, where winter cooling of the surface waters produces deep reaching vertical mixing, the nitrate content of sea water follows a fairly regular cycle with high values in autumn, winter and early spring and low values in late spring and summer [7, 11].

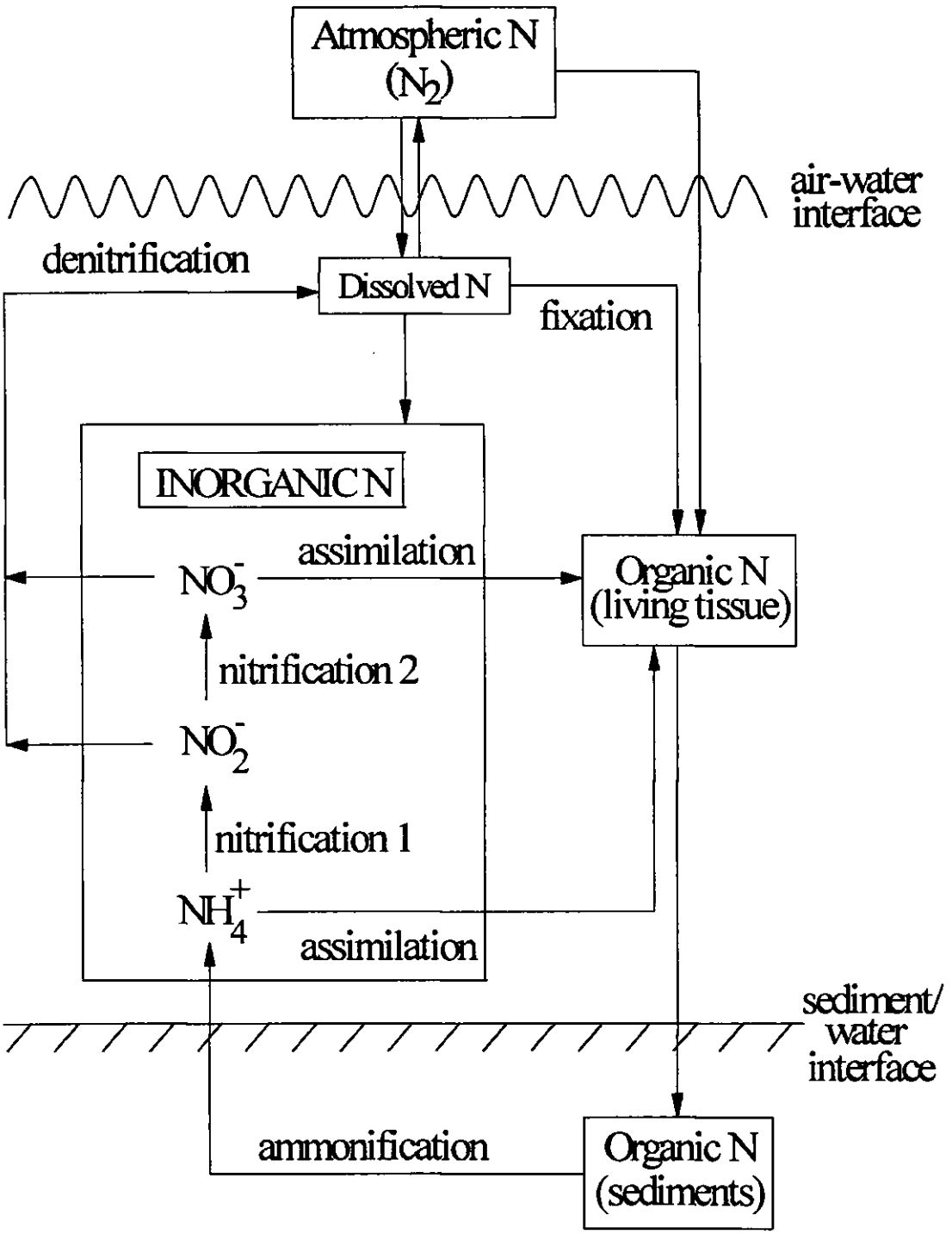

Figure 1.1. The nitrogen cycle.

1.2.2. Nitrogen Fixation

Marine counterparts of terrestrial and freshwater organisms able to fix atmospheric nitrogen have been found in sea water, e.g. *Clostridium* have been found in marine sediments. However, since the fixation process is endothermic, and requires a plentiful supply of organic material as an energy source, it is unlikely that these organisms, although abundant in the sea, fix significant amounts of nitrogen. In tropical and subtropical waters where thermal stratification occurs with depleted surface water nutrient levels, *Trichodesmium* have been shown to fix nitrogen on a large scale even though the concentrations of organic matter are low. Dugdale and Goering [12] found that *Trichodesmium* assimilates ammonium-nitrogen more rapidly than elemental nitrogen or nitrate-nitrogen. Some species of blue-green algae (e.g. *Calothrix scopulorum*) liberate extracellular nitrogen to the water as they grow and this has been utilised by a variety of algae, fungi and bacteria.

1.2.3. Assimilation of Fixed Nitrogen

Some form of nitrogen is required by phytoplankton for the synthesis of their cellular amino acids. They satisfy most of their needs by utilising the ammonia, nitrite and nitrate present in the water. Although all three sources of nitrogen can be absorbed by most species of phytoplankton, ammonia is usually used preferentially. Uptake is virtually confined to the euphotic layer of the sea since it is a consequence of photosynthesis [13, 14].

It has been observed that there is a hyperbolic relationship between the concentration of nitrate or ammonia and its rate of uptake. When these forms of nitrogen become severely depleted in the water (total N $<10\ \mu g\ l^{-1}$), nitrogen deficient organisms are produced before cell division finally ceases. These deficient cells are able to take up ammonia and nitrate, but not nitrite, in the absence of light, converting them to organic compounds such as chlorophyll.

Before it can be incorporated into amino acids by algae for protein synthesis, the assimilated

nitrate must first be converted to ammonia. A hydrogen donor, and a source of high energy phosphate (e.g. adenosine triphosphate) is required to bring about this endothermic reduction process. Although these may be produced by respiration, they are more usually produced by photosynthetic mechanisms. The reduction of nitrate to ammonia takes place in four stages involving the consecutive production of nitrite, hyponitrite and hydroxylamine.

$$NO_3^- + 2H^+ + 2e^- \longrightarrow NO_2^- + H_2O$$
$$2NO_2^- + 4H^+ + 4e^- \longrightarrow N_2O_2^{2-} + 2H_2O$$
$$N_2O_2^{2-} + 6H^+ + 4e^- \longrightarrow 2NH_2OH$$
$$NH_2OH + 2H^+ + 2e^- \longrightarrow NH_3 + H_2O$$

The first step, the reduction of nitrate by a molybdenum containing nitrate reductase is catalysed by the reduced coenzyme II which is produced by the chloroplasts. Ammonia produced by nitrate reduction or assimilated directly from the water, is converted into glutamic acid by the reaction with α-ketoglutaric acid in the presence of reduced adenine nicotinamide dinucleotide phosphate (NADPH).

$$\underset{\text{α-ketoglutaric acid}}{HOOC.CO.(CH_2)_2.COOH} + NH_3 + NADPH + H^+ \longrightarrow HOOC.CH(NH_2)CH_2CH_2.COOH + NADP^+ + H_2O$$
glutamic acid

The twenty or so other amino acids required as building blocks for algal proteins are formed from glutamic acid by transamination. Thus the reaction of glutamic acid with pyruvic acid gives rise to alanine with the reformation of α-ketoglutaric acid.

$$\underset{\text{pyruvic acid}}{CH_3COCOOH} + HOOC.CH(NH_2)CH_2CH_2.COOH \longrightarrow CH_3CH(NH_2)COOH + HOOC.CO(CH_2)_2.COOH$$
alanine

Proteins are then produced by linking together the various amino acids by complicated

reaction sequences involving RNA and DNA with energy provided by adenosine triphosphate.

1.2.4. Regeneration of Nitrate

The regeneration processes by which the organic nitrogen compounds are reconverted via ammonia to the nitrate ion are believed to be mainly bacterial [1]. Bacteria may occur both free floating and attached to organic and inorganic suspended matter. Aerobic species use suspended and dissolved organic matter as food, and satisfy their energy requirements through oxidation of organic matter to carbon dioxide using dissolved oxygen. In anoxic waters, some bacterial species use alternative sources of oxygen such as nitrate and sulphate. If there is an absence of nitrogen and phosphorus in the organic matter, certain species can utilise the dissolved inorganic species of the elements. When a food source becomes exhausted or non-viable conditions develop, the bacterial cells die and undergo rapid autolysis liberating ammonia and phosphate. If, however adequate food is available and conditions are suitable, the bacteria will flourish and multiply.

1.2.5. Decomposition of Organic Nitrogen to Yield Ammonia

Decomposition of soluble and particulate nitrogen compounds of dead organisms and those excreted by plants and animals is brought about by various bacterial species to yield ammonia, and occurs at all depths of the sea. Levels of free or dissolved amino acids do not build up because the decomposition is quite efficient, although stable organic nitrogen compounds resist and sink into the marine sediments as humus.

1.2.6. Nitrification

Nitrification is a two-stage oxidation process mediated by such species as *Nitrosomonas* (NH_3 to NO_2^-) and *Nitrobacter* (NO_2^- to NO_3^-). In this exothermic reaction more energy for

biosynthesis is obtained from the oxidation of NH_4^+ to NO_2^- (-84 kcal mol^{-1})

$$NH_4^+ + OH^- + 1^1/_2O_2 \longrightarrow H^+ + NO_2^- + 2H_2O$$

than the subsequent oxidation to NO_3^- (-18 kcal mol^{-1}).

$$NO_2^- + {}^1/_2O_2 \longrightarrow NO_3^-$$

The net reaction is:

$$NH_4^+ + 2O_2 \longrightarrow NO_3^- + H_2O + 2H^+$$

The oxidation of ammonia to nitrite by *Nitrosomonas* is usually rate-limiting, so nitrite is rarely present in appreciable concentrations. Nitrate, the end-product, is highly oxidised, soluble and biologically available.

Nitrification is oxygen demanding and can, in some aquatic systems, create anoxic conditions. This is because *Nitrosomonas* and *Nitrobacter* are strict aerobes, requiring minimum oxygen concentrations of around 2 mg l^{-1} to function efficiently. However as this reaction is autotrophic, CO_2 may be used as a carbon source and the amount of free oxygen finally used may be less than the stoichiometric requirement (4.33 mg oxygen per mg ammonia).

The nitrifying bacteria are also pH and temperature susceptible, with an optimum pH of 8.4-8.6 and a temperature requirement of greater than 15 °C. A high rate of nitrification is essential for efficient nitrogen cycling, particularly as nitrate is an important substrate for denitrification. Chemoautrophic nitrifying bacteria are usually dominant in freshwaters and their activity is generally highest at the sediment-water interface where ammonium-nitrogen generation is also at its highest.

1.2.7. Denitrification

Denitrification may be considered as the biological reduction of nitrate to nitrogen or nitrous oxide [15]. Micro-organisms, such as some *Pseudomonas* species, which are able to reduce nitrate to molecular nitrogen are known to exist in aquatic systems. These bacteria when they grow in anoxic, or almost anoxic, waters use nitrate ions as alternative electron

acceptors to oxygen in the oxidation of organic matter. The rate and extent of denitification is controlled by the oxygen supply and the available energy produced by organic matter.

1.2.8. Seasonal Cycles

Tropical and subtropical waters are the most stable marine environments with respect to nitrate. They are extremely oligotrophic (low nutrient levels), but can exhibit temporarily elevated concentrations through atmospheric inputs and periodic storm induced mixing of the deeper waters. Temperate waters undergo seasonal variations in surface nitrate concentrations of between 0 and 100 $\mu g\ l^{-1}$ N as shown in Figure 1.2. Nitrate concentrations are usually uniform from the surface to the bottom in nearshore environments because strong mixing (tides) ensures a well-mixed water column. In the winter, this vertically uniform and generally decreasing concentration pattern continues across the shelf until full oceanic conditions persist. During the summer months, when there are extremes of solar input, marked thermal stratification is set up, caused by heating of the sea surface, which becomes relatively buoyant and tends to form two distinct layers. The boundary between the two layers (the thermocline) is invariably narrow and distinct, and the temperature may fall by several degrees over a vertical distance of 1 or 2 m. The formation of thermal stratification is of major importance in regulating the distribution of nitrate.

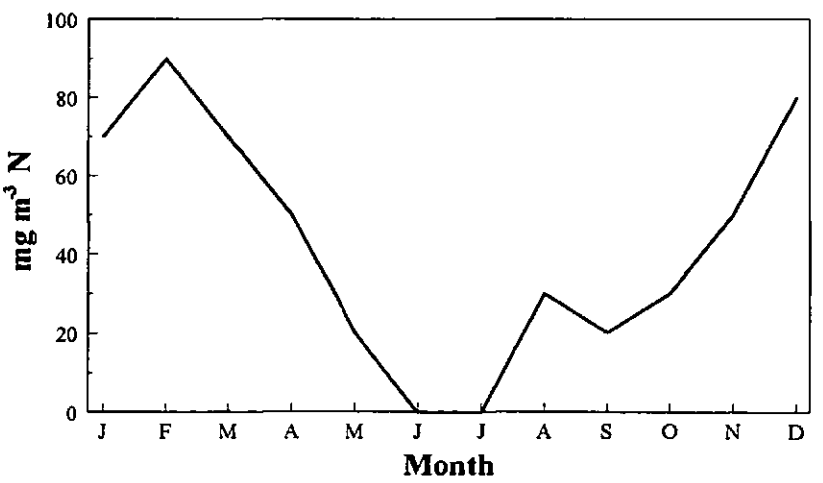

Figure 1.2. Typical seasonal variation in nitrate surface water concentration in temperate zones [10].

This distribution is brought about because the upper layer becomes essentially isolated from inputs of nitrate from deep, offshore waters by the strong density boundary imposed by the thermocline. This boundary is sufficiently robust to prevent the normal mixing processes occurring. This, combined with biological removal of nitrate, forms an upper layer which becomes progressively more depleted in nitrate throughout the summer. Nitrate concentrations typically fall from 50 μmol l^{-1} to <10 μmol l^{-1} during the formation and development of stratified conditions. These conditions give rise to a characteristic vertical profile of nitrate as shown in Figure 1.3.

Upwelling systems exhibit large fluctuations in surface nitrate concentrations. Upwelling is the phenomenon whereby sub-surface (100-300 m in depth) water is brought to the surface in response to the offshore horizontal transport of surface water, thus introducing nitrate (and other nutrients) to the surface water.

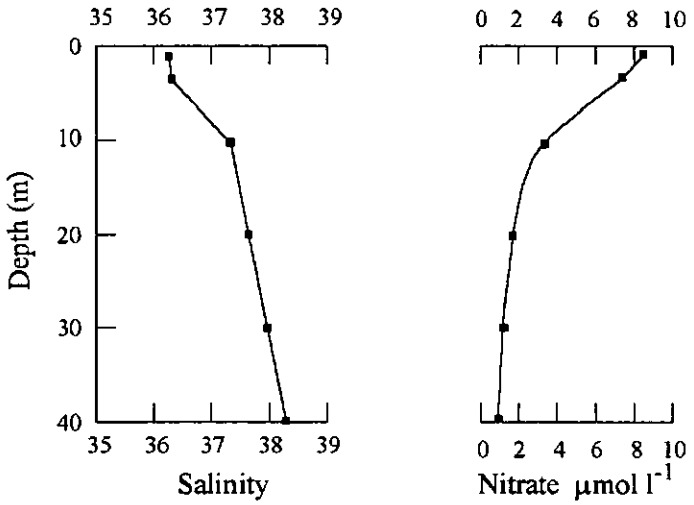

Figure 1.3. Typical winter salinity and nitrate depth profiles of the temperate zone in the Northern hemisphere.

1.2.9. Estuaries

From a chemical standpoint, an estuarine environment may be simply defined as one in which sea water is substantially diluted with freshwater entering from land drainage. This applies only to estuaries which are positive [16]. Negative estuaries are ones in which sea water mixes with more saline waters. The classical, positive estuary is typical of the

majority of mid-latitude estuaries, whereas negative estuaries are confined to low-latitude, arid regions (*e.g.* the Red Sea) or polar latitudes (*e.g.* the Ross Sea). The physical features of estuaries are important in determining the concentrations and distribution of nitrate. Mixing in an estuary occurs between natural waters of very different chemical composition and physico-chemical properties. For instance, although the salinity of sea water is high as compared with the total salt content of river waters, for some dissolved components, such as the plant nutrient elements nitrogen, phosphorus and silicon and many of the transition metals, concentrations in freshwater are often considerably higher in the marine environment. As well as ionic strength (salinity), physico-chemical parameters which may change during estuarine mixing include pH and redox potential. Estuarine waters will also contain suspended sediment derived from the in-flowing river and sea water or by resuspension of settled sediment as a result of tidal stirring.

Estuaries can be classified into three general hydrodynamic categories, resulting from the balance of the freshwater and tidal flows, and in each case an estuary may change its category over periods of time ranging from days (in response to river spates), through weeks (in response to the neap-spring tide), to months (in response to seasonal variations in river flow). The hydrodynamical features of the estuary are fundamental to determining the horizontal and vertical distribution of nitrate within an estuary [17].

In a situation where the residence time of the water in the estuary is short, relative to the timescale of biological activity, and there is only one source of nitrate (e.g. a single riverine input), a simple nitrate-salinity dilution relationship results. This is known as 'conservative behaviour', and under such circumstances, there is no net removal or addition of nitrate. In contrast 'non-conservative behaviour' can occur, resulting in deviations from the idealised salinity-nitrate relationship (Figure 1.4).

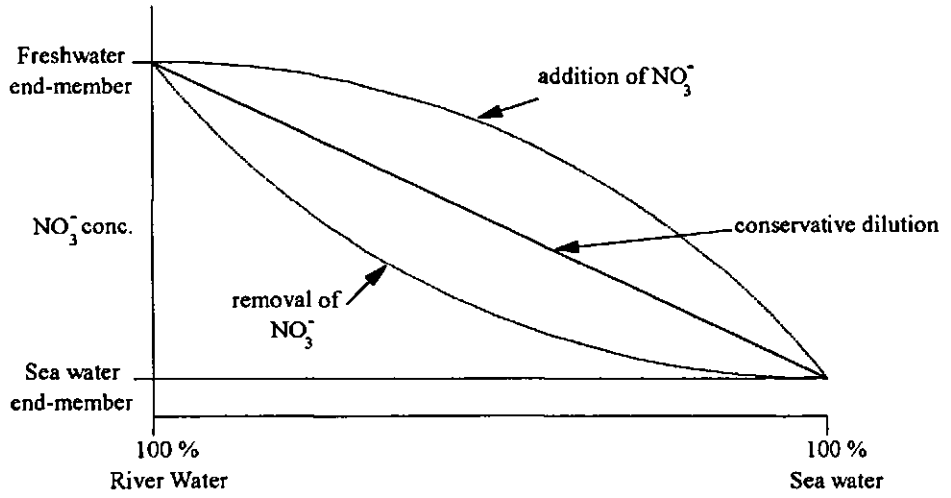

Figure 1.4. Conservative and non-conservative behaviour in estuaries.

Deviations above the salinity dilution will occur where there are point-source inputs within the estuary (e.g. from industrial waste inputs). However, deviations below the conservative dilution line are commonly observed and generally indicate biological removal processes occurring within the estuary. Furthermore, deviations from conservative behaviour are not always unequivocal if there are variations in nutrient concentrations in the end-members, i.e. the freshwater and sea water ends (0 - 35 ‰). Estuaries also exhibit widely fluctuating seasonal cycles in nitrate concentrations, caused by riverine inputs due to seasonal river flow and the regular spring-neap tidal cycle.

1.3. PHOSPHORUS

The total phosphorus (TP) content of natural waters comprises both particulate and dissolved forms, the latter being operationally defined as the fraction which will pass through a 0.45 μm membrane. However, the so-called dissolved fraction can also contain significant amounts of high relative molecular mass colloidal organic phosphorus species.

The total dissolved inorganic phosphorus (DIP) comprises of both orthophosphate, found in sea water as H_3PO_4, HPO_4^{2-} and PO_4^{3-}, and condensed phosphates (DCP), in the form of inorganic polyphosphates, metaphosphates and branched ring structures. The dissolved

organic phosphorus (DOP) fraction includes nucleic acids, phospholipids, inositol phosphates, phosphamides, phosphoproteins, sugar phosphates, aminphosphonic acids, phosphorus containing pesticides and organic condensed phosphates.

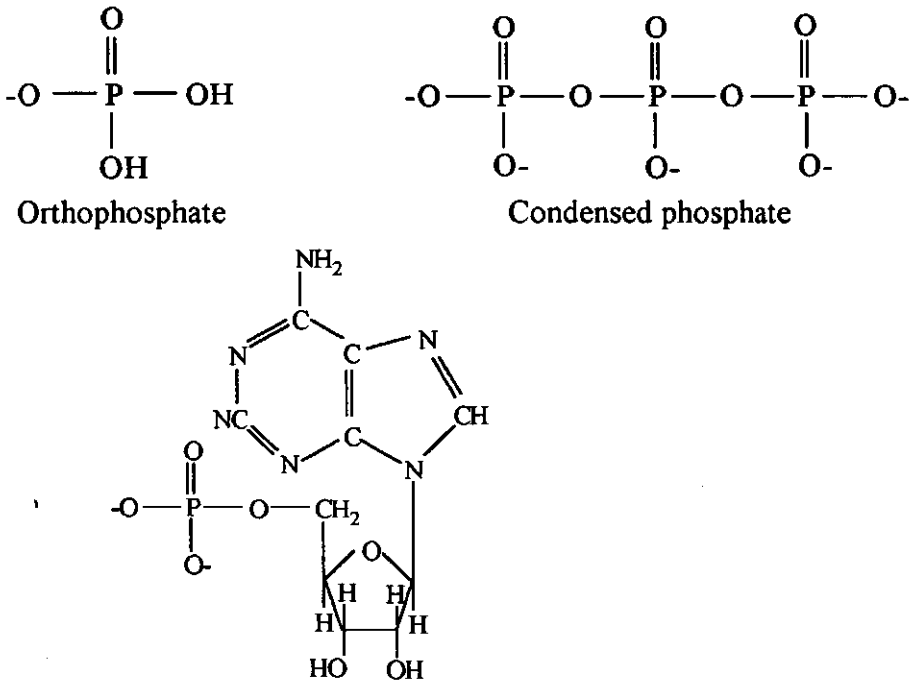

Figure 1.5. Structures of some dissolved phosphorus species found in the aquatic environment.

1.3.1. The Phosphorus Cycle

The distribution of the various forms of phosphorus in the sea (Figure 1.6) is broadly controlled by biological and physical agencies that are similar to those which influence the marine chemistry of nitrogen [18].

1.3.2. Uptake of Phosphorus

Phosphorus compounds, such as adenosine triphosphate and nucleotide coenzymes play a key role in photosynthesis and other processes in plants. Phytoplankton normally satisfy their requirements for the element by direct assimilation of ortho-phosphate and its subsequent conversion to organic phosphorus compounds proceeds at all times, even in the dark. At phosphate concentrations above 10 μg P l^{-1} the rate of growth of many species of

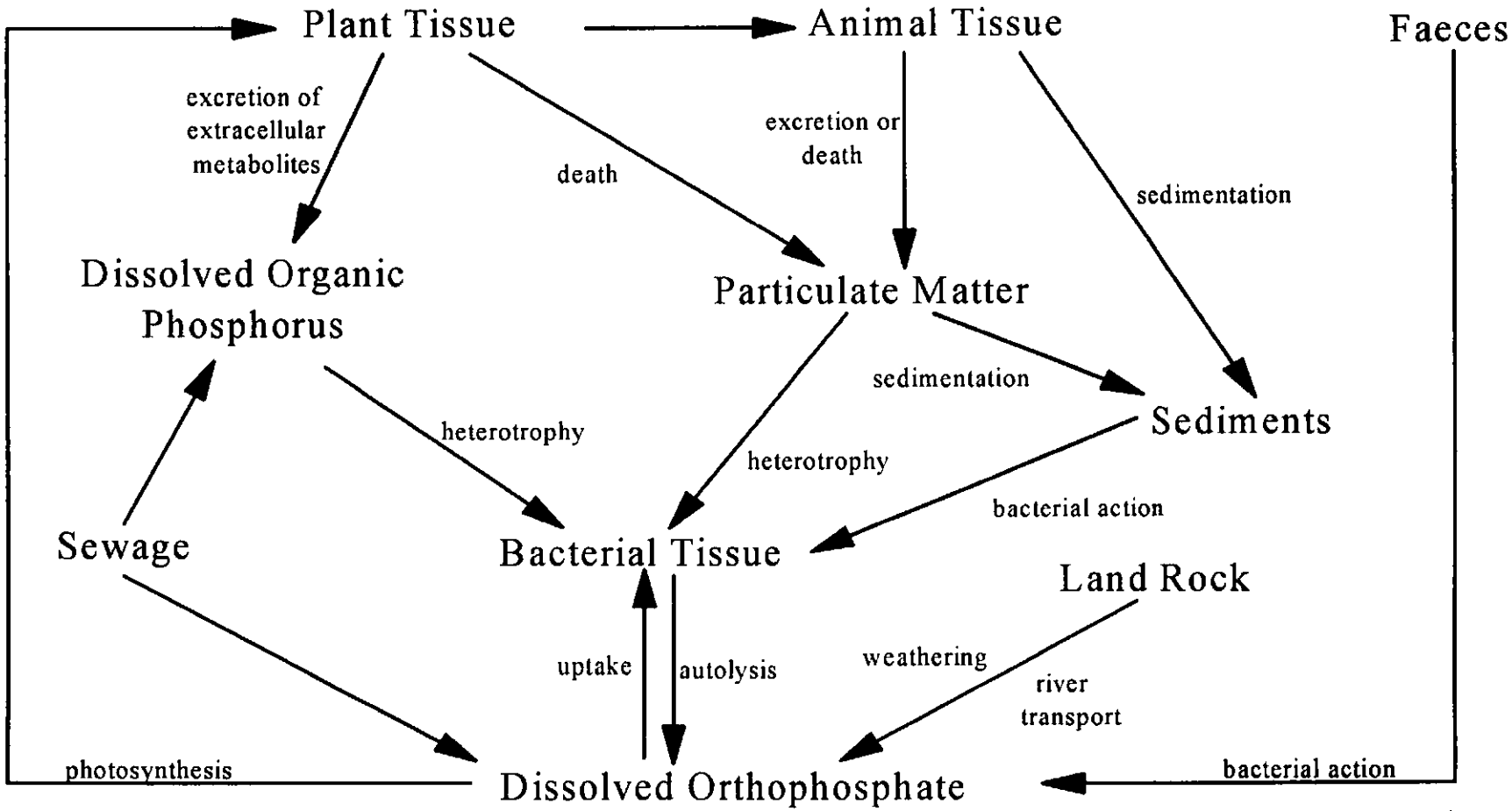

Figure 1.6. The phosphorus cycle.

phytoplankton is independent of the phosphate concentration. However, as the concentration decreases below this critical level, cell division becomes increasingly inhibited and photosynthesis ceases. It is doubtful whether phosphorus deficiency is ever a growth-limiting factor in the sea, since nitrate is usually exhausted before the phosphate concentration falls to a critical level. Bacteria normally satisfy their phosphorus requirements from the organic detritus on which they live. However, if this food source is insufficiently rich in phosphorus they are able to assimilate dissolved inorganic phosphate from the water.

1.3.3. Regeneration of Phosphorus

When phytoplankton and bacteria die, the organic phosphorus in their tissue is rapidly converted to phosphate through the agency of the phosphatases in their cells. In the sea most of the phytoplankton are consumed by zooplankton, which obtain their phosphorus requirements in this way. Part of the phytoplankton is assimilated and the unassimilated material is lost in faecal pellets which contain appreciable amounts of organic phosphates in addition to orthophosphate. Hydrolysis of the organic phosphates proceeds rapidly in the faecal pellets through the action of phosphorylases which are also present. Inorganic phosphate is soon leached from the faecal pellets and passes into the sea water together with any undecomposed organic phosphorus compounds. The latter is then rapidly broken down to orthophosphate by bacterial or enzymatic action.

1.3.4. Seasonal Cycles

Coastal Waters

In shallow coastal waters at temperate latitudes, seasonal variations occur in both the phosphate and dissolved organic phosphorus concentrations. During the winter most of the phosphorus is present as orthophosphate. However, this decreases rapidly in March when it

is utilised by phytoplankton as they proliferate. Zooplankton and fish grazing on the phytoplankton return phosphorus to the water in their excretions as both phosphate and organic phosphorus compounds. The latter becomes the predominant form of dissolved phosphorus in the Northern hemisphere, in May-June, when phosphate may have decreased to levels as low as 2 μg P l^{-1} in the euphotic zone. After the bloom, regeneration of phosphate from phytoplankton, detritus and the dissolved organic phosphorus compounds sets in rapidly. Very high nutrient levels may build up in estuaries and land locked bodies of water as a result of the discharge of sewage and of effluents containing detergents rich in polyphosphates. These may be further augmented by nitrate and phosphate introduced from run-off water from farm land to which excessive amounts of fertiliser have been applied. Such conditions frequently lead to very rapid proliferation of phytoplankton which, when they die and decay, soon strip the water of its dissolved oxygen. It is probable that phosphorus is the main cause of such eutrophication, since even in the absence of combined inorganic nitrogen, nitrogen fixing algae will continue to flourish, provided that sufficient phosphate is available.

Oceanic Waters

The distribution of phosphate in the open oceans closely parallels that of nitrate. The concentration in the surface layer depends on the amount of exchange with the deeper water. It is high in regions such as the eastern boundaries of the oceans, where upwelling replenishes the surface layers. Over the rest of the ocean its level is usually low (<10 μg l^{-1} P), particularly in regions of convergence. Phosphate increases rapidly with depth in the neighbourhood of the permanent thermocline, as a result of the oxidation of detritus falling from the surface, and also because of the activities of zooplankton as shown in Figure 1.7.

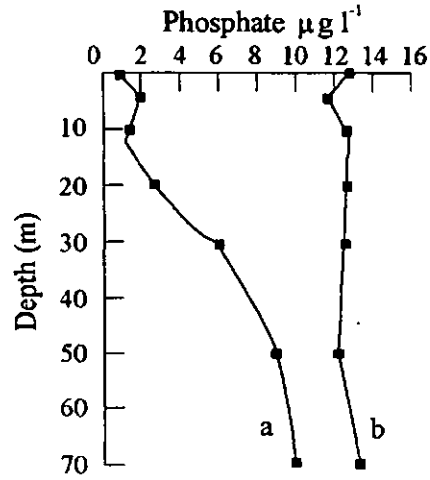

Figure 1.7. Typical phosphate depth profiles in the Northern hemisphere temperate zone during a. summer and b. winter

1.3.5. Nitrogen:Phosphorus Ratio

Phytoplankton biomass (indicated by chlorophyll concentration) in a waterbody appears to be proportional to its nutrient load up to a point. The concept of limiting nutrients in waterbodies relies on the fact that both absolute and relative quantities of essential nutrients regulate primary productivity (mainly algal biomass) in the waterbody. Therefore it is assumed that the ratio at which nutrients are taken up and used by algae reflect the relative composition of these nutrients in their cellular material.

Nitrogen and phosphorus are assimilated from sea water in an approximately constant proportion of 15:1, and although this ratio holds true for many water masses, variations occur in some areas. For example higher than average ratios are found in the Mediterranean Sea, and lower than average ratios in the South Atlantic. N:P ratios of between 5:1 and 8:1 are common in inshore waters and in surface waters in which the ratio may approach zero after phytoplankton growth has removed the greater part of the nitrate. The N:P ratio of zooplankton is higher than that of phytoplankton, and the soluble excretion products of these animals, therefore, have a relatively low N:P ratio, which may account for the low values often observed during the summer in surface waters [10].

1.3.6. Eutrophication

In freshwater lakes the impact of unnaturally large additions of nutrients are well known leading to changes in primary production and species composition, intense algal blooms and generally harmful effects, such as oxygen depletion, with consequent effects on water quality and living resources [2]. For some time, similar events were thought to be unlikely in the marine environment which, being larger and more dynamic, would have the capacity to absorb nutrient inputs. It is recognised, however, that enhanced productivity does occur naturally in estuarine and nearshore waters where as much as 80 - 90 % of the nutrient input is taken up by primary production. This observable effect of excessive nutrient input can manifest in the frequent occurrence of algal blooms as in lake waters. Limited increases are desirable in terms of enhanced production, but large inputs will degrade the environment in a number of ways, especially if the oxygen demand of the decaying plant material from large blooms leads to hypoxia and the death of sensitive organisms such as fish.

The rate of primary production in the sea is limited by a number of factors including the availability of nutrients and certain trace substances, light, temperature, water column stability and suitable population of phytoplankton. However, the maximum size of this population is critically determined by the availability of nutrients such as phosphorus and nitrogen compounds. While phosphate has in certain areas (e.g. in the Adriatic), been shown to be the growth-limiting nutrient, inorganic nitrogen compounds usually play this role to a greater degree.

The inputs in different localities vary widely, depending on a range of factors including population density, land use, effluent treatment, estuarine topography, dispersal rates and natural marine sources of the nutrients. In some enclosed waters and coastal seas these inputs have led to clearly detectable and sustained increases in nutrient concentrations in the water. The areas thus affected are numerous and geographically widespread but all have the common feature of limited water exchange with the open sea [19, 20].

In the Baltic Sea, systematic monitoring since 1980 has produced evidence of eutrophication, as seen in progressively decreasing oxygen concentrations and increasing levels of nutrients. Recorded biological effects over the same period indicate higher summer rates of primary production and productivity of fish, but exceptional and unwelcome blooms of algae have also occurred. Although it is recognised that some events are related to climatological and hydrological variations in the Baltic, the documented increases in nutrient input to this enclosed sea are a matter of major concern [20].

The coastal areas of the southern North Sea have very high winter levels of nutrients and correspondingly high primary production in the spring, with notable seasonal changes in phytoplankton species composition. Macrobenthos mortality due to oxygen deficiency has occurred in the past and more extensively in recent years [21]. The northern Adriatic also shows signs of eutrophication as a result of high inputs of nutrients through rivers and coastal developments. This has been associated with seasonal occurrences of algal blooms and, in limited areas, with anoxic conditions leading to mass mortality of fish and benthic invertebrates in shallow waters. In the summer of 1988, possibly owing to the climatic conditions (calm and hot weather) prevailing in that year, an unusual proliferation of algae fouled beaches along both the Italian and Yugoslav coasts [22].

1.4. DETERMINATION OF NITRATE

The Griess-Ilosvay method has been widely used for the colorimetric determination of nitrite [23, 24]. It is based on a two step reaction:

a). Diazotisation, the reaction of nitrite with an aromatic amine in acidic solution to form an intermediate diazonium ion.

b). Coupling, the reaction of a diazonium ion with an aromatic compound containing amino or hydroxy substituents to form an azo dye.

Several authors have used a number of compounds for diazotisation (Table 1.3) and coupling (Table 1.4).

Table 1.3. Compounds used in diazotisation step.

COMPOUND	REFERENCE
4-Aminobenzotrifluoride	25
Sulphanilamide	26, 27, 28
Sulphanilic acid	29
1-Naphthylamine	30
ρ-D aminodiphenyl sulphone	31

Table 1.4. Compounds used in coupling step.

COMPOUND	REFERENCE
1-Naphthol	25, 30
N-(1-Naphthyl) ethylenediamine	26, 27, 28
1- Naphthylamine	29

The now generally accepted method for sea water analysis is based on the method proposed by Shinn [32] and adapted for sea water by Bendscheider and Robinson [33]. A comprehensive study of the interferences of the method has been carried out [34]. A number of ions such as lead, barium and silver interfere by precipitating as chloride. Chromium, nickel and cobalt interfere by reason of the colour of their ions, and a number of other ions interfere in diverse ways, e.g. bromide, copper, iodide. But many of these ions are not present at their interfering levels in natural waters. Sulphanilamide hydrochloride is used as the amino compound which is coupled with N-(1-naphthyl) ethylenediamine dihydrochloride, shown in Figure 1.8. The amount of the azo dye formed is proportional to the initial concentration of nitrite over a wide range (e.g. 0 - 15 mg l^{-1} NO_2-N) of concentrations. The most sensitive and generally applied methods for the determination of nitrate in sea water are based on the reduction of nitrate to nitrite which is then determined by formation of an azo dye as described above. The reduction can be performed by a

homogeneous or a heterogeneous reaction. Methods based on the homogeneous reduction of nitrate by hydrazine in the presence of copper ions as a catalyst have been proposed [35-41]. This procedure suffers from a number of disadvantages: the reduction takes 24 hours and is inhibited at temperatures above 26 °C, and no reduction takes place in waters containing hydrogen sulfide due to the poisoning of the copper catalyst. The reduction of nitrate in heterogeneous systems using zinc [42, 43], or amalgamated zinc [44], are characterised by low and variable yields of nitrite. In spite of any health considerations, practical difficulties in preparing the columns/coils, concerns over column efficiency [45-47] and several

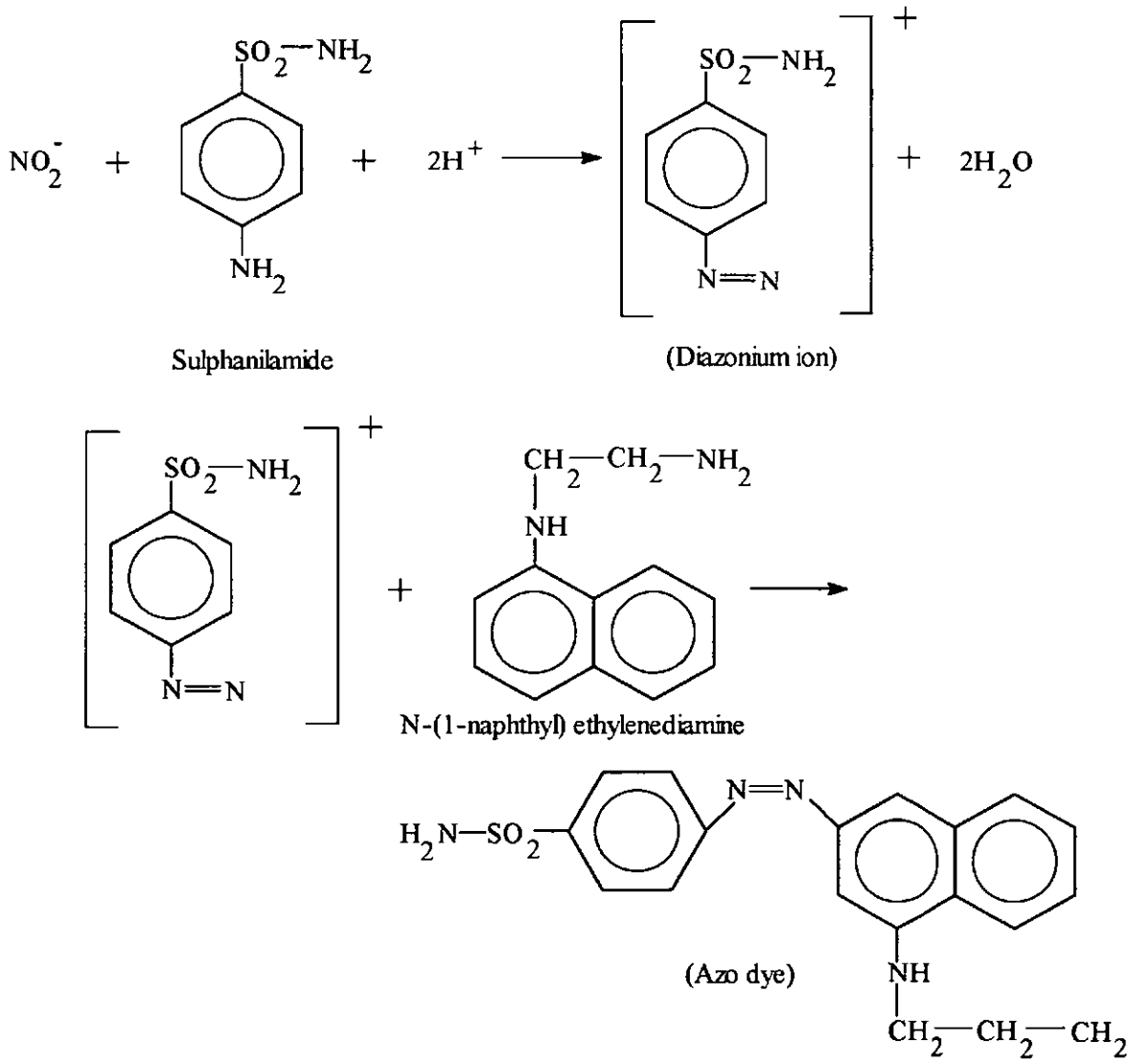

Figure 1.8. Diazotisation and coupling reaction.

interferences in the reduction step [48], the cadmium reduction procedure remains the most widely used for nitrate analysis [49-51]. Various forms of cadmium have been used including cadmium filings [52, 53], amalgamated cadmium [54], copperised cadmium in granular form [49], copperised cadmium wire [55] and a copper/cadmium alloy [56]. The copperised cadmium reduction method is widely used in automated systems such as the AutoAnalyzer® [26, 57-59] and more recently with FI [60-69]. A comparison of manual, AutoAnalyzer® and flow injection procedures for the analysis of nitrate in waters using some form of cadmium as the reductor followed by the diazotisation and coupling with sulphanilamide and N-(1-Naphthyl) ethylenediamine dihydrochloride is given in Table 1.5.

A reductor filled with copper coated cadmium granules is most commonly used method for the reduction of nitrate to nitrite. The conditions of the reduction are adjusted so that the nitrate is quantitatively converted to nitrite and not reduced further.

The principal reaction is:

$$NO_3^- + Me_{(s)} + 2H^+ \longrightarrow NO_2^- + Me^{2+} + H_2O$$

The yield of the reduction of the nitrate to nitrite depends upon the metal used in the reductor, the pH of the solution and the activity of the metal surface. Reaction solutions which are too alkaline, or inactive metal surfaces result in only partial reduction; solutions which are too acidic, the use of highly electronegative metals, or too active surfaces result in the nitrate being reduced further than the nitrite step.

In both cases the analysis will result in nitrate values which are too low. The standard electromotive forces (E_o) of the two reactions in acid solution are similar.

$$NO_3^- + 3H^+ + 2e^- \longrightarrow HNO_2 + H_2O \qquad (E_o = +0.94\ V)$$

$$NO_3^- + 4H^+ + 3e^- \longrightarrow NO + 2H_2O \qquad (E_o = +0.97\ V)$$

In a neutral or alkaline solution the reaction is

$$NO_3^- + H_2O + 2e^- \longrightarrow NO_2^- + 2OH^- \qquad (E_o = +0.015\ V)$$

Table 1.5. Nitrate analysis in waters using cadmium reduction followed by diazotisation and coupling.

METHOD	SAMPLE	[N1NED]	[SULPHANILAMIDE]	BUFFER	REDUCTION	STANDARDS	FLOW RATES (ml min^{-1})	SAMPLE LOOP	LINEAR RANGE	LOD	SAMPLE THROUGHPUT (hr^{-1})	REF.
Auto Analyzer	Seawater	0.1 % w/v	1 g / 90 ml + 1 ml HCl	2.5 g/100 ml EDTA pH 6.5 - 7.0	Cd filings (20 mesh) not copperised	N/A	N/A	N/A	0 - 400 g/L NO_3-N	N/A	30	65
Manual	Seawater	1 g/L	10 g/L + 100 ml 12 N HCl	38 g/L EDTA	Cd filings 20 g/L $CuSO_4$	N/A	N/A	N/A	0 - 60 g-at/L NO_3-N	0.05 g-at/L	N/A	44
FI	Seawater potable and waste waters	0.25 g/ 250 ml + 10g NaCl	2.5 g/ 250 ml + 13 ml HCl	0.4 M NH_4Cl + 0.3 M NaCl	Cd granules <0.3 mm 1 % $CuSO_4$ w/v 60 mm long 1 mm i.d.	0.001 M Stock in 0.7 M NaCl	Buffer 1.0 Sulph. 0.23 N1NED 0.23	200 µl	N/A	0.1 µM	30	55
Auto Analyzer	Waters	1 g/L	10 g/L + 200 ml H_3PO_4	100 g/L NH_4Cl + 20 g sodium tetraborate + 1 g EDTA	Stainton Cd/Ag wire alloy	N/A	Sample 0.8 Buffer 0.16 Sulph. 0.1 N1NED 0.1	N/A	N/A	N/A	N/A	66
FI	Waters	1g N1NED + 20 g Sulph./L + 100 ml 80 % H_3PO_4		100 g NH_4Cl 20 g sodium tetraborate 1 g EDTA	20 - 40 mesh Cd filings 5.2 cm long	1000 ppm NO_3N (6.07 g $NaNO_3$)	1.6 ml/min	75 µl and 15 µl	0 - 5 mg/L	N/A	75 or 90	56
rFI	Seawater	1 g/L +10 g NH_4Cl	10 g/L + 100 ml HCl	10 g/L NH_4Cl pH 8	Cd powder (100 mesh) 1 cm long 20 ml 5 % $CuSO_4$	Contains 25 g NaCl	N/A	20 µl	N/A	0.1 µM	75 or 30	59
Manual	Waters	0.5 g/500 ml	5 g/500 ml + 50 ml HCl	0.1 M NH_4Cl pH 8-9	Amal. Cd 1 % w/v $HgCl_2$	100 g/L NO_3-N (7.14 M KNO_3)	N/A	N/A	2-100 g/L NO_3-N	N/A	30	46

METHOD	SAMPLE	[N1NED]	[SULPHANILAMIDE]	BUFFER	REDUCTION	STANDARDS	FLOW RATES ml/min	SAMPLE LOOP	LINEAR RANGE	LOD	SAMPLE THROUGHPUT hr^{-1}	REF.
FI	Surface, ground	2 g N1NED + 40 g Sulph. /L + 100 ml 85 % H_3PO_4		30 g NH_4Cl + 0.2 g EDTA pH 6.6	Copperised Cadmium Tube	N/A	N/A	300 µl	0 - 2 mg/L NO_3-N	0.05 mg/L	50	65
FI	Natural waters	0.5 g/L N1NED + 10 % H_3PO_4 + 25 g/L Sulph. + 10 % H_3PO_4		10 g/L NH_4Cl	Cd powder 100 (mesh) 50 ml $CuSO_4$ (10 g/L) 40 mm long	100 mg/L NO_3-N	Buffer 0.7 Colour Reagent 0.7	30 µl	0 - 12 mg/L NO_3-N	N/A	N/A	72
Auto Analyzer	Seawater	1 g/250 ml + 5 drops BRIJ 35	10 g/500 ml + 100 ml HCl	10 g/L NH_4Cl	Copperised Cd granules	N/A	Sample 2.5 NH_4Cl 0.1 Sulph. 0.1 N1NED 0.05	N/A	0 - 5000 nmol/L and 0 - 35 mol/L	N/A	40	58
FI	Natural waters	0.25 g/250 ml + 10 g NaCl	2.5 g/250 ml + 13 ml HCl in carrier	0.4 M NH_4Cl 0.3 M NaCl	Cd microcolumn, Cd granules 1 % $CuSO_4$	Contain 0.7 M NaCl	N/A	N/A	N/A	N/A	60	69
FI	Waters	0.5 g/500 ml	5 g / 500 ml + 26 ml HCl	0.1 M NH_4Cl	Cd granules 1 % $CuSO_4$	1000 mg/L NO_3-N	Sample 1.4 Buffer 2.4 Sulph. 0.9 N1NED 0.9	200 µl and 30 µl	0.05 - 1.0 mg/L 0.5 - 10 mg/L	0.025 mg/L	60	73
Auto Analyzer	Seawater	500 mg/L	5 g/L + 50 ml HCl + 1 ml BRIJ	10 g/L NH_4Cl	Copperised Cd granules	N/A	Sample 1.6 NH_4Cl 0.32 Sulph. 0.1 N1NED 0.1	N/A	0 - 100 nM	N/A	20 - 30	59
FI	Seawater and fresh water	0.3 % w/v	2 % w/v in 15 % v/v HCl	2 % w/v NH_4Cl	Stainton Cd wire 1 m (copperised)	2.5 mM stock	Buffer 0.1 Sulph. 0.1 N1NED 0.1	0.3 ml	1- 20 µM NO_3^-	0.1 µM	30 - 35	74

Copper coated cadmium filings or fine granulate are very suitable for the heterogeneous reduction step, but in a neutral or weak alkaline medium the cadmium ions formed during the reduction of nitrate react with hydroxyl ions and form a precipitate. Furthermore the reduction potential needed for the reduction of nitrate to nitrite is dependent on the hydrogen ion activity according to the Nernst equation:

$$E = E_0 - \frac{RT}{nF} \cdot \ln \frac{a_{NO_2^-} \cdot a_{OH^-}}{a_{NO_3^-}}$$

E = Electromotive force or Zero current cell potential (V)

E_o = Standard cell potential (V)

R = Universal gas constant ($J\ K^{-1}\ mol^{-1}$)

F = Faraday constant ($C\ mol^{-1}$) T = Temperature (K)

This implies that the pH is changed if the solution is not buffered especially in the vicinity of the metal surfaces. Seawater pH rarely falls outside the limits 7.7 - 8.2, and for sea water remote from contaminated or anoxic regions, the pH is mainly buffered by the carbonic acid system ($CO_2/HCO_3^-/CO_3^{2-}$) and to a lesser extent, by borate, phosphate, silicate and arsenate [1]. Therefore, ammonium chloride is added both as a complexant and as a buffer:

$$2NH_4^+ \longrightarrow 2NH_3 + 2H^+$$

$$Cd^{2+} + 2NH_3 \longrightarrow [Cd(NH_3)_2]^{2+}$$

The two hydroxyl ions formed are balanced and the ammonia is bound in the diamine complex. Under controlled conditions, the nitrite originally present in the seawater sample passes the reductor without further reduction. This amount of nitrite should be considered and subtracted from the total amount of nitrite measured. After the reduction procedure, the nitrate analysis is continued exactly as for the determination of nitrite in seawater.

The variables of direct importance in the reduction of nitrate to nitrite by cadmium have been discussed by Nydahl [75]. The nitrite yield from the reduction of nitrate using various types of reductor cadmium was compared, and the effect of pH, temperature, chloride

concentration and flow rate (i.e. contact time) through a packed reductor column was investigated. Maximum yield approaches 100 %, at pH 9.5 and temperature has little effect between 20 - 30 °C, but at 10 °C the reduction is noticeably slower.

Chemiluminescence (CL) techniques have been used to determine nanomolar quantities of nitrate and nitrite in sea water [76]. Nitrite can be determined for example on the basis of the quenching of peroxyoxalate chemiluminescence after HPLC separation [77]. Another method involves the oxidation of iodide by nitrite; the iodine formed is extracted and detected by the CL reaction with an alkaline solution of luminol [78]. A further method utilises the acid decomposition of nitrite to NO and NO_2 followed by transfer of the gases into an alkaline luminol solution by a stream of purified air from which the CL emission light is measured [79, 80]. The majority of methods currently used for the CL determination of nitrite are based on the conversion of nitrite to nitric oxide which is transferred into the gas phase [81] and detected by a CL reaction with ozone. Ascorbic acid [82], iodide [83, 84] or vanadium (III) [85] have been recommended for the reduction of nitrite to NO.

The sequence of reactions involved in the chemiluminescence determination of nitrite is,

$$NO_2^- + H^+ \rightleftharpoons HONO \longrightarrow NO$$

$$NO + O_3 \longrightarrow NO_2^* \longrightarrow NO_2 + h\nu$$

A large number of methods have been proposed that utilise the direct ultraviolet absorption of the nitrate ion at 210 nm for the determination of nitrate in waters. The sample is filtered then acidified with sulphuric acid to remove hydrogen carbonate and sulphamic acid added to remove nitrite. Although reliable results can be obtained for natural waters low in organic matter (e.g. humic acids), waters containing significant amounts of organic matter and/or iron give a positive bias and a correction factor has to be applied. The correction factor is normally determined by measuring the solution absorbance at 275 nm where the nitrate ion has a negligible absorbance, and multiplying this absorbance by a determined empirical factor. The difference between the two absorbances is then related to the nitrate

concentration. The main problem with this method is that the empirical factor is dependent on the nature of the water. Various manual correction methods have been proposed to overcome this interference: coagulation with aluminium hydroxide followed by filtration [86], zinc-copper coupled reduction of nitrate to assess non-nitrate absorbance contribution [87], and measurement at 205, 210, 215, 220, 225 and 230 nm, followed by an empirical correction procedure [88]. Rennie et al. [89] overcame the problem by selectively removing interfering species by making the sample alkaline with sodium hydroxide solution (pH = 12.6) and passing it through an activated charcoal filter. The main drawback to all of these correction methodologies is that they cannot be readily automated.

The speed of response of the nitrate selective electrode makes it potentially useful for nitrate determinations on a large number of samples. The nitrate ion electrode develops a potential across a thin, porous, inert membrane that holds in place a water-immisible liquid ion exchanger. The electrode responds to nitrate ion activity between 0.14 to 1400 mg l^{-1} NO_3-N which is not sensitive enough for levels typically found in sea water [90]. A further drawback with the method is that chloride and bicarbonate ions interfere when their weight ratios to nitrate are >10 and >5 respectively. Although the electrodes function satisfactorily in buffers over the pH range 3 to 9, erratic responses have been noted when pH is not held constant. Because the electrode responds to NO_3^- activity rather than concentration, ionic strength must be constant in all samples and standards. To minimise these problems a buffer solution containing silver sulphate is often used to remove Cl^-, Br^-, I^-, S^{2-} and CN^-, sulphamic acid to remove NO_2^- and buffer at pH 3 used to eliminate HCO_3^- and to maintain a constant pH and ionic strength. Due to these difficulties work has recently been carried out on the development of new electrode coatings to overcome interferences and enhance sensitivity. Examples include an $[Os(bipy)_2(pvp)_{10}Cl]Cl$ modified glassy carbon electrode [91] and a ruthenium containing polymer modified electrode [92].

Various chromatographic techniques have been proposed for the determination of nitrate and nitrite, including ion chromatography [93], ion-exclusion chromatography [94] and ion-interaction chromatography [95]. Nitrate and nitrite analysis in sea water and other matrices containing high concentrations of chloride (e.g. brines) [96] can be difficult because of near co-elution of the three ions. This problem is overcome by using reversed-phase ion-interaction chromatography [95]. The major advantage of chromatographic techniques is the ability to simultaneously determine a range of ions including nitrate, chloride and sulphate. A comparison of ion chromatography, segmented flow analysis and FI for nitrate determination [97] favours ion chromatography and segmented flow analysis for lower detection limits, but the sampling rate for FI at 30 - 60 samples per hour is significantly better than that for ion chromatography at 10 samples per hour.

1.5. DETERMINATION OF DISSOLVED INORGANIC PHOSPHATE

The most commonly measured forms of phosphorus in aquatic ecosystems are dissolved reactive phosphorus (DRP), total dissolved phosphorus (TDP) and total particulate phosphorus (TPP). These operationally defined fractions were originally chosen as a compromise between ease of measurement and predictive power with regard to biological and environmental effects e.g. bioavailability and nutrient budget calculations.

The majority of manual and automated methods of phosphate determination are based on the spectrophotometric determination of orthophosphate as phosphomolybdenum blue [90, 98].

$$PO_4^{3-} + 12MoO_4^{2-} + 27H^+ \longrightarrow \underset{\text{12-molybdophosphate}}{H_3PO_4(MoO_3)_{12}} + 12H_2O$$

$$H_3PO_4(MoO_3)_{12} \xrightarrow{\text{Reductant}} \text{Phosphomolybdenum blue}$$

Many modifications of this method has been reported, usually involving the use of different reductants, e.g. tin(II) chloride, ascorbic acid, 1-amino-2-naphthol-4-sulphonic acid, sodium sulphate, hydrazine sulphate, or combinations thereof [99], or different acid strengths, in attempts to improve the selectivity and stability of the chromophore produced [100]. The most widely used methods for batch and automated analyses are variants of the Murphy and Riley method [101], which utilises ascorbic acid reduction with an antimony potassium tartrate catalyst. The method suffers little interference from silica, which is however a common problem in many other phosphomolybdenum blue based procedures. Ascorbic acid is usually preferred to tin(II) chloride because the latter has the following limitations:

1. Absorbance of the product is temperature dependent.

2. The product of the reaction is relatively unstable, and therefore accurate time intervals for reaching the absorbance maximum are necessary.

3. There is an appreciable positive salt error.

4. Copper interferes above 50 $\mu g\ l^{-1}$ Cu.

Spectrophotometric DRP measurements have been shown to overestimate orthophosphate because of molybdate and/or acid-induced hydrolysis of labile organic and condensed phosphorus species [102-104]. Segmented continuous flow techniques using photometric detection have been applied extensively to the analysis of DRP [105]. FI was adopted for the determination of various phosphorus species in waters and has been used for the shipboard determination of DRP [106] and the in situ analysis of rivers [107]. Techniques such as FI may enable chemistries that are unsatisfactory in batch mode to be used advantageously in automated mode. In batch mode, for example, the tin(II) chloride reduction of 12-phosphomolybdic acid is prone to problems as stated above. However, with FI these deficiencies can be overcome because the timing of reagent addition and mixing sequences are well controlled and frequent recalibration is possible. Typical detection limits and experimental conditions for the spectrophotometric determination of

orthophosphate in natural waters are shown in Table 1.6. Injection of reagents into a flowing sample stream (reverse FI or rFI) has been reported by Casey and Smith [108]; this approach has advantages in terms of minimising reagent consumption, which is critical with on site monitors, and sensitivity enhancement. With rFI the acidity of the carrier stream is critical [109], the optimum colour formation with fast kinetics was found to occur at $[H^+]/[MoO_4^{2-}]$ ratios of 70 [110, 111].

Methods based on spectrophotometric measurement as phosphomolybdate suffer two disadvantages; low sensitivity and interference from several other anions e.g. arsenic and silicon. In order to be suitable for measurement of phosphate in natural waters a method with a detection limit of 1 $\mu g\ l^{-1}$ P or less is desirable. Apart from reduction to molybdophosphate blue, various techniques have been used to enhance sensitivity and specificity. Solvent extraction using solvents such as amyl alcohol, isobutanol, butyl acetate and benzene [99], either before or after the reduction step, have been used. Solvent extraction procedures are tedious, time consuming and often involve toxic solvents, although they may be more acceptable if they can be performed on a micro-scale, e.g. on-line FI solvent extraction using minimal solvent.

Some dye substances and organic molecules (e.g. methylene blue, methyl violet, rhodomine B, crystal violet) form extractable ion pair complexes with phosphomolybdate in acidic solution [99]. It has been found that extracting phosphate with malachite green using either spectrophotometry [112] or spectrofluorimetry [113] the sensitivity is enhanced 30 times, but the ion association complex must be stabilised by the addition of a phosphate free surfactant.

A number of potentiometric methods have been reported for the determination of orthophosphate. These include direct methods [114, 115] using phosphate specific electrodes and indirect methods involving lead [116], calcium [117] or cadmium [118] ion selective electrode (ISEs). For dilute waters, ISEs suffer from lack of sensitivity and in the

Table 1.6. Phosphate determination in natural waters.

METHOD.	REAGENTS	STANDARDS	FLOW RATES ml/min.	SAMPLE VOLUME µl.	LINEAR RANGE	LOD	THROUGHPUT h^{-1}	COMMENTS	REF.
Spectrophotometric. Sea Water.	Molybdate + Antimony, Ascorbic Acid	Prepared in ASW or in low phosphate sea water.	Sample 2.0	20	N/A	0.05 µM	90	Precision 1.5 % at 3 µM 885 nm	106
Spectrophotometic. River water.	Molybdate + Malachite Green + Ethanol, Sulphuric Acid.	Potassium dihydrogen phosphate	1.3	240	0 - 0.8 mg l^{-1}	N/A	40	650 nm	113
Spectrophotometric. Natural Waters.	Molybdate, Ascorbic Acid.	Potassium dihydrogen phosphate	Sample 1.1	30	0 - 2000 µg l^{-1}	12 µg l^{-1}	N/A	660 nm	107
Colorimetric. Surface Waters.	Molybdate, Tin (II)Chloride + Hydrazinium, Ethanol	Sodium dihydrogen phosphate + Mercury (II) Chloride.	Molybdate 1.6 Tin (II) 0.8 Ethanol 2.0	1200	0 - 500 µg l^{-1}	0.01 mg l^{-1}	90	660 nm	122
Spectrophotometric. Industrial Wastewaters, Sea Water	Potassium peroxodisulfate, Malachite green, Molybdate, Sodium thiosulfate, Platinum capillary digester.	Potassium dihydrogen phosphate.	Carrier, Oxidising agent and reducing agent 1.0 Molybdate 0.4	N/A	0 - 500 ng ml^{-1} 10 - 50 ng ml^{-1}	2 ng ml^{-1}	N/A	160 °C heater, 650 nm	123
Spectrophotometric. Natural Waters.	Molybdate, Tin (II) Chloride. Carrier - Water or Potassium Chloride with anion-exchange column	N/A	Molybdate 0.31 Tin (II) 0.31 Carrier 0.77	580	0 - 100 µg l^{-1}	0.6 µg l^{-1}	N/A	N/A	124
Spectrophotometric. Waters.	Molybdate + Rhodamine B, Carrier-Water, polyvinyl chloride	N/A	Reagent 0.6 Carrier 0.94 PVA 0.29	200	7 - 600 ppb	ppb level	55	586 nm	125
Spectrophotometric. Waters	PVA, Molybdate, Crystal Violet, Nitric Acid.	Ammonium dihydrogen orthophosphate	PVA 1.5 Molybdate 0.1 Crystal Violet 1.5 Nitric Acid 1.5	250	0 - 5 µg ml^{-1}	0.02 µg ml^{-1}	60	560 nm	126
Spectrophotometric. Domestic, and Industrial waste waters.	Molybdate + Antimony, Ascorbic Acid. Carrier - Potassium sulphate	Potassium dihydrogen phosphate	Sample 1.8 Carrier 2.4 Molybdate 2.4 Ascorbic 0.5	30 and 200	0.5 -. 25 mg l^{-1} 0.025 - 1 mg l^{-1}	0.010 mg l^{-1}	N/A	660 nm	127
Spectrophotometric.	Molybdate, Tin (II) Chloride + Hydrazinium, Ascorbic Acid.	N/A	N/A	200	0 - 2 mg l^{-1}	0.05 mg l^{-1}	N/A	670 nm	128

case of indirect methods, from a lack of selectivity. Ion chromatography (IC) can be used for phosphate separations, but is generally slow, insensitive (0.2 - 1.0 mg l^{-1} P), and usually unsuited to samples with high ionic strength. Detection of low levels of phosphate is possible if large injection volumes or trace enrichment techniques are used [119, 120] and improved sensitivity of phosphorus detection may also be achieved by post-column reaction with molybdate [121]. Other analytical techniques available for phosphorus include atomic absorption spectrometry, voltammetry, inductively coupled plasma atomic emission spectrometry, inductively coupled plasma-mass spectrometry and gas chromatography, although for various reasons none of these have been widely applied to water analysis.

1.6. FLOW INJECTION ANALYSIS

1.6.1. Basic Principles

Flow injection (FI) is based on the injection of a liquid sample into a moving, unsegmented carrier stream of a suitable liquid. The injected sample forms a zone which is transported towards a detector that continuously records the absorbance, electrode potential or other parameter as the sample passes through the flow cell [129-131].

FI is finding increasing applications in research, routine analysis, teaching of analytical chemistry, monitoring of chemical processes, sensor testing and development, and enhancing the performance of various instruments as well as measurement of diffusion coefficients, reaction rates, stability constants, composition of complexes and extraction constants and solubility products [132-137]. The versatility of FI has allowed the method to be adapted to different detection systems such as electrochemistry, molecular spectroscopy and atomic spectroscopy, using numerous manifold configurations (e.g. Figure 1.9). FI systems may be designed to dilute or to preconcentrate the analyte; to perform separations based on solvent extraction [138], ion exchange [139], gas diffusion or

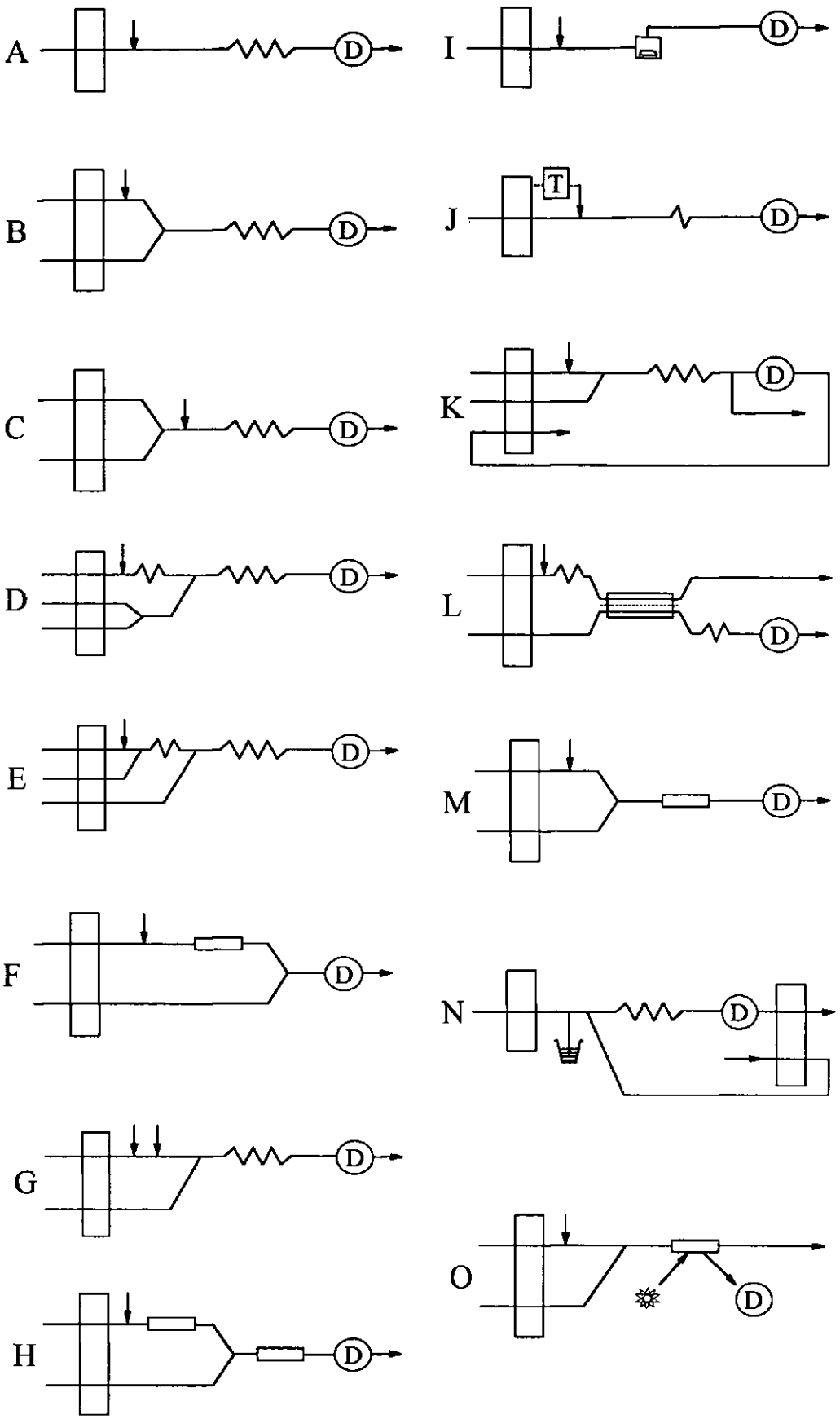

Figure 1.9. Types of FI manifolds. A, single line; B, two line with a single confluence point; C, reagent premix into a single line; D, two line with a single confluence point and reagent premix; E, three line with two confluence points; F, packed reactor in line; G, double injection and single confluence (zone penetration); H, sequential reactors (with immobilised enzymes); I, single line with mixing chamber; J, single line, stopped flow; K, solvent extraction; L, dialysis, ultrafiltration, or gas diffusion; M, two lines, single confluence, incorporating a packed reactor; N, hydrodynamic injection; O, two line, one confluence, optosensing on solid surface.

dialysis [140]; and to prepare unstable reagents in situ. Optimisation and design of the flow channels to achieve maximum sampling frequency, best reagent and sample economies, and proper exploitation of the chemistries is possible through understanding of the physical and chemical processes taking place during the movement of the fluids through the FI channel.

The simplest FI analyser consists of a pump, which is used to propel the carrier stream through a narrow tube; an injection port, by means of which a well-defined volume of a sample solution is injected into the carrier stream in a reproducible manner; and a microreactor in which the sample zone reacts with the components of the carrier stream, forming a species that is sensed by a flow through detector and recorded. A typical recorder output has the form of a peak (Figure 1.10a.), the height H, width W, or area A of which is related to the concentration of the analyte. The time span between the sample injection S and the peak height H, is the residence time T during which the chemical reaction takes place. With rapid response times, typically in the range of 5 - 20 seconds, a sampling frequency of two samples per minute can be achieved. The injected sample volumes may be between 1 and 200 µl which in turn requires no more than 0.5 ml of reagent per sampling cycle. This makes FI a simple, automated microchemical technique, capable of having a high sampling rate and a low sample and reagent consumption.

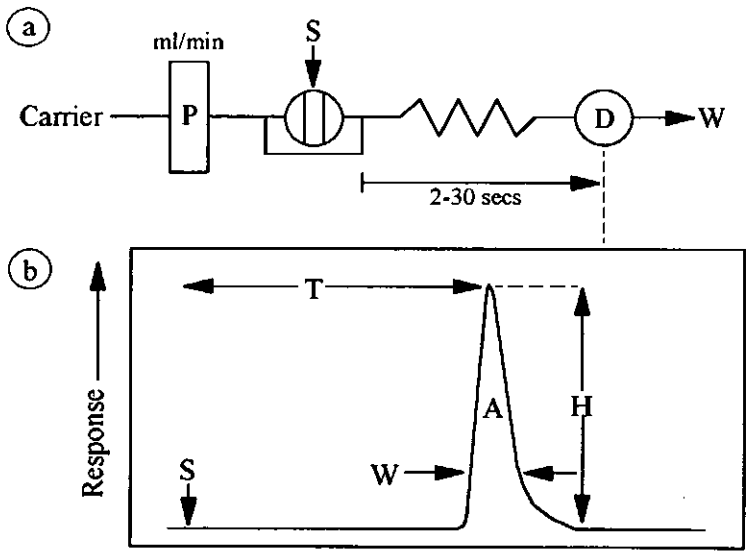

Figure 1.10. a.) Simple FI manifold; P is the pump, S is the injection valve, D is the flow-through detector and W is waste. b.) Chart recorder Output; the recording starts at S, H is the peak height, W is the peak width, A is the peak area and T is the residence time corresponding to the peak height.

FI is based on a combination of three principles: sample injection, controlled dispersion of the injected sample zone, and reproducible timing of its movement from the injection point to the detector. The chemical reactions take place whilst the sample material is dispersing within the reagent, the concentration gradient of the sample zone being formed by the physical dispersion process, where the sample zone broadens as it moves downstream and changes from the original asymmetrical shape to a more symmetrical and eventually Gaussian form [131]. What happens to one injected sample happens in exactly the same way to all other subsequently injected samples.

1.6.2. Dispersion Coefficient (D)

A sample contained in the sample loop of the injection valve is homogeneous and has an original concentration C° that, if it could be scanned by a detector, would give a square signal the height of which would be proportional to the sample concentration. When the sample zone is injected, it follows the movement of the carrier stream, forming a dispersed zone, the form of which depends on the geometry of the channel and the flow velocity [141]. Therefore, the response curve has the shape of a peak reflecting a continuum of concentrations, (concentration gradient). This continuum of concentrations can be viewed as being composed of individual elements of fluids, each having a certain concentration, C. The dispersion coefficient, D is defined as the ratio of concentrations of sample material before and after the dispersion process.

$$D = C° / C$$

If D = 2, the sample solution has been diluted 1:1 with the carrier stream. For convenience, sample dispersion has been defined as limited (D = 1 - 3), medium (D = 3- 10), and large (D > 10). The FI peak is a result of two kinetic processes that occur simultaneously: the physical process of zone dispersion and the chemical process resulting from reactions between sample and reagent species. The underlying physical process is well reproduced

for each individual injection cycle; yet it is not a homogeneous mixing, but a dispersion, the result of which is a concentration gradient of sample within the carrier stream. The dispersion coefficient is a theoretical concept, which does not correspond to any actual concentration within the dispersed sample zone. A dispersed sample zone is not composed of discrete elements of fluid, but only imagined by the detector at any time as an apparent discrete section of the concentration gradient. The D value is always related to a certain time, which is the period elapsed from the sample injection, to the moment the dispersed element of sample material passes through the observation field of the detector.

1.6.3. Effect of Peak Height with Sample Volume

By injecting increasing volumes of solution, a series of curves will be recorded, all starting from the same point of injection S, where the height of the individual peaks will increase until an upper limit 'steady state' has been reached. At this final level the recorded absorbance will correspond to the concentration of undiluted sample C°, and D = 1. The rising edge of all curves coincides and has the same shape regardless of the injected volumes. Where $n = S_v / S_{1/2}$, S_v is the sample volume, and $S_{1/2}$ is the volume of the sample solution necessary to reach 50 % of the steady state value, corresponding to D = 2. By injecting two $S_{1/2}$ volumes, 75 % of C° is reached, corresponding to D = 1.33; and so on. Injection of five $S_{1/2}$ volumes results in D = 1.03 and injection of seven $S_{1/2}$ volumes results in D = 1.008, corresponding to 99.2 % of C°. An increase in peak height and in sensitivity of measurement is achieved by increasing the volume of the injected sample solution. Dilution of overly concentrated samples is best achieved by reducing the injected volumes.

1.6.4. Effect of Peak Height with Channel Length and Flow Rate

The microreactor between the injection port and the detector may have different lengths, diameters, and geometry. The influence of coil length L and inner diameter of the tubing d

on the dispersion has been studied in detail [129]. The use of tubing of a small diameter will result in lower $S_{1/2}$ values, because the same sample volume will occupy a longer length of tube (θ), since $S_v = \pi(0.5d)^2\theta$ and will, owing to the restricted contact with the carrier stream, be less easily mixed and dispersed. If the tube diameter d is halved, the sample will occupy a fourfold longer portion of the tube (θ), and, hence, the $S_{1/2}$ value will be four times smaller. There are practical considerations that prevent the use of channels with too narrow a bore or too tightly packed reactors because: the flow resistance will increase; the system might easily become blocked by solid particles; and the flow cell used in spectrophotometric detection must have an optical path with an inner diameter of 0.5 - 1 mm, to allow sufficient light to pass through. The optimum internal diameter of tubes (usually PTFE) connecting the injection port and the detector is 0.5 mm although 0.75 mm internal diameter is useful for the construction of systems with large dispersion, and 0.3 mm for systems with limited dispersion.

The mean residence time T will depend, for a reaction system made of tubing of uniform internal diameter, on the tube length L, the tube diameter d, and the pumping rate Q. For systems of medium dispersion where the sample has to be mixed and made to react with the components of the carrier stream, one would tend to increase the tube length L in order to increase T. However, one can expect that dispersion of the sample zone to increase with the distance travelled, and this band broadening will eventually result in loss of sensitivity and lower sampling rate. So, instead of increasing the length L, one can decrease the pumping rate Q and keep L as short as is practically possible.

1.6.5. Effect of Peak Height with Channel Geometry

The effectiveness of various mixing geometries is shown in Figure 1.11. The coiled tube is the most frequently used geometric form of the FI microreactor. There are however different channel geometries; these are straight tube, coiled tube, mixing chamber, single

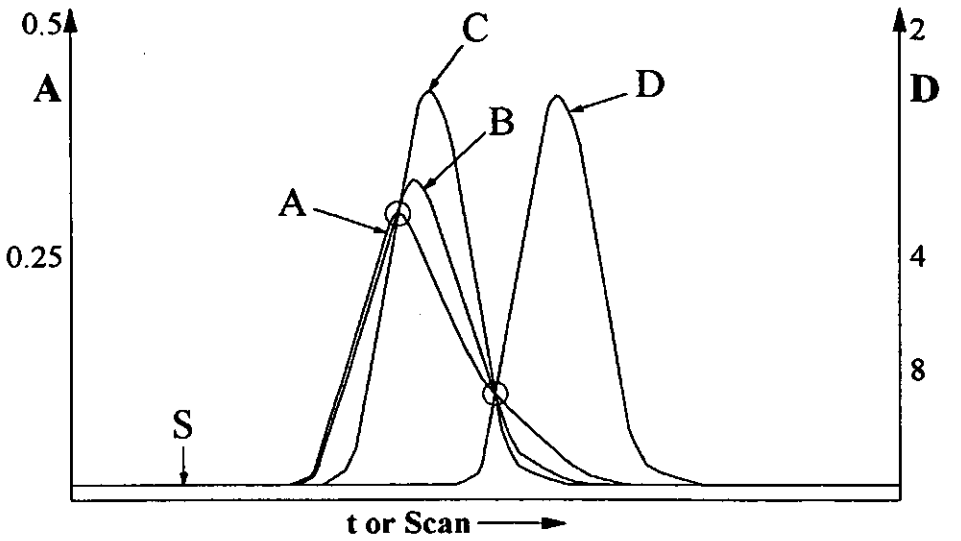

Figure 1.11. Dispersion of a dye, injected as a sample zone into: A, straight tube; B, coiled tube; C, 'knitted tube'; and D, a SBSR reactor. Peaks were recorded with microreactors of identical length, but different geometry [129].

bead string reactor, and 3-D or 'knitted' reactor. The function of these reactors is to increase the intensity of radial mixing. Thus, the reagent becomes more readily mixed with the sample , and the axial dispersion of the sample zone is reduced.

In a straight tube of uniform diameter, the parabolic profile formed by laminar flow remains undisturbed up to a flow velocity not normally reached in a typical FI system, and since the radial diffusion occurring in the time frame of an FI experiment is not sufficient to offset the axial dispersion initially formed during sample injection, an asymmetrical peak is recorded.

A coiled tube is the most frequently used reactor geometry, since it can conveniently accommodate any length of tubing in an experimental set-up and also because secondary flow within the coiled tubing promotes mixing in the radial direction. The result is a more symmetrical, higher and narrower peak than if an identical straight tube length had been used. The tighter the coiling of the tube is, the more pronounced this effect. Also, the longer the tube is, the longer the time for mixing and therefore the more symmetrical the obtained peak.

The mixing chamber was first used in the early FI titration systems [129] where a magnetic stirrer was used to promote reproducible homogeneous mixing of sample and reagents. But

the use of this type of geometry has many drawbacks, such as large dispersion giving reduced sensitivity, low sample throughput and large sample and reagent volumes, which is undesirable for systems which need to moderate their consumption. A single bead string reactor (SBSR) [142] is the most effective device to promote radial mixing in a tubular reactor. The SBSR allows symmetrical peaks to be obtained within the time domain and channel length of a typical FI manifold. However, small air bubbles and solid particles tend to be trapped in SBSR which may increase carryover and flow resistance. A three dimensional disoriented (3-D reactor) or 'knitted' reactor can be made by tightly and irregularly knotting a suitable length of tubing. The chaotic movement of the carrier stream through a spatially disoriented path promotes radial dispersion almost as effectively as a SBSR without its drawbacks.

1.7. IN SITU MONITORING

Quantitative knowledge of nutrient status and primary production is essential for investigating the ecology and/or biogeochemistry of aquatic ecosystems as well as providing information on the possible occurrence and impact of eutrophication, as discussed in Section 1.3.6. Chemical oceanographers study the processes that control the composition of the ocean by measuring the spatial and temporal distribution of elements in sea water. However, the resolution of chemical measurements of sea water is rather coarse and subject to systematic error. The limitations of conventional sampling techniques and analytical methods only allow the collection and analysis of more than a few samples per hour. In addition the sampling process greatly increases the possibility of contamination and chemical and biological reaction. Chemical analyses done in situ minimises these problems. Advances in analytical chemistry have made it feasible to perform a variety of chemical analysis in situ. The development of flow injection and light-emitting diode photometric

detectors have been particularly important in this respect. In situ FI [143] sample treatment can provide rapid analysis, high sampling frequency, robust construction to withstand harsh chemical matrices, easily maintained simple design, ability to be automated with unattended analyses and self-calibration, and low construction and operating costs.

For environmental monitoring FI field monitors have been developed for such parameters as nitrate [72], phosphate [144], ammonia [145] and aluminium [146] using solid state photometric detection [147], but these early designs were based on commercial mains-powered microcomputer systems and are thus unsuitable for use in a portable battery powered monitor. Recent developments in microchip technology have led to the production of specialised microcontroller devices for control and automation applications. This technology has been used in the development of in situ monitors with solid state detection for the analysis of both nitrate and phosphate [148, 149] in river waters. The computer system has been designed to automate all the functions required for field-based operation, i.e. control of peristaltic pumps, injection valve and switching valve and data acquisition, processing and logging. The systems are powered by a 12 V sealed lead-acid battery, which has an operational lifetime of many weeks.

For in situ monitoring of sea water, there are added constraints; the chemical monitors must be submersible and obtain immediate measurements whilst in the water column. Johnson and co-workers pioneered the use of continuous-flow submersible systems (SCANNERS) for nitrate [150, 151]. FI technologies have enabled chemical sea water parameters to be analysed underwater at depths of up to 2500m [150] and pressures of 1000 bar. The external parameters such as temperature (4 - 30 °C), pressure (2 - 30 bar) and salinity of sample (0 - 34 ‰) influencing the flow analysis and the chemistries incorporated into these monitors have been studied [152].

An absolute requirement for successful use of an autonomous functioning of flow analysis is an accurate and completely reliable reagent and sample delivery system. Taylor et al. [153]

have developed a three-channel positive displacement piston pump to work with an in situ continuous flow analyser. It is similar in concept to those used in high performance liquid chromatography and capable of delivery of fluids against a substantial flow resistance. Each channel consisted of four pump heads that were responsible for delivery of each of three possible reagents and sample (or standard). Each 10 μl pump head was operated at 30 to 60 strokes per minute by a rotating swash plate, which produced a sinusoidal 'pulsed' flow giving thorough mixing.

Osmotic pumps [154] have been developed to monitor nitrate in freshwater and sea water. Flow within an osmotic pump is caused by the osmotic pressure created across a rigid semi-permeable membrane separating a saturated salt solution from a solution of lower salinity. The diffusion of water through the membrane results in a net flow from dilute to the more saline solution. This flow of water through the rigid membrane then squeezes a flexible bag containing the reagents to be pumped, driving a reagent flow. This type of pump is dependent on temperature giving variable flow rates and can not be used where high response rates are essential.

Peristaltic pumps are the most common type of propulsion system used in FI. They are inexpensive, use simple technology, reliable, robust, physically small, easily automated and multichannel, therefore, they are ideal for in situ determination of nutrients in sea water.

1.8. RESEARCH OBJECTIVES

The overall objective was to design and optimise flow injection based chemistries for the determination of the seawater nutrients, nitrate and phosphate, for shipboard and in situ monitoring.

Specific objectives were:

1. To design and optimise an FI manifold for the determination of nitrate in estuarine, coastal and open ocean waters with a limit of detection of 0.1 μmol l^{-1} and a linear range of 0 - 73 μmol l^{-1} NO_3-N.
2. To achieve stability of reagents and standards for at least 30 days.
3. To demonstrate the accuracy of the method by participation in interlaboratory comparisons.
4. To validate the method on natural water samples of varying salinity (0 - 35 ‰) in the laboratory and on-board ship.
5. To design and optimise an FI manifold for the determination of orthophosphate in sea water with a limit of detection of 0.1 μmol l^{-1} and a linear range of 0 - 73 μmol l^{-1} PO_4-P.
6. To apply the method to the determination of orthophosphate in natural water samples of varying salinity (0 - 35 ‰).
7. To compare the FI method for the shipboard determination of nitrate with the traditional continuous flow methodology (AutoAnalyzer®), during a North Sea cruise.
8. To carry out a comparative study between a photomultiplier and a charged coupled device (CCD), two-dimensional array detector for the determination of nitrite and nitrate.

Chapter Two
Determination of Nitrate

2. DETERMINATION OF NITRATE

2.1. INTRODUCTION

This chapter describes the development and optimisation of an FI method for the determination of nitrate in sea water, with adaptations made to cover the levels found in freshwaters (0 - 15 mg l^{-1} NO_3-N) and estuarine waters (0 - 0.5 mg l^{-1} NO_3-N) and the varying salinity (0 - 35 ‰). Concentration units quoted for nitrate vary depending on the specific discipline involved, for example marine scientists use µmol l^{-1} NO_3 and EC legislation quote, mg l^{-1} N. Table 2.1, therefore shows the conversion factors between the most commonly used units.

Table 2.1. Nitrate concentration unit conversions.

Nitrate-Nitrogen (NO_3-N)	1 mg l^{-1} = 71.43 µmol l^{-1}
Nitrate (NO_3)	1 mg l^{-1} = 16.1 µmol l^{-1}

2.2. EXPERIMENTAL

2.2.1. Reagents and Standards

All solutions were prepared from ultra-pure de-ionised water supplied by a Milli-Q system (Millipore Corp.), and all reagents were AnalaR® (BDH) unless otherwise stated. The carrier stream was prepared by dissolving ammonium chloride (10 g) in 1 l of water. The N-(1-naphthyl)ethylenediamine dihydrochloride (NINED, Sigma) and sulphanilamide reagents were prepared by dissolving 0.5 and 25 g, respectively in 1 l of water containing 10 % ($^{v}/_{v}$) orthophosphoric acid. The colour reagent solution was prepared by mixing equal

volumes of the N1NED and sulphanilamide reagents in a brown glass bottle. The cadmium reductor was prepared by stirring 5 g cadmium powder (325 mesh, 99.5 % purity, Johnson-Matthey Metals) in 50 ml of a copper (II) sulphate solution (10 g l^{-1}) for 2 min. The copperised cadmium was then washed with 2 M hydrochloric acid and ammonium chloride solution (10 g l^{-1}), packed into a glass tube (40 mm, 2 mm i.d.) and plugged with glass wool. When not in use the cadmium column was stored in ammonium chloride solution (10 g l^{-1}). A stock nitrate solution (100 mg l^{-1}) was prepared by dissolving 0.7220 g of potassium nitrate in water. Working standards were prepared by serial dilution with water.

2.2.2. Instrumentation and Procedures

The initial FI manifold used for the determination of nitrate is shown in Figure 2.1. Peristaltic pumps (FIAstar 5020 Analyzer) and flexible modified PVC pump tubing (Anachem) were used to propel the ammonium chloride (0.23 ml min^{-1}) carrier stream and colour reagent (0.16 ml min^{-1}) through PTFE tubing (0.8 mm i.d.). The standards and samples (260 µl) were injected into an ammonium chloride carrier stream, passed through the cadmium reductor column and then merged with the colour reagent in a 200 cm reaction coil. The resultant pink-purple azo dye was detected using a FIAstar 5023 spectrophotometer (λ_{max} 540 nm) filled with a 10 mm path length flow cell (18 µl). Although absorbance is dimensionless, A.U. is used to denote absorbance in all subsequent discussions.

2.3. RESULTS AND DISCUSSION

2.3.1. Univariate Optimisation of Reagent Concentrations

A univariate optimisation was carried out on the reagent concentrations, sulphanilamide and N-(1-naphthyl) ethylenediamine, and the concentration of orthophosphoric acid contained in

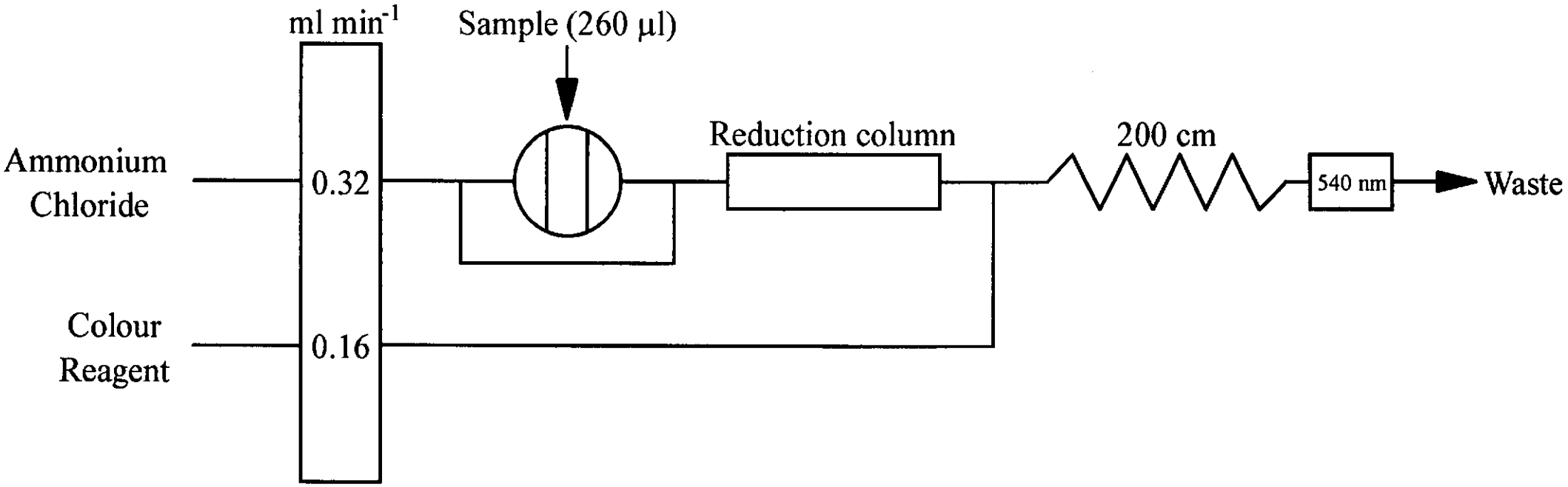

Figure 2.1. FI manifold for the determination of nitrate in waters

the colour reagent. The manifold shown in Figure 2.1 was used for the optimisation of the acid, but for the optimisation of the sulphanilamide and N1NED concentrations the colour reagent stream was split into two. For the optimisation experiments the reagent concentrations were 25 g l^{-1} sulphanilamide, 0.5 g l^{-1} N1NED, both in 10 % ($^{v}/_{v}$) orthophosphoric acid with 0.5 mg l^{-1} NO_3-N used throughout. Figure 2.2 shows the results of the univariate optimisation of sulphanilamide in the range 5 - 40 g l^{-1} containing 10 % ($^{v}/_{v}$) orthophosphoric acid. The absorbance signal increases with increasing sulphanilamide concentration up to 20 g l^{-1} after which there is only a small increase. A minimum excess of 25 g l^{-1} sulphanilamide was used for subsequent work.

The effect of N1NED concentration was studied in the range 0.2 - 1.4 g l^{-1} in 10 % ($^{v}/_{v}$) orthophosphoric acid, as shown in Figure 2.3. There is an increase in absorbance with increase in N1NED between 0.2 and 0.5 g l^{-1} followed by a decrease in signal at higher concentrations. For further work a N1NED concentration of 0.5 g l^{-1} was used.

The orthophosphoric acid concentration of the mixed colour reagent, sulphanilamide (25 g l^{-1}) and N1NED (0.5 g l^{-1}), was studied in the range 5 - 30 % ($^{v}/_{v}$), shown in Figure 2.4. There is a decrease in absorbance signal with an increase in orthophosphoric acid concentration. A 10 % ($^{v}/_{v}$) orthophosphoric solution was chosen so as to buffer the diazotisation step against samples of high pH.

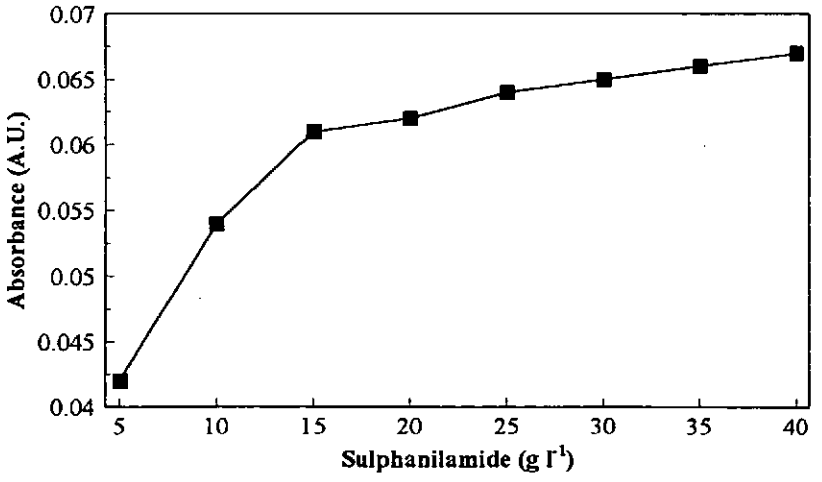

Figure 2.2. Univariate optimisation of sulphanilamide concentration.

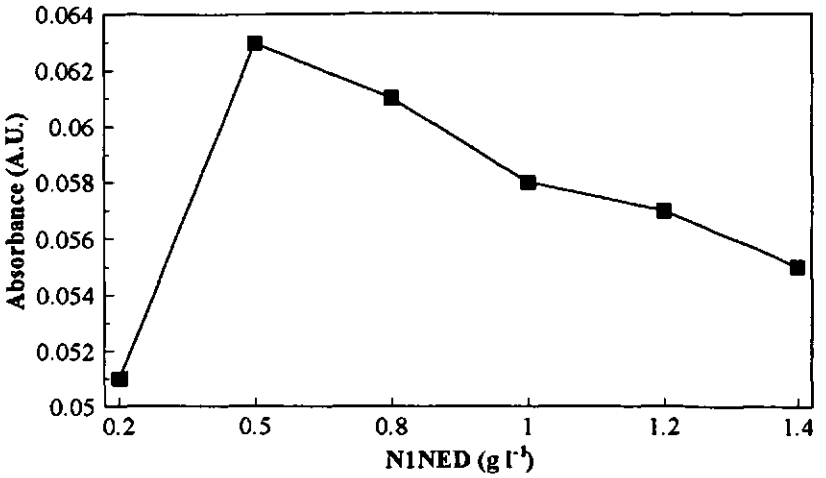

Figure 2.3. Univariate optimisation of N-(1-naphthyl)ethylenediamine concentration.

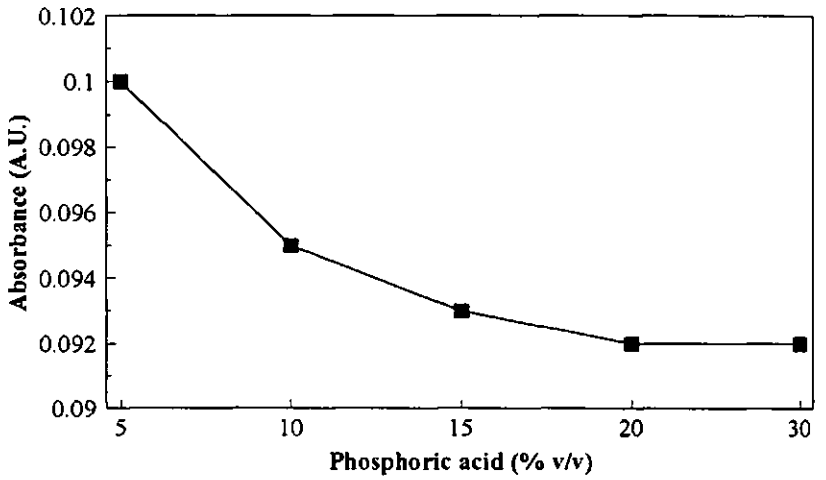

Figure 2.4. Univariate optimisation of orthophosphoric acid concentration.

2.4. SIMPLEX OPTIMISATION

2.4.1. Principles

Simplex optimisation is a multivariate optimisation technique which was first proposed by Spendly et al. to assist in the efficient running of an industrial process [155]. It works by locating the summit of the response surface defined by the system variables. The summit is assumed to be the optimal system conditions (e.g. conditions which give the highest signal to noise ratio). Simplex optimisation may be applied when all the factors are continuous

variables. A simplex is a geometrical figure which has n + 1 vertices when a response is being optimised with respect to n factors. For example, for two factors (V_1 and V_2) the simplex will be a triangle. The method of optimisation is illustrated by Figure 2.5. The initial simplex is defined by the points labelled 1, 2 and 3. In the first experiment the response is measured at each of the combinations of factor levels given by the vertices of the simplex. The worst response would be found at point 1 and it would be logical to conclude that a better response would be obtained at a point which is the reflection of 1 with respect to the line joining 2 and 3, i.e. at 4. The points 2, 3 and 4 form a new simplex and the response is measured for the combination of factor levels given by 4. Comparing the responses for the points 2, 3 and 4 will show that 2 gives the worst response. The reflection procedure is repeated to give the simplex defined by 3, 4 and 5. It can be seen that no further progress beyond the stage shown, since points 9 and 13 both give a worst response than 11 [156].

In order to improve the performance of the simplex method various modifications have been proposed, incorporating extra rules to allow the simplex to change shape and size, increasing the efficiency of the procedure [157-162].

If the initial simplex is taken as a regular figure in n dimensions, then positions taken by the vertices in order to produce such a figure will depend on the scales used for the axes. The scales should be chosen so that unit change in each factor gives roughly the same change in response. The choice of the size of the initial simplex is not critical if it can be expanded or contracted as the method proceeds.

Once an optimum has been found, the effect on the response when one factor is varied while the others are held at their optimum levels can be investigated for each factor in turn. This procedure can be used to check the optimisation. It also indicates how important deviations from the optimum level are for each factor.

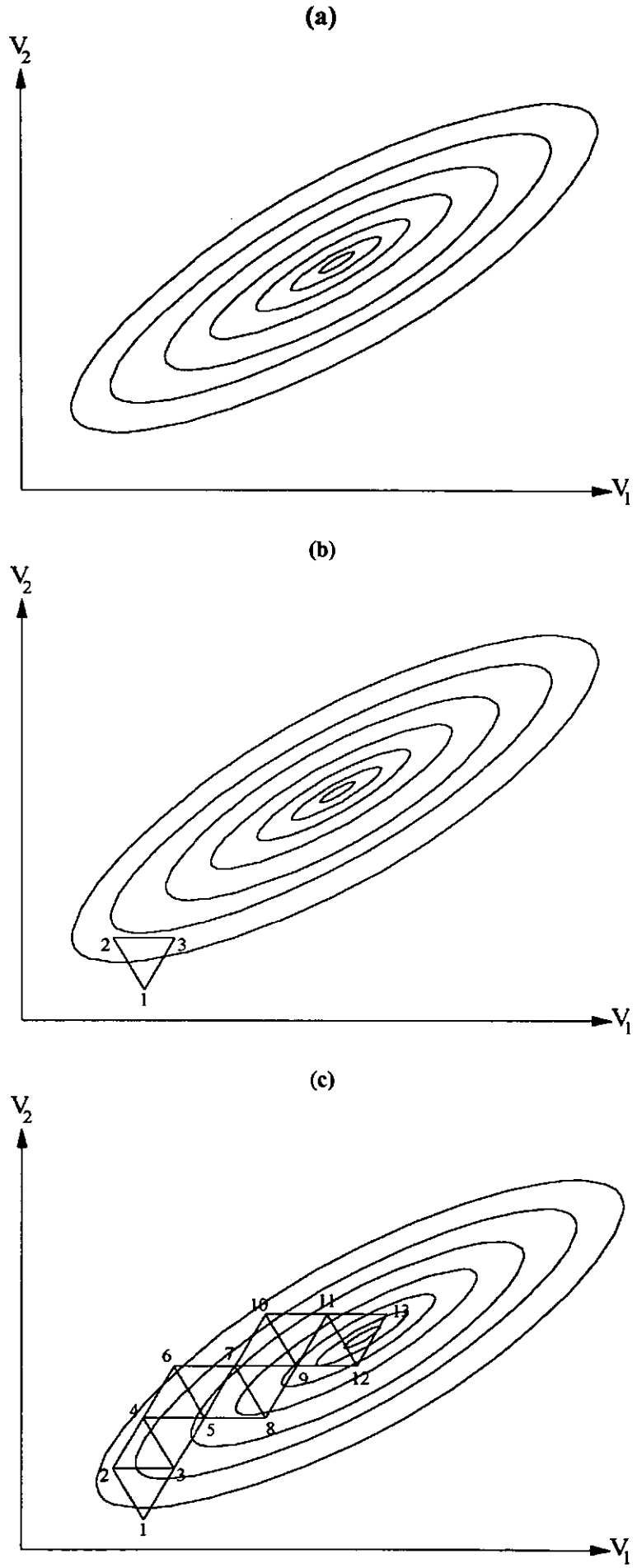

Figure 2.5. Simplex Optimisation for a two variable System. (a) response surface: (b) initial vertex (starting conditions) and (c) complete fixed step size simplex optimisation procedure for a two variable system.

2.4.2. Simplex Optimisation of Nitrate FI Manifold.

A simplex algorithm [163] written in BASIC was used to optimise the nitrate method. The key variables for maximising the absorbance signal were considered to be the flow rates of the ammonium chloride carrier stream, the colour reagent stream and the sample stream, the sample loop volume and the reaction coil length. The starting conditions for each variable are shown in Table 2.2 including the range, step size and precision. The range is the minimum and maximum limits of each variable, the step size is the increments in which the variables increase or decrease between each simplex experiment, and the precision is the smallest value that the variable can be measured. The reagent concentrations, previously univariately optimised, used in the simplex experiments were 10 g l^{-1} ammonium chloride and mixed colour reagent, 25 g l^{-1} sulphanilamide, 0.5 g l^{-1} N1NED containing 10 % ($^{v}/_{v}$) orthophosphoric acid.

Table 2.2. Conditions used for simplex optimisation.

VARIABLE	UNITS	RANGE	STEP SIZE	PRECISION	STARTING CONDITIONS
Sample Loop Volume	µl	25 - 300	10	5	25
Carrier Flow Rate	ml min^{-1}	0.16 - 1.0	0.1	0.1	0.16
Reagent Flow Rate	ml min^{-1}	0.16 - 1.0	0.1	0.1	0.16
Sample Flow Rate	ml min^{-1}	0.16 - 1.0	0.1	0.1	0.42
Reaction Coil Length	cm	50 - 300	25	10	100

The absorbance at peak maximum measured at 540 nm was used as the response surface during the optimisation procedures, using a 0.5 mg l^{-1} NO_3-N standard. Table 2.3 shows the variable conditions for each simplex experiment and Figure 2.6 shows the simplex history in terms of the response.

Table 2.3. Simplex history for each variable.

EXPERIMENT NUMBER	SAMPLE LOOP VOLUME μL	CARRIER FLOW RATE ml/min	REAGENT FLOW RATE ml/min	SAMPLE FLOW RATE ml/min	REACTION COIL cm	RESPONSE
1	25	0.16	0.16	0.42	100	0.098
2	90	0.16	0.16	0.42	100	0.211
3	60	0.80	0.16	0.42	100	0.097
4	60	0.42	0.80	0.42	100	0.090
5	60	0.42	0.42	1.20	100	0.133
6	60	0.42	0.42	0.60	175	0.140
7	70	0.16	0.16	0.80	125	0.163
8	70	0.16	0.42	1.20	150	0.130
9	120	0.42	0.42	1.20	150	0.223
10	170	0.42	0.60	1.20	175	0.246
11	130	0.42	0.42	0.42	125	0.258
12	160	0.60	0.16	0.16	100	0.206
13	200	0.16	0.16	0.42	100	0.378
14	220	0.16	0.16	0.42	175	0.400
15	240	0.16	0.16	0.60	125	0.416
16	260	0.23	0.16	0.80	200	0.480
17	240	0.16	0.16	0.60	125	0.416
18	260	0.23	0.16	0.80	200	0.480

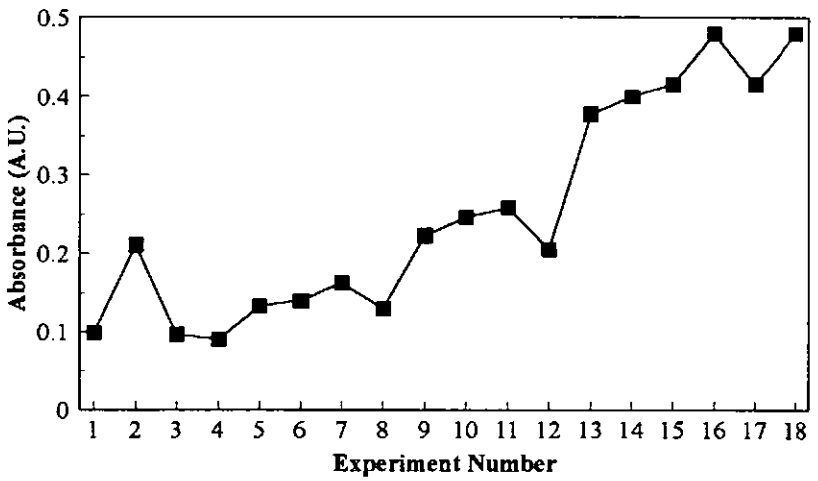

Figure 2.6. Simplex history for initial optimisation.

After sixteen experiments of the initial simplex the absorbance signal was increased to 0.480 A.U.; almost a five-fold increase. From Table 2.3 it can be seen that the key variables were

the sample loop volume, and carrier, and colour reagent flow rates. This is due to the increase in time for the formation of the azo dye and longer contact time for the nitrate with the cadmium in the reduction column.

2.4.3. Univariate Optimisation of Nitrate FI Manifold

In order to asses the performance of the simplex optimisation each of the variables were also univariately optimised to investigate their effects on the method. The basic conditions for the optimisation involved the manifold shown in Figure 2.1, with reagent concentrations of 10 g l^{-1} ammonium chloride carrier and a mixed colour reagent containing 25 g l^{-1} sulphanilamide, 0.5 g l^{-1} N1NED and 10 % ($^{v}/_{v}$) orthophosphoric acid. All experiments were carried out using 0.1 mg l^{-1} NO_3-N.

Figures 2.7 and 2.8 show the optimisation of the carrier flow rate in the range 0.16 - 1.2 ml min^{-1} and colour reagent flow rate from 0.16 - 0.8 ml min^{-1}. As, the flow rate increases the absorbance signal decreases, this is because the diazonium ion formed between the sulphanilamide and the reduced nitrate in the sample has less time to react with the N1NED, also the contact time between the nitrate and the copperised cadmium in the reduction column decreases with increasing flow rate, so the nitrate is less reduced to nitrite, hence the response signal decreases. For further work a carrier and colour reagent flow rate of 0.23 and 0.16 ml min^{-1} respectively were used. From Figure 2.9 it can be seen that the absorbance signal increases with increasing sample flow rate, this is because a 10 second sample loop filling time was used. So, obviously at lower flow rates the loop is not being fully filled. A 10 second filling time was chosen so as to have a fast sample throughput which is important for automation and field deployment. Figure 2.10 shows the optimisation of the sample loop volume in the range 25 - 300 µl. As, expected the absorbance increases with increasing sample volume, reaching an optimum at about 200 µl.

In order to achieve a lower limit of detection , a sample volume of 260 µl, as optimised by simplex was used for further work.

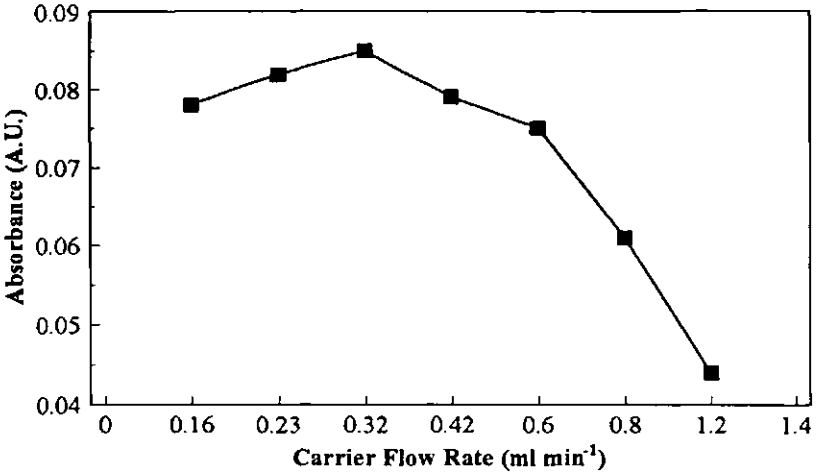

Figure 2.7. Univariate optimisation of ammonium chloride carrier flow rate.

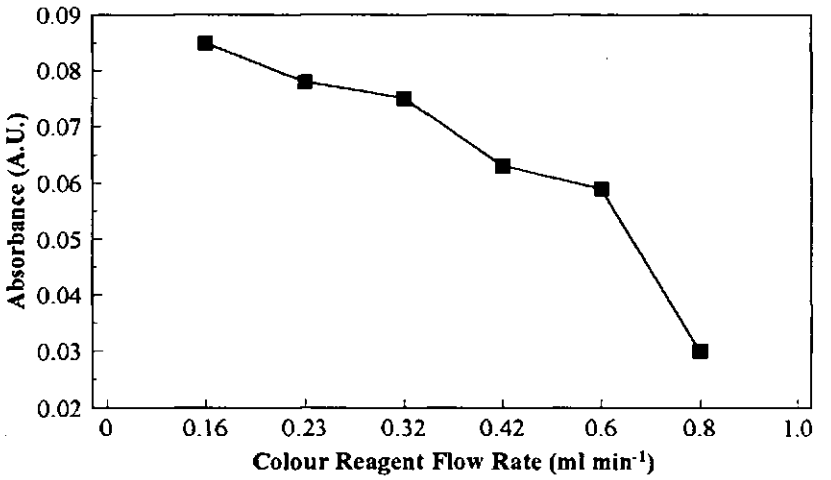

Figure 2.8. Univariate optimisation of colour reagent flow rate.

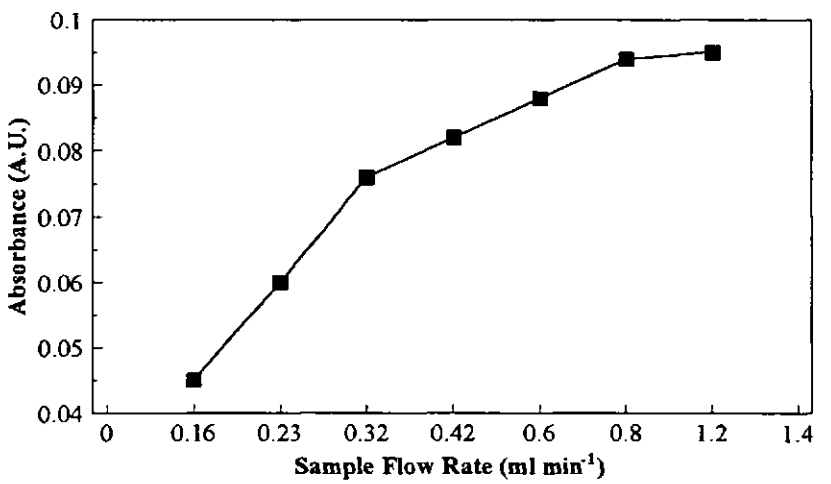

Figure 2.9. Univariate optimisation of sample flow rate.

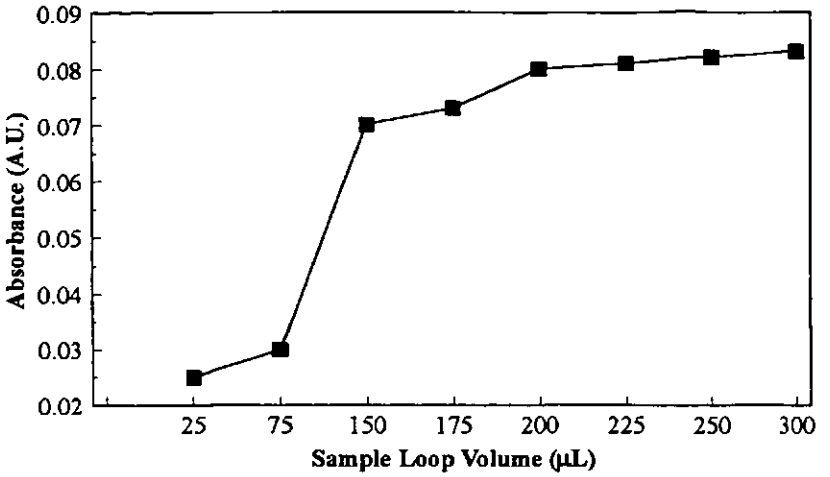

Figure 2.10. Univariate optimisation of sample loop volume.

2.5. THE SCHLIEREN EFFECT

2.5.1. Principles

Sensitivity in FI spectrophotometry is often limited by differences in refractive indices between the sample and carrier solutions [164-166]. The Schlieren signal is highly dependent on the chemical species, involved being less pronounced for species with a rapid dissolution ability (e.g. low viscosity). This phenomenon becomes more evident in single line systems with limited dispersion if the sample reaches the detector without being properly mixed with the carrier stream. In this situation, a number of liquid interfaces acting as mirrors are randomly established between fluid elements with different refractive indices so that the amount of light reaching the detector becomes erratic. As a consequence, the recorded peak is noisy, and the sensitivity and reproducibility deteriorate. The effect is more pronounced at the front and tailing portions of the sample zone where the concentration, and hence refractive index gradients are highest. Therefore, FI systems based on gradient exploitation are usually more susceptible to this effect.

The refractive index effect in FI was reported for the first time when a turbidimetric procedure for sulphate determination was proposed [167] and quotes '**a mixing boundary (Schlieren pattern) could be seen very clearly when the flow through cuvette was**

removed from the spectrophotometer and observed visually after injecting a blank or sample. The phenomenon becomes less pronounced as the mixing conditions are improved.'

Under good mixing conditions, a continuous concentration gradient is established along the processed sample. As the flow injection analyser operates under laminar flow conditions, isolines of different refractive indices acting as lenses are established. The liquid lenses may either focus light on the detector or scatter it during the passage of the sample zone through the flow cell. The effect was discussed when an LED transducer for the use in FI measurements was designed [164]; the flow cell was removed from the spectrophotometer and observed with the naked eye. As the sample passed through the flow cell, the image was initially magnified and then diminished. In practice, this means a reproducible positive peak followed by a smaller negative peak. The heights of these peaks, proportional to the concentration of the injected solution, are highly dependent on the optical performance of the spectrophotometer.

If a well mixed sample zone reaches the flow cell in a pulsed fashion, the Schlieren effect may manifest itself as an undulation on the recorded peak. Usually the superimposed modulated frequency is determined by the pulsation of the peristaltic pump. The effect is due to the intermittent presence of concentrated and diluted portions of the sample zone in the spectrophotometer light beam. A steady state Schlieren signal may be observed in FI systems with merging streams with pronounced differences in concentrations. Under non-ideal mixing conditions, the baseline becomes noisy with a sinusoidal oscillation.

An appropriate way to reduce the refractive index problem is to match the concentrations of the sample and carrier solutions. For higher sensitivity, sample injection into a chemically inert solution with a similar matrix composition is to be preferred [165, 168], the reagents then being added by confluence. An example for sea water analysis [166] involved the sample channel split and reagents added in defined proportions to both branches in order to

provide streams of similar salinity. Thereafter, a sample/reagent aliquot was selected and injected into the other sample/reagent stream. With this approach, however, sample replacement is difficult, impairing the analytical frequency.

There are situations, however, where concentration matching is a limiting factor in system design. As examples, analyses of sample batches with high and variable salinity, such as estuarine samples where the salinity may vary between 0 - 35 ‰, intercalation of an ion exchange resin column in the eluent solution, sample injection into a concentrated reagent and addition of confluent streams with pronounced differences in concentrations can be pointed out.

Dual-wavelength spectrophotometry, currently exploited in liquid chromatography to suppress solvent peaks can be utilised to circumvent the Schlieren effect in FI [169]. A dual-wavelength beam passes through the flowing sample, the emergent light is dispersed and the resulting monochromatic beams are measured simultaneously by separate detectors, the difference in absorbance constituting the measurement basis. Real-time subtraction of the wavelength independent noise is then achieved.

Parameters affecting dispersion, such as injection volume, reactor length, flow rates and confluent stream addition, also have a marked effect on the Schlieren signal. In FI systems with large dispersion, the magnitude of the Schlieren signal increases with increasing injection volume. It was found that when increasing the sampling loop the Schlieren and analytical signals showed similar behaviour. This means that the signal to noise ratio does not improve with variations in sample volume. For larger volumes, two distinct Schlieren regions are observed because the mixing boundaries predominate at the front and tailed portions of the sample zone. In this situation, increasing the sample volume results in a better separation between these regions. If sensitivity is limited by the Schlieren effects and the sampling rate is not critical, the sample volume should be as large as possible, yielding a sample zone with a central portion less affected by light scattering.

Increasing the analytical path length decreases both the Schlieren effect and analytical signals. However, the decrease in the Schlieren effect is more pronounced than the analytical signal attenuation because it depends on dispersion and available mixing time, whereas the analytical signal attenuation depends only on dispersion. In practice, this means an improvement to the signal to noise ratio by increasing the reaction coil length. However, this coil cannot be increased at will because the analytical signal should be preserved.

The influence of the total flow rate on the Schlieren signal is less pronounced for higher flow rates, and the addition of a confluent stream diminishes the magnitude of the Schlieren signal. At the confluence point, the concentration of each fluid element of the sample zone is reduced, allowing better homogenisation of the final sample zone. The merging reagent should be added to the sample zone at a high flow rate to reduce the Schlieren effect.

2.5.2 Refractive Index Correction

Figure 2.11 shows the shape of the FI peaks for nitrate concentrations < 0.8 μmol l^{-1} using the manifold shown in Figure 2.1 which has no refractive index correction. There is a clear negative peak followed by an enhanced positive signal, as interpolated from the calibration graph, giving an elevated calculated nutrient concentration. Figure 2.12 shows the manifold developed to eliminate refractive index problems arising from samples of varying salinity [170]. To ensure thorough mixing between the sample and carrier a glass bead mixing column (20 mm, 3 mm i.d., column filled with 1.5 to 2 mm o.d. glass balls) was introduced before the reduction column. The samples were injected into a sodium chloride matrix matching stream. It was found that a sodium chloride concentration of 12.5 ‰ eliminated the refractive index effects caused from samples of 0 - 35 ‰ salinity. So, the manifold is suitable for the analysis of fresh, estuarine and sea water samples without the need to change any parameters or make any corrections.

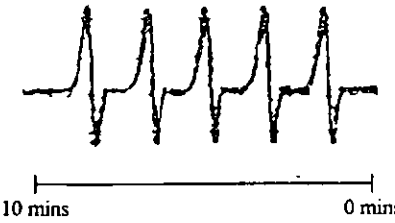

Figure 2.11. Typical FI peak shape for low level nitrate (< 0.8 μmol l^{-1} NO_3-N).

2.5.3. Calibration Data and Figures of Merit

The manifold shown in Figure 2.12 achieves a limit of detection of 0.1 μmol l^{-1} NO_3-N (3σ) and a linear calibration range of 0.1 - 73 μmol l^{-1} NO_3-N ($n = 6$; $r^2 = 0.9995$). Table 2.4 shows calibration data for NO_3-N standards over the range 0.7 - 21.0 μmol l^{-1} NO_3-N at salinities ranging from 0 - 30 ‰. This adequately covers the range of nitrate concentrations and salinities expected in estuarine and coastal waters. Figure 2.13 shows the FI peaks for nitrate calibration at 0 - 30 ‰.

2.6. INTERLABORATORY COMPARISONS

An intercomparison has a number of aims:

1. to detect the pitfalls of a commonly applied method and to ascertain its performance in practice.

2. to measure the quality of a laboratory or a part of a laboratory.

3. to improve the quality of a laboratory in collaborative work in mutual learning process.

4. to certify the contents of a reference material (CRM). Such an exercise is one of the most powerful tools to detect and remove sources of error due to a particular technique as applied within a laboratory. In general, analytical errors in all inorganic analysis may stem from: a). inadequate sample storage.

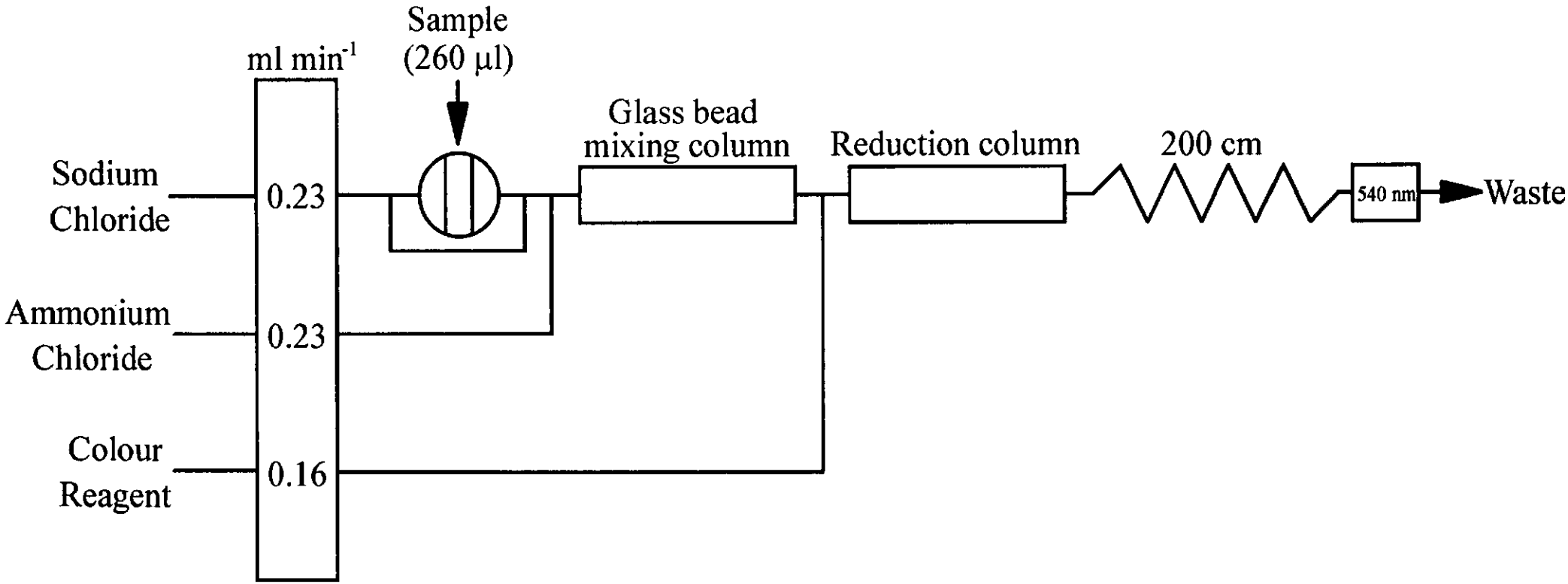

Figure 2.12. FI manifold for the determination of nitrate in estuarine and coastal waters

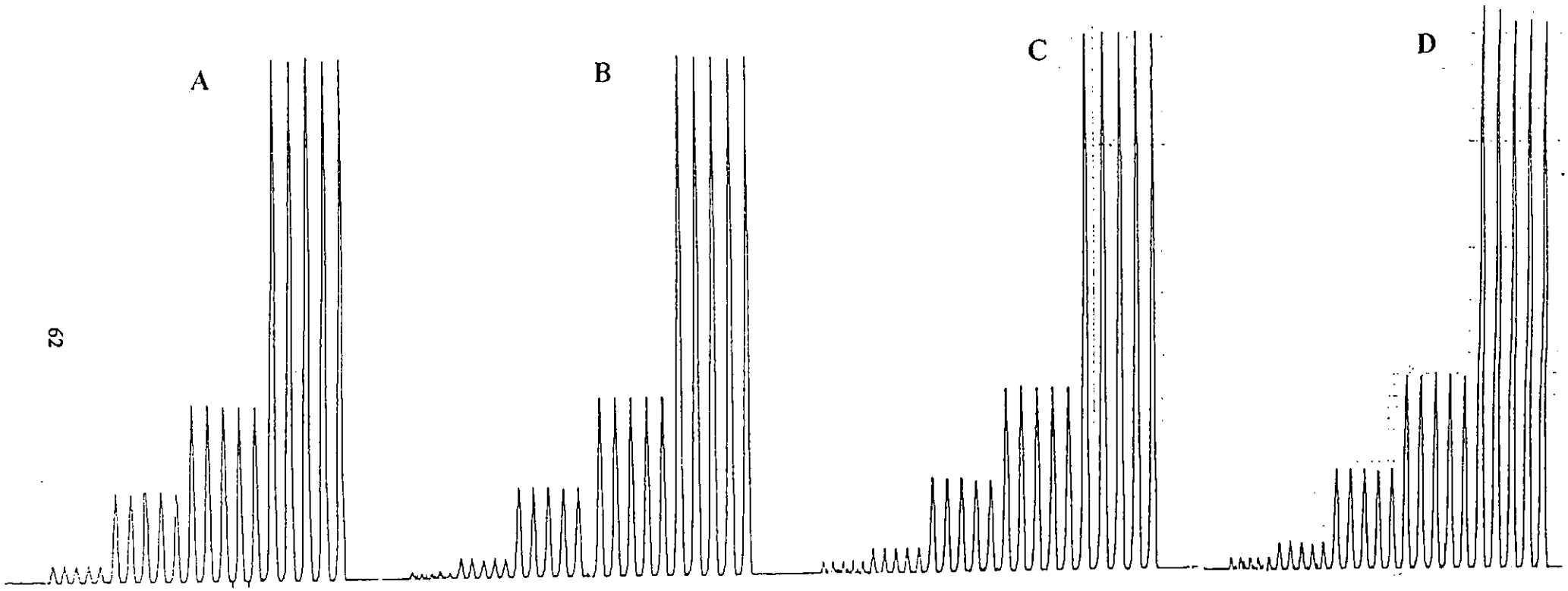

Figure 2.13. FI peaks for nitrate calibrations (0, 0.01, 0.05, 0.1 and 0.5 mg l^{-1}) in salinities of A, 20 ‰, B, 10 ‰, C, 0 ‰ and D, 30 ‰.

Table 2.4. NO_3-N calibration data covering the 0 - 30 ‰ salinity range.

NO_3-N (µmol l^{-1})	Salinity (‰)	Absorbance Signal (A.U.)	RSD (%) (n = 5)	r^2 (n = 5)	Gradient (b)	Error in gradient (S_b)	Intercept (a)	Error in intercept (S_a)
0	0	0.006	0	0.9997	0.012	2.10×10^{-4}	3.25×10^{-3}	2.11×10^{-3}
0.7		0.011	0					
3.5		0.045	1.2					
7.0		0.088	0.5					
21.0		0.262	0.2					
0	10	0.002	22.8	1.0000	0.012	4.80×10^{-5}	1.28×10^{-3}	1.19×10^{-4}
0.7		0.009	6.4					
3.5		0.043	1.2					
7.0		0.086	0					
21.0		0.254	0.1					
0	20	0.000	0	1.0000	0.012	1.25×10^{-4}	0.000	7.32×10^{-4}
0.7		0.008	0					
3.5		0.042	1.3					
7.0		0.084	0.6					
21.0		0.256	0.3					
0	30	0.002	0	0.9999	0.012	7.91×10^{-5}	4.2×10^{-4}	7.93×10^{-4}
0.7		0.009	0					
3.5		0.041	0					
7.0		0.083	0					
21.0		0.252	0.3					

b). the method of sample pre-treatment (e.g. digestion, preconcentration, dilution).

c). the method of final measurement; the influence of blanks is particularly critical for nitrate determinations.

d). the laboratory infrastructure.

e). the data treatment.

All of the experimental work reported below as coming from the University of Plymouth was carried out by T. McCormack.

2.6.1. Community Bureau of Reference (BCR), Nitrate in Freshwater Intercomparison

Preparation of the candidate reference materials [171]

The two reference material CRM 479 and 480 were prepared (at the University of Cordoba, Spain) from ultra-pure water to which freshly prepared solutions of the different compounds described in Table 2.5 were added (amounts in g added to approximately 150 litres of ultra-pure water). The final pH values of the solutions were ~ 6.8. The homogenisation of the solutions was achieved with a mechanical shaker during the addition of the solutions. The clear glass ampoules were filled with the CRM solutions after previously cleaned with detergent, rinsed with ultra-pure water and air dried for two days. After heat sealing the ampoules were then stored at ambient temperature in the dark.

The pH of the solution was considered to be critical for the stability. The evaporation of carbon dioxide as well as the precipitation of calcium carbonate were considered to be possible sources of inhomogeneity and instability. Sodium carbonate (530 mg l^{-1}) was added to maintain the pH against the air, the resulting pH ranged between 9 and 9.5 so acid (0.5 ml of 10 mol l^{-1} HCl) was added in order to achieve a pH of 6.8 similar to that observed in natural water. Lauryl sulphate (2 mg l^{-1}) was added to the samples to simulate

Table 2.5. Amounts of compounds added to the two candidate CRMs.

COMPOUND	CONCENTRATIONS g 150 ml^{-1}
Potassium nitrate (KNO_3)	3.670 and 12.475
Sodium Carbonate (Na_2CO_3)	79.500
Calcium Chloride ($CaCl_2 \cdot 4H_2O$)	13.755
Magnesium Sulphate ($MgSO_4 \cdot 7H_2O$)	18.450
Potassium phthalate	0.750
Lauryl sulphate	0.300
Phenylmercury acetate	1.500

the presence of humic acids, it has a wide absorption range in the U.V. Finally, phenyl mercury acetate was added to avoid microbial growth. The levels of nitrate concentrations were chosen to be in the range found in freshwaters. Nitrates were added in the form of high purity salts (KNO_3) dissolved in Milli-Q water. The water was boiled, homogenised with a mechanical shaker and filtered with sterile filters of 0.2 μm. Calcium chloride, magnesium sulphate, and sodium carbonate were added to simulate the hardness of a natural water.

2.6.2. Analysis and Results

Two ampoules of each CRM (479 and 480) containing nitrate in freshwater were received from BCR Brussels in June 1993. An ampoule of each CRM was carefully broken open and the contents were analysed on five separate days. As the concentration of nitrate in each sample was so high, the manifold shown in Figure 2.1 was used with a 30 μl sample loop, plus the samples were diluted by a factor of 10. Tables 2.6 and 2.7 show the concentration in CRM 479 and 480 determined on five separate occasions by the University of Plymouth (Laboratory 15). Table 8 shows a summary of the techniques used by the fifteen participating laboratories,

Table 2.6. Nitrate in CRM 479 determined by the University of Plymouth.

Analysis Number	Mean Total Signal	Mean Net Signal (Total - Blank)	Concentration in Solution (μmol ml^{-1}) x 10^{-4}	Blank (μmol kg^{-1} NO_3)	RSD (%)	Content in Sample (μmol kg^{-1} NO_3)
1	0.054	0.052	2.84	0.16	0.00	202
2	0.059	0.056	2.98	0.07	0.00	213
3	0.057	0.055	3.02	0.05	1.46	216
4	0.055	0.053	2.97	0.23	0.81	212
5	0.054	0.052	2.94	0.09	1.00	210

Table 2.7. Nitrate in CRM 480 determined by the University of Plymouth.

Analysis Number	Mean Total Signal	Mean Net Signal (Total - Blank)	Concentration in Solution (μmol ml^{-1}) x10^{-3}	Blank (μmol kg^{-1})	RSD (%)	Content in Sample (μmol kg^{-1})
1	0.241	0.239	1.25	0.16	0.17	891
2	0.248	0.246	1.23	0.07	0.61	880
3	0.227	0.225	1.21	0.05	0.36	865
4	0.230	0.228	1.22	0.23	0.36	871
5	0.235	0.232	1.25	0.09	0.42	889

Table 2.8. Summary of techniques as applied in the nitrate determination.

Sample Pre-treatment and Calibration	Final Determination	Lab. No.
Reduction on Cd column; addition of sulphanilamide and N-(1-naphthyl)ethylenediamine dihydrchloride Calibrant: KNO_3 (purity ≥ 99.99 %) in water	SPEC of diazo compound at 540 nm	01
No pre-treatment Calibrant: KNO_3 (purity > 99 %)	IC Conductivity	02
Addition of HCl Calibrant: KNO_3 (purity > 99 %)	IC Conductivity	03
No pre-treatment Calibrant: KNO_3 (purity > 99 %)	IC Conductivity	04
No pre-treatment Calibrant: $NaNO_3$ (purity 99.995 %) verified against KNO_3 (purity 99.99 %)	IC Conductivity	05
Addition of NH_4Cl buffer (pH=8.2); reduction on Cd column; addition of sulphanilamide and N-(1-naphthyl)ethylenediamine Calibrant: $NaNO_3$ (purity 99.995 %) verified against KNO3 (purity 99,99 %)	SPEC (SFA) of diazo compound at 540 nm	05
Addition of NH_4Cl buffer (pH=8.2); reduction on Cd column; addition of sulphanilamide and N-(1-naphthyl)ethylenediamine Calibrant: KNO_3 (purity > 99 %)	SPEC of diazo compound	06
No pre-treatment Calibrant: $NaNO_3$ (purity ≥ 99.5 %) in water	IC Conductivity	07
No pre-treatment Calibrant: KNO_3 (purity ≥ 99.5 %) in water	IC Conductivity	08a
UV-irradiation Calibrant: KNO_3 (purity ≥ 99.5 %) in water	IC Conductivity	08b
No pre-treatment for CRM 479; gravimetric dilution for CRM 480 Calibrant: KNO_3 (purity >99 %) in water verified against $NaNO_3$	IC Conductivity	09
Addition of NH_4Cl buffer (pH=8.2); reduction on Cd column; addition of sulphanilamide and N-(1-naphthyl) ethyleneamine Calibrant: commercial solution	SPEC (SFA) of diazo compound at 540 nm	10
Addition of NH_4Cl buffer; reduction on Cd column; addition of sulphanilamide and N-(1-naphtyl) ethylenediamine Calibrant: $NaNO_3$ (purity ≥ 99.99 %) in water	SPEC (SFA) of diazo compound at 540 nm	11

Sample Pre-treatment and Calibration	Final Determination	Lab. No.
No pre-treatment for CRM 479; dilution for CRM 480 Calibrant: KNO_3 (purity > 99 %) in water verified with control solutions	IC Conductivity	12
No pre-treatment Calibrant: $NaNO_3$ (purity ≥ 99 %) in water verified against quality reference standard	IC	13
Reduction by hydrazine addition with a copper catalyst; addition of sulphanilamide and N-(1-naphthyl) ethylenediamine Calibrant: KNO_3 (purity > 99.99 %) in water	SPEC of diazo compound at 540 nm	14
Addition of NH_4Cl buffer; reduction on Cd column; addition of sulphanilamide and N-(1-naphthyl) ethylenediamine dihydrochloride Calibrant: KNO_3 (purity ≥ 99.5 %) in water	SPEC of diazo compound at 540 nm	15

seven laboratories used spectrophotometric determination and the remainder used ion chromatography, with laboratory 05 using both.

The precision of the nitrate concentrations are presented in Table 2.9; calculated both from each single measurements performed in each laboratory, and from the mean values of each laboratory. The small difference between the two estimations of precision indicate that the variance among laboratories predominates over the variance of the single laboratories.

Table 2.9. Statistics of the certification measurements.

	No. Data	Mean	Std. Dev.	Variance	CV %
CRM 479 all data	106	214.1	7.43	55.20	3.5
CRM 479 means	16	213.6	7.08	50.13	3.3
Difference				5.08	
CRM 480 all data	96	887.2	25.97	674.44	2.9
CRM 480 means	15	886.0	20.15	406.02	2.3
Difference				268.42	

From Figures 2.14 and 2.15 it can be seen that the results from Plymouth University (Laboratory 15) overlap the certified mean for both CRM 479 and 480. The participants agreed that the content of nitrate in the CRM 479 could be certified on the basis of the results of Laboratories 01, 03, 05, 10, 11, 14, 15, and 17 (all spectrophotometric methods), and 02, 04, 05, 07, 09, 12, 13 and 16 (all ion chromatography methods). The value proposed for certification was 213.5 ± 3.9 μmol kg^{-1} compared with 210.6 ± 5.27 μmol kg^{-1} as determined by Plymouth University.

The contents of nitrate in the candidate CRM 480 could be certified on the basis of the results of Laboratories 01, 03, 05, 10, 11, 14, and 15 (all spectrophotometric methods), and 02, 04, 05, 07, 08, 09, 13 and 16 (all ion chromatography methods). The value certified was 886 ± 13 μmol kg^{-1} compared to 879.2 ± 11.23 μmol kg^{-1} as determined of the University of Plymouth.

2.6.3. Youden's Plot of BCR Intercomparison Data

Information on the type of errors associated with the measurements performed by each laboratory may be obtained by using Youden's plot. This procedure, used in collaborative studies, compares the results obtained on two solutions with different concentrations, analysed with the same analytical method. Results are plotted in a scatter diagram. Alternatively, the median values of the results can be used. The diagram is divided into four quadrants by the two straight lines representing the expected values for the two samples. In a hypothetical case, when the analysis is affected by random errors only, the results will be spread randomly over the four quadrants. However, the results are usually located in the lower left and upper right quadrant, forming a characteristic pattern along the 45° line passing through the expected values. This is due to systematic errors which underestimate or overestimate the concentration in both samples.

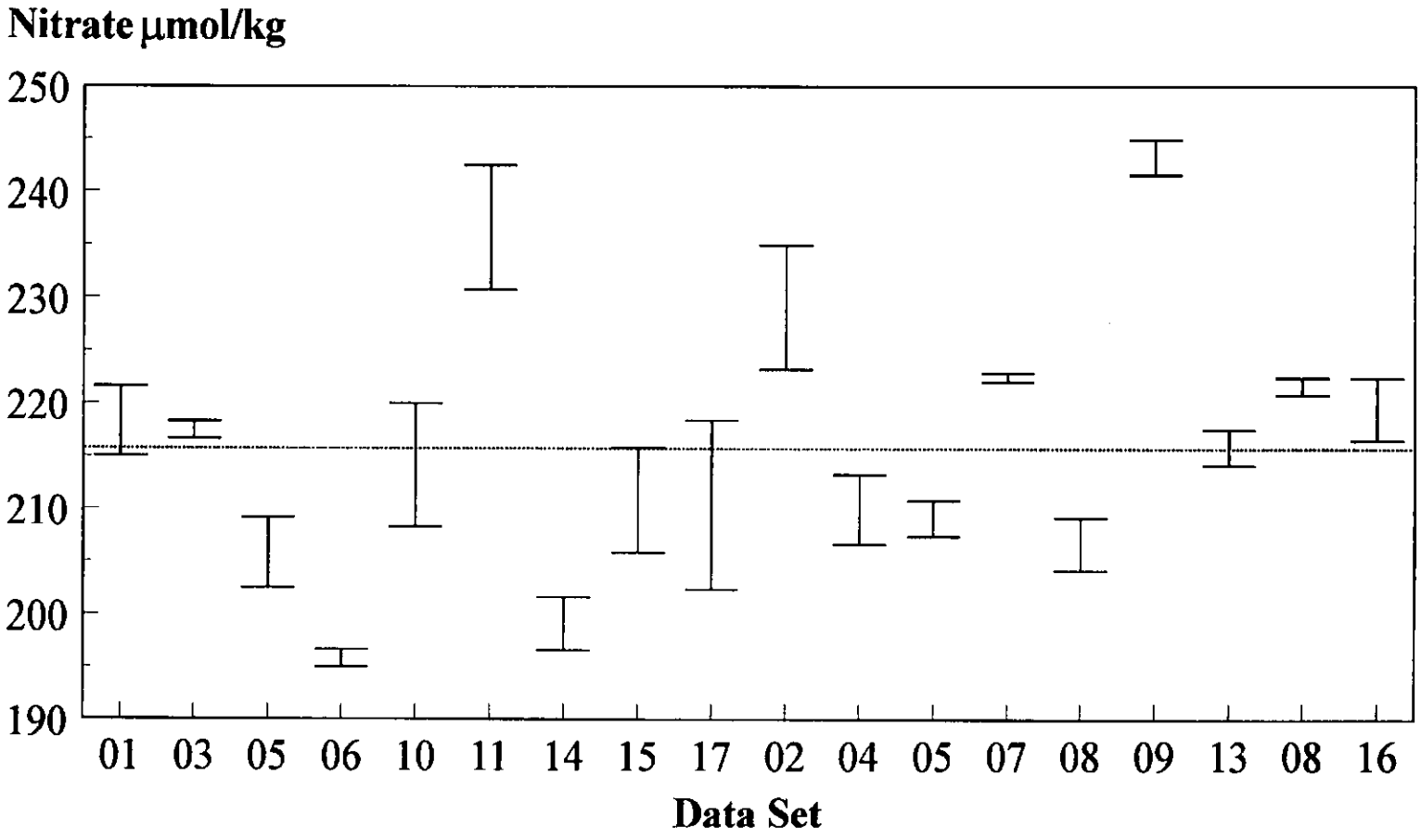

Figure 2.14. Data from the participating laboratories for the nitrate concentration of CRM 479. The Plymouth data is Lab. 15.

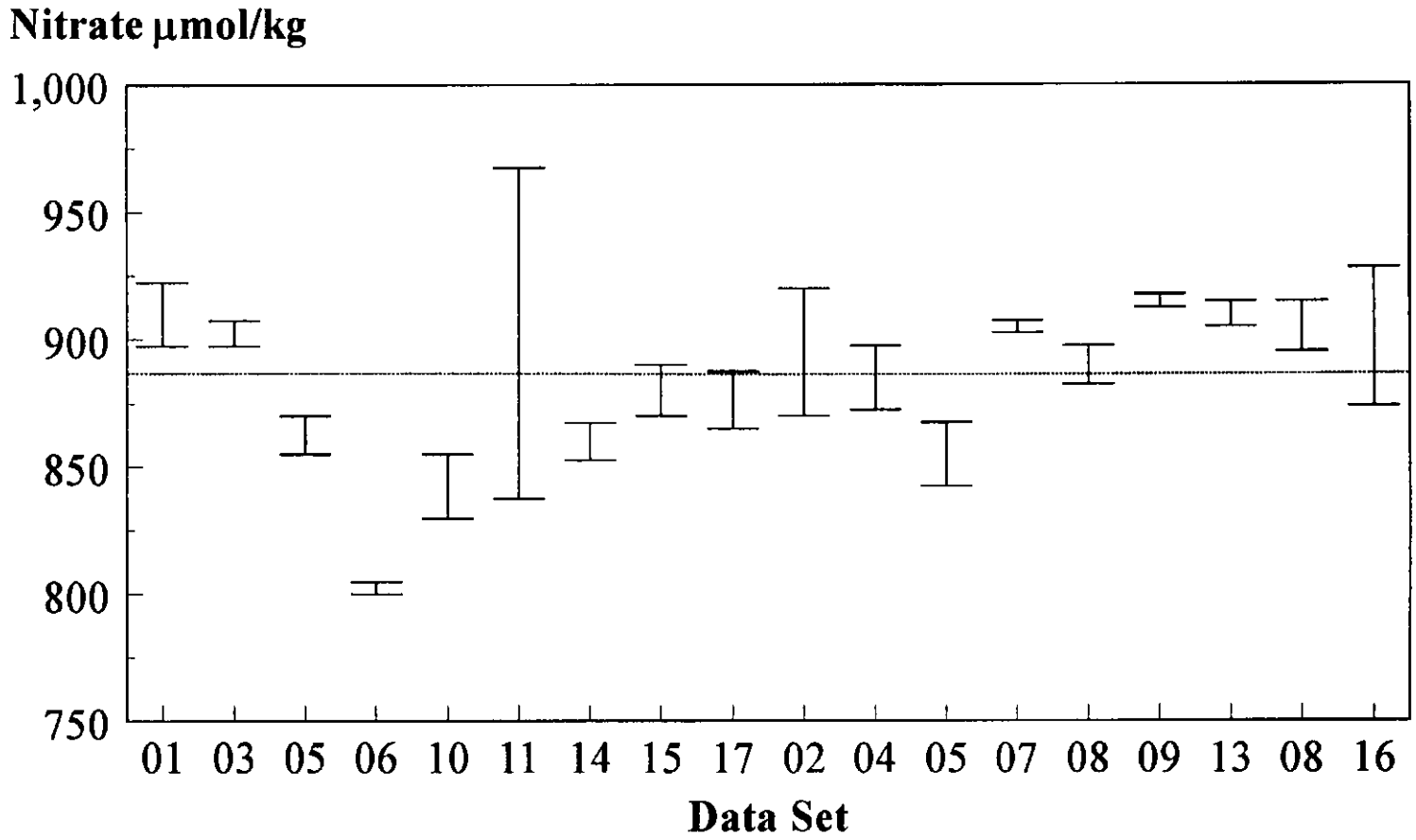

Figure 2.15. Data from the participating laboratories for the nitrate concentration of CRM 480. The Plymouth data is Lab. 15.

The Youden's graph (Figure 2.16) for nitrate in CRMs 479 and 480, obtained using the mean values of each laboratory, shows clear systematic errors, as 12 out of 14 data are located in the upper right and lower left quadrants. On the other hand, the plot does not reveal differences due to the two analytical methods used. The graph shows the University of Plymouth, slightly underestimated both CRM 479 (difference 2.9 μmol l^{-1}) and CRM 480 (difference 6.8 μmol l^{-1}), but the standard deviation limits for each reference material overlaps the centroid.

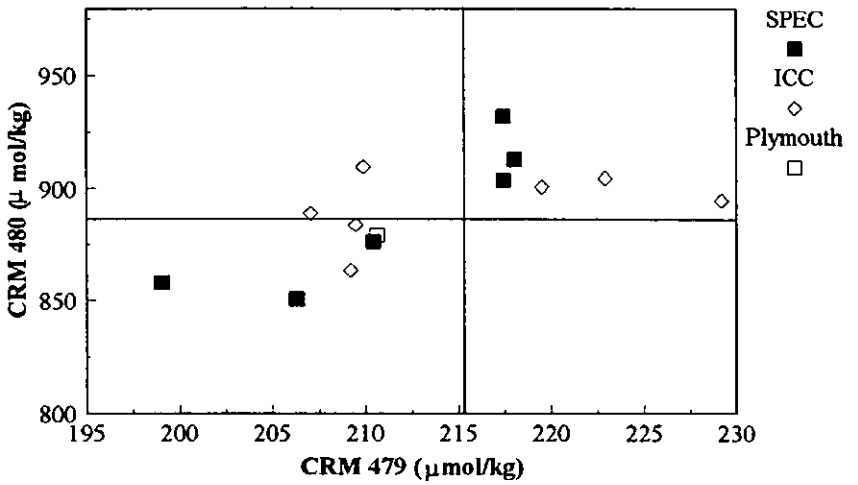

Figure 2.16. Youden plot for CRM 479 against CRM 480 analysed using spectrophotometry and ion chromatography.

2.6.4. The Fifth ICES Intercomparison Exercise for Nutrients in Sea Water (NUTS I/C 5)

In sea water studies the needs are increasing parallel to the development of international oceanic collaboration programs as well as environmental shelf sea monitoring. The GESREM (Group of Experts on Standards and Reference Material, co-sponsored by IOC, IAEA and UNEP) has clearly pointed out (UNESCO) [172, 173] the necessity of giving high priority to developing production of reference material for nutrients in sea water. The main source of nutrient variation in sea water is micro-organism activity. Therefore, production of a reference material for nutrients first depends on biological inactivity of

samples. Several other requirements must also be met, such as preventing potential enzymatic activity, keeping the natural matrix unchanged, avoiding interference in analytical methods, ensuring leakproof closure for long-term storage, using adequate container material with respect to exchanges with container walls (leaching/adsorption) and permeability to atmospheric contamination (nitrogeneous compounds) [174].

2.6.5. History of ICES Intercomparisons

The first intercalibration, including nutrients was carried out in the Baltic in 1965. Three ships met in Copenhagen with each contributing freshly collected bulk samples. Each ship then carried out the determination of oxygen, salinity, chlorinity, alkalinity and phosphate on board on the same day [175].

The second exercise [176], in 1966, involving the newly formed ICES Working Group on the Intercalibration of Chemical Methods took place in Leningrad with four ships determining the parameters as before, and in Copenhagen with the inclusion of further participants and the addition of nitrate, nitrite and silicate to the list of determinants. The nitrate and nitrite results at the time were not included in the report, it was during the early days of heterogeneous cadmium based nitrate/nitrite reduction techniques and some of the associated problems were presumably not fully appreciated at the time.

The third exercise took place in 1969/70 [177] and involved 45 laboratories from 20 countries. Nutrients were studied separately from oxygen, salinity, chlorinity and pH. Standard solutions were prepared and distributed in Japan and the participants carried out the analysis in their own laboratories. The overall accuracy, particularly for phosphate and nitrate, was disappointing.

It was not until 1988 that the fourth exercise took place as NUTS I/C 4 [178]. The test samples were natural making the exercise an intercomparison, participants were unaware that 'blank' samples were included and anonymity as in the third exercise was abolished. 69

laboratories from 22 countries submitted results. It was found that 58 laboratories were consistent in phosphate, 51 in nitrate and 48 in both phosphate and nitrate, including 12 whose results were especially close to the concentrations present.

The fifth exercise (NUTS I/C 5) began with distribution in 1993 and the intention was to include every laboratory anywhere that measures nutrients in sea water.

2.6.6. Analysis and Results

Three bottles were received from Ifremer, Brest, numbered 1, 2 and 3 containing nitrate and nitrite. The concentrations of the nutrients were assumed to be < 40 μmol l^{-1} for both nitrate and nitrite with salinities of 35.3 ± 0.1 ‰. No preservatives were to be added and the samples were to be stored in the dark at room temperature. The two parameters in each bottle were determined on the same day, as instructed, and to minimise the dissolution of glass by the sample the analyses were performed within three months of arrival.

Table 2.10 shows the results for Total Oxidised Nitrogen (TON, nitrate + nitrite) nitrate and nitrite for the three samples as determined by this laboratory. Table 2.11 shows the concentrations of nutrients believed to be in each sample. There is good correlation between the TON results, but the FI manifold (Figure 2.1) used does not have refractive index correction, so that the low level nitrate and nitrite levels were over estimated. Figures 2.17 and 2.18 show the results from all the 132 participating laboratories, as can been seen there is good distribution correlation for the three samples for TON and nitrite.

Table 2.10. Concentration of nutrients determined by the University of Plymouth.

LAB.	SAMPLE	$NO_3 + NO_2$ (μmol)	NO_2 (μmol)	NO_3 (μmol)
	1	10.48	1.57	8.91
118	2	2.05	1.48	0.57
	3	27.82	2.29	25.53

Table 2.11. Concentration of nutrients contained in samples 1, 2 and 3.

SAMPLE	$NO_3 + NO_2$ (μmol)	NO_2 (μmol)	NO_3 (μmol)
1	10.485	0.505	9.98
2	1.473	0.143	1.33
3	27.436	1.406	26.03

2.7. STABILITY TRIALS

2.7.1. Stability of Reagents and Standards

A necessary requirement for the deployment of an in situ or shipboard monitor incorporating the manifold shown in Figure 2.12 is that all the reagents and standards are stable for the duration of the deployment period. In this application the target unattended deployment time is 30 days.

A nitrate (100 mmol l^{-1}) stock standard and a mixed stock standard containing nitrate (100 mmol l^{-1} N), nitrite (10 mmol l^{-1} N), phosphate (20 mmol l^{-1} P) and silicate (100 mmol l^{-1} Si), were prepared in Milli-Q water. These nutrient concentrations in the mixed stock standard represent the concentration ratio found in sea water (10:1:2:10). Chloroform (0.1 % $^{v}/_{v}$) was added to both stock solutions as a preservative. Working standards containing 1, 20 and 50 μmol l^{-1} NO_3-N were prepared from both the nitrate and mixed stock standards and left at ambient temperature throughout a 40 day period over which the standards were analysed. The laboratory temperature ranged from 14 to 25 °C during this period, thus providing a reasonable indication of stability for in situ deployment.

Figures 2.19 and 2.20 show the result of using glassware as supplied. The response decreases markedly after 15 days for all standards, for the 50 μmol l^{-1} NO_3-N standard, the signal decreases by 40 % in 30 days. Therefore a rigorous cleaning protocol was developed

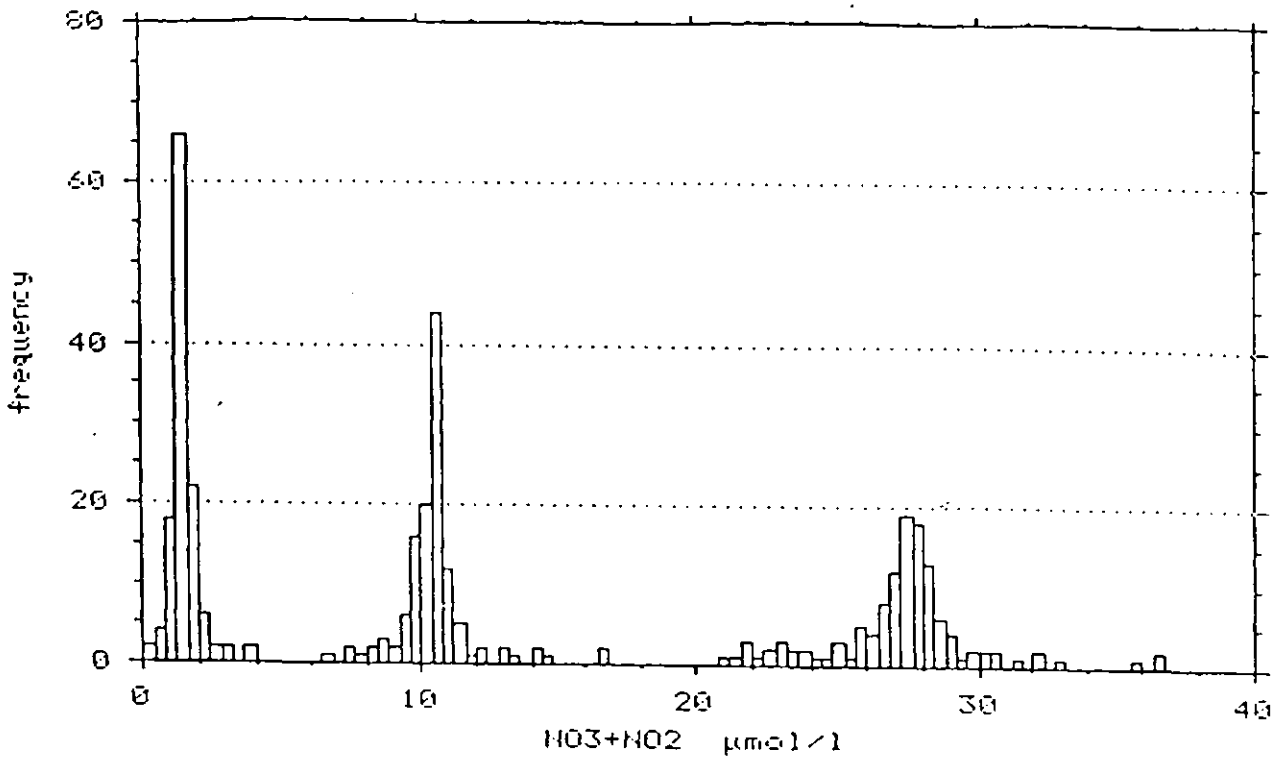

Figure 2.17. Histogram of TON results from the 132 laboratories participating in 'NUTS I/C 5'

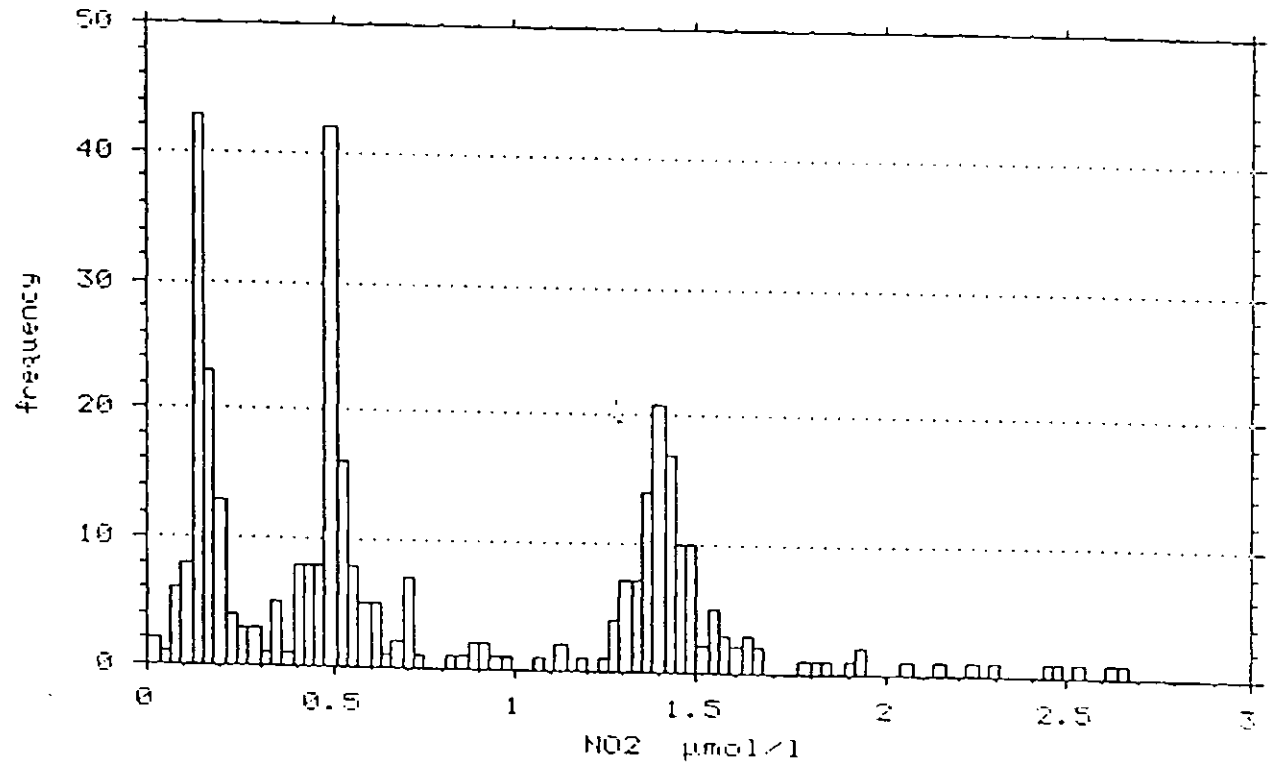

Figure 2.18. Histogram of nitrite results from the 132 laboratories participating in 'NUTS I/C 5'

for all glassware in order to minimise contamination and microbial growth. Hence, all glassware was first soaked in Decon 90 for 2 days, washed with hydrochloric acid (10 %) and Milli-Q water and oven dried (110 °C). Figures 2.21 and 2.22 show a repeat of the experiment after thorough washing of the glassware. There was no significant reduction in response over 40 days, even in the presence of other nutrient species, and that after more than 700 injections the copperised-cadmium column retained its efficiency. The small absorbance changes observed were due to fluctuations in the ambient temperature (Figure 2.23), and hence in reaction rate, over the 40 day period. This does not affect accuracy providing that frequent calibration is used.

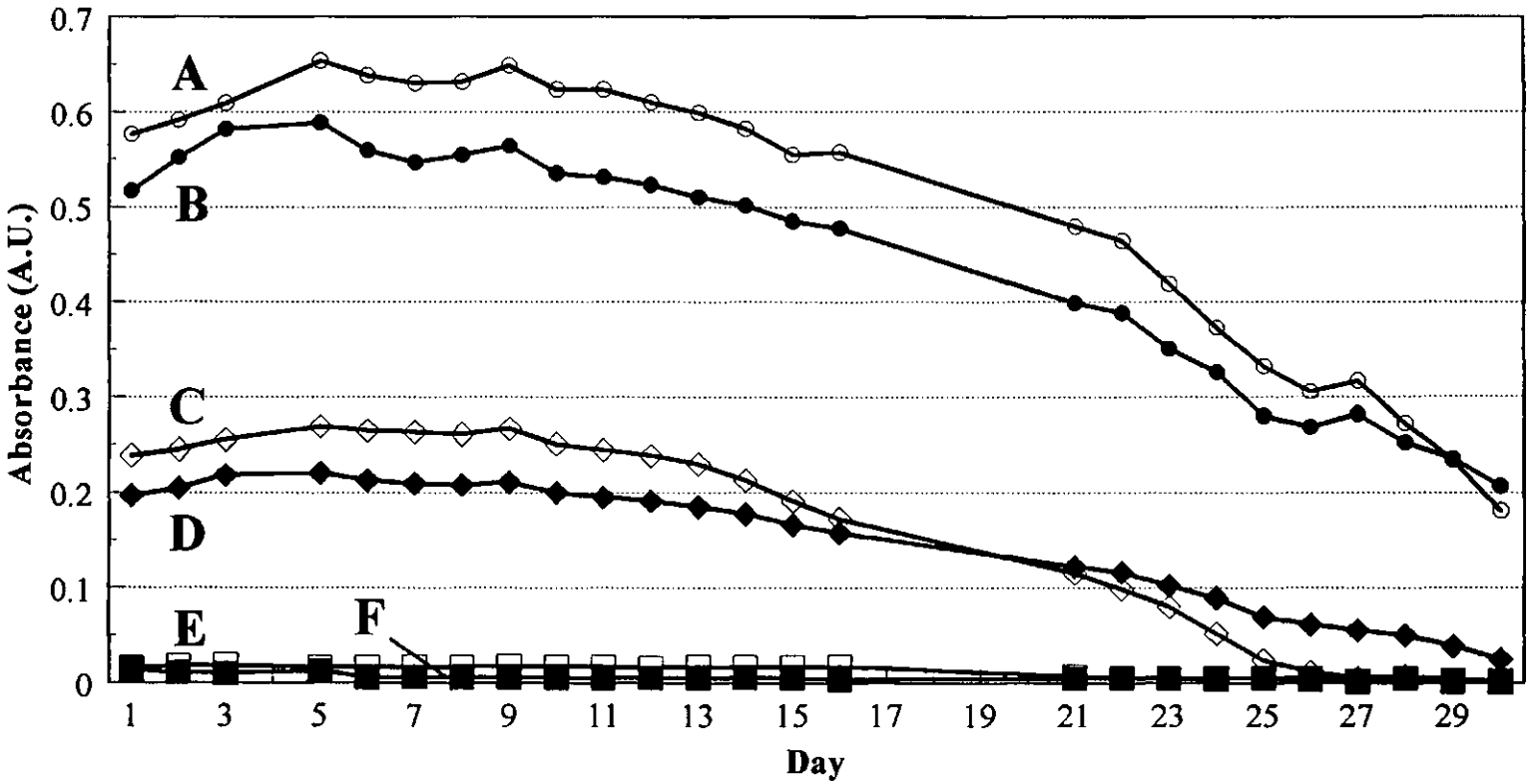

Figure 2.19. Stability of response for a standard and a mixed standard (containing NO_3-N. NO_2-N, PO_4-P and Si) over 30 days. Concentrations are: A, 50 μmol l^{-1} NO_3-N + 5 μmol l^{-1} NO_2-N; B, 50 μmol l^{-1} NO_3-N; C, 20 μmol l^{-1} NO_3-N + 2 μmol l^{-1} NO_2-N; D, 20 μmol l^{-1} NO_3-N; E, 1 μmol l^{-1} NO_3-N + 0.1 μmol l^{-1} NO_2-N; F, 1 μmol l^{-1} NO_3-N.

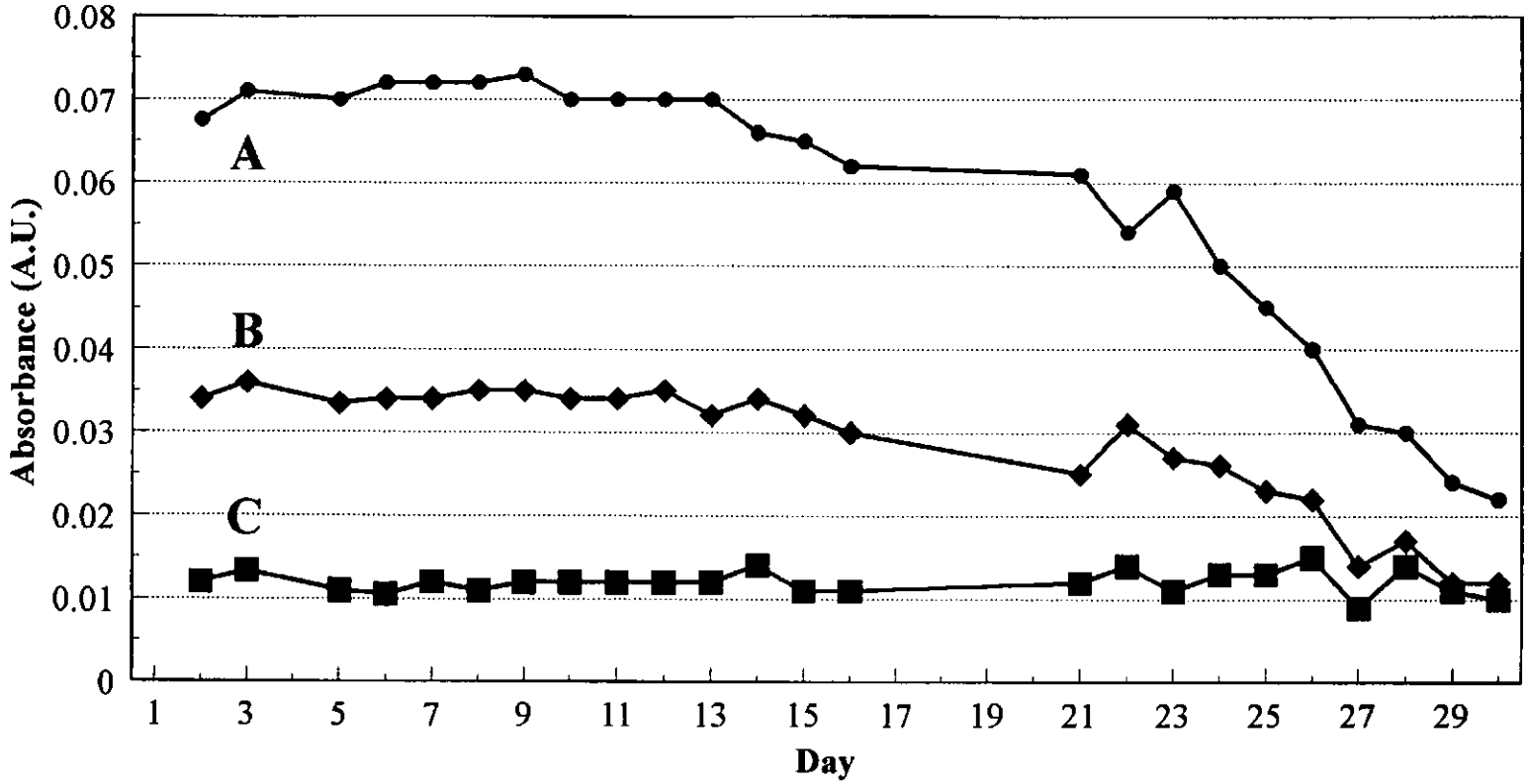

Figure 2.20. Stability of response for a standard and a mixed standard (containing NO_3-N. NO_2-N, PO_4-P and Si) over 30 days. Concentrations are: A, 5 μmol l^{-1} NO_2-N; B, 2 μmol l^{-1} NO_2-N; C, 0.1 μmol l^{-1} NO_2-N.

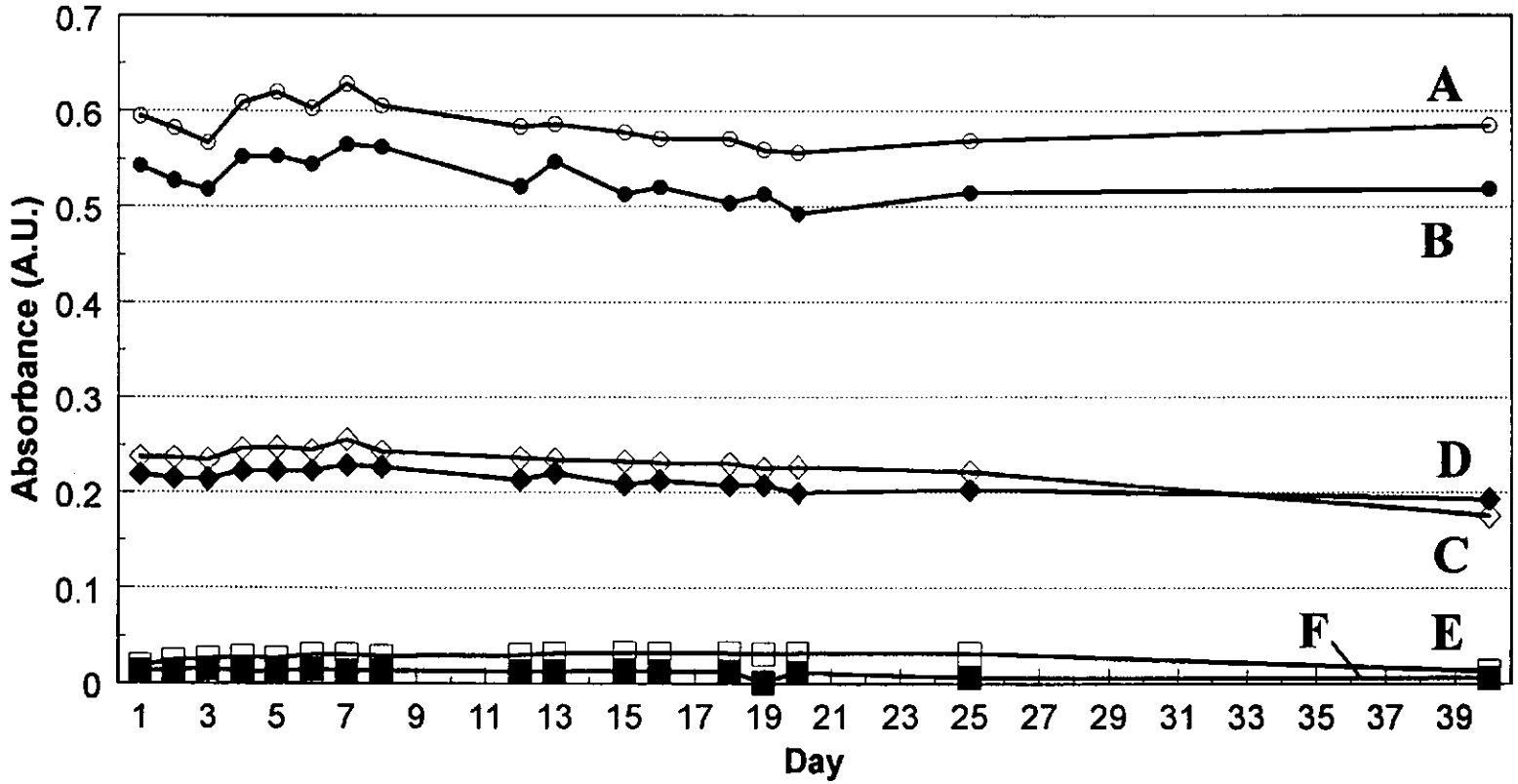

Figure 2.21. Stability of response for a standard and a mixed standard (containing NO_3-N. NO_2-N, PO_4-P and Si) over 40 days. Concentrations are: A, 50 μmol l^{-1} NO_3-N + 5 μmol l^{-1} NO_2-N; B, 50 μmol l^{-1} NO_3-N; C, 20 μmol l^{-1} NO_3-N + 2 μmol l^{-1} NO_2-N; D, 20 μmol l^{-1} NO_3-N; E, 1 μmol l^{-1} NO_3-N + 0.1 μmol l^{-1} NO_2-N; F, 1 μmol l^{-1} NO_3-N.

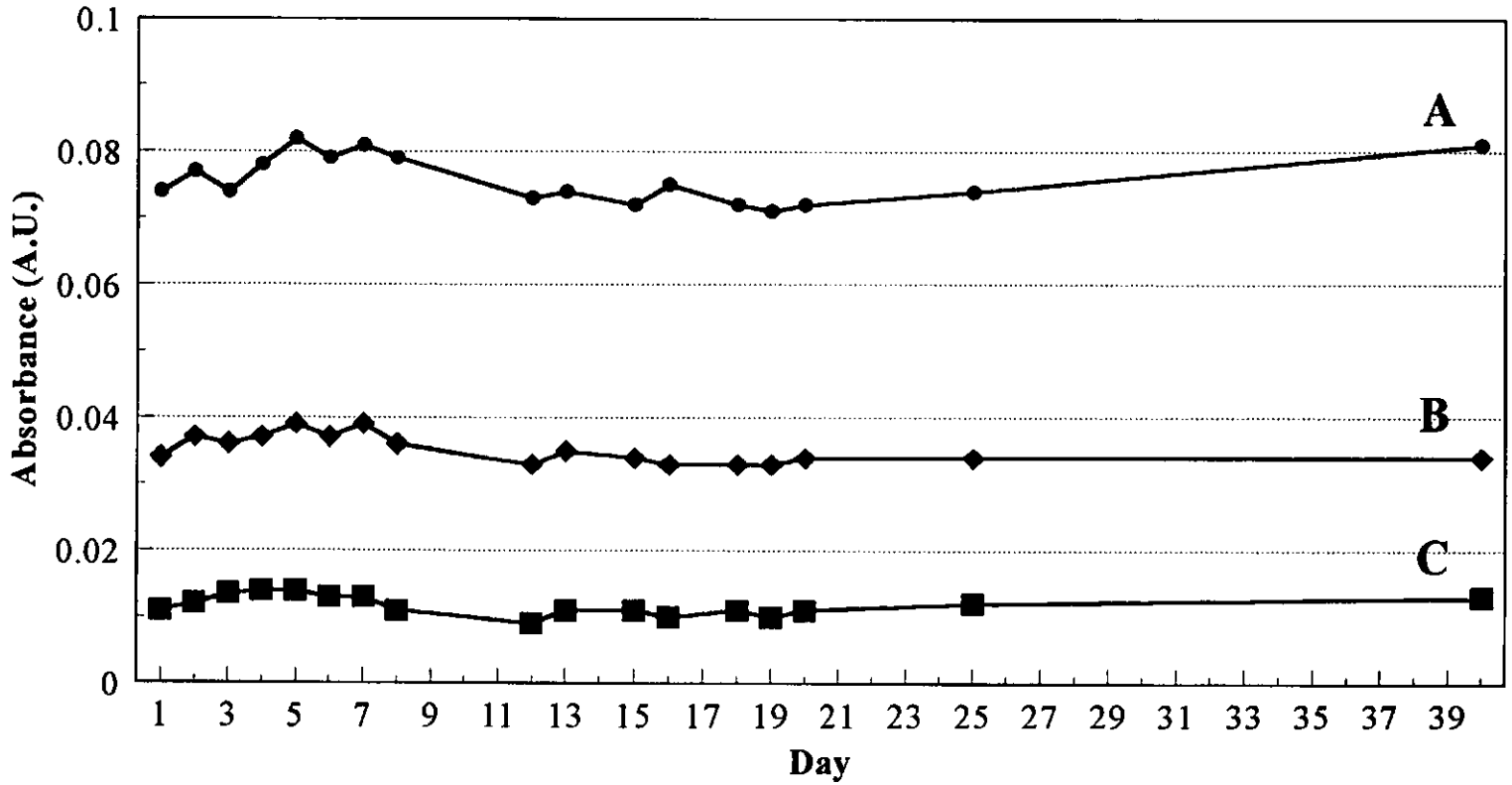

Figure 2.22. Stability of response for a standard and a mixed standard (containing NO_3-N. NO_2-N, PO_4-P and Si) over 40 days. Concentrations are: A, 5 μmol l^{-1} NO_2-N; B, 2 μmol l^{-1} NO_2-N; C, 0.1 μmol l^{-1} NO_2-N.

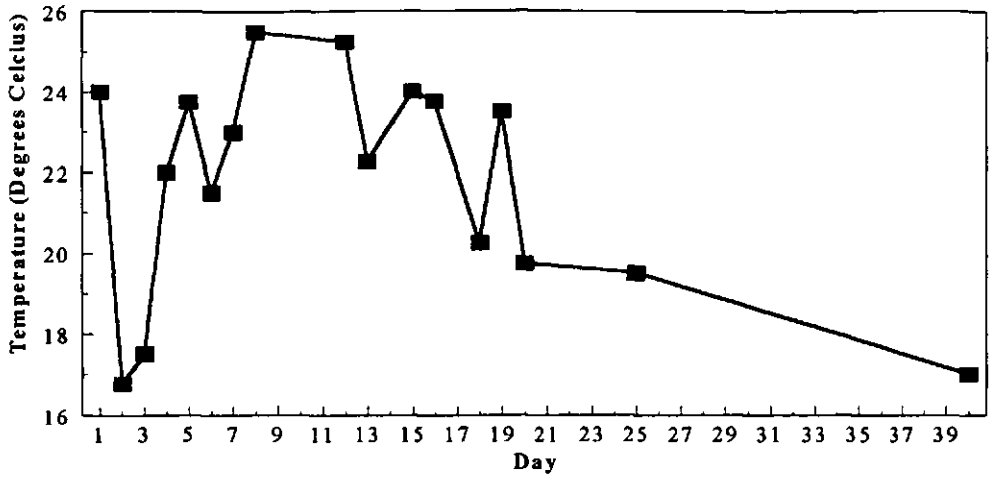

Figure 2.23. Room temperature at time of analysis during the stability trial over 40 days.

2.8. CONCLUSIONS

1. The optimised FI method is applicable to the determination of nitrate in samples of varying salinity (0 - 35 ‰).
2. The method achieves the limit of detection (0.1 μmol l^{-1} NO_3-N) and linear range (0.1 - 73 μmol l^{-1}) required for monitoring nitrate in estuarine, coastal and sea waters.
3. The reagents, cadmium reduction column and standards are stable for at least 40 days provided a glassware cleaning protocol of soaking in Decon 90 for 2 days followed by washing with hydrochloric acid (10 %) and Milli-Q water and oven drying (110 °C) is used.

Chapter Three
Determination of Orthophosphate

3. DETERMINATION OF ORTHOPHOSPHATE

3.1. INTRODUCTION

This chapter compares the analytical merits of rFI and FI methods, using ascorbic acid and tin(II) chloride as the reducing agents, for the determination of phosphate in riverine, coastal and oceanic waters. Investigations are made in order to increase the sensitivity of the methods and overcome both the high phosphate blank and salt error.

3.2. EXPERIMENTAL

3.2.1. Reagents and Standards

All glassware was cleaned by soaking in phosphate free detergent (Decon 90), then in 10 % $^{v}/_{v}$ sulphuric acid and rinsing in deionised water. All solutions were prepared from ultra-pure-deionised water supplied by a Milli-Q system (Millipore Corp.) and all reagents were AnalaR® (BDH). A stock phosphate solution (100 mg l^{-1}, PO_4-P) was prepared by dissolving potassium dihydrogen orthophosphate (0.4390 g) in 1 l of water. All reagents were stored in brown glass bottles.

rFI manifold. The acid molybdate reagent was prepared by dissolving ammonium heptamolybdate (5 g) and antimony potassium tartrate (0.1 g) in 1 l nitric acid (0.4 M, 69 % $^{v}/_{v}$). The L-ascorbic acid (10 g) was dissolved in 1 l of glycerol solution (10 % $^{m}/_{v}$).

FI manifold. The acid molybdate reagent was prepared by dissolving ammonium heptamolybdate (5 g) and antimony potassium tartrate (0.1 g) in 1 l nitric acid (0.4 M, 69 % $^{v}/_{v}$). The L-ascorbic acid (10 g) was dissolved in 1 l of glycerol solution (10 %, $^{m}/_{v}$).

Tin(II) chloride manifold. The acid molybdate reagent was prepared by dissolving ammonium heptamolybdate (10 g) in sulphuric acid (0.6 M). Tin(II) chloride-2-hydrate (0.2 g) and hydrazinium sulphate (2 g) were dissolved in 1 l of sulphuric acid (0.3 M).

Salinity compensation manifold. The acid molybdate reagent was prepared by dissolving ammonium heptamolybdate (10 g) in 1 l of sulphuric acid (0.3 M). Tin(II) chloride-2 hydrate (0.2 g) and hydrazinium sulphate (2 g) were dissolved in 1 l sulphuric acid (0.2 M). The sodium chloride (6 %) was dissolved in 1 l of water.

3.2.2. Instrumentation and Procedures

Peristaltic pumps (Ismatec Mini-S 820) and flexible modified PVC pump tubing (Anachem) were used to propel all solutions through PTFE tubing (0.8 mm i.d.). Sample and reagent injections were made using 6-port rotary injection valves (Rheodyne). All absorbance measurements were taken at 660 nm using a LKB Biochrom Ultrospec II 4050 UV/VIS spectrophotometer containing a 10 mm (18 μl) path length flow cell (Hellma). Most methods using ascorbic acid as the reductant for the determination of phosphate use a λ_{max} of 880 nm. For in situ monitoring, LEDs are used as sources for photometric detectors due to their small size and low power consumption. A constraint in the use of LEDs however, is the limited spectral range covered by such devices in the UV/VIS region [147]; only red (λ_{max} = 650 nm), orange (λ_{max} = 620 nm), yellow (λ_{max} = 583 nm), green (λ_{max} = 565 nm) and blue (λ_{max} = 470 nm) LEDs having band widths of 30 - 40 nm, are readily available. Therefore, 660 nm was used as the detection wavelength in this work in order to be compatible with the potential use of a red LED as the light source for an in situ phosphate monitor [144, 149].

rFI manifold. A schematic of the manifold used is shown in Figure 3.1. The acid molybdate (0.8 ml min^{-1}) and ascorbic acid (0.8 ml min^{-1}) streams were merged and injected

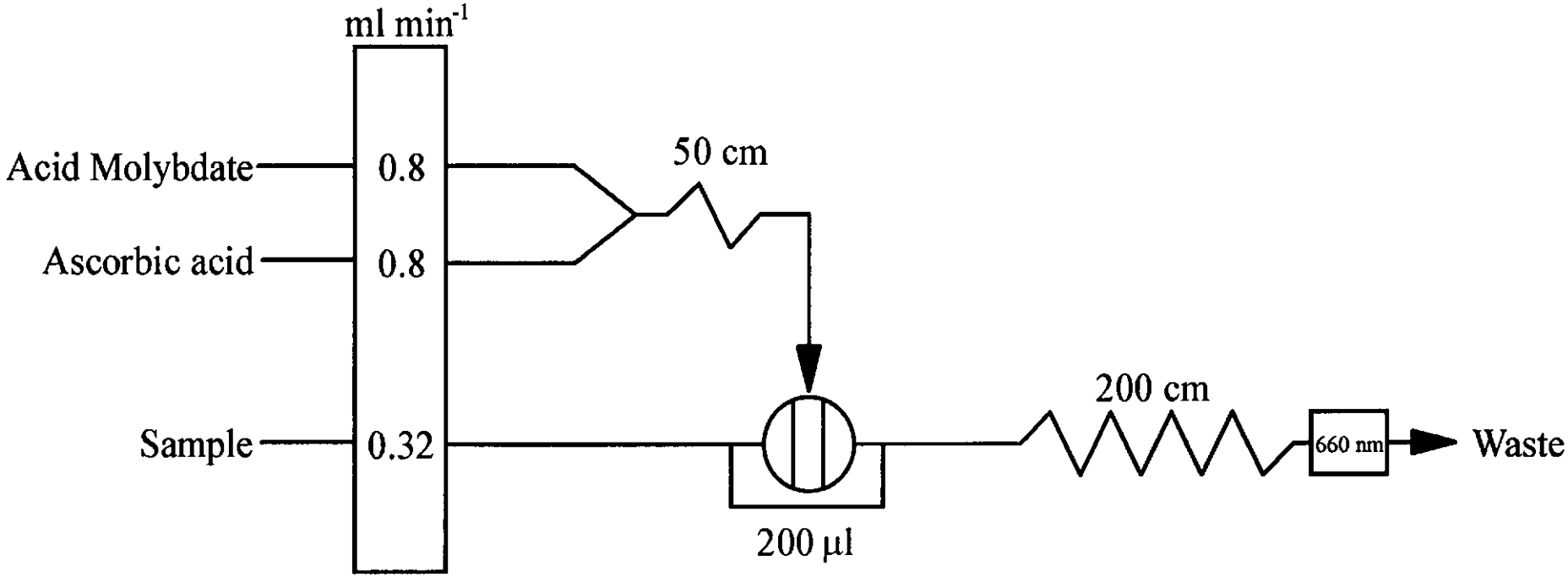

Figure 3.1. rFI manifold for the determination of orthophosphate with ascorbic acid as the reductant

(200 µl) into a sample or phosphate standard stream (0.32 ml min^{-1}) and mixed in a 200 cm reaction coil.

FI manifold. The manifold used is shown in Figure 3.2. The standards and samples (300 µl) were injected into a Milli-Q water stream (0.6 ml min^{-1}) and transported to a T piece via a 30 cm mixing coil. Acid molybdate (0.6 ml min^{-1}) and ascorbic acid (0.23 ml min^{-1}) was added at this point and the sample zone transported to the detector via a 100 cm reaction coil.

Tin(II) chloride manifold. Figure 3.3 shows the schematic of the manifold used. The standards and samples (200 µl) were injected into a Milli-Q water stream (0.6 ml min^{-1}) and transported to a T piece via a 30 cm mixing coil. Acid molybdate (0.23 ml min^{-1}) was added at this point and after another 30 cm reaction coil a tin(II) chloride stream (0.16 ml min^{-1}) was added and the sample zone transported to the detector via a 60 cm reaction coil.

Salinity compensation manifold. The manifold used is shown in Figure 3.4. The acid molybdate was injected (200 µl) into a sample or standard stream (1.2 ml min^{-1}) and mixed in a 60 cm coil, sodium chloride (2.0 ml min^{-1}) and tin(II) chloride (2.0 ml min^{-1}) streams were introduced and mixed in a 30 cm reaction coil.

3.3. RESULTS AND DISCUSSION

The majority of methods currently used for the determination of orthophosphate in sea water are based on the formation of 12-molybdophosphoric acid (Mo(VI)) and its subsequent reduction to a phosphomolybdenum blue complex, the absorbance of which is measured at a suitable wavelength (typically 660 nm or 880 nm).

$$PO_4^{3-} + 12MoO_4^{2-} + 27H^+ \longrightarrow \underset{\text{12-phosphomolybdic acid}}{H_3PO_4(MoO_3)_{12}} + 12H_2O$$

$$H_3PO_4(MoO_3)_{12} \xrightarrow{\text{Reductant}} \text{Phosphomolybdenum blue}$$

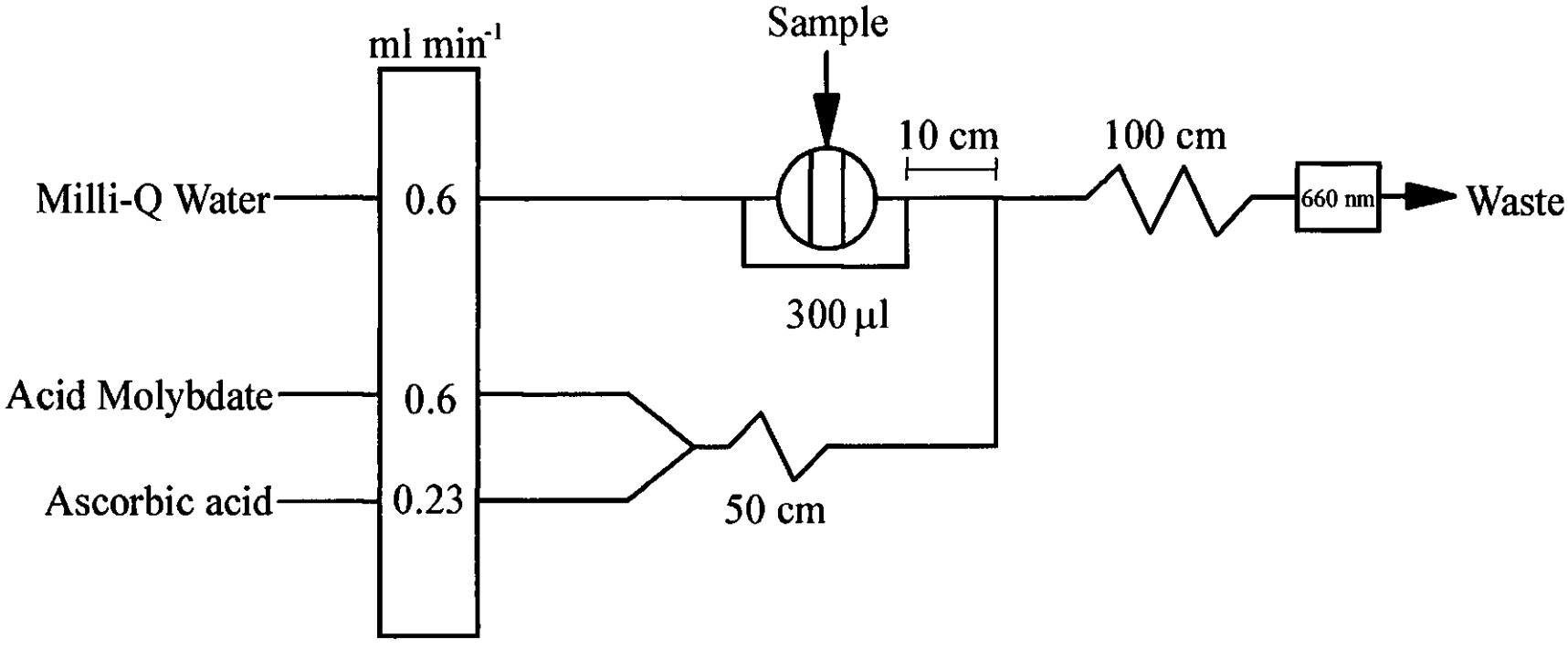

Figure 3.2. FI manifold for the determination of orthophosphate with ascorbic acid as the reductant

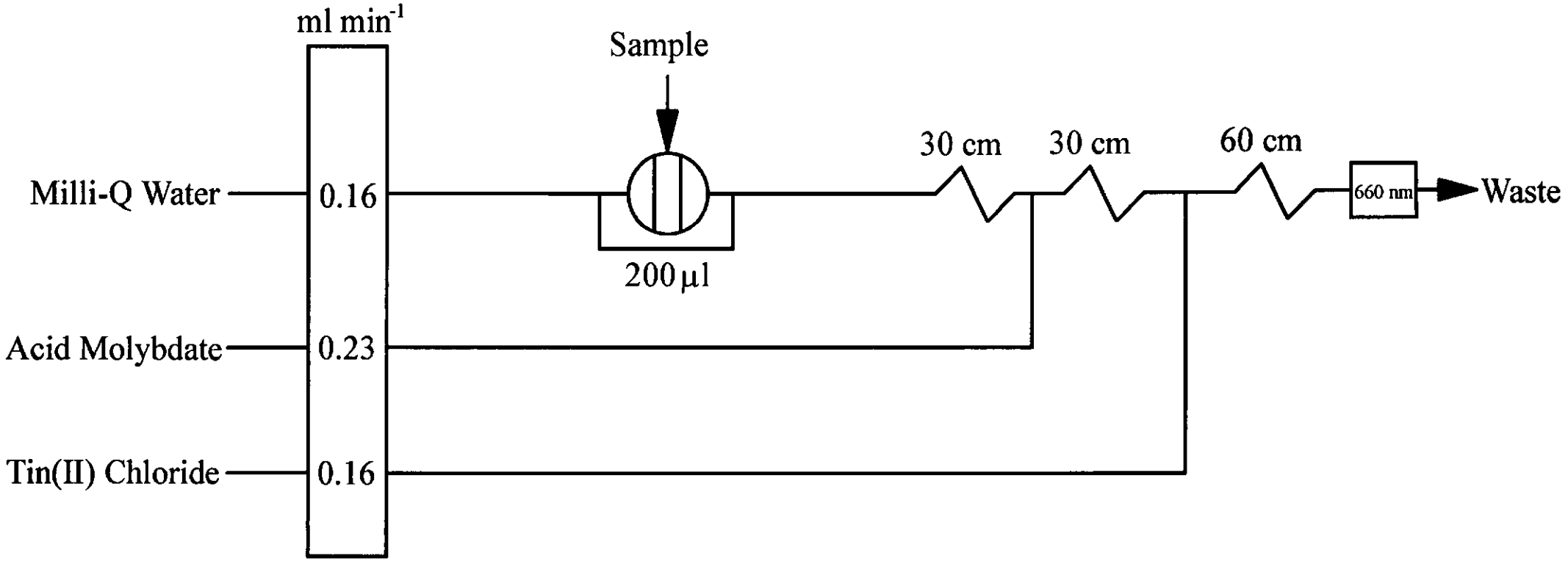

Figure 3.3. FI manifold for the determination of orthophosphate with tin(II) chloride as the reductant

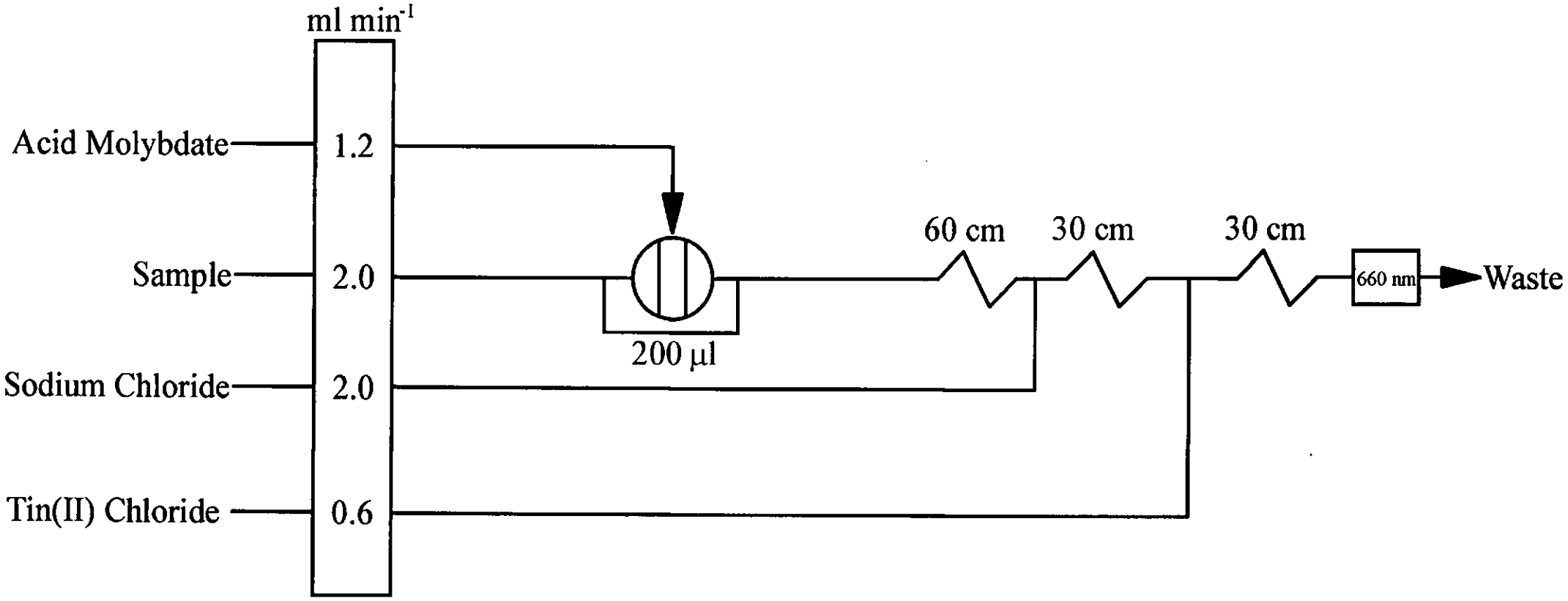

Figure 3.4. Salinity compensation manifold for the determination of orthophosphate with tin(II) chloride as the reductant

Although several reducing agents are capable of bringing about this reduction, relatively few produce a molybdenum blue complex having a sufficiently high molar absorptivity to permit them to be used for the determination of phosphate at sea water levels i.e. sub nM. The most frequently used reductants are therefore tin(II) chloride and ascorbic acid. The methods using tin(II) chloride suffer from a number of disadvantages, including the instability of the colour, the dependence of the rate of reduction on temperature and salinity, and the salt error. The use of ascorbic acid as a reductant in the determination of orthophosphate in sea water was first suggested by Greenfield and Kalber [179]. Their technique was subsequently modified by Murphy and Riley [180] to produce a single solution method which was free from most of the difficulties associated with the use of tin(II) chloride. However, because colour development was slow, Murphy and Riley [96] modified their procedure by adding antimony(III) to the molybdate reagent. Johnson and Petty [106] showed that using antimony-ascorbic acid in a flow injection manifold at room temperature the extent of reaction was less than 10 %, even with residence times in the reaction tube of several minutes. An extent of reaction greater than 90 % was obtained within 15 s when 80 cm of a 1 m tube was placed in a water bath at 50 °C but, the need to incorporate a heater into the system is disadvantageous because raising the temperature increases the rate of reaction of silicate with the molybdate reagent [181, 182]. It is also unsuitable for in situ monitoring as it is an added power drain on the system. The reaction is thought to involve the formation of a mixture of two isomeric heteropoly acids. Chalmers [183] showed that 12-phosphomolybdic acid exists in an unstable β-form which is produced when deca- or dodeca-molybdate ion is the principle molybdate species in the solution. This isomer undergoes spontaneous transformation to the α-form. The α-form is also produced directly from phosphate when the reacting species is the octa-molybdate ion. It is essential that the acidity and molybdate concentration in the solution are carefully controlled since these, together with the $[H^+]$:$[MoO_4^{2-}]$ ratio, control the species of molybdate present [184].

Examination of the literature reveals that a wide range of concentrations of molybdate, pH, antimony and reductants are used, as shown in Table 3.1. Drummond and Maher [110] studied the conditions under which the phosphoantimonylmolybdenum blue species is formed. Optimum colour formation was found to occur at $[H^+]:[MoO_4^{2-}]$ ratios between 50:1 and 80:1 and at pH values between 0.36 - 1.06. Conditions above a $[H^+]:[MoO_4^{2-}]$ ratio of 80:1 result in incomplete colour formation, whereas below a ratio of 50:1 the molybdate undergoes self-reduction even in the absence of phosphate.

Table 3.1. Variations in final reagent concentrations using the molybdenum blue method.

pH	H^+ (mM)	MoO_4^{2-} (mM)	$H^+:MoO_4^{2-}$	Sb(III) (mM)	Ascorbic Acid (mM)	Reference
-0.03	1080	11.2	71.4	-	11.4	185
0.4	400	5.46	73.3	0.07	5	101
0.4	400	5.46	73.3	0.32	23	186
0.22	600	9.59	70 ±10	0.82	2.3	111
0.4	400	5.44	73.5	0.04	5.7	187
0.5	300	4.1	73.5	-	-	188
0.4	400	5.6	73.3	0.06	0.4	189
0.7	200	2.61	76.6	0.054	10.7	24

Doubts also exists over the specificity of the reaction using antimony-ascorbic acid as the reductant because a number of such methods have been shown to overestimate phosphate concentrations. In biological materials, hydrolysis of labile organic and condensed phosphorus compounds is observed when using antimony-ascorbic acid [99, 103, 104]. These labile compounds are of two types, namely organic and inorganic phosphates that hydrolyse by splitting P-O-P links, and phosphate esters of aldehydes or ketones that hydrolyse by splitting C-O-P links. Adenosine triphosphate, for example, has two labile phosphorus atoms, and therefore interferes in the determination of phosphate [186]. Any

chemical species capable of forming heteropoly blue compounds can interfere, particularly silicate and arsenate, but such interference only occurs at concentrations many times higher than those typically found in coastal and oceanic waters [101, 190]. The molybdosilicate complex exists in two forms depending on pH. The α isomer is formed at pH 3.5 - 4.5 whereas the β isomer is formed more rapidly in the pH range 0.8 - 2.5 [24]. But, at room temperature and with the high $[H^+]:[MoO_4^{2-}]$ ratio used for the determination of phosphate the formation of the silicomolybdenum blue is inhibited. Fluoride concentrations greater than 20 mg l^{-1} F result in slower colour development of phosphoantimonylmolybdenum blue, but fluoride is usually found at concentrations of 1 - 2 mg l^{-1} in ocean water and therefore it is not a significant interference when analysing these waters for orthophosphate content.

3.3.1. rFI Manifold.

In normal FI the solution containing the determinand is injected into an inert eluent, or into an eluent containing an excess of reagent, and is determined either directly or as a derivative. Johnson and Petty [106] were the first to introduce reverse flow injection (rFI) as a technique, where the roles of sample and carrier are reversed, a fixed volume of reagent solution being injected into a sample carrier stream. They determined phosphate by injecting a molybdate reagent into a sample carrier stream and monitoring the 12-molybdophosphate formed by visible spectrophotometry. The rFI method was found to be five times more sensitive than the FI method described by Ruzicka and Hansen [129] because phosphate is determined with very little dilution in rFI. The main advantages of rFI are that it is economical in terms of reagent consumption (particularly useful when the reagents are expensive and/or hazardous), it generates less waste than FI and it is possible to make several different determinations on the same sample solution stream, by the sequential injection of different reagents. The only requirement is that there needs to be

sufficient sample which is generally not a problem when analysing natural waters. The rFI signals are different in shape to conventional FI signals [191]. In FI the product is initially formed at the extremities of the sample zone and, with sufficient dispersion, the reagent also mixes with the centre of the sample zone and the result is a transient peak with a sharp rising edge and a more gradual decay. With rFI the sample is initially present in infinite supply as the carrier stream. The equivalent concentration of sample throughout the reagent zone increases from zero to a value approaching that in the carrier stream. Whether this sample is converted completely into product, however, depends on whether the reagent concentration remains sufficiently high and also whether there is sufficient time for the reaction to go to completion. Clearly, the reagent is injected at as high a concentration as possible but is diluted rapidly during dispersion and its concentration eventually becomes limiting. If the determinand is fully formed throughout the reagent zone under conditions of high dispersion, the signal will be rectangular in shape, i.e. a steep-sided flat-topped peak. With slightly less dispersion, the equivalent determinand concentration at the extremities of the bolus will be very close to that in the carrier stream but in the centre it will be lower. Hence the predicted shape at this lower dispersion is a hollow-topped peak. At even lower dispersions a double peak would be expected.

3.3.2. Univariate Optimisation of Reagent Concentrations for the rFI Manifold

A univariate optimisation was carried out on the reagent concentrations of ammonium heptamolybdate and ascorbic acid using the manifold shown in Figure 3.1. In order to achieve the best signal to blank ratio, absorbance of 1 mg l^{-1} and 0 mg l^{-1} PO_4-P standards were measured and compared. Figure 3.5 shows the results of the univariate optimisation of molybdate in 0.4 M nitric acid over the range 0.5 - 10 g l^{-1}. An ascorbic acid concentration of 10 g l^{-1} was used for all experiments. As the availability of molybdate was increased from 0.5 to 10 g l^{-1}, the absorbance increased by 0.159 AU with the 1 mg l^{-1} PO_4-

P standard. But, the absorbance signal for the blank does not change significantly with increased molybdate concentration. For further work a molybdate concentration of 5 g l^{-1} was used, as at this concentration the best signal to blank ratio was achieved.

The effect of ascorbic acid concentration was studied in the range 0.5 - 70 g l^{-1} with 1 mg l^{-1} and 0 mg l^{-1} PO_4-P standards and a molybdate concentration of 5.0 g l^{-1} in 0.4 M nitric acid and the results are shown in Figure 3.6. As the ascorbic acid concentration increased the absorbance signal increased due to the increased rate of reaction. Further addition of

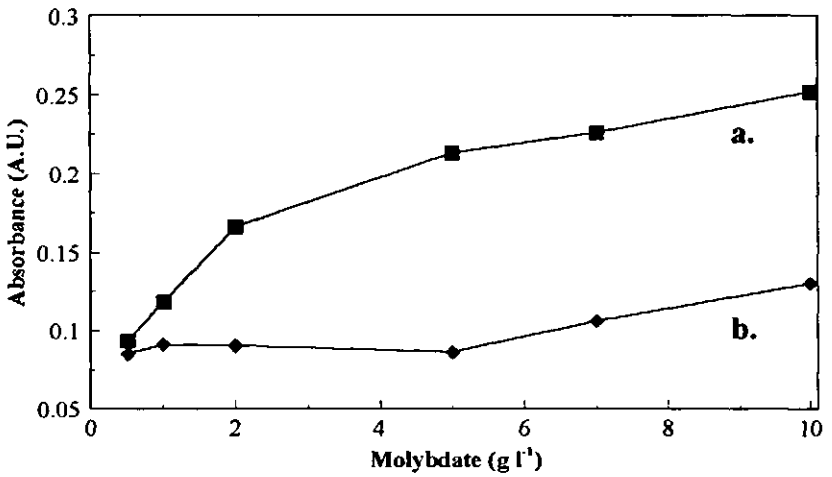

Figure 3.5. Univariate optimisation of molybdate concentration with; a. 1 mg l^{-1} and b. 0 mg l^{-1} PO_4-P.

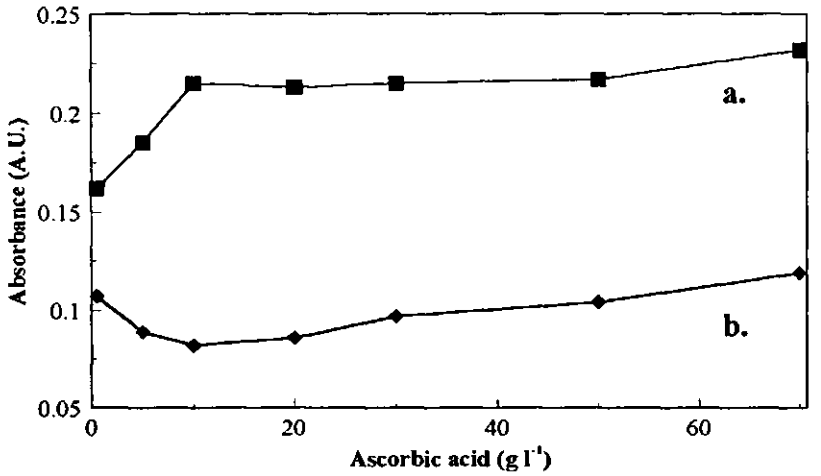

Figure 3.6. Univariate optimisation of ascorbic acid concentration with; a. 1 mg l^{-1} and b. 0 mg l^{-1} PO_4-P.

ascorbic acid above 10 g l^{-1} did not increase the rate of reaction, therefore the absorbance signal remained constant above this concentration of reductant. The absorbance of the blank remained relatively constant with varying ascorbic acid concentration. A 10.0 g l^{-1}

ascorbic acid concentration was used for further work in order to achieve the best signal to blank ratio and reaction kinetics.

3.3.3. Simplex Optimisation of the rFI Manifold

A simplex optimisation, as described in section 2.4, was carried out using the rFI manifold shown in Figure 3.1. The key variables for maximising the absorbance signal were considered to be the flow rates of the molybdate, ascorbic acid and sample streams, the sample loop volume and the reaction coil length. The starting conditions, range, step size and precision for each variable are shown in Table 3.2. The reagent concentrations used in the simplex experiments were as previously optimised i.e. 5.0 g l^{-1} molybdate in nitric acid (0.4 M) and 10.0 g l^{-1} ascorbic acid. Due to the high blank signal with this method the absorbance difference between 1 mg l^{-1} and 0 mg l^{-1} PO_4-P standards at the FI peak maximum, measured at 660 nm, was used as the response surface during the optimisation procedures in order to maximise the sample to blank ratio. Table 3.3 shows the variable conditions for each simplex experiment and Figure 3.7 shows the simplex history in terms of the response.

Table 3.2. Conditions used for simplex optimisation.

VARIABLE	UNITS	RANGE	STEP SIZE	PRECISION	STARTING CONDITIONS
Injected Reagent Volume	µl	25 - 300	10	5	200
Molybdate Flow Rate	ml min^{-1}	0.16 - 1.0	0.1	0.1	0.6
Ascorbic Flow Rate	ml min^{-1}	0.16 - 1.0	0.1	0.1	0.6
Sample Flow Rate	ml min^{-1}	0.16 - 1.0	0.1	0.1	0.23
Reaction Coil Length	cm	50 - 300	25	10	50

Table 3.3. Simplex history for each variable.

EXPERIMENT NUMBER	INJECTED REAGENT VOLUME (µl)	MOLYBDATE FLOW RATE (ml min^{-1})	ASCORBIC FLOW RATE (ml min^{-1})	SAMPLE FLOW RATE (ml min^{-1})	REACTION COIL (cm)	RESPONSE (AU)
1	200	0.6	0.6	0.23	50	0.174
2	200	1.0	0.6	0.23	50	0.158
3	200	0.8	1.0	0.23	50	0.176
4	200	0.8	0.8	0.6	50	0.180
5	200	0.8	0.8	0.32	50	0.153
6	125	0.8	0.8	0.32	150	0.166
7	25	0.8	0.8	0.32	100	0.087
8	150	0.8	0.8	0.32	50	0.147
9	150	0.6	1.0	0.42	100	0.170
10	125	0.42	1.0	0.6	100	0.114
11	100	1.0	0.8	0.32	50	0.125
12	100	0.8	0.8	0.4	50	0.124
13	125	0.8	0.8	0.32	100	0.148
14	50	1.0	0.6	0.23	50	0.124
15	125	0.8	1.0	0.42	100	0.146
16	125	1.0	1.0	0.42	100	0.143
17	100	0.8	0.8	0.32	50	0.130
18	125	0.8	0.6	0.42	100	0.133
19	100	0.8	0.8	0.32	50	0.132
20	75	0.8	0.8	0.8	50	0.072
21	125	0.42	1.0	0.42	100	0.148
22	100	1.0	0.8	0.32	50	0.140
23	100	0.8	0.8	0.42	50	0.132
24	125	0.8	0.8	0.32	100	0.161
25	200	0.8	0.8	0.32	200	0.187
26	125	0.8	0.8	0.32	100	0.161
27	200	0.8	0.8	0.32	200	0.187

After twenty five experiments of the initial simplex the response was increased from 0.174 AU to 0.187 AU. From Table 3.3 it can be seen that the critical factors were injected reagent volume and reaction coil length. This was demonstrated by the low responses

achieved by experiments 7 and 20, in which the small reagent volumes injected, 25 and 75 µl respectively, were quickly depleted. In addition, the short reaction coil length of 50 cm for experiment 20 meant that the residence time and hence the extent of reaction was limited, resulting in a low absorbance signal.

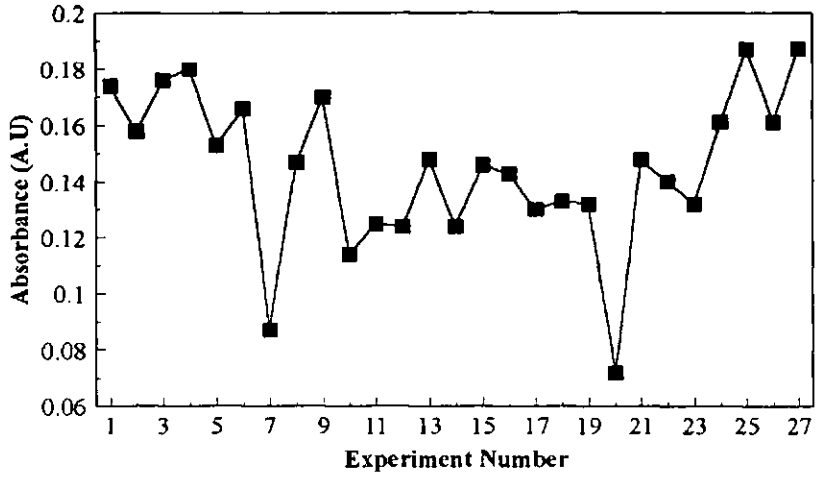

Figure 3.7. History of simplex.

Increasing the volume of reagent injected into the reaction stream from 25 to 125 µl increased the peak height by 85 %. However the signal due to the refractive index change, which precedes the analyte signal, increased with the larger volume. This obscured small analyte peaks and outweighed any advantage gained by the increase in sensitivity [106]. An uneven distribution of the sample in the radial dimension of the conduit is a consequence of laminar flow. This makes the sample zone in the flow cell act as a lens, either focusing the incident light better or dispersing it away from the photodetector the other side of the flow cell. Consequently an absorbance signal resulting from this Schlieren effect (see Section 2.5), is superimposed on the true absorption signal because of the refractive index (RI) difference between the sample and carrier streams. The magnitude of this effect is dependent on a number of factors, e.g. the RI difference between the sample and the carrier, the extent of sample dispersion and the flow cell design [192, 193]. The RI effect can be overcome in FI by increasing dispersion with further mixing and/or matrix matching the sample and carrier streams. With the rFI manifold matrix matching is difficult to achieve as

an additional stream would further dilute the reagents. Increasing the concentrations of reagents to overcome this dilution would increase the coating of the molybdenum blue product on the walls of the PTFE tubing and flow cell which would make this approach unsuitable for long term in situ deployment. A linear calibration graph, $r^2 = 0.9894$ was obtained for phosphate standards in Milli-Q water with an equation of y(AU) = 0.112 + 0.107 PO_4-P (mg l^{-1}). The method achieved a LOD of 28 μg l^{-1} PO_4-P (defined as 3 times the standard deviation of 5 replicates of the blank) compared to that achieved by Johnson and Petty [106] which was 2 μg l^{-1} PO_4-P using a detection limit definition of 2 times the detector baseline noise. This difference in LODs was subsequently attributed to a high blank absorbance signal due to possible contamination of the Milli-Q water supply and the RI effect. This issue is discussed below but the main aim of this aspect of the work was to directly compare rFI with FI for the shipboard and in situ determination of PO_4-P in estuarine and coastal waters. Therefore the results from the rFI manifold (Figure 3.1) were compared with those obtained using an FI manifold (Figure 3.2).

3.3.4. FI Manifold

The manifold shown in Figure 3.2 was adapted from Ruzicka's high sensitivity FI manifold [129] and used for this work. The formation of double peaks in the mixed sample/reagent zone caused by insufficient reagent must be avoided. The reagent has to penetrate into the core of the sample zone through the leading and trailing edges. Thus, the larger the sample volume and the smaller the cross section of the channel, the more likely the formation of a double peak. Where there is insufficient reagent a trough in the centre of the FI peak is observed. Double peaks can be eliminated by increasing the residence time, increasing the mixing and/or decreasing the injected volume. Therefore, in the experiments, the sample was injected into a stream of water, merged at a confluence point with the combined reagent stream of molybdate and ascorbic acid and mixed in a 'knitted' coil to minimise

axial dispersion of the sample zone. A linear calibration graph, $r^2 = 0.9915$ was obtained for phosphate standards in Milli-Q water represented by the equation y(AU) = 0.110 + 0.105 PO_4-P (mg l^{-1}). The method achieved a LOD of 19 μg l^{-1} PO_4-P, which was lower than that achieved by the rFI manifold (Figure 3.1). Dispersion coefficients (D) were calculated for both the rFI and FI manifolds as described by Ruzicka [129]. For the rFI manifold D was 10.8, compared with 8.5 for the FI manifold. Therefore, as the same reagent concentrations were used for both methods the lower sensitivity achieved by the rFI manifold, was due in part to the greater dispersion.

The accurate analysis for low-level reactive phosphate in sea water is inherently blank limited. A common difficulty in preparing reagent blanks is the possibility of their contamination with phosphate. Many reagent grade salts e.g. AnalaR® at the appropriate dilutions contain phosphate at concentrations comparable with those found in surface sea water, e.g. 5 g l^{-1} AnalaR® ammonium molybdate contains 8.2 μg l^{-1} PO_4-P. The phosphate contamination of the reagents would be more significant in the rFI manifold, because the phosphate content of the reagents is measured in addition to that contained in the sample. With the FI method however any reagent phosphate contamination is subtracted when the baseline is set to zero, as the reagents are continually flowing through the flow cell at a constant concentration. It would be possible to use exceptionally pure reagents e.g. Aristar®, if available, to reduce the phosphate contamination, but the cost of these reagents is prohibitive for routine analysis.

3.3.5. Effect of Antimony(III) as a Catalyst in the FI Manifold

Using the manifold shown in Figure 3.2 an investigation was carried out on the effect of the presence of antimony potassium tartrate on the sensitivity of the method. Figure 3.8 shows the effect of 0.1 g l^{-1} Sb(III) on a series of phosphate standards (0.0 - 1.0 mg l^{-1} P) made up in Milli-Q water. The absorbance signal for a 1 mg l^{-1} PO_4-P standard increased from 0.215

to 0.565 AU in the presence of Sb(III), but at lower phosphate concentrations, i.e. <0.1 mg l^{-1}, the sensitivity was not improved significantly. This supports the observations of Towns [188] who found that the addition of Sb(III) resulted in higher sensitivity when phosphorus concentrations were greater than 1 mg l^{-1}.

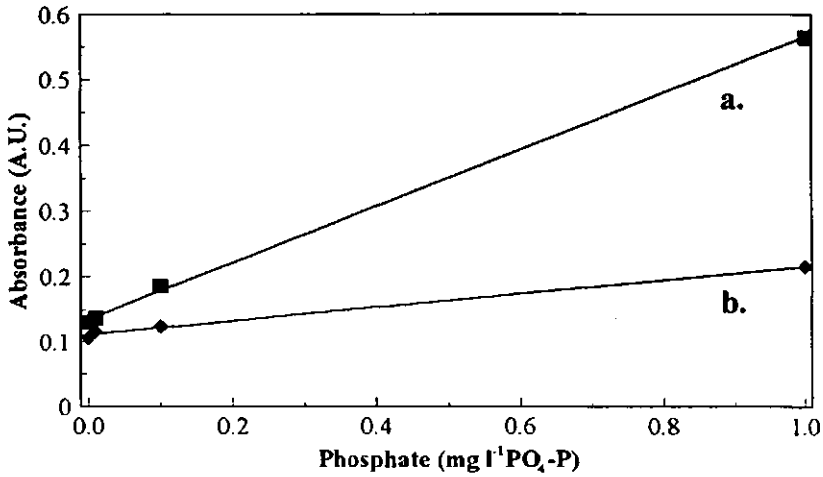

Figure 3.8. Effect on absorbance; a. with 0.1 g l^{-1} antimony(III) and b. without antimony(III).

Spectral studies [111] have shown that antimony is present in the complex in a 2:1 (Sb:P) ratio and the stoichiometry of the reduced molybdoantimonylphosphoric acid is $PSb_2Mo_{12}O_{40}$. From these results it is recommended that 0.1 g l^{-1} Sb(III) is used as a catalyst when ascorbic acid is the reductant of choice.

3.3.6. Investigation of the Blank Signal using the FI manifold

Both the rFI and FI manifolds described above have a high blank signal, with intercepts on the y axis of 0.112 and 0.110 AU respectively. This is probably due to the presence of phosphate in the Milli-Q water used to prepare the standards. It was therefore decided to use low nutrient sea water in order to try to reduce the blank signal. Table 3.4 shows a calibration comparison for phosphate standards made up in Milli-Q water and in a commercial Low Nutrient Sea Water (LNS, Ocean Scientific, Wormley, Surrey). The blank absorbance signal was reduced from 0.106 AU for Milli-Q to 0.065 AU with the use of LNS. The LNS is quoted as containing <0.05 μM phosphate (i.e. 1.5 μg l^{-1} PO_4-P) and this

suggests that the high blank for Milli-Q was due to phosphate contamination. The sensitivity of the method was enhanced by the use of LNS and the LOD was improved from 19.0 μg l^{-1} PO_4-P in Milli-Q water to 6.3 μg l^{-1} PO_4-P. LNS is therefore recommended for use in all phosphate determinations below 100 μg l^{-1} over the range 0 - 200 μg l^{-1} PO_4-P.

Table 3.4. Comparison of phosphate standards in Milli-Q and LNS.

MATRIX	CALIBRATION LINE	r^2	LOD (μg l^{-1} PO_4-P)	RSD (%)
Milli-Q	y = 0.105x + 0.110	0.9915	19.0	1.7
LNS	y = 0.158x + 0.064	0.9996	6.3	0.6

y is in AU and x is in mg l^{-1} PO_4-P.

3.3.7. Addition of Glycerol

Using the FI manifold shown in Figure 3.2 with phosphate standards in LNS the presence of glycerol (10 %) on the absorbance signal, especially that of the blank, was investigated. Harvey [194] and Ruzicka [129] reported the use of glycerol to minimise precipitation of reaction products which adhere to the sides of the PTFE tubing and walls of the flow cell. In addition ascorbic acid has been reported to be stable in distilled water and sulphuric acid for up to 7 days [24] whereas in 10 % glycerol it is stable for 30 days [110, 144]. The gradients of the calibration lines were the same (Figure 3.9) but the absorbances were increased by about 0.030 AU with the presence of glycerol. This was due to the higher viscosity of the glycerol causing greater RI differences between the sample zone and the carrier stream. However the results show that glycerol could be used for long term deployment of the manifold with no detrimental affect on the LOD or sensitivity.

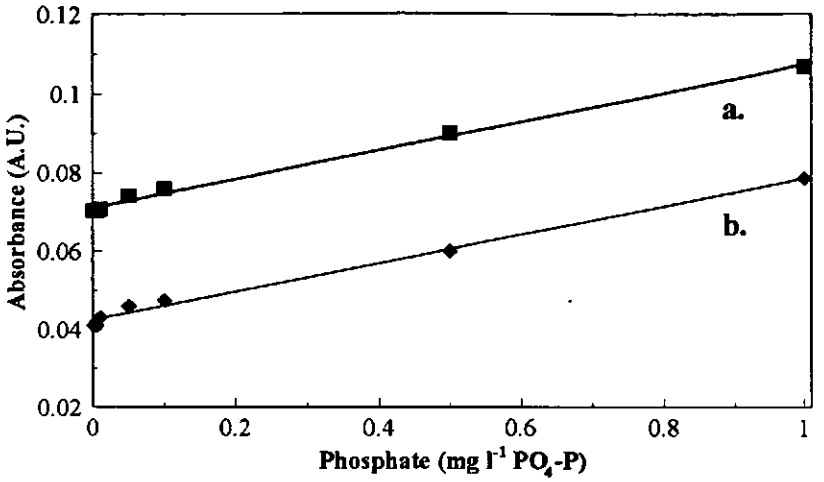

Figure 3.9. Effect on absorbance; a. with glycerol and b. without glycerol.

3.3.8. Univariate Optimisation of Reagent Concentrations for the Tin(II) Chloride Manifold

Ascorbic acid, with or without glycerol, is the recommended reductant for applications in which the manifold is left unattended for days or weeks at a time. For short term (i.e. daily) deployments and for laboratory use however, tin(II) chloride may be preferred if a lower LOD is required. A univariate optimisation was therefore carried out on the reagent concentrations of ammonium heptamolybdate and tin(II) chloride using the manifold shown in Figure 3.3. For the optimisation the reagent concentrations were 10.0 g l^{-1} molybdate in 0.3 M sulphuric acid and 0.2 g l^{-1} tin(II) chloride-2-hydrate containing 2.0 g l^{-1} hydrazinium sulphate with a 0.1 mg l^{-1} PO_4-P standard. The effect of molybdate concentration was studied in the range 2 - 20 g l^{-1} and the results are shown in Figure 3.10. The absorbance increased with increasing molybdate concentration up to 10 g l^{-1}, and this concentration was used for all further experiments.

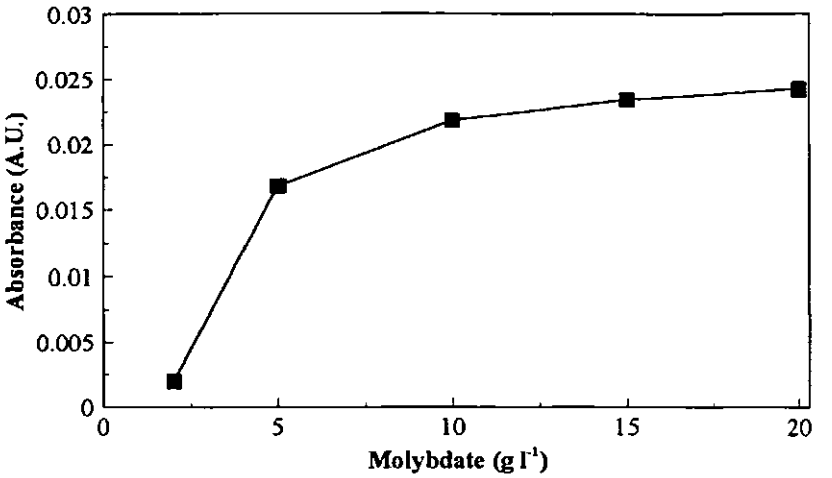

Figure 3.10. Univariate optimisation of molybdate concentration.

Figure 3.11 shows the results of the univariate optimisation of tin(II) chloride concentration in the range 0.05 - 1 g l^{-1}. The absorbance signal increased as the concentration of tin(II) chloride increased because more of the molybdate in the molybdophosphoric acid was reduced. The main disadvantage of using tin(II) chloride as a reducing agent is its poor stability, which can potentially lead to poor precision and a shift in the baseline [122]. By using a low concentration, e.g. 0.2 g l^{-1} for further work and adding hydrazinium sulphate [195], the tin(II) can be stabilised for 5 days. Using this method a linear calibration graph, $r^2 = 0.9997$ was obtained for standards in Milli-Q water represented by the equation y(AU) = 0.001 + 0.232 PO_4-P (mg l^{-1}), the method achieved a LOD of 4.3 μg l^{-1} PO_4-P which is an improvement on that reported by Janse et al. [128] of 10 μg l^{-1} PO_4-P.

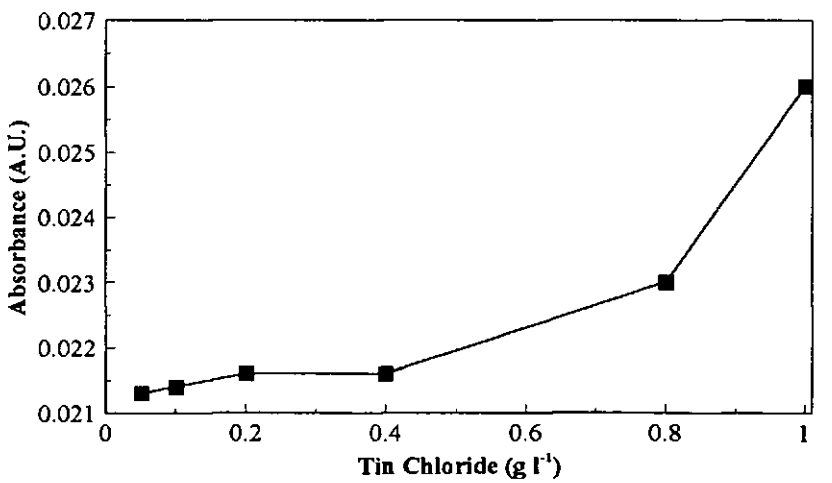

Figure 3.11. Univariate optimisation of tin(II) chloride concentration.

3.3.9. The Salt Error

The use of tin(II) chloride as the reductant has long been recognised as having a salt error [196]. Figure 3.12 demonstrates this fact; as salinity decreases the absorbance decreases, although at salinities >10 ‰ the response is constant. These results are similar to those reported by Harvey [194] who showed that increasing salinity decreased the response up to 25 ‰ and that the salt error was constant between 25 and 35 ‰. These results show that the method is suitable for the analysis of coastal and open ocean waters without the need for correction providing the standards are also prepared in 35 ‰ sea water e.g. LNS. However the results also show that for the analysis of estuarine waters, where salinity can vary from 0 - 35 ‰ a correction or modified manifold is required.

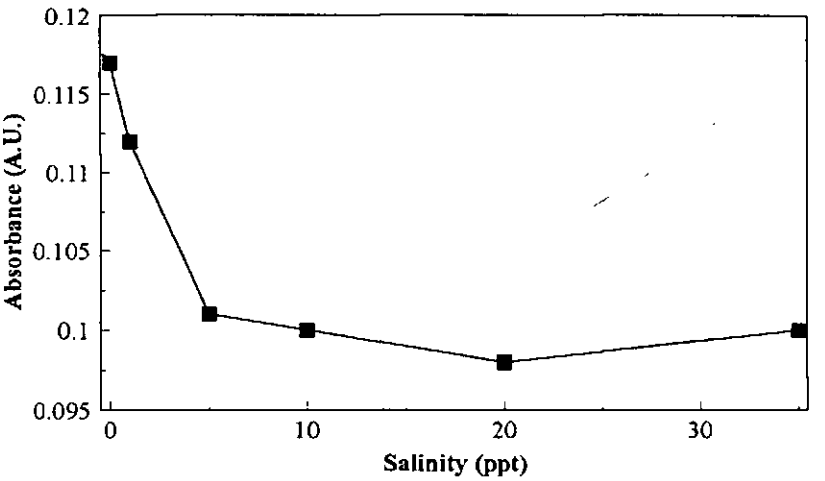

Figure 3.12. Effect of sample salinity on absorbance measurement.

3.3.10. Salinity Compensation Manifold

The manifold shown in Figure 3.4 was developed in order to overcome the major problem with using tin(II) chloride, i.e. the salt error. As with the nitrate manifold shown in Figure 2.12, a matrix matched sodium chloride stream was incorporated into the manifold. Figure 3.13 and Table 3.5 show calibration data for phosphate standards of various salinities (prepared by adding sodium chloride) in Milli-Q water. The method achieved a LOD of 4.5 $\mu g\ l^{-1}$ PO_4-P, which was comparable with the FI method using tin(II) chloride reduction described above (Section 3.3.8).

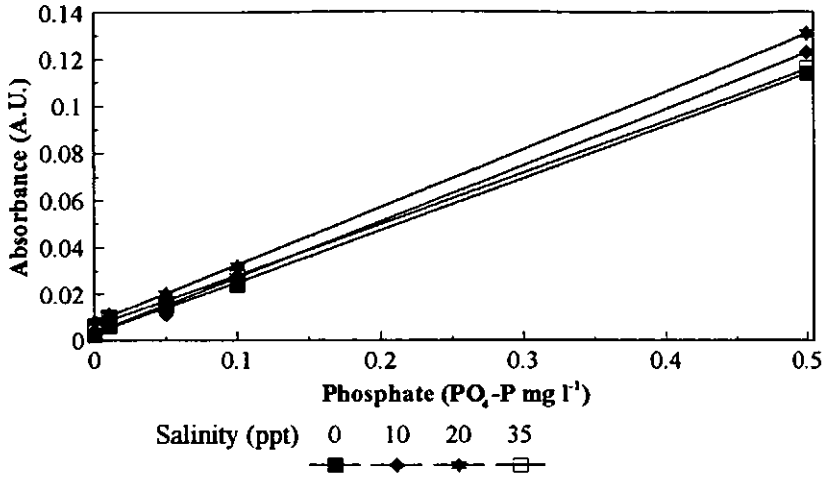

Figure 3.13. Calibration lines for standards of various salinities.

Table 3.5. Calibration data for standards of varying salinities.

SALINITY (‰)	CALIBRATION LINE	r^2
0	y = 0.222x + 0.002	0.9995
10	y = 0.239x + 0.003	0.9975
20	y = 0.245x + 0.007	0.9999
35	y = 0.219x + 0.006	0.9994

y is in AU and x is in mg l^{-1} PO_4-P.

This manifold is therefore applicable to the determination of PO_4-P in riverine, estuarine, coastal and oceanic waters, where the salinity varies from 0 - 35 ‰, without the need to apply a correction for the salt error. This manifold is therefore recommended for laboratory analysis and short term shipboard deployments. Results from shipboard deployment in the Tamar Estuary are presented in Chapter 4.

3.4. CONCLUSIONS

1. The ascorbic acid-antimony(III) method with glycerol is recommended for long term deployments, i.e. greater than one day.
2. Low nutrient sea water is preferred to Milli-Q for preparing phosphate standards for the determination of phosphate in sea water, particularly when the detection limit is low.
3. The use of high purity reagents, particularly nitric acid and molybdate is recommended in order to reduce possible phosphate contamination.
4. Tin(II) chloride is recommended as the reductant to achieve the lowest detection limit (4.3 $\mu g\ l^{-1}$ P) for the analysis of coastal and open ocean waters.
5. The salinity compensation manifold can be used to determine phosphate over the range 0 - 0.5 $mg\ l^{-1}$ P in estuarine waters (salinity range 0 - 35 ‰).

Chapter Four
Determination of Nitrate and Orthophosphate in the Tamar Estuary and Sutton Harbour

4. DETERMINATION OF NITRATE AND ORTHOPHOSPHATE IN THE TAMAR ESTUARY AND SUTTON HARBOUR

4.1. INTRODUCTION

This chapter discusses shipboard validation of the FI methods for the determination of TON and orthophosphate in estuarine and riverine waters. TON and orthophosphate levels from eight surveys of the Tamar Estuary are presented. Additional field data collected from Sutton Harbour before and after impoundment with lock gates are shown and related to biogeochemical processes and interactions taking place within the area.

4.2. EXPERIMENTAL

4.2.1. Reagents and Standards

All solutions were prepared a day prior to the surveys in accordance with sections 2.2.1 and 3.2.1 for the determination of nitrate and phosphate respectively.

4.2.2. Instrumentation

Tamar Surveys. The FI manifold shown in Figure 2.12 was used for all surveys for the determination of TON on board the *R.V.S. Tamaris*. A sample injection volume of 30 µl was used in order to extend the linear range of the method to cover the expected nitrate levels found in the Tamar Estuary (typically 0 - 5 mg l^{-1} N [17]). Nitrite determinations were carried out in the laboratory on the collected discrete samples using the FI manifold (Figure 2.12) without the cadmium reduction column. The salinity compensation manifold shown in Figure 3.4 was used for the ship-board determination of phosphate in the Tamar Estuary.

A primary supply of estuarine water was provided by a submersible pump fixed at a depth of 1 m. Discrete samples were taken from this surface water supply and passed through a 0.45 μm pore-sized filter (Supelco) fixed to the sample inlet of the FI manifolds.

Sutton Harbour Surveys. Both TON and orthophosphate nutrients were analysed in the laboratory; TON using the FI manifold shown in Figure 2.12 and orthophosphate using the antimony-ascorbic acid chemistry with the manifold shown in Figure 3.2. Salinity was measured using a calibrated TDS-7 salinometer.

4.2.3. Sampling of the Tamar Estuary

The Tamar Estuary lies to the west of the City of Plymouth and borders the counties of Devon and Cornwall. The Rivers Tavy and Lynher flow into the Estuary before it finally drains into Plymouth Sound which is an open bay with an artificial breakwater at its entrance and Drake's Island to the northwest. The estuary is tidal for about 30 km (to the Weir) and these tidal flows are dominant over river flows. Nutrients from the river due to land drainage keep the nutrient concentrations at a higher level than found at sea, so abundant phytoplanktonic populations can develop.

Nitrate Surveys. Seven surveys of the Tamar Estuary were carried out between April 1994 and February 1995 aboard a Rotock Sea-truck (*R.V.S. Tamaris*) for the determination of TON. Table 4.1 shows the specific dates of the surveys and the state of the tides on those days. The sampling stations spanned the entire estuary starting from a point south of Drakes Island in the Sound and continuing at regular intervals up-stream (approximately every 5 ‰ surface salinity change) through the brackish/freshwater interface [197], to the freshwater at Calstock. Figure 4.1 shows a schematic of the Tamar Estuary with bars drawn at 5 kilometre intervals along the axis of the estuary from the mouth to the Weir in

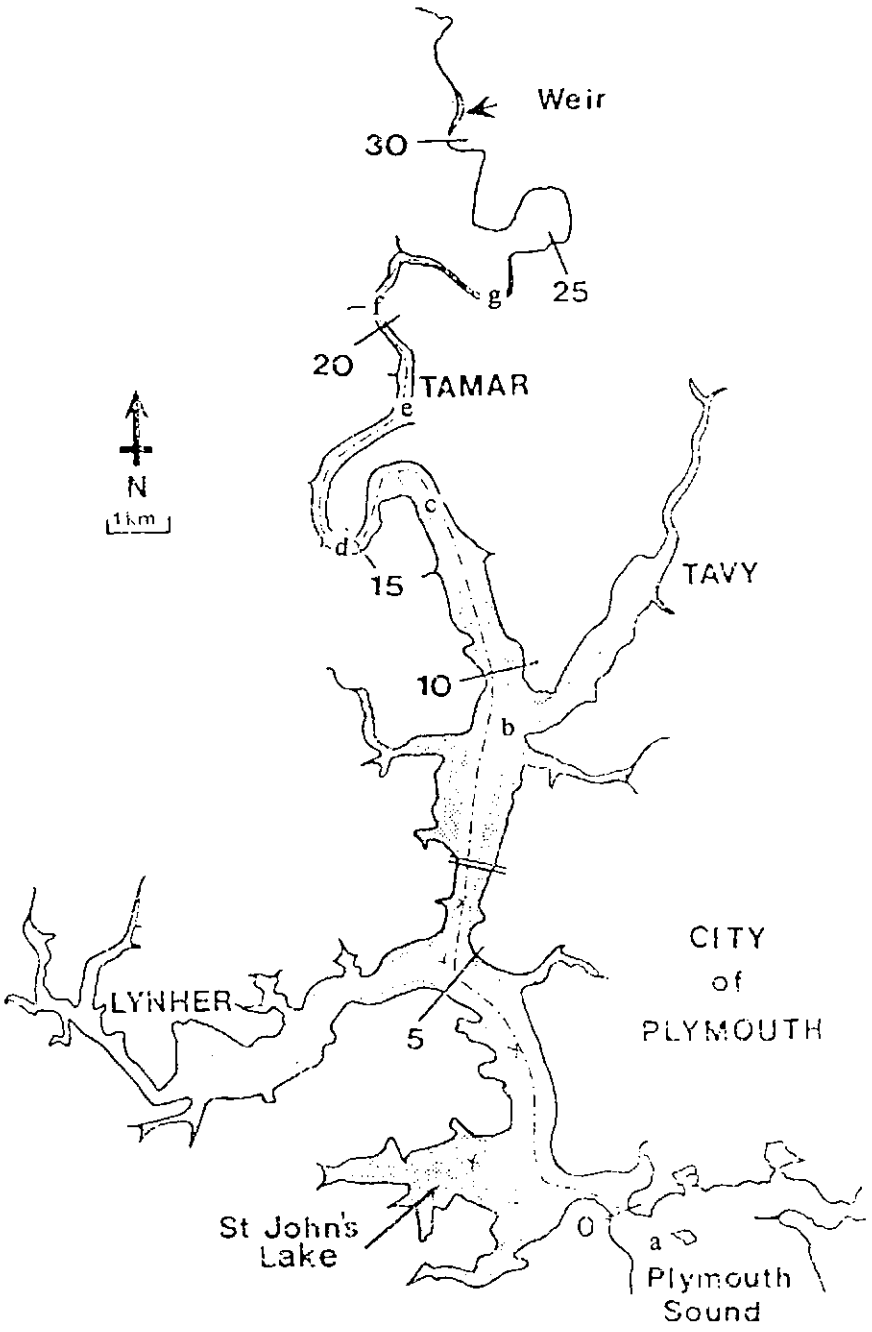

Figure 4.1. Schematic of the Tamar Estuary with Sampling Stations a) Drake's Island, b) Skinham Point, c) Weir Quay, d) Tinnel, e) Whitsam, f) Museum and g) Calstock.

the north. The sampling sites used upstream were: Drake's Island, Skinham Point (8 km), Weir Quay (13 km), Tinnel (15 km), Whitsam (18 km), the Museum (21 km) and Calstock (23 km).

Phosphate Survey. A survey was carried out on October 19th 1995 to assess the salinity compensation phosphate manifold on-board the *R.V.S Tamaris* with samples of differing salinity from the Tamar Estuary and to discuss distribution of this nutrient within an estuarine environment. Discrete samples were taken at regular intervals both up-stream from the estuary mouth in the Sound to the freshwater at Calstock and down-stream back to the high-saline waters of the Sound. The state of the tide on the date of sampling and analysis is shown in Table 4.1.

Table 4.1. Tide times at Port of Devonport on survey days.

DATE	TIDE	HEIGHT (m)	TIDE	HEIGHT (m)	ANALYTE
April 19th 1994	HW 10:54	4.2	HW 23:21	4.4	N
	LW 04:26	2.0	LW 17:09	2.2	
May 18th 1994	HW 10:35	4.4	HW 22:56	4.6	N
	LW 04:16	1.7	LW 16:44	1.9	
June 13th 1994	HW 08:13	4.8	HW 20:22	5.1	N
	LW 01:57	1.1	LW 14:11	1.2	
July 27th 1994	HW 08:32	5.0	HW 20:39	5.2	N
	LW 02:33	0.7	LW 14:46	0.9	
September 28th 1994	HW 10:22	4.4	HW 22:49	4.2	N
	LW 03:33	2.2	LW 16:15	2.4	
November 9th 1994	HW 09:42	5.2	HW 22:16	4.8	N
	LW 03:27	1.4	LW 15:56	1.5	
February 6th 1995	HW 09:25	4.9	HW 21:44	4.7	N
	LW 03:33	1.4	LW 15:52	1.5	
October 19th 1995	HW 01:11	4.2	HW 13:39	4.5	P
	LW 07:18	2.4	LW 19:57	2.1	

4.2.4. Sampling of Sutton Harbour

Sutton Harbour is situated in the south east of the City of Plymouth, within the historic Barbican area at the mouth of the Plym Estuary. The harbour covers an area of 1 x 10^5 m^2 and contains a fish dock and marina for fishing and recreational vessels. Historically the disadvantages of Sutton Harbour as a main fishing port were:

1. The harbour had insufficient water depth at low water to enable large beam trawlers to operate efficiently,

2. The existing fish market was too small,

3. Its location presented traffic difficulties for traders,

4. Most importantly the Barbican was prone to periodic flooding several times a year.

Therefore, in April 1992 a £7 million flood prevention scheme financed by the NRA, MAFF and the Sutton Harbour Company was put into operation to impound the harbour with lock gates. In addition a greater operational depth, enabling continual access to vessels, together with large areas of reclaimed land for a new fish market on the eastern side and easier road transport access were achieved. Work began in April 1992 with site preparation and construction of the lock in the eastern arm of the harbour in dry dock, they were then floated and sunk into place at the harbour mouth, with final completion and commission in April 1994. A full environmental study before and after impoundment was carried out by Smith [198, 199], who monitored the water and sediment quality within the harbour before and after installation of the lock gates. As part of that study, the TON and orthophosphate concentrations of the collected samples were analysed by this author.

Surveys were conducted on adjacent spring and neap tides (six to eight days apart) commencing in November 1991. Each survey involved the collection of water samples at the surface and bottom at HW and LW from each of five sampling stations throughout the spring and neap tidal cycle. Figure 4.2 shows a schematic of Sutton Harbour and the

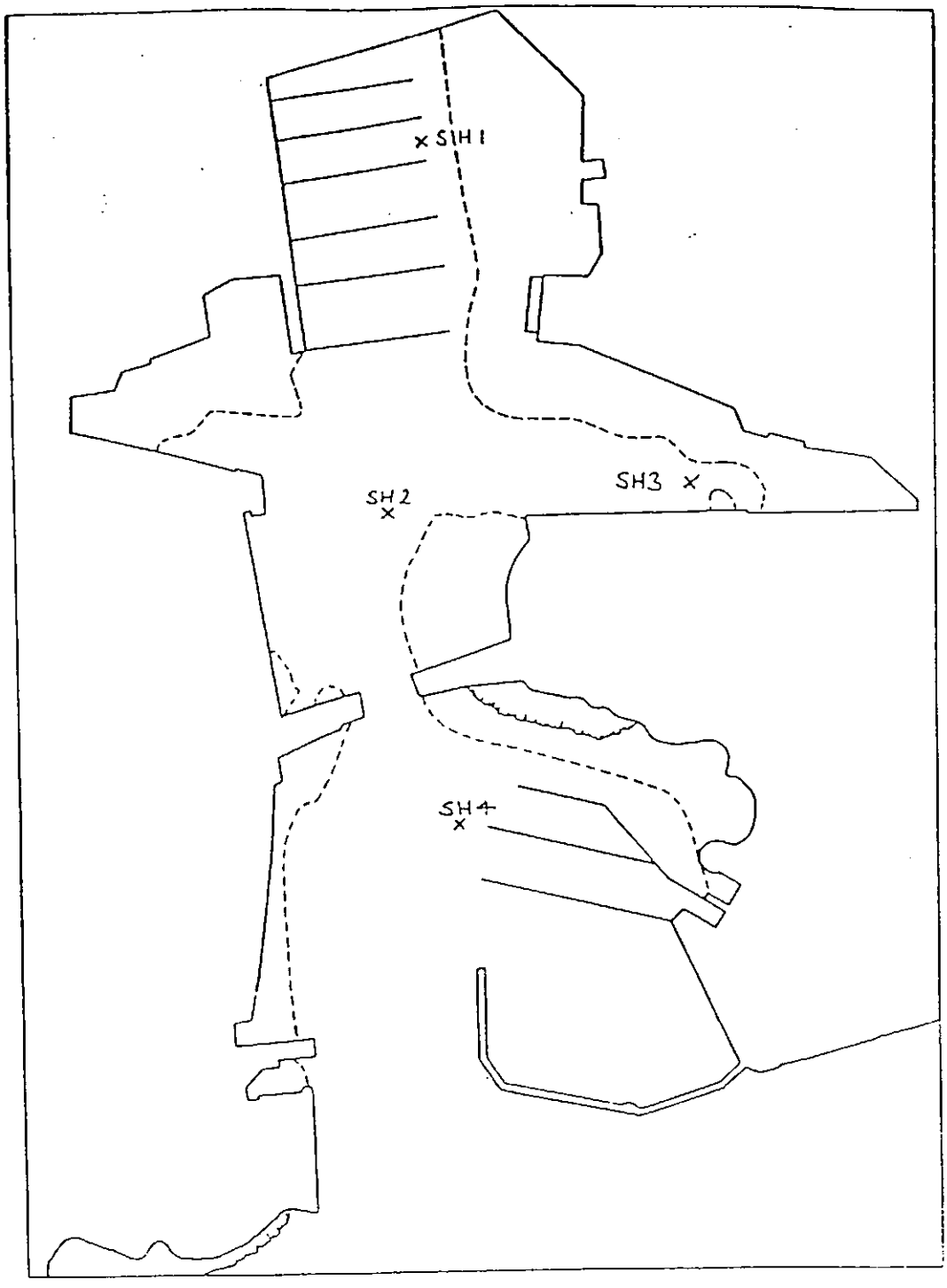

Figure 4.2. Schematic of Sutton Harbour.

location of the sampling sites. The stations were chosen in order to represent varying conditions inside the harbour. Station 1 (SH1) was in the north of the harbour furthest from the entrance and was likely to suffer from long water renewal times. Station two (SH2) was positioned centrally, in line with the axial flow through the harbour entrance, and therefore received most tidal flushing. Station three (SH3) was located in the eastern arm of the harbour, where water renewal is thought to be slow due to low current velocities. This station is also close to a land reclamation site and the location of initial lock gate construction. Stations four (SH4) and five (SH5) serve as controls and are located outside the harbour. Station five is close to untreated sewage discharges along the Plymouth waterfront and also to the Plym Estuary. Samples were collected surface (0.5 m depth) and bottom at each station using an IOS water bottle, consisting of a cylindrical polypropylene body with hinged rubber caps at either end that were triggered shut from the surface, thus enclosing a water sample from the required depth. At each station the bottle was primed by cocking the caps and closing the taps. It was then lowered by a line marked at 1.0 m intervals to the necessary depth, a messenger was clipped to the line and released to close the top and bottom caps and then the water sample was retrieved. An aliquot (50 ml) for each nutrient (TON and phosphate) was drawn into a polypropylene syringe from the IOS bottle and passed through a 0.45 μm pore size Swinnex filter holder into a previously acid washed (10 % HCl) and Milli-Q water rinsed brown glass bottle (250 ml). The samples were stored in the dark at 4 °C for analysis within 6 hours. A further sample aliquot was taken and measured for salinity on immediate return to the laboratory.

4.3. RESULTS AND DISCUSSION

4.3.1. Nitrate in the Tamar Estuary

Figure 4.3 shows the levels of TON found on the seven surveys at each of the seven sampling sites. Substantial concentration differences were found between the highly saline waters at the lower end of the estuary and the waters of lower salinity at the upper end of the estuary. Nitrate levels in the Sound varied between 0.01 - 0.39 mg l^{-1} N, whilst those at Calstock were much higher, between 1.2 - 3.3 mg l^{-1} N. These values compare well with the nutrient concentrations found on previous surveys of the Tamar Estuary, as shown in Table 4.2. There was also a clear seasonal pattern in TON concentration at most sites, with high levels in winter and late spring (>3 mg l^{-1} N at Calstock) decreasing in the summer especially in June when the rate of photosynthetic removal of nitrate i.e. greater than the rate of nitrate replacement to the estuary from riverine sources.

Figure 4.4 shows plots of TON concentration against salinity for each of the seven surveys. The surveys for April, May, June, July and February show conservative behaviour for TON within the estuary, i.e. an inverse linear relationship between TON concentration and salinity. This shows that there are no significant sources or sinks for TON within the survey area and that riverine inputs from upstream of Calstock dominate the system. The profiles for September and especially November were obtained at a time of exceptional weather conditions when continuous heavy rainfall for several days prior to the survey had considerably increased the water level of the estuary. This resulted in higher than normal inputs of nitrate from within the catchment of the survey area due to enhanced run off and storm effects at high rainfall. This was compounded by the fact that at Skinham Point (at the junction with the Tavy) and at Weir Quay (downstream of the sharp river bends and mud flats in the 13 - 16 km region), water masses can be temporarily isolated from the main

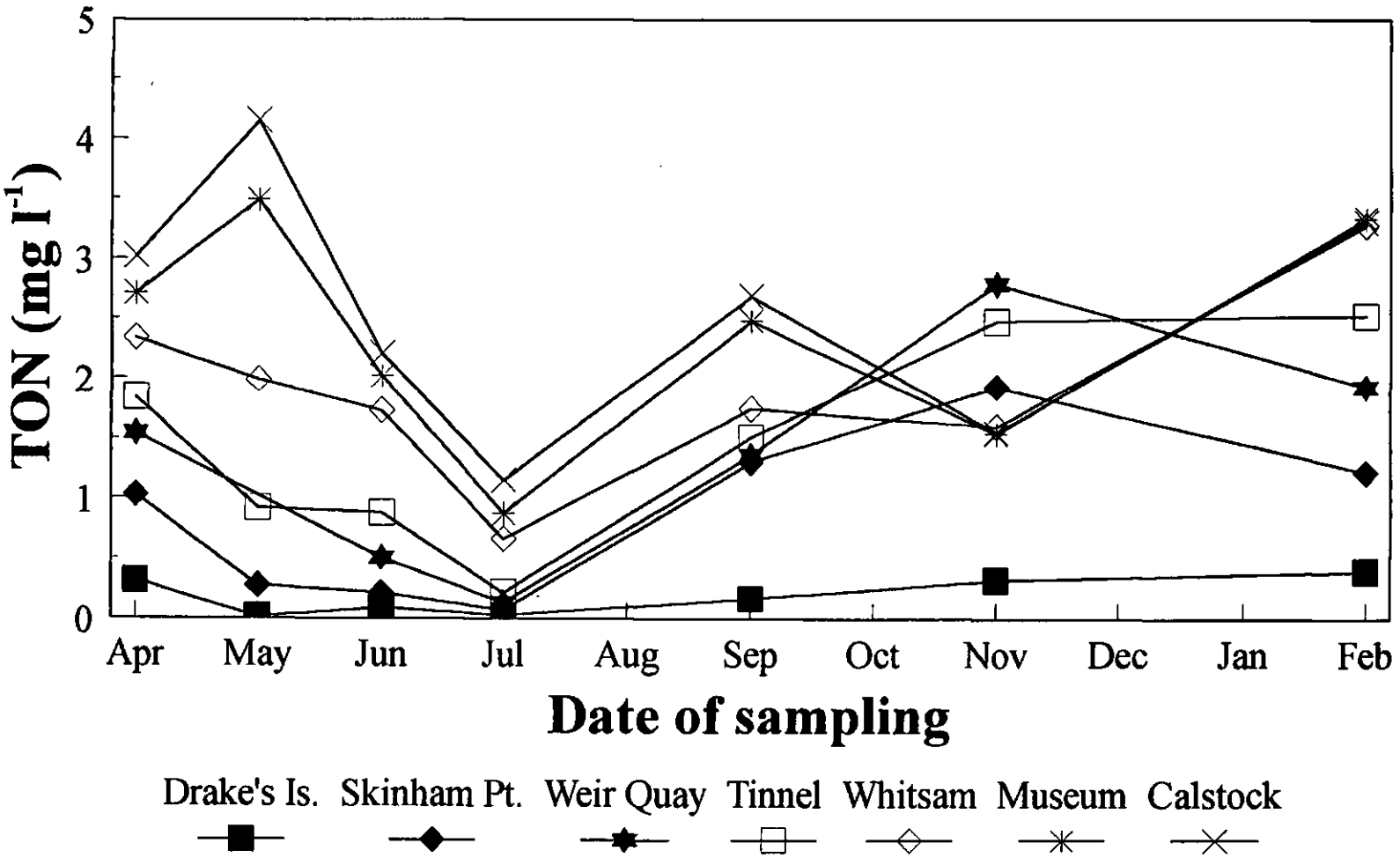

Figure 4.3. TON concentrations at each sampling station on the seven Tamar surveys

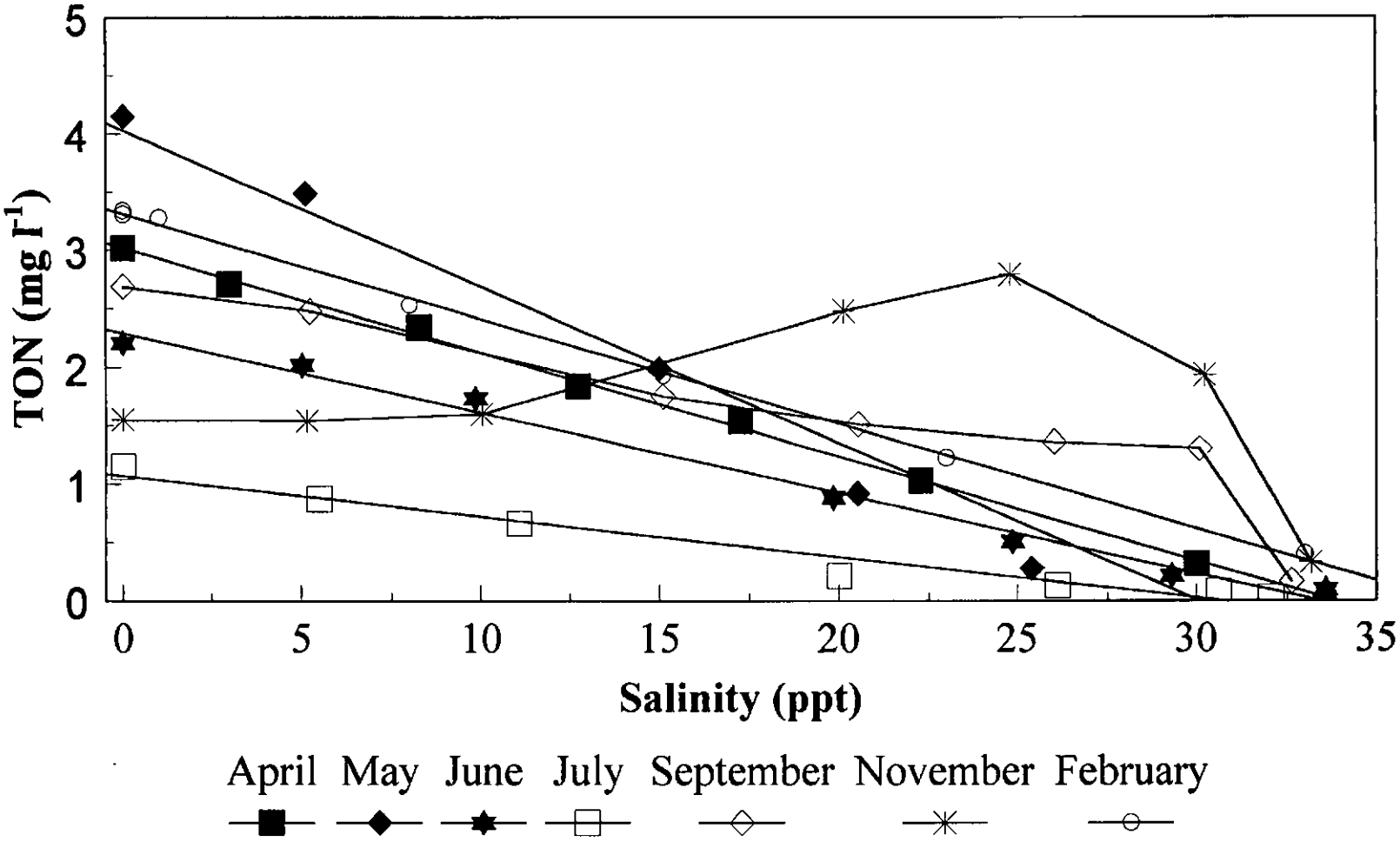

Figure 4.4. TON concentration against salinity for each of the seven Tamar surveys.

tidal stream, leading to inhomogeneity in the water column and localised regions of high nutrient content [200, 201].

Table 4.2. Literature values for nutrient concentrations in the Tamar Estuary.

REFERENCE	NITRATE (mg l^{-1} N) at SALINITY		NITRITE (mg l^{-1} N) at SALINITY		PHOSPHATE (µg l^{-1} P) at SALINITY	
	0 ‰	32 ‰	0 ‰	32 ‰	0 ‰	32 ‰
200	1.0 - 3.5	0.1 - 0.3	-	-	20 - 40	5.0 - 40
201	0.8 - 3.4	0.2 - 0.4	0.01	0.02	-	-
202	-	-	0.01	0.03	-	-
203, 204	-	-	-	-	-	20 - 30
205	-	0.1 - 0.4	-	0.02	-	20 - 60

Nitrite is an important nitrogen species in the aquatic nitrogen cycle. It occurs as an intermediate in the microbial reduction of nitrate or and oxidation of ammonia. As its rate of consumption nearly equals its rate of formation, nitrite rarely accumulates in natural systems. In estuaries nitrite is found at concentrations in the range 0 - 30 µg l^{-1} N; higher values indicate polluted waters and can reach levels as high as 2 mg l^{-1} [93]. Figure 4.5 shows the levels of nitrite found in the Tamar Estuary over the period of the survey at the seven sampling stations. Nitrite concentrations varied between 0 and 30 µg l^{-1} N, as found on previous surveys (Table 4.2). There was no evidence of seasonal variation with levels very low in July and November for all samples, and above 5 µg l^{-1} N in April, June and February. Nitrite concentrations were generally higher at sampling stations in the upper 5 km and lower 10 km of the estuary at Calstock and the Museum, and Skinham Point and Drake's Island respectively, with lower nitrite concentrations within the central 10 km of the estuary at Weir Quay, Tinnel and Whitsam. No marine chemical interpretation can be made without further work and correlation with variables such as turbidity, chlorophyll-a measurements and ammonium concentration. Knox et al [201] and Morris et al [202]

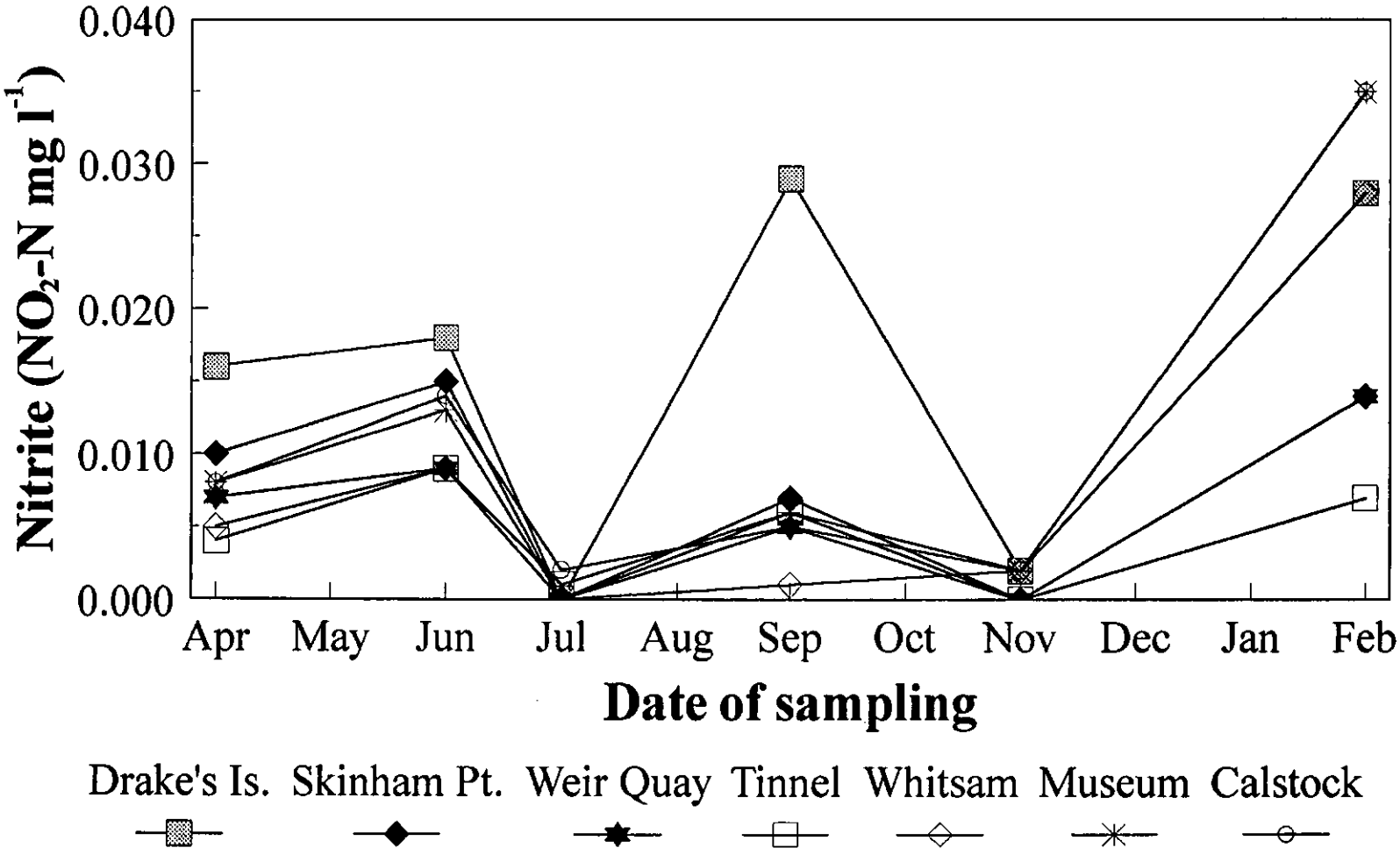

Figure 4.5. Nitrite concentration at each sampling station on the seven Tamar surveys

observed persistent maxima in the nitrite profiles, especially in the low salinity upper 10 km of the estuary. The nitrite profiles were also significantly correlated with those of ammonium which also show persistent estuarine maxima. These correlations could indicate either that the nitrite is produced by oxidation of ammonium throughout the water column or that nitrite production takes place within the sediment and that the two components are released and mixed into the water column in a constant ratio. Morris et al [202] found spring-neap periodicity in nitrite concentrations, reflecting variations in the degree of tidal sediment disturbance and that peak nitrite concentrations were persistently confined within the low salinity zone close to the site of the turbidity maximum. This evidence suggests a sediment source of nitrite and/or that the nutrient is generated within the water column by a localised biological process.

4.3.2. Orthophosphate in the Tamar Estuary

Samples for orthophosphate determination were taken up-stream with the flood-tide and down-stream with the ebb-tide at regular intervals (~10 mins). Figure 4.6 shows the levels of phosphate at each of the sampling sites, concentrations varied between 5 - 65 $\mu g\ l^{-1}$ P, as with previous surveys (Table 4.2), with the considerably higher levels found at the lower 5 km of the estuary on the flood-tide and not on the ebb. These pronounced localised maxima in concentration encountered in the lower 5-10 km of the estuary were indicative of significant inputs of phosphate to this region. Figure 4.7 shows the location of the sewage outfalls in the region of Plymouth and the Tamar Estuary and provides a guide to the volume discharged based on the population served and whether the sewage is untreated, partially treated (settlement in septic tank) or fully treated [206, 207]. Discharges into the Tamar are mostly treated, whilst those into the Sound and lower estuary are substantial and untreated. On the flood tide the inputs in the Sound are washed up into the lower estuary causing the higher than expected levels of orthophosphate whilst on the ebb tide the

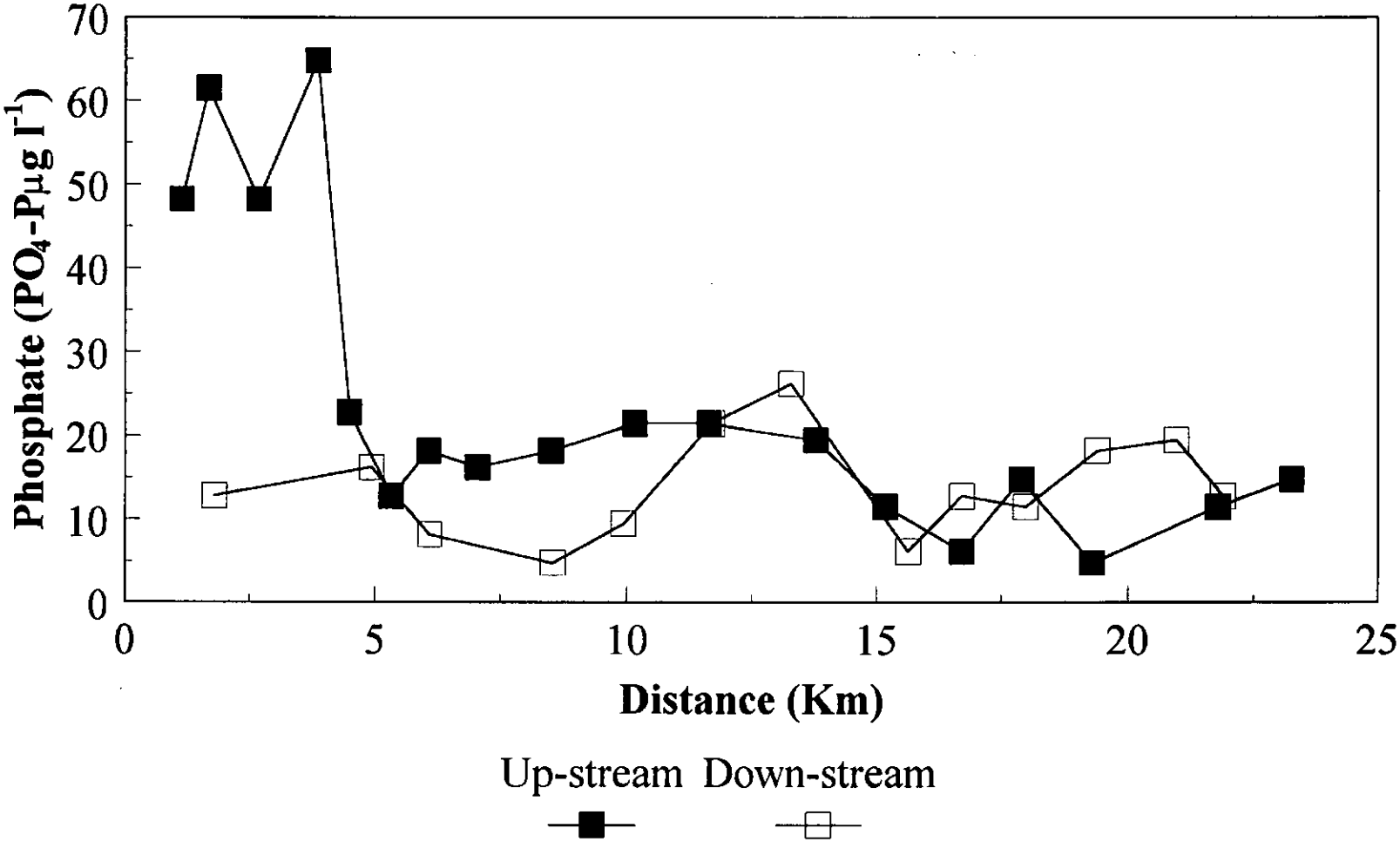

Figure 4.6. Orthophosphate concentrations in the Tamar Estuary.

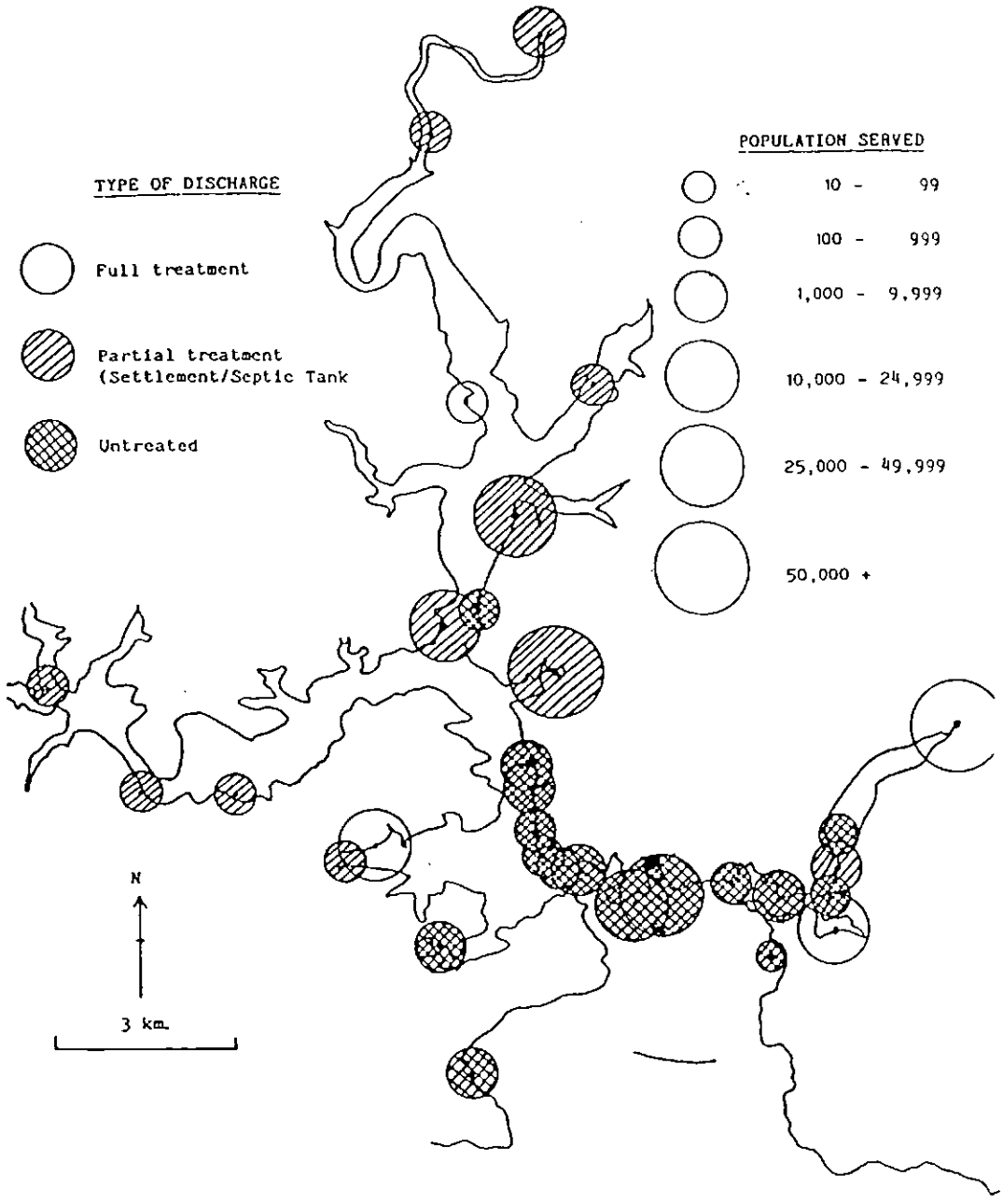

Figure 4.7. Sewage outfalls in the Sound and Tamar Estuary.

estuarine water flows back into the Sound taking with it the pollutant orthophosphate. These results are concordant with whose reported by Mommaerts [203, 204].

Figure 4.8 shows salinity plotted against the phosphate concentration of samples taken up-stream and down-stream. Unlike the linear relationship with salinity exhibited by nitrate, phosphate levels, except for those at flood tide in the lower 10 km of the estuary, are generally invariant over the whole salinity range of the estuary (0 - 32 ‰) at a concentration of approximately 20 $\mu g\ l^{-1}$ P. This means that either the end members of the mixing series contain virtually identical concentrations of phosphate, or there is some sort of buffering process in the estuarine water which maintains dissolved phosphorus levels close to 20 $\mu g\ l^{-1}$ P, irrespective of changes in salinity. This second possibility is supported by the work of Butler and Tibbitts [205]. In order to constitute a true buffer system the estuarine sediment must be capable of both removing phosphate from phosphate-rich water and adding it to water low in phosphate. The effect of salinity, coupled with those of pH and phosphate concentration, all tend to decrease the change in phosphate levels between the fresh (phosphate-rich) and saline (phosphate-poor) parts of an estuary. At the freshwater end the high phosphate concentration, low salinity and possibly low pH all favour removal, whereas in the sea water all these factors are reversed. Uptake of phosphate occurs by a two-stage process consisting of a rapid initial adsorption of PO_4^{3-} onto the sediment surface, followed by a much slower reaction in which the phosphorus is incorporated into the structure of the solid phase. The PO_4^{2-} is held in the solid phase as a Fe(III) phosphate complex, but when the sediment becomes reducing such as under anoxic conditions the ferric iron is reduced to soluble Fe(II) which allows the phosphorus to escape to the overlying water.

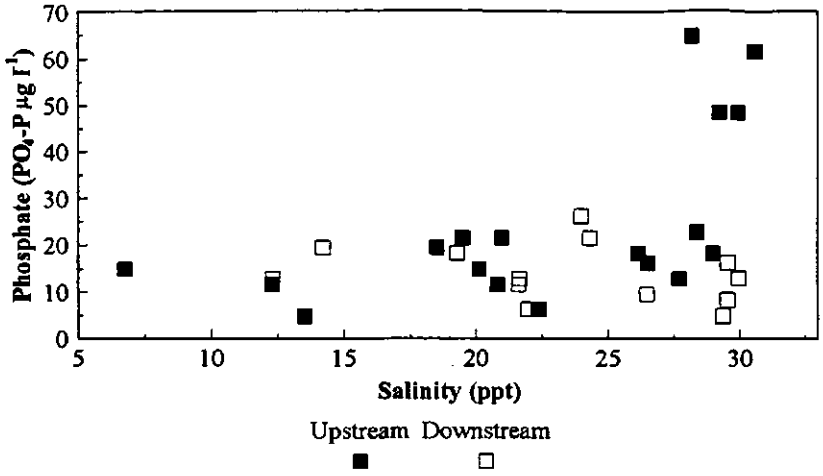

Figure 4.8. Orthophosphate concentration against salinity for samples from the Tamar Estuary

4.3.3. Nutrient Variability in Sutton Harbour

The mean spring and neap tidal ranges for Sutton Harbour (Plymouth Devonport) are 4.7 m and 2.2 m respectively. These differing tidal ranges lead to variations in mixing and advection, the more energetic spring tides cause greater mixing of the water column and bring a greater volume of water across the harbour/estuary interface. Therefore the spring-neap tidal cycle, with a period of about 14.5 days causes sympathetic variations in water quality. Figures 4.9 and 4.10 show the surface and bottom sample salinities inside the harbour (SH1-SH3) at neap and spring tides. The seasonal variations in salinity were dominated by pulses of brackish water during the winter periods when the River Plym was in spate (flood), particularly during the January 1993 and February 1994 surveys, leading to a high degree of stratification within the water column. Whilst during the summer there is greater mixing and a lower river flow, this leads to an increase in surface salinity and a reduced difference between surface and bottom water salinities i.e. July surveys.

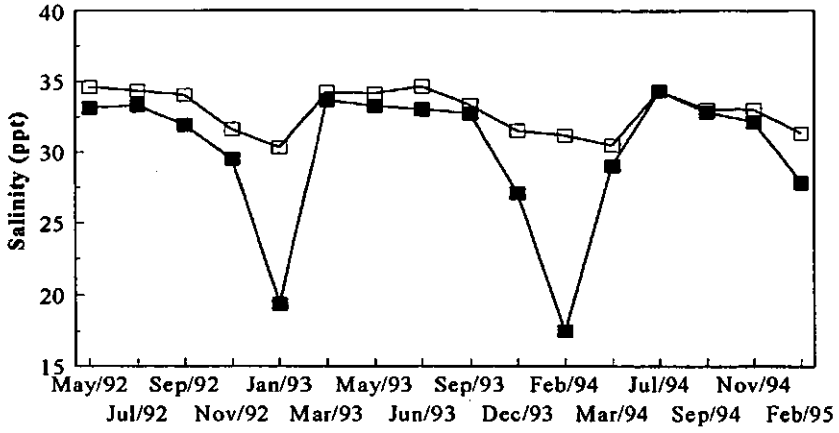

Figure 4.9. Salinity at neap tide. Filled squares represent samples near surface and open squares near bottom.

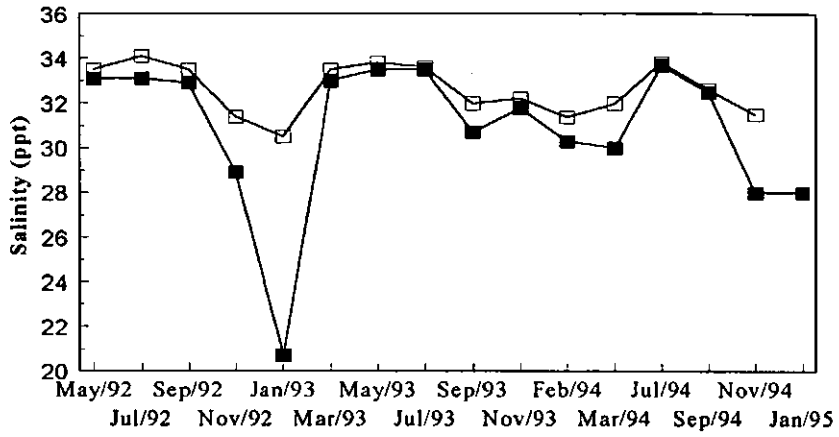

Figure 4.10. Salinity at spring tide. Filled squares represent samples near surface and open squares near bottom.

TON and phosphate concentrations at high and low water at the neap tide are shown in Figures 4.11 and 4.12, and 4.13 and 4.14 respectively. The response of the nutrient concentrations to the winter pulses of brackish water was particularly evident when increased stratification increased the surface-bottom concentration gradients. TON and phosphate concentrations exhibited distinctive seasonality, with surface and bottom maxima between November and March and minima between May and September each year. Surface concentrations of both nutrients were generally greater than bottom concentrations inside and outside the harbour (SH4) with maximum vertical differences between November and March and minimum vertical differences between May and September, these patterns are concordant with salinity and primary productivity variations.

The response to the brackish water from the Plym on TON and phosphate was less clearly evident at the spring tide, as shown in Figures 4.15 and 4.16 for TON and Figures 4.17 and 4.18 for phosphate. Seasonal cycles in nutrient concentration were apparent, with maxima between November and March and minima between May and September each year. Unseasonally high rainfall before the spring survey of September 1993 resulted in higher TON concentrations compared to the levels found the previous week at the neap tide, as well as very high concentration of phosphate in November 1993 and 1994. A reduction in river flow between the neaps and springs in February 1994 lowered the orthophosphate concentration considerably [5]. As for the neap surveys surface nutrient concentrations were generally higher than those for bottom water samples.

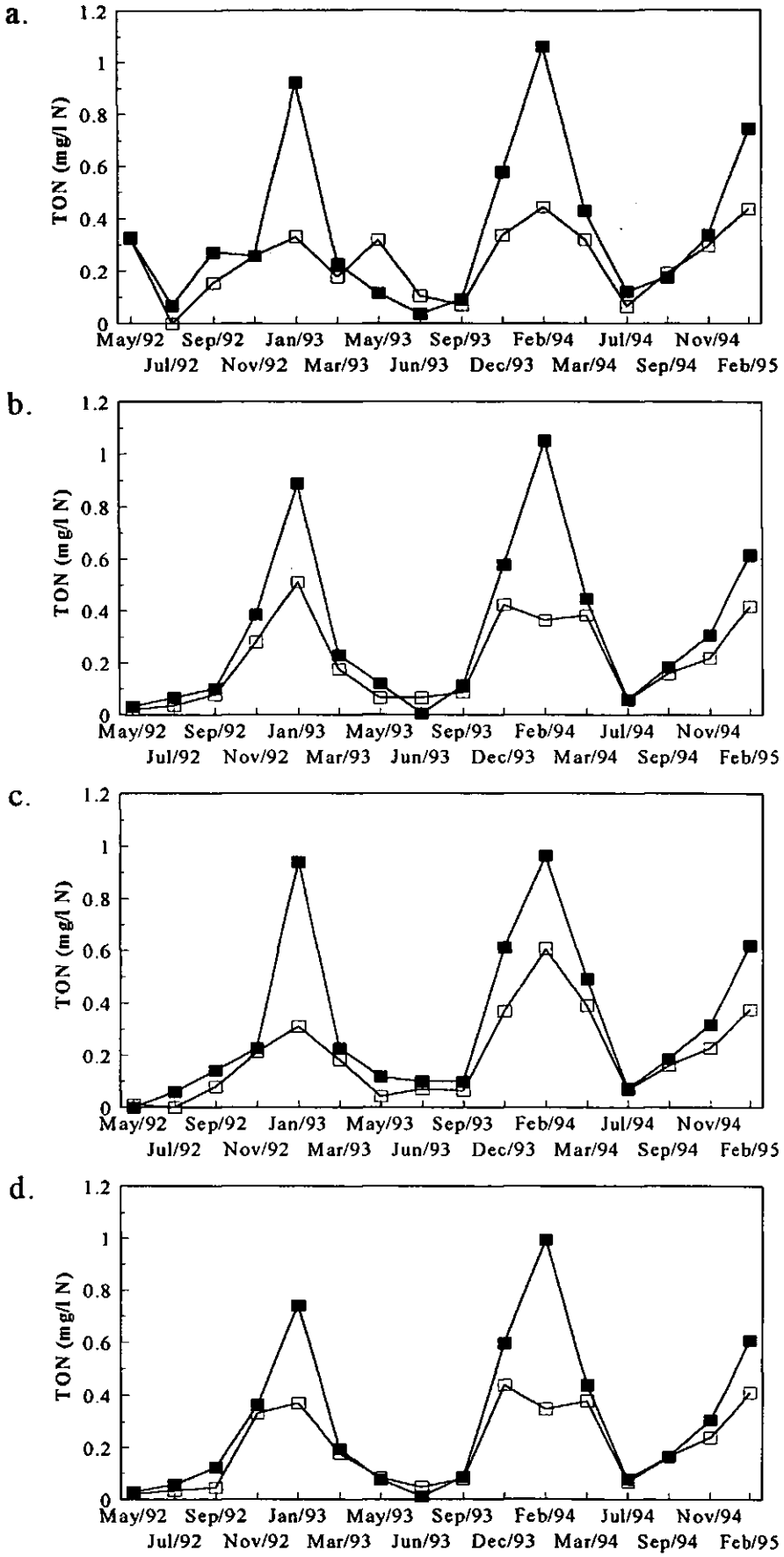

Figure 4.11. Concentrations of TON at neap tide, high water for: a. SH1, b. SH2, c. SH3, d. SH4. Filled squares represent samples near-surface and open squares near bottom.

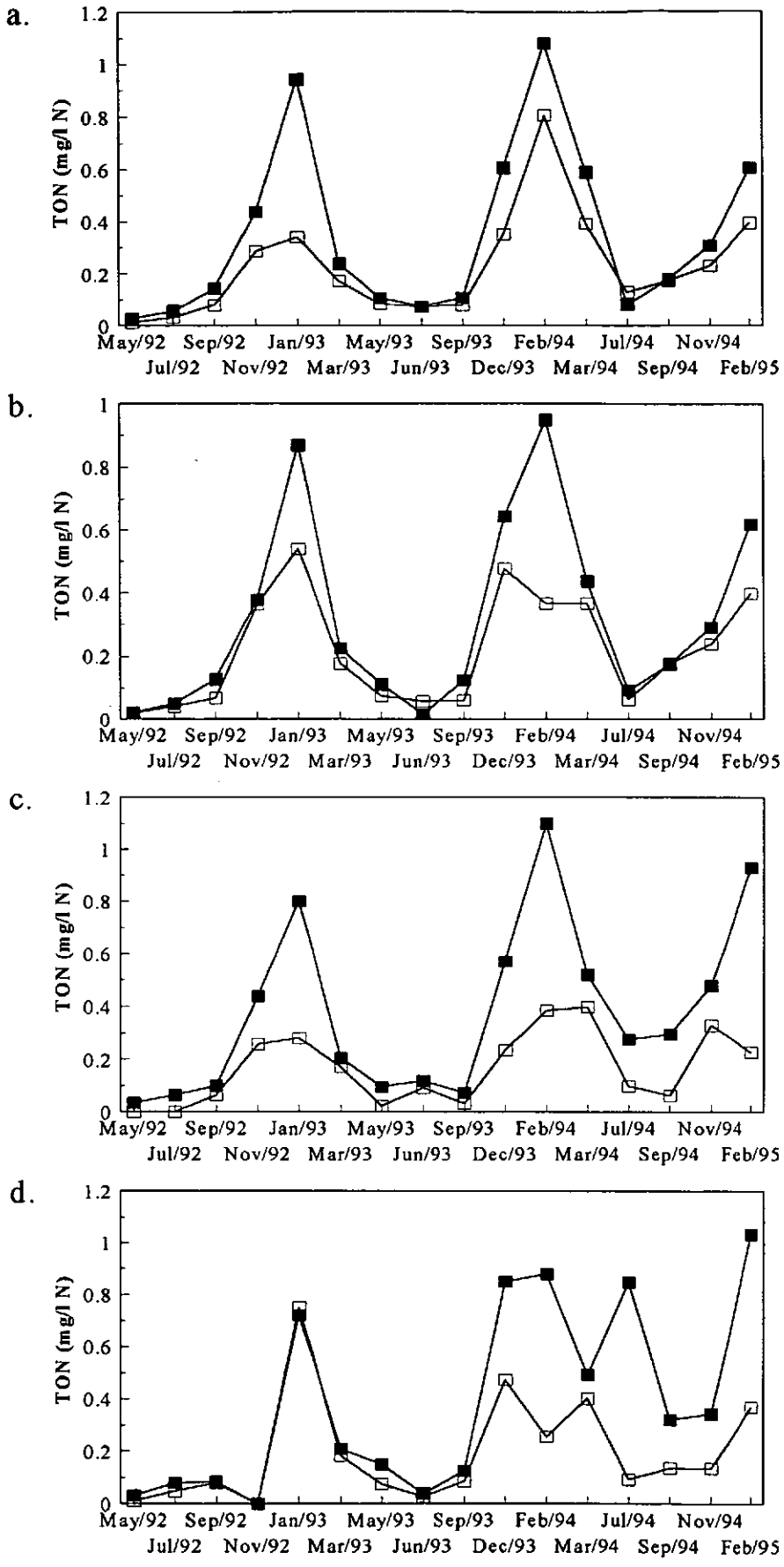

Figure 4.12. Concentrations of TON at neap tide, low water for: a. SH1, b. SH2, c. SH3, d. SH4. Filled squares represent samples near-surface and open squares near bottom.

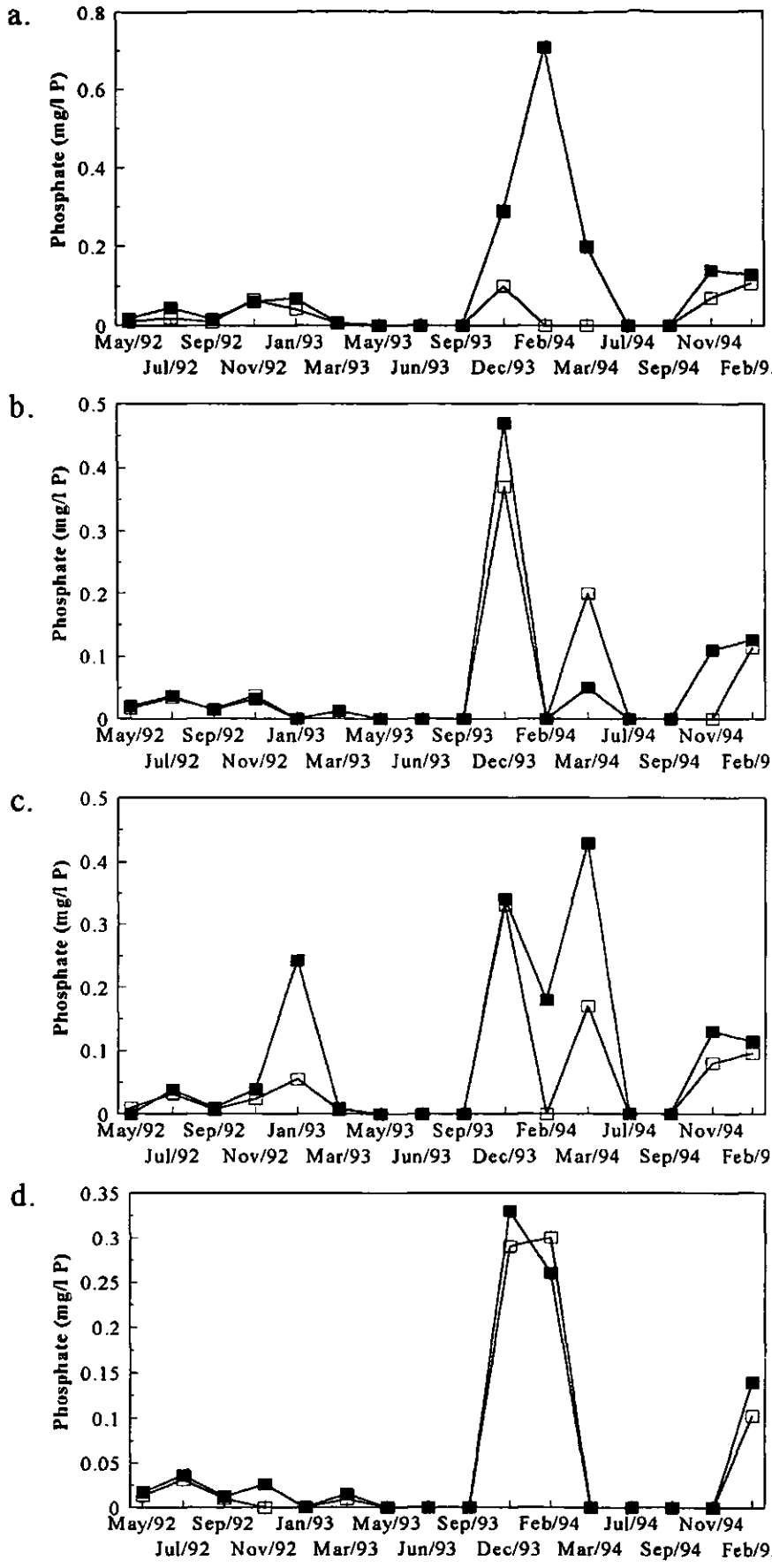

Figure 4.13. Concentrations of orthophosphate at neap tide, high water for: a. SH1, b. SH2, c. SH3, d. SH4. Filled squares represent samples near-surface and open squares near bottom.

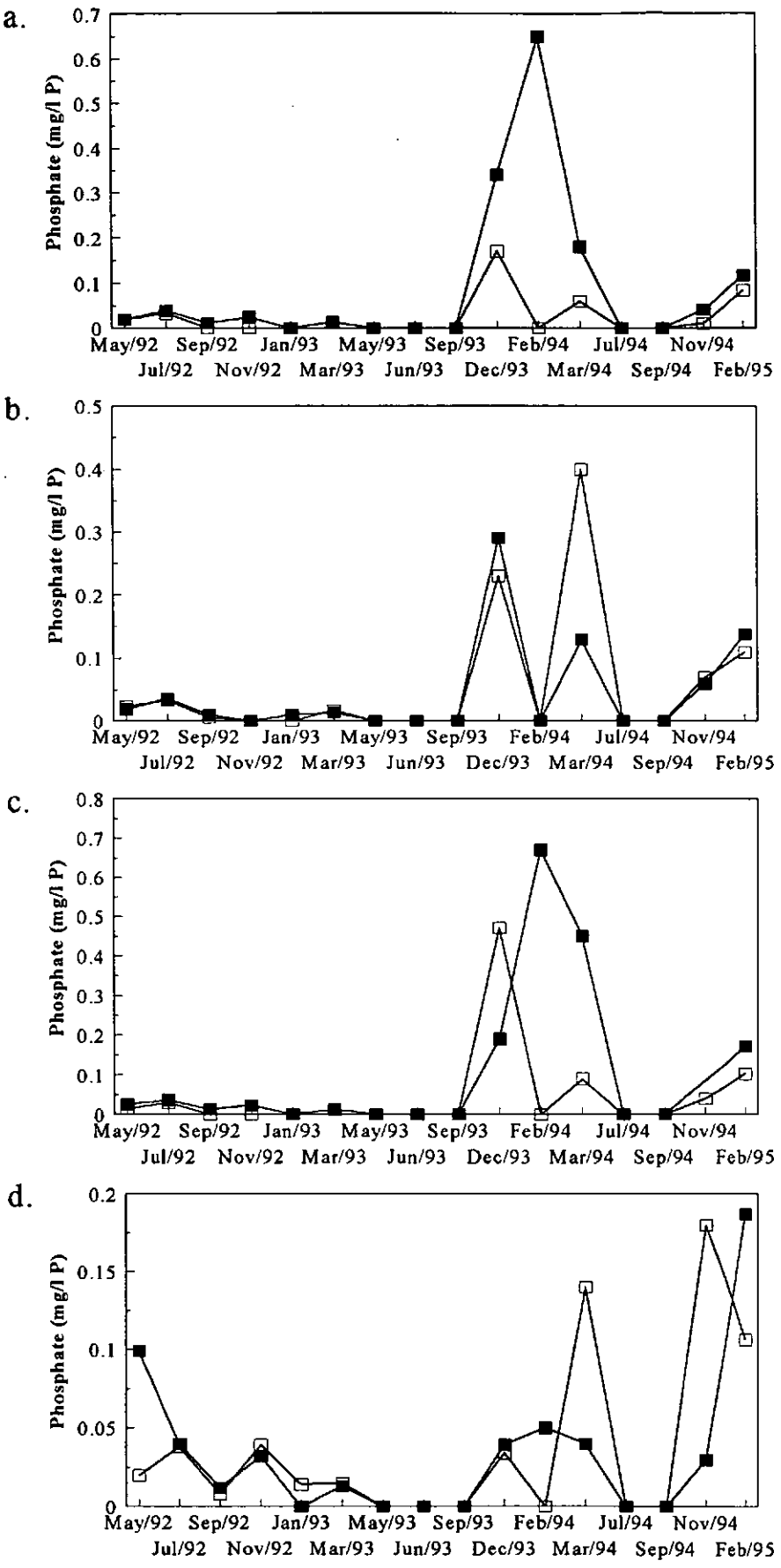

Figure 4.14. Concentrations of orthophosphate at neap tide, low water for: a. SH1, b. SH2, c. SH3, d. SH4. Filled squares represent samples near-surface and open squares near bottom.

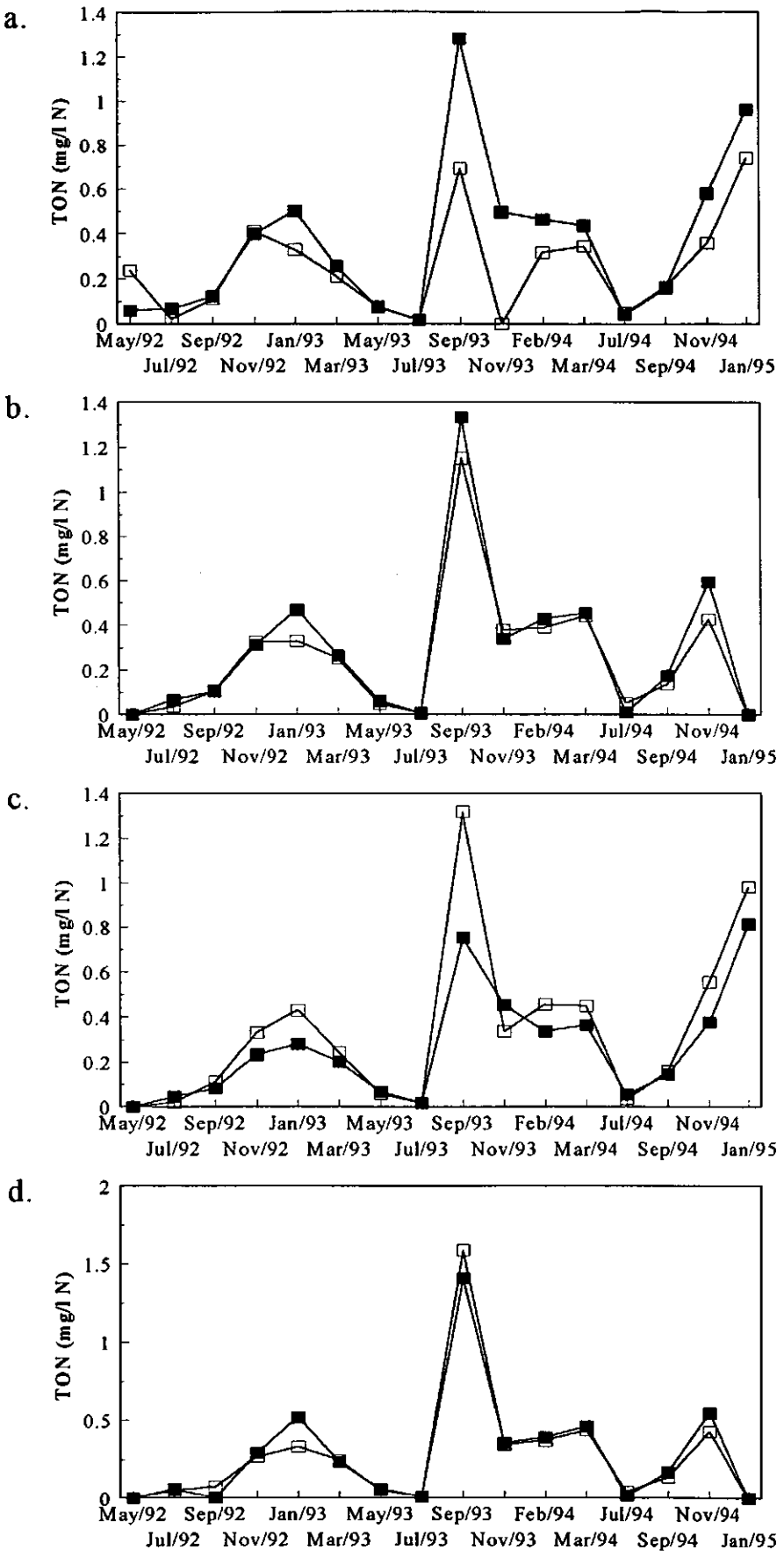

Figure 4.15. Concentrations of TON at spring tide, high water for: a. SH1, b. SH2, c. SH3, d. SH4. Filled squares represent samples near-surface and open squares near bottom.

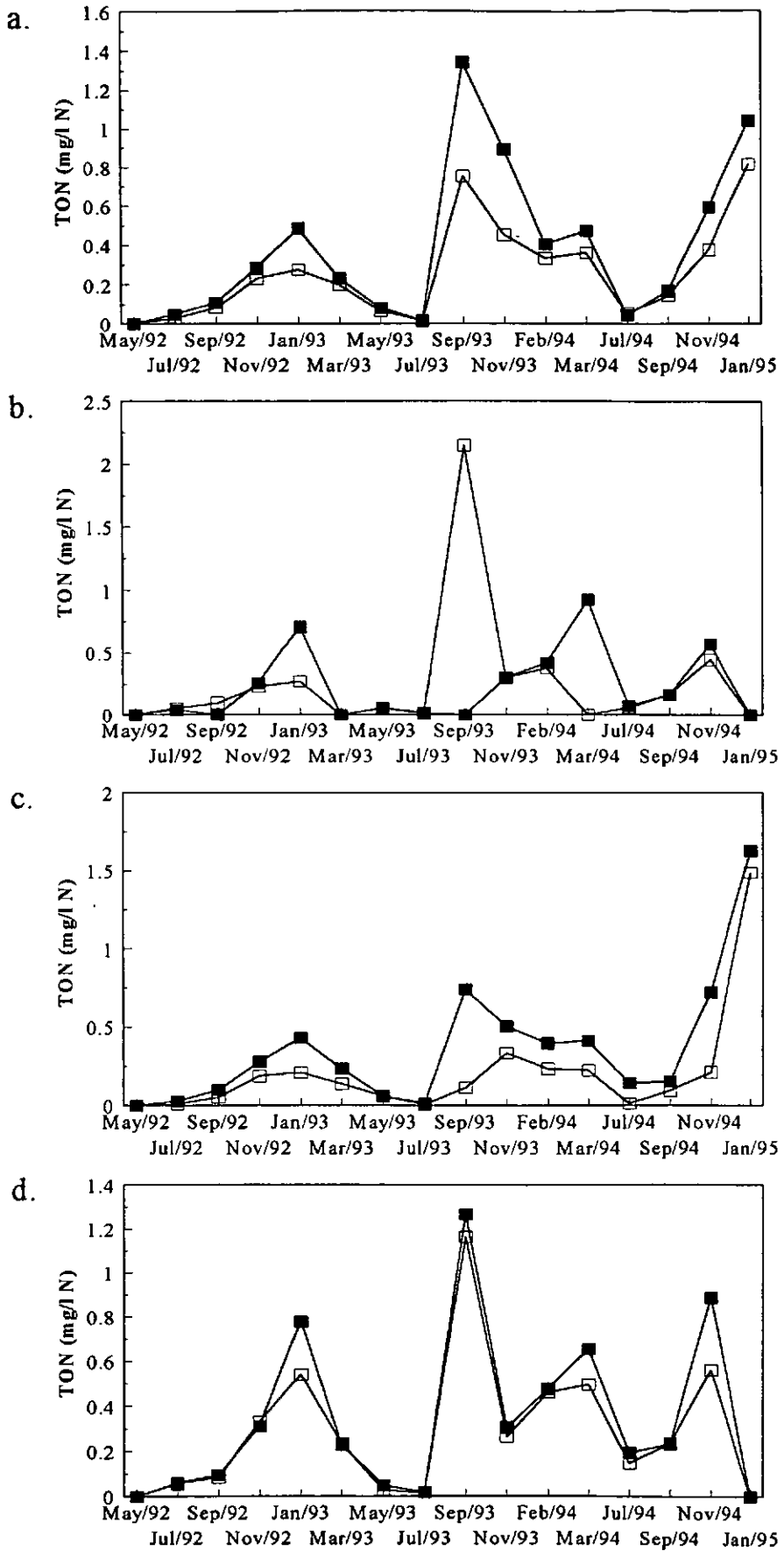

Figure 4.16. Concentrations of TON at spring tide, low water for: a. SH1, b. SH2, c. SH3, d. SH4. Filled squares represent samples near-surface and open squares near bottom.

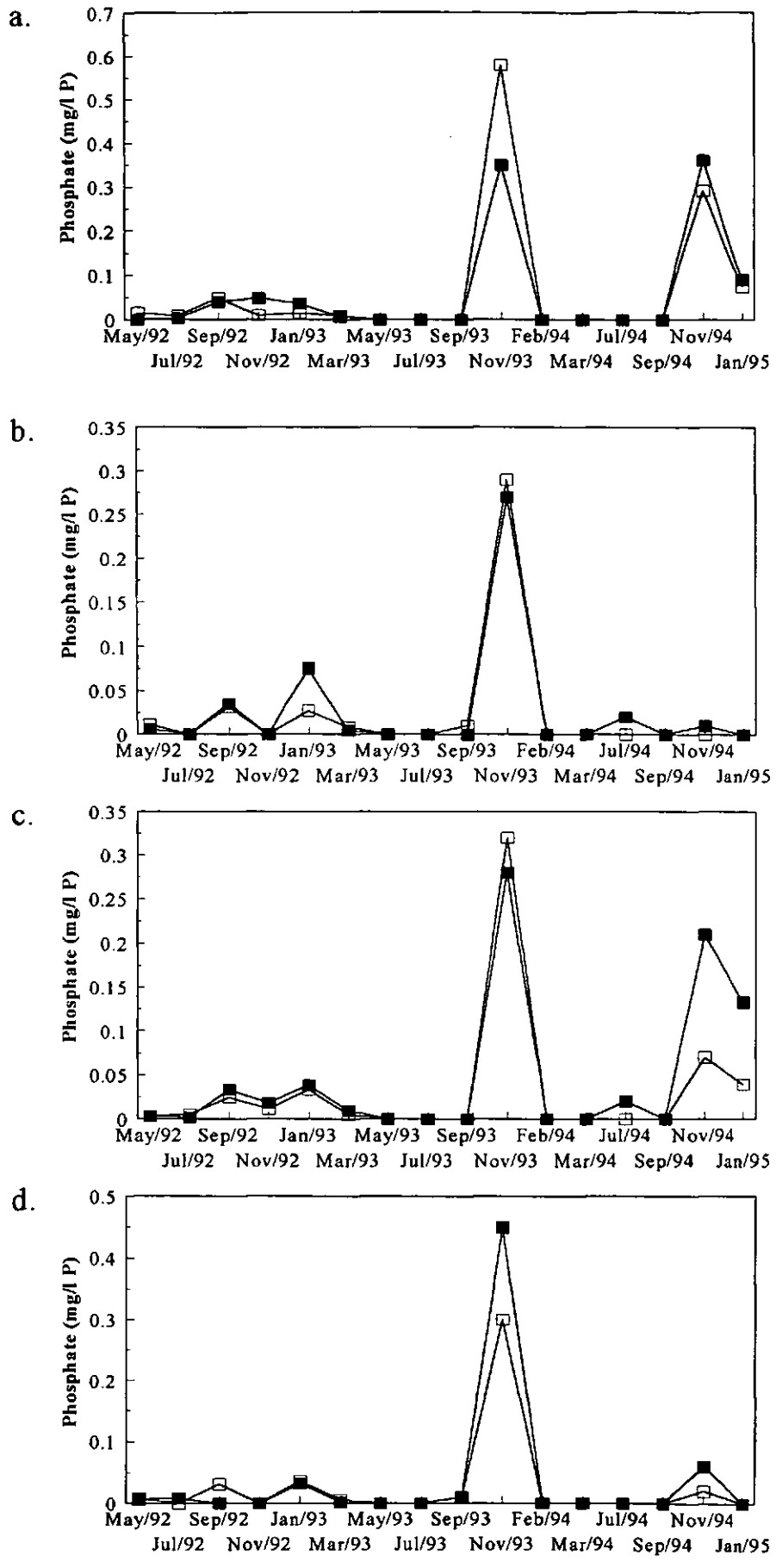

Figure 4.17. Concentrations of orthophosphate at spring tide, high water for: a. SH1, b. SH2, c. SH3, d. SH4. Filled squares represent samples near-surface and open squares near bottom.

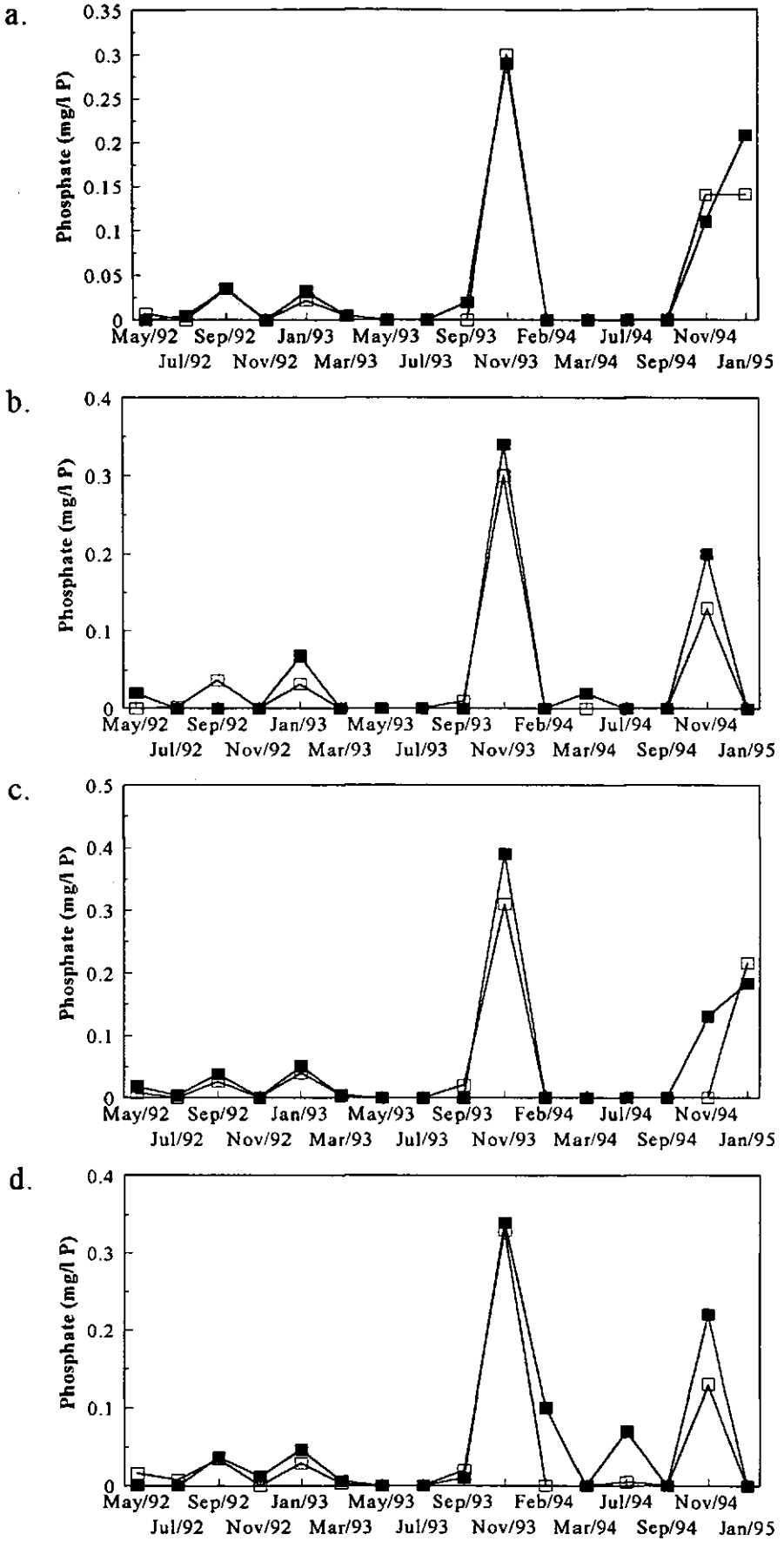

Figure 4.18. Concentrations of orthophosphate at spring tide, low water for: a. SH1, b. SH2, c. SH3, d. SH4. Filled squares represent samples near-surface and open squares near bottom.

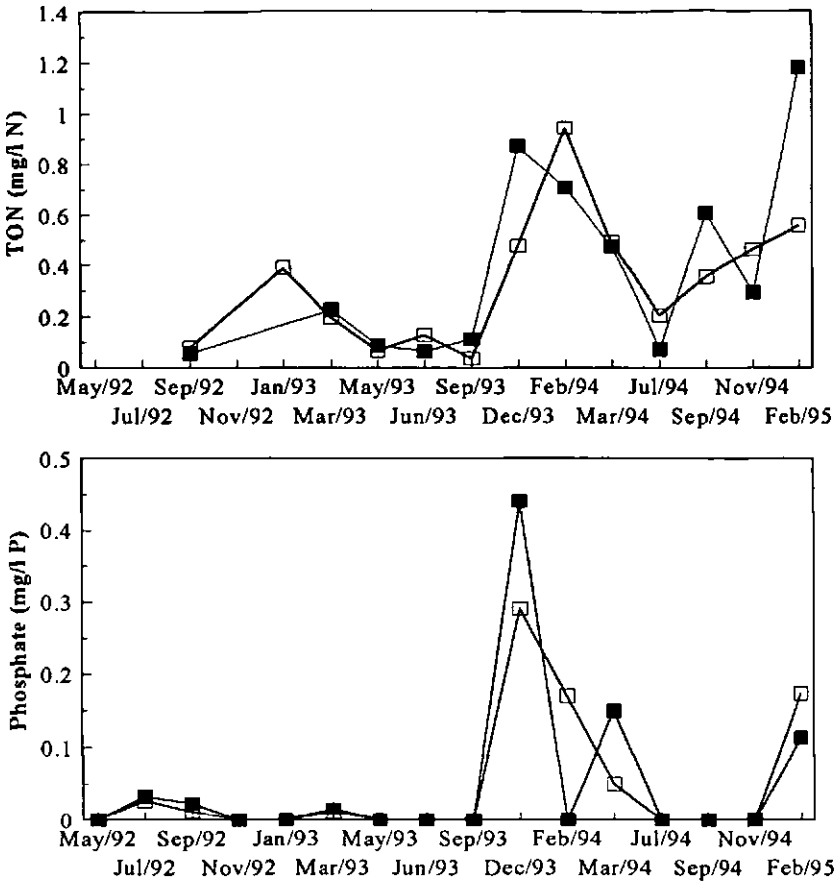

Figure 4.19. Concentrations of TON and orthophosphate at neap tide for samples from the Sound (SH5). Open squares represent samples at high water and filled squares low water.

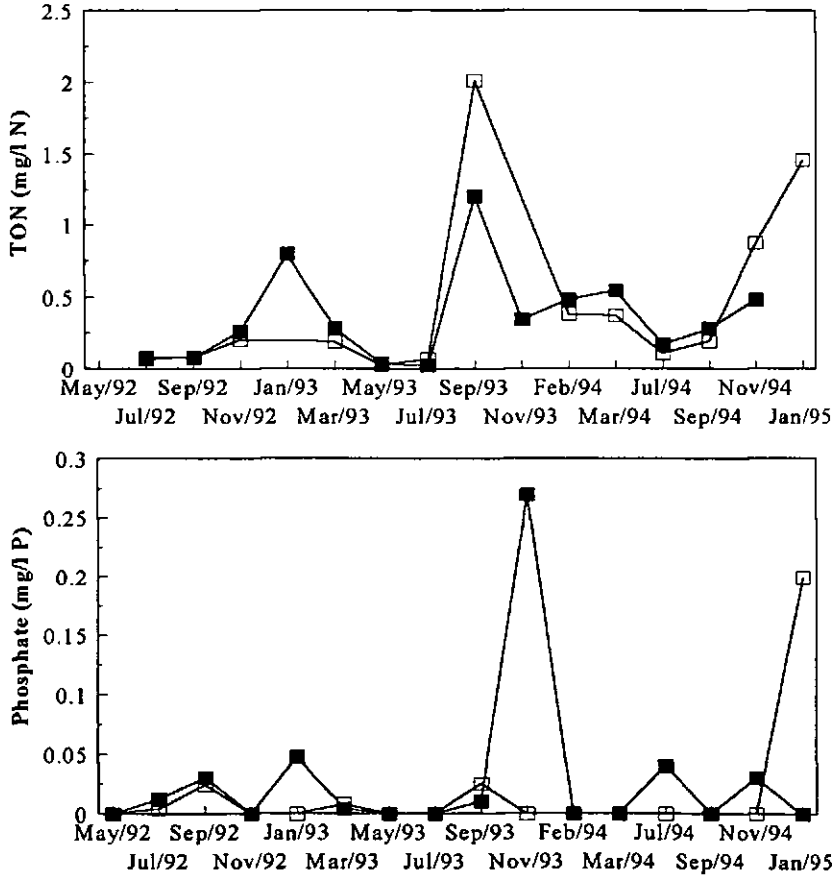

Figure 4.20. Concentrations of TON and orthophosphate at spring tide for samples from the Sound (SH5). Open squares represent samples at high water and filled squares low water.

Seasonal variability in dissolved nutrient concentration was driven to varying extents by seasonal cycles in river flow (a nutrient source) and seasonal variability in primary production (a nutrient sink). If the main source of nutrients is the River Plym, then plots of dissolved nutrient concentration against salinity should be linear if there is no other alternative source or sink. Correlation coefficients (r^2) for TON and orthophosphate concentration plotted against salinity for samples taken at the neap and spring tides, surface and bottom at high and low waters inside the harbour (SH1-SH3) are shown in Table 4.3.

Table 4.3. Correlation coefficients (r^2) for nutrient concentration against salinity.

NUTRIENT	NEAP HW		NEAP LW		SPRING HW		SPRING LW	
	Surface	Bottom	Surface	Bottom	Surface	Bottom	Surface	Bottom
TON	0.897	0.553	0.918	0.718	0.124	0.265	0.065	0.023
Phosphate	0.478	0.180	0.108	0.137	0.035	0.041	0.015	0.000

TON concentrations show a strong inverse correlation with salinity in surface and bottom waters at the neap tide, although there was greater correlation for surface samples with salinity as shown in Figures 4.21 and 4.22. For samples taken at the spring tide there was less of a correlation with salinity because of the greater mixing and therefore lower extent of stratification caused by the more energetic tide. Phosphate concentration was found to show no correlation with salinity at either the neap or spring tide which means that phosphate was entering the system either via a source other than that of the Plym, possibly from anthropogenic inputs such as the sewage outfalls in the Sound and/or the release of phosphate from the sediments, as discussed in Section 4.3.2.

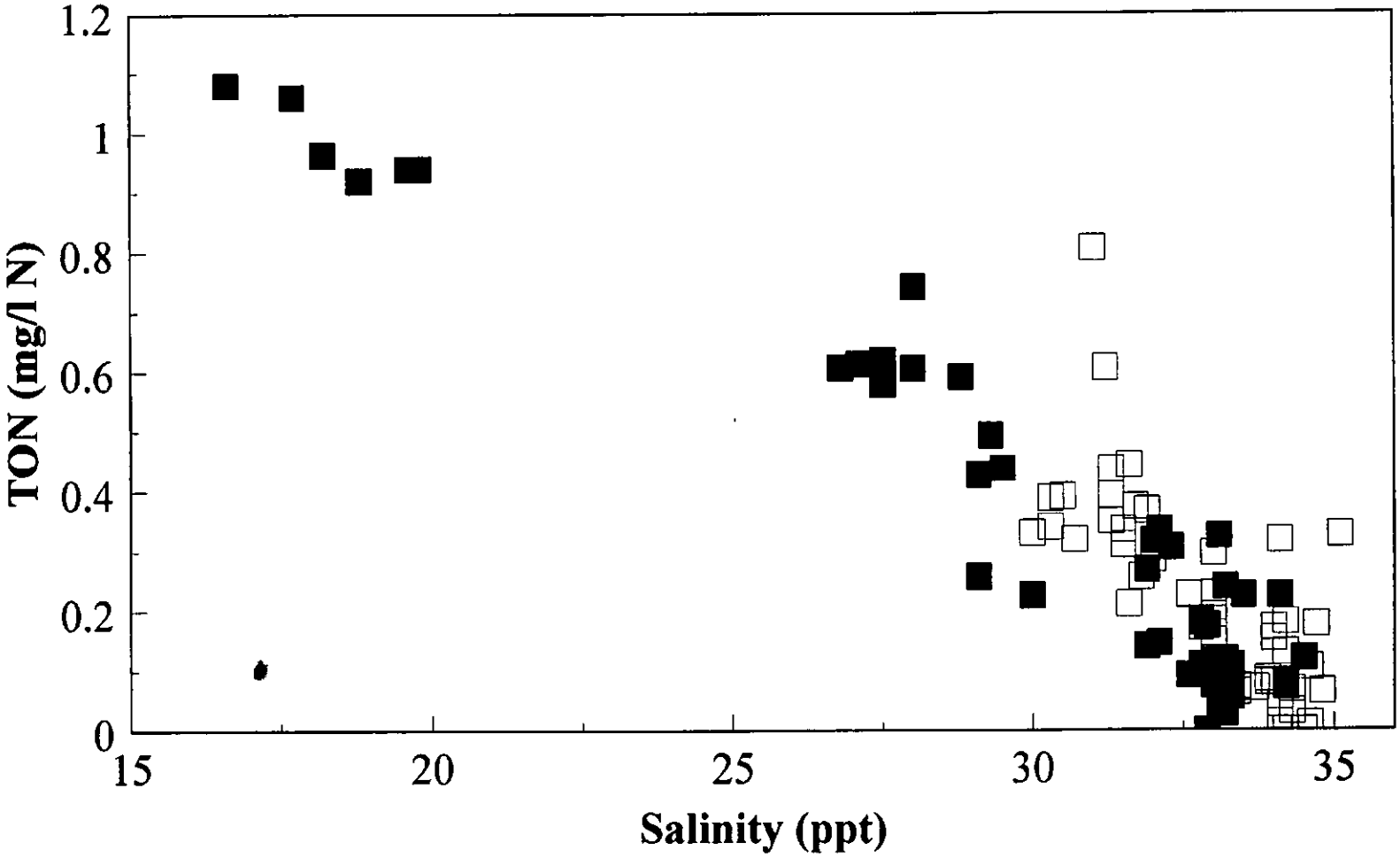

Figure 4.21. TON concentration against salinity for samples at the high water neap tide. Filled squares represent samples near surface and open squares near bottom.

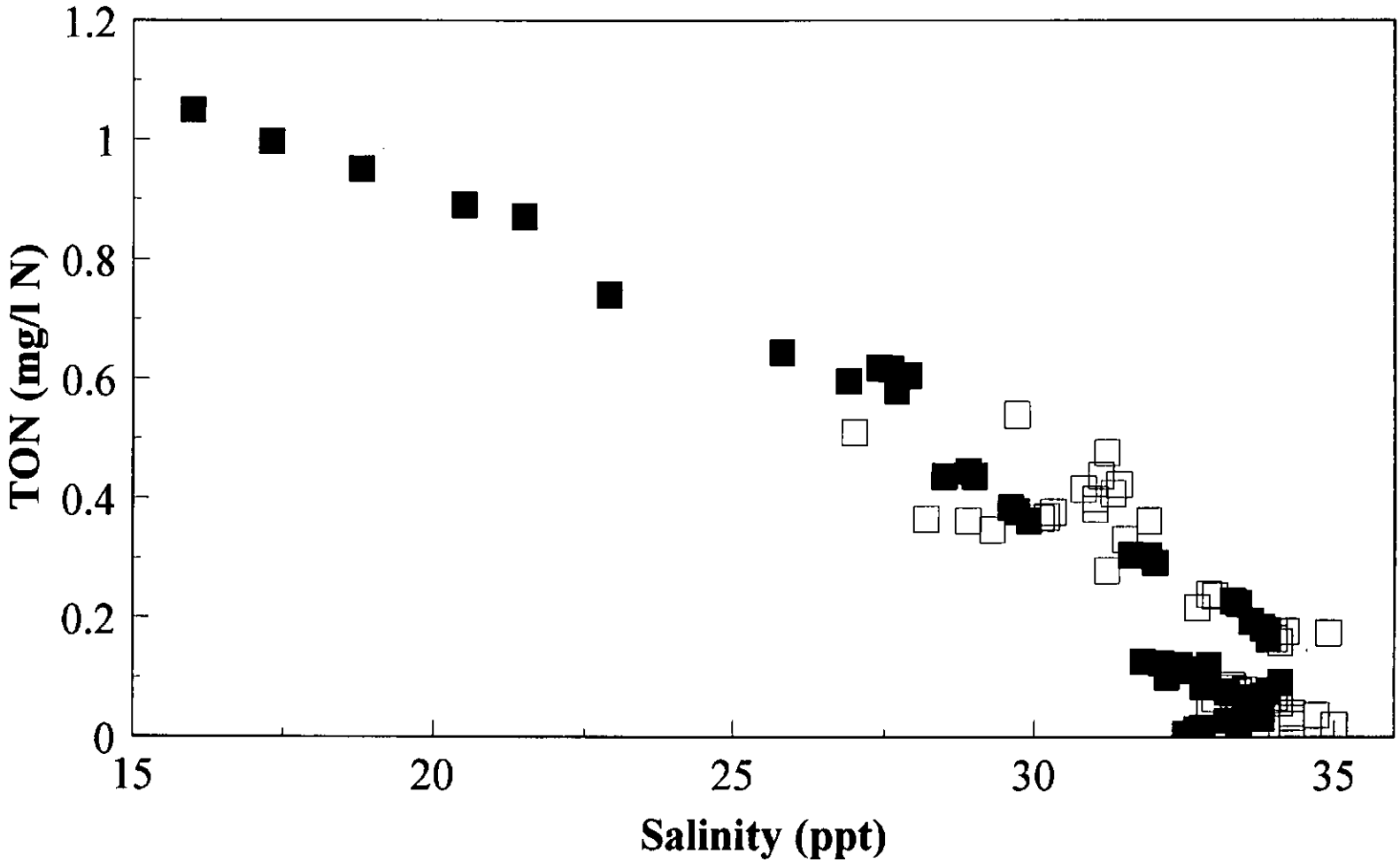

Figure 4.22. TON concentration against salinity for samples at the low water neap tide. Filled squares represent samples near surface and open squares near bottom.

4.4. CONCLUSIONS

1. The FI manifold optimised in Chapter 2 for the determination of nitrate is suitable for the shipboard analysis of riverine and estuarine waters over the range 0 - 5 mg l^{-1} N.
2. The salinity compensation FI manifold developed in Chapter 3 for the determination of orthophosphate is suitable for the shipboard analysis of riverine and estuarine waters over the range 0 - 0.1 mg l^{-1} P.
3. FI is suitable for survey work carried out on board a ship because the instrumentation is portable quick to assemble and is flexible in terms of chemistries and linear ranges.
4. There is seasonal variability in TON concentration in both the Tamar Estuary and Sutton Harbour as well as a strong inverse correlation with salinity.
5. The buffering of phosphate by the sediments and suspended solids leads to a relatively constant concentration throughout the Tamar Estuary (20 μg l^{-1}), although anthropogenic sources to the lower 5 km is evident.

Chapter Five
Determination of Nitrate in the North Sea

5. DETERMINATION OF NITRATE IN THE NORTH SEA

5.1. INTRODUCTION

This chapter discusses shipboard validation of the FI method in coastal waters with regular sampling over three sections of the Humber-Tweed coastal track and compares the results with those obtained using the traditional shipboard AutoAnalyzer® method. Additional field data collected during the cruise are related to nitrate levels and marine biogeochemical processes.

5.1.1. Cruise CH119a

A berth was obtained onboard *R. R. S. Challenger* in June 1995 for a cruise of the North Sea along the North East English coastline, stretching from the Humber Mouth in the South to the Tweed in the North. The cruise was commissioned to form part of the River-Atmosphere-Coast Study (RACS) which is part of the Land-Ocean Interaction Study (LOIS). The LOIS Community Research Project (CRP) is a collaborative multidisciplinary study which is being undertaken by scientists from the Natural Environmental Research Council (NERC), Higher Education Institutes (HEIs) and other organisations. It is built upon the results and expertise of previous and existing NERC programmes, such as the North Sea Project (NSP), Biogeochemical Ocean Flux Study (BOFS) and Terrestrial Initiative in Global Environmental Research (TIGER). The aim of the LOIS CRP is to provide for the first time an integrated, holistic view of how coastal ecosystems work, and how they are likely to respond to future changes caused by the activities of man on land and at sea.

The main cruise objectives for RACS are:

1. To quantify hydrodynamical transports and the processes affecting transformations, interactions and fates of particles, biogeochemically important elements and representative contaminants from land sources to the coastal zone.

2. To provide the first integrated environmental data base for a UK coastal region covering seasonal cycles and interannual variability and incorporating measurements of the fluxes of materials and rates of biological productivity.

3. To generate new quantitative understanding of estuarine and coastal zone processes controlling the fluxes and reactivities of both natural and anthropogenic materials.

4. To provide models of these processes as building blocks for comprehensive coastal zone system models which will realistically predict the affects of future environmental change.

Cruise CH119a was perfectly suited to shipboard validation of the developed FI method for the determination of nitrate in coastal waters. It gave an opportunity to assess the system for both its physical and analytical robustness. In addition, FI could be compared to the AutoAnalyzer® system which has been traditionally used at sea for the determination of nutrients. *R. R. S. Challenger* was a fully equipped scientific research vessel (54.3 m in length) operated by NERC. The 119th cruise was operated by 18 crew-members and officers and involved a total of 15 scientists.

5.2. EXPERIMENTAL

5.2.1. Reagents and Standards

All solutions were prepared one day prior to the cruise in accordance with section 2.2.1.

5.2.2. Instrumentation

The FI system shown in Figure 2.12 was used throughout the cruise. A non-toxic supply of surface sea water was pumped up from 4 metres depth into the laboratory. This water supply was attached to a filtration unit (Figure 5.1.) described by Morris et al. [208]. It consisted of a machined 'Perspex' block (75 x 75 x 40 mm) containing a nylon net and membrane filter through which a primary seawater supply was pumped at up to 10 l min^{-1}. The sample line of the FI manifold was attached to the filtration block via a stainless steel capillary tube and samples were taken at 15 minute intervals.

5.2.3. Cruise Track

The track for cruise CH119a is shown in Figure 5.2, beginning in the Humber Mouth at Spurn Head on the 8th of June 1995 and ending at Grimsby on the 12th of June.

5.3. RESULTS AND DISCUSSION

5.3.1. Overall Performance

Samples were analysed at intervals on three separate sections of the Humber-Tweed Coastal Track: 1, Holy Island and the Tweed, 2, The Tyne and Wear, and 3, Bridlington Bay and Humber/Wash.

The FI system performed continuously with no problems over the three track sections, being of 8, 11 and 10 hours duration respectively and analysed up to 120 samples. Nitrate standards (0 - 22.5 μmol l^{-1}) were analysed before, during and after the cruise. Table 5.1 shows the calibration lines and the reproducibility of the absorbance signal throughout the cruise. There was no significant difference between the three calibration lines at the 95 % confidence level as determined by three separate paired t-tests. In addition to these calibrations one of the five standards (0, 1, 7.5, 15, or 22.5 μmol l^{-1}) was analysed every

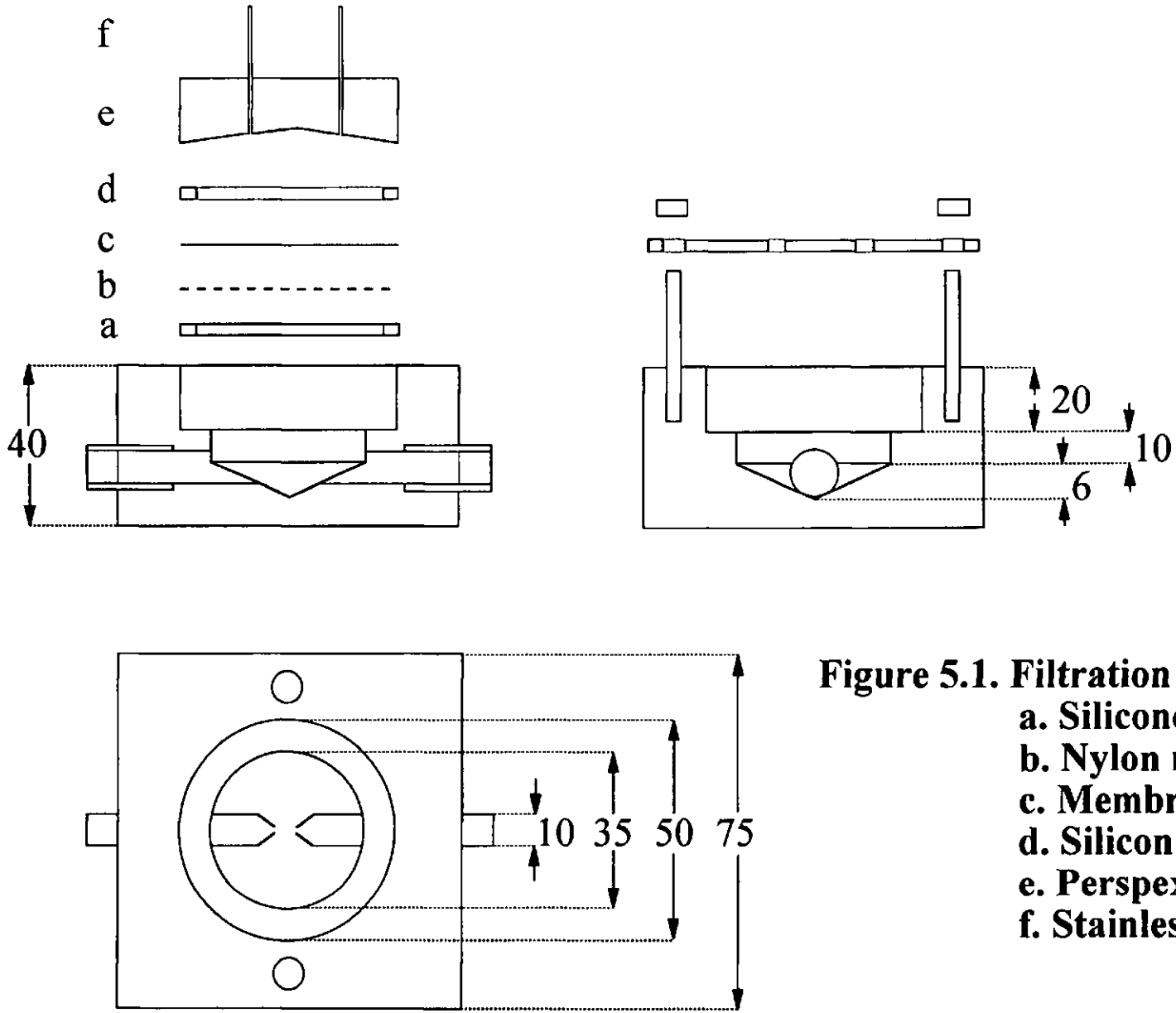

Figure 5.1. Filtration unit.
a. Silicone rubber washer,
b. Nylon net,
c. Membrane filter,
d. Silicon rubber washer,
e. Perspex cylinder,
f. Stainless steel capillary tube

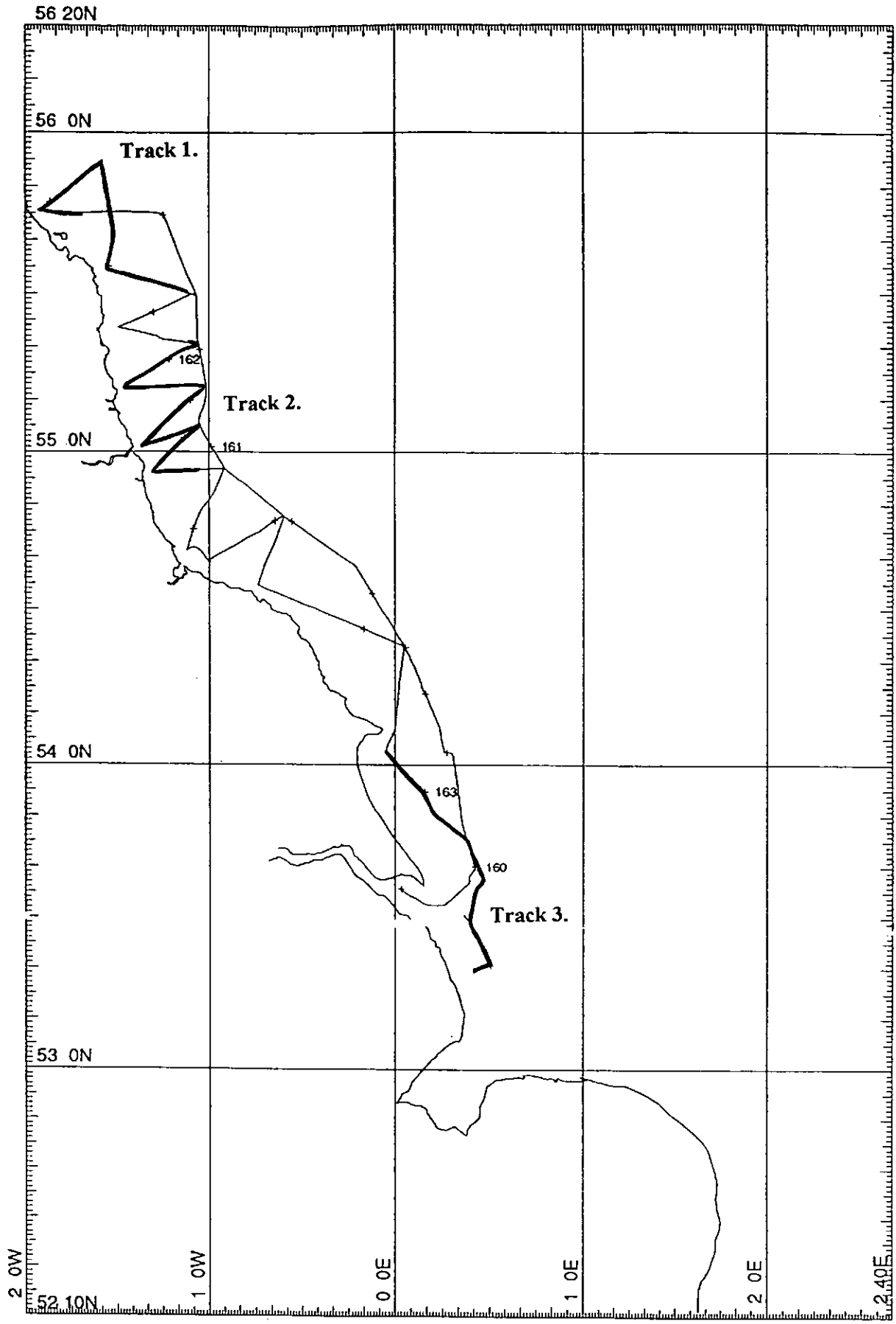

Figure 5.2. CH119a cruise track.

hour to validate the chemical and physical performance of the system and to allow for diagnosis of any problems at an early stage. Again there was no significant difference between these individual results and those from the calibration runs.

Table 5.1. Calibration data for nitrate standards run on the cruise.

NITRATE (μmol l^{-1})	MEAN ABSORBANCE (A.U.)		
	10/06/95	10-11/06/95	11-12/06/95
0	0.004	0.002	0.004
1	0.011	0.011	0.013
7.5	0.060	0.057	0.061
15	0.127	0.128	0.120
22.5	0.182	0.185	0.185
Calibration Equation	y (AU) = 0.003 + 0.008 (μmol l^{-1})	y (AU) = 0.000 + 0.008 (μmol l^{-1})	y (AU) = 0.003 + 0.007 (μmol l^{-1})
r^2	0.9988	0.9981	0.9991

Figures 5.3, 5.4 and 5.5 show the TON levels found both by the FI method and the Technicon AutoAnalyzer II® over the three track sections. There is good correlation between the TON levels determined by both systems during track 3 where the TON concentrations are high (up to 20 μmol l^{-1}). For tracks 1 and 2 however where the TON levels were much lower, the FI method gave tenfold higher results than the AutoAnalyzer® method. The AutoAnalyzer® was reporting levels in the ranges of 0 - 0.11 and 0 - 0.13 μmol l^{-1} TON for tracks 1 and 2 respectively, which is close to the detection limit of the method.

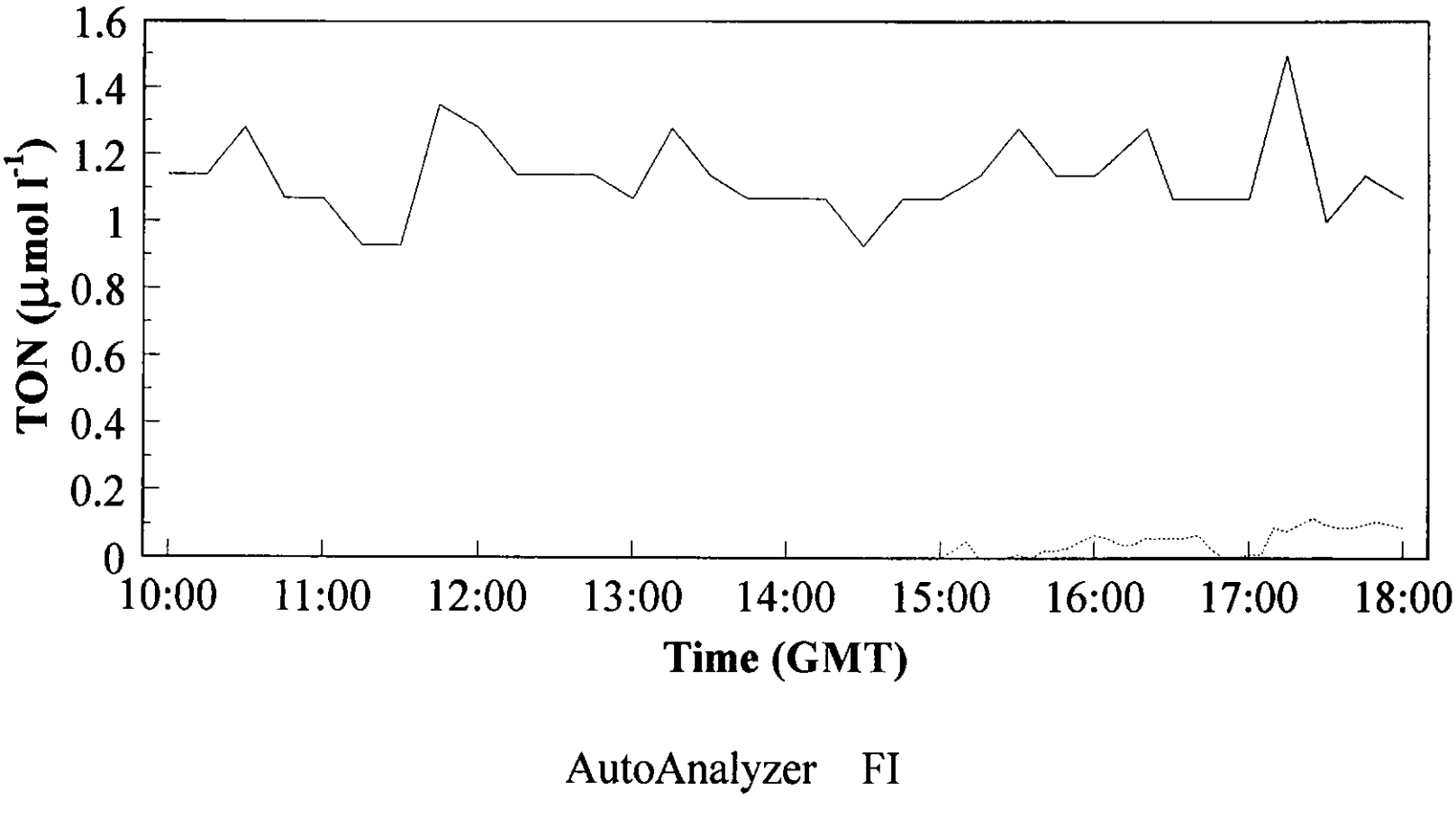

Figure 5.3. TON levels determined by FI and the AutoAnalyzer on the 10th June 1995 on track 1.

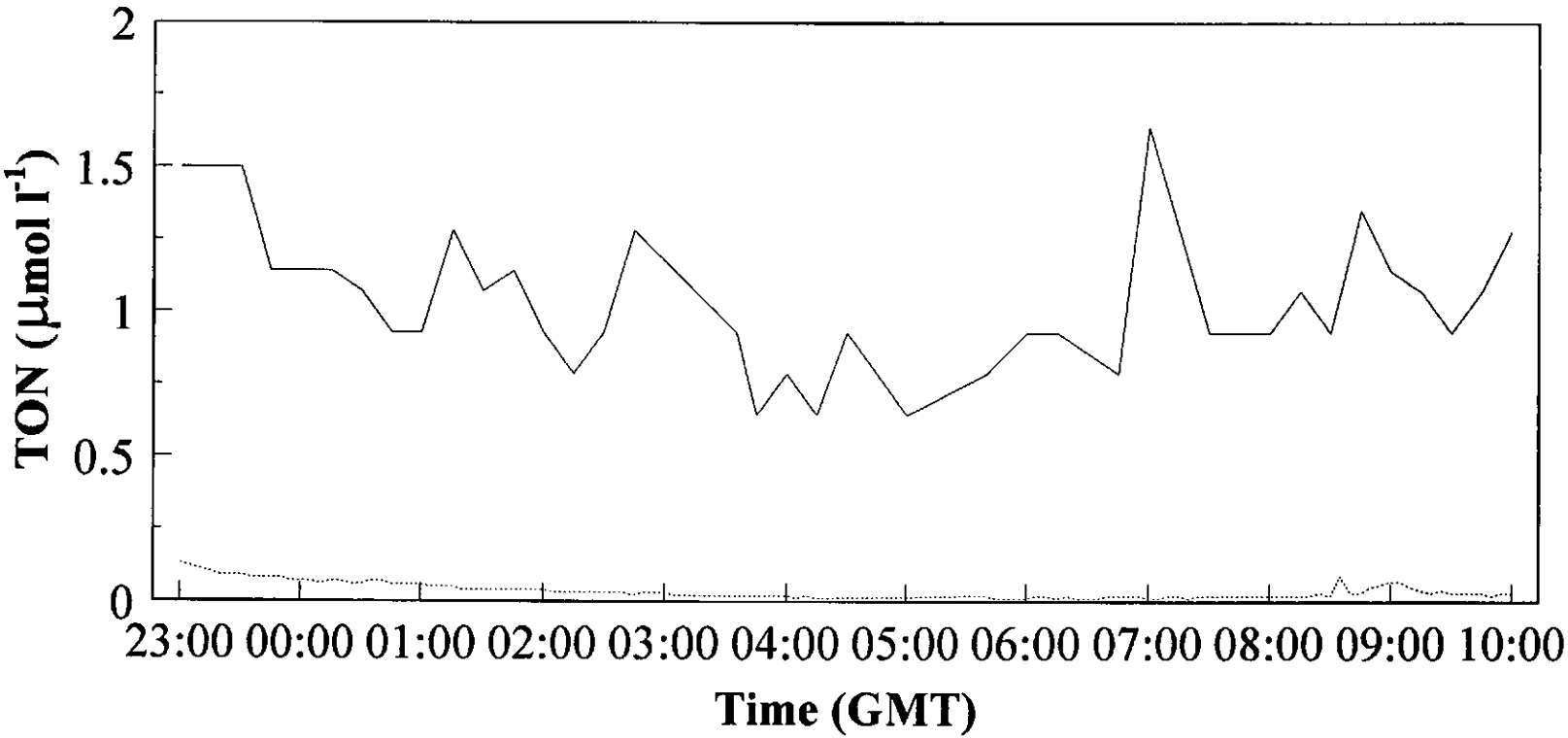

Figure 5.4. TON levels determined by FI and the AutoAnalyzer on the 10th-11th June 1995 on track 2.

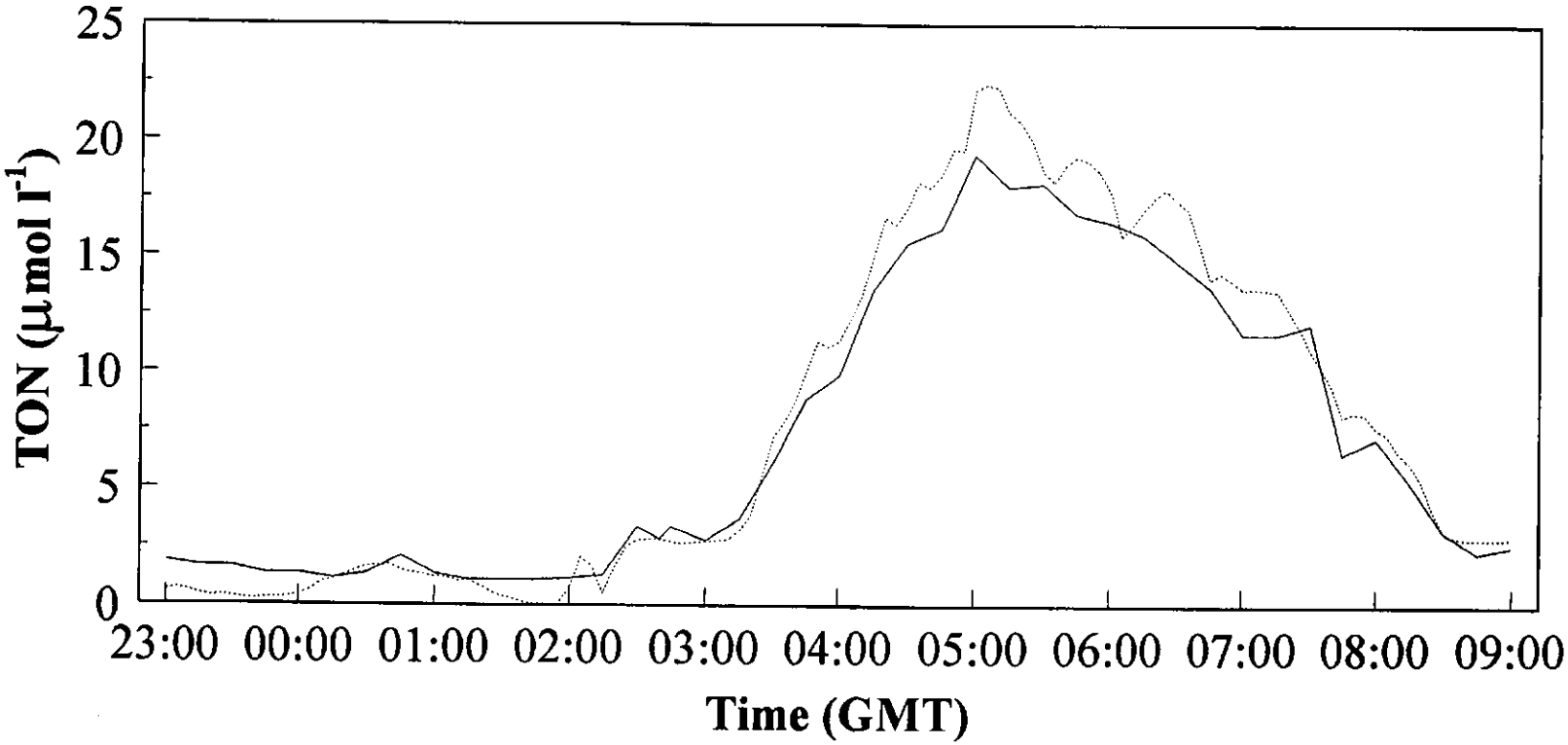

Figure 5.5. TON levels determined by FI and the AutoAnalyzer on the 11th-12th June 1995 on track 3.

5.3.2. Comparative Analytical Performance of FI and Air Segmented Continuous Flow Analyzer (AutoAnalyzer®)

Figure 5.6. shows the AutoAnalyzer® manifold used for the determination of nitrate during cruise CH119a. The manifold is more complex than the FI manifold, with more streams (eight) pumped at faster flow rates. The continuously aspirated sample was first air-segmented before being merged with the ammonium chloride carrier stream and the air bubbles were then removed at a debubbler before passing the sample through the cadmium coil. Air bubbles were reintroduced after the column before mixing with the separate sulphanilamide and NINED streams. A second debubbler was incorporated prior to the flow cell. The copperised cadmium reduction coil used with the AutoAnalyzer® was made of a 1 m long cadmium wire, as described by Stainton [55]. This type of reductor has a number of drawbacks; it is not easy to completely copperise and there are often many uncopperised 'blank spots' leading to a relatively rapid breakdown. In addition it causes larger dispersion compared with the short granulated cadmium columns and it often degrades with residual particles breaking off, so that an additional filter is needed downstream.

During the cruise a continuous sample was taken from the non-toxic supply via the filtration block, but the whole system had to be stopped to run any nitrate standards. For convenience, and to obtain a continuous sample profile, the operator only calibrated the system at the beginning and at the end of the cruise. Therefore if any problems arose, e.g. due to drift, degradation of the individual reagents or change in the operating temperature, they would not be identified until after the cruise. This is in contrast to the continuous calibration protocol permitted by the FI method. The nitrate levels found on this cruise (which were typical of UK surface waters in summer), showed minimal variation over the 15 minutes between each event and therefore allowed regular between sample calibration without any loss in environmental information. The FI approach not only permits frequent calibration but also means that reagent consumption can be kept to a minimum. In addition,

because of the high particulate loading found in Humber waters (typically >100 mg l^{-1}), the filters of the filtration block had to be changed on an hourly basis [208]. For the FI method where discrete samples were taken every fifteen minutes it was not a problem to stop the flow and replace the filter between samples. For the AutoAnalyzer® method however the bubble pattern would be seriously disrupted if the manifold had to be stopped every hour. Therefore the FI method is better suited to 'continuous' operation over long periods of time (e.g. one tidal cycle of 13 hours), particularly when the sample has a high particulate loading.

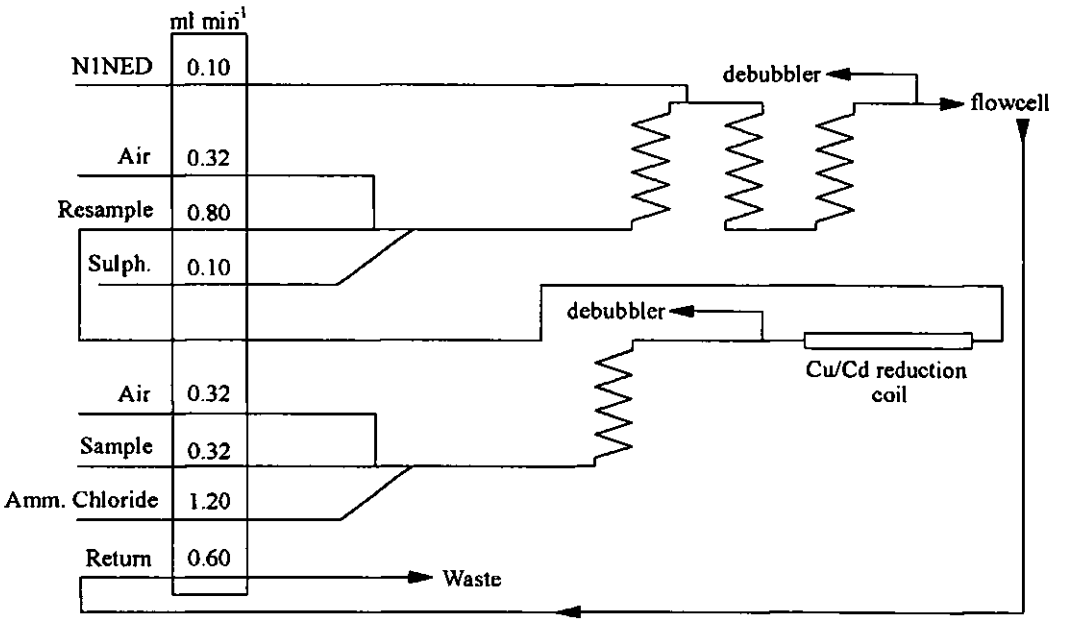

Figure 5.6. AutoAnalyzer® manifold used on cruise CH119a with 1 m long copperised cadmium reduction coil, sulphanilamide (5 g l^{-1} in HCl solution), N1NED (0.5 g l^{-1}) and Ammonium chloride (10 g l^{-1}).

AutoAnalyzer® methods in most situations, must allow the reaction to proceed to completion in order to achieve a steady-state reading at the detector and have limited flexibility, especially in terms of timing. It is difficult to interrupt the system to introduce random samples or standards also, unless preplanned and it is difficult to adapt the system to different chemistries. The primary drawback to the air-segmented systems is the need for a reproducible bubble pattern which can be particularly difficult to achieve in the rough conditions likely to be encountered at sea. Air bubbles are compressible, thereby creating

pulsations in the flowing stream. For most detectors the air bubble must be removed before the sample passes through it, unless electronic gating is used. In, addition, the precision of the bubble size can be difficult to control. This variation in bubble size adds to the irreproducibility of the system. The most important advantages gained by elimination of the air bubbles are:

1. Introduction of a reproducible sample volume into the system by injection.
2. Reproducible handling in the system with reduced pulsation.
3. No predetector bubble separation needed.
4. The flow rate of carrier and reagent streams can be reproducibly controlled including predefined intermittent step and run periods.

5.3.3. Biogeochemistry of the Humber Plume

Chemical transport and biogeochemical interactions within estuarine plume zones are key factors in a number of important processes, including biological production and geochemical cycling. They may also be dominant in controlling fluxes of land-derived natural and pollutant chemicals into shelf seas. An estuarine plume is primarily a coastal sea region which is significantly influenced by land-derived discharge emanating from an estuary. It can be identified and characterised as a region with a significant salinity gradient although considerably weaker than that of an estuary. An essential characteristic of estuarine plumes is that, like estuaries, they are highly dynamic, i.e. they depend strongly on river discharges, tidal conditions and wind stress.

In order to quantify the influence of estuarine plume zones in the transfer of land-derived material to coastal seas, a 'mixing curve' method [209], generally applied to estuarine studies, can be utilised. With this approach the concentration distribution of a chemical constituent within the plume is compared with that of a conservative tracer derived from the same source, usually the fraction of freshwater as quantified by salinity. This provides an

assessment of the net effect of all non-conservative processes occurring within the plume zone, without specifically identifying those processes. The relatively weak concentration gradients in plumes require analytical chemistry methods of high accuracy and precision in order to obtain adequate resolution using the 'mixing curve' approach, and it also relies on the assumption of steady-state conditions.

Continuous recordings of water properties at a depth of 3 m were obtained throughout the cruise. Salinity and temperature were recorded using a thermosalinograph; water transmittance using a transmissometer and chlorophyll *a* fluorescence using a fluorometer. In addition to TON, the concentrations of the nutrients, nitrite, phosphate and silicate were also recorded using a Technicon AutoAnalyzer II®. Data recorded along track 3 (Figure 5.2.) on the 11th and 12th June 1995 is shown in Figures 5.7 - 5.13 below. The data are given in μmol l^{-1} as this is the standard unit for the marine discipline. Conversion factors are given in Table 5.2.

Table 5.2. Nutrient concentration conversion factors

Nitrate-Nitrogen (NO_3-N)	0.1 mg l^{-1} ≡ 7.1 μmol l^{-1}
Phosphate-Phosphorus (PO_4-P)	0.1 mg l^{-1} ≡ 3.2 μmol l^{-1}
Silicate-Silicon (SiO_2-Si)	0.1 mg l^{-1} ≡ 3.6 μmol l^{-1}

It can be seen that at approximately 03:00 (GMT), on entering the Humber estuary plume from the north, salinity decreases, whilst temperature and TON (Figure 5.5), nitrite, phosphate and silicate concentrations increase. This is due to the input of nutrient rich, low salinity river water from the Humber dominating the profile. This plume spreads southward towards the Wash in a narrow strip close to the shore before dispersing into high salinity, low nutrient sea water to the south and east. This is in accord with the basic pattern of residual (non-tidal) flow in the region which, in the absence of wind forcing, runs parallel to the coastline in a southerly to south-easterly direction across the Humber mouth, turning

east off the Wash under the influence of the Norfolk coastline. These observations are in agreement with those made by Morris et al [210].

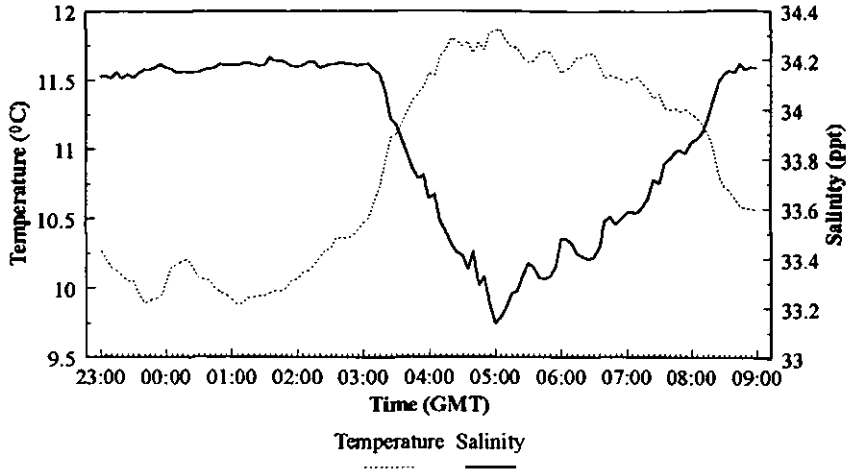

Figure 5.7. Temperature and salinity of surface waters on the 11th and 12th June 1995, on track 3.

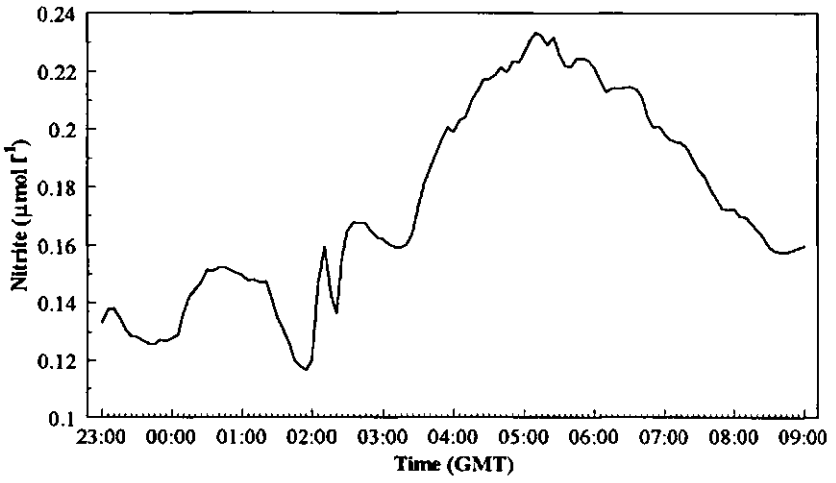

Figure 5.8. Nitrite levels determined by the AutoAnalyzer® on the 11th and 12th June 1995, on track 3.

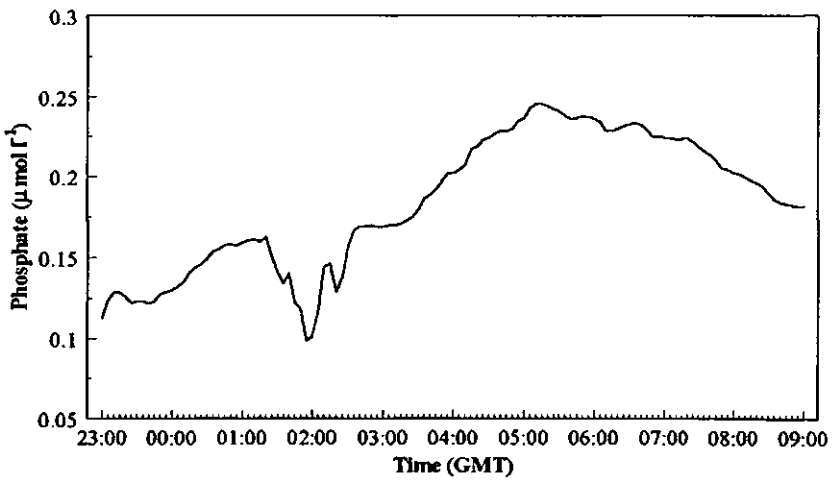

Figure 5.9. Phosphate levels determined by the AutoAnalyzer® on the 11th and 12th June 1995, on track 3.

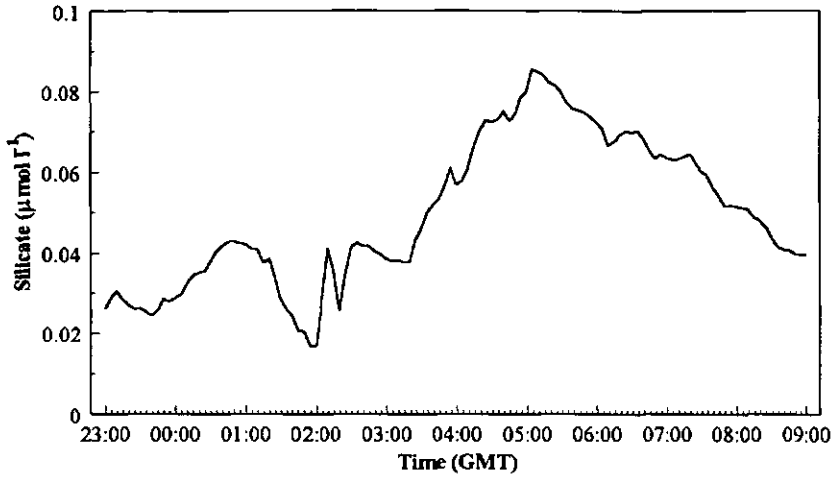

Figure 5.10. Silicate levels determined by the AutoAnalyzer® on the 11th and 12th June 1995, on track 3.

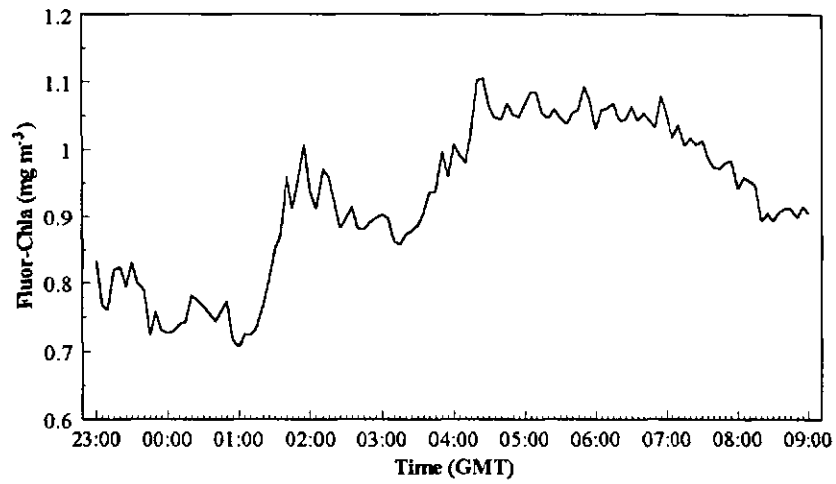

Figure 5.11. Chlorophyll levels of surface waters on the 11th and 12th June 1995, on track 3.

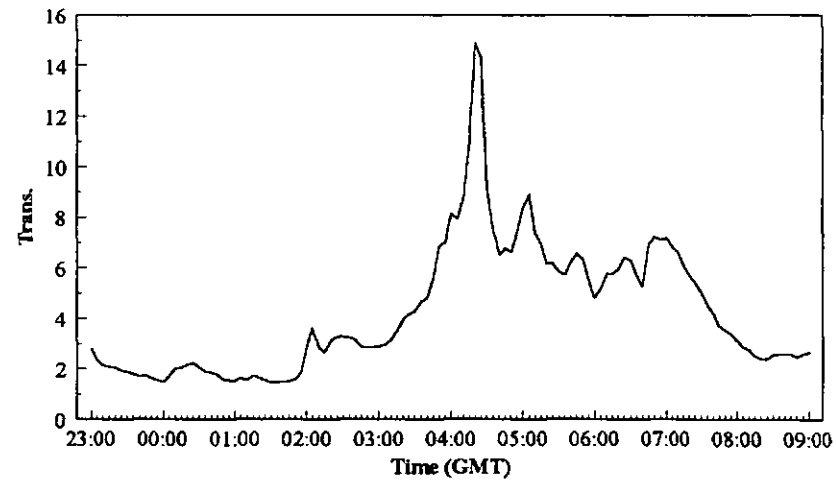

Figure 5.12. Transmittance of surface waters on track 3, on the 11th and 12th June 1995.

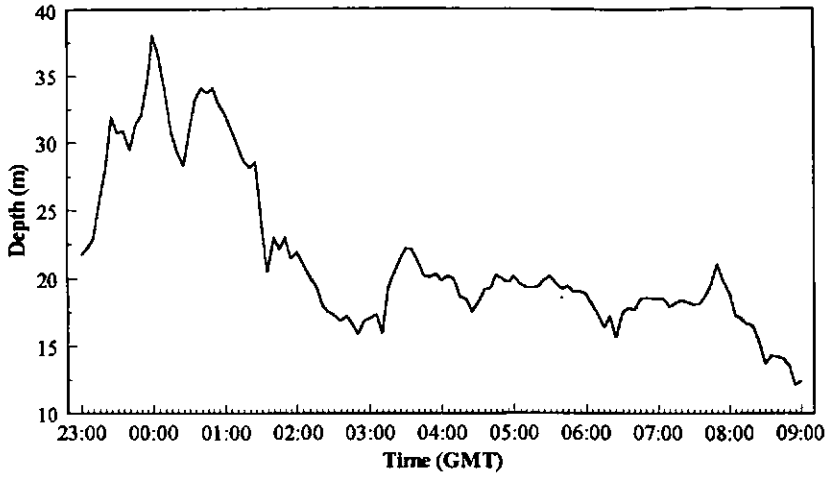

Figure 5.13. Depth of water on track 3, on the 11th and 12th June 1995.

Figures 5.14, 5.15 and 5.16 show the mixing curves for salinity plotted against TON, phosphate and silicate respectively.

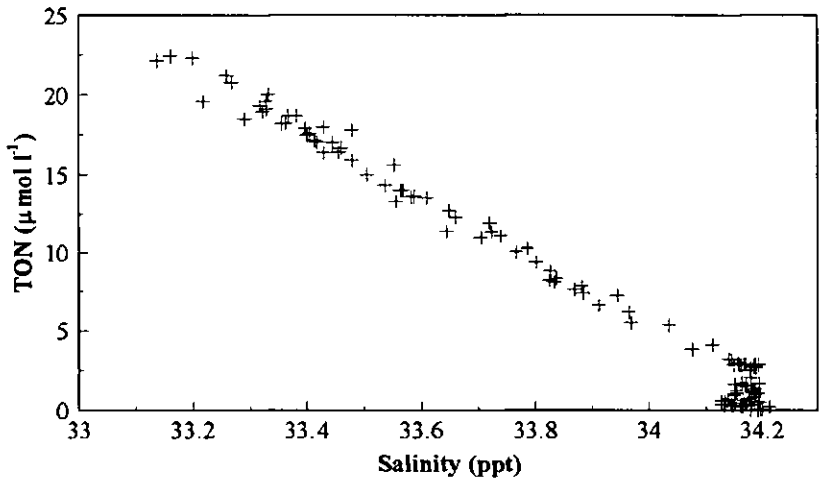

Figure 5.14. Mixing curve for TON on track 3, on the 11th and 12th June 1995.

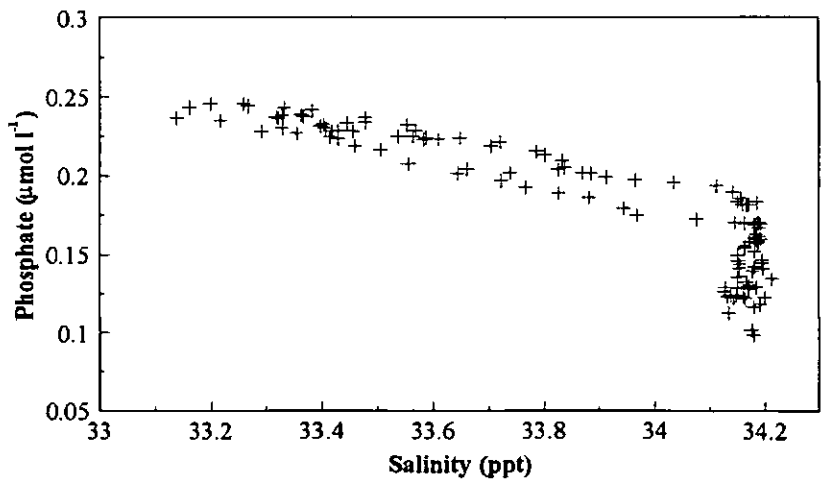

Figure 5.15. Mixing curve for phosphate on track 3, on the 11th and 12th June 1995.

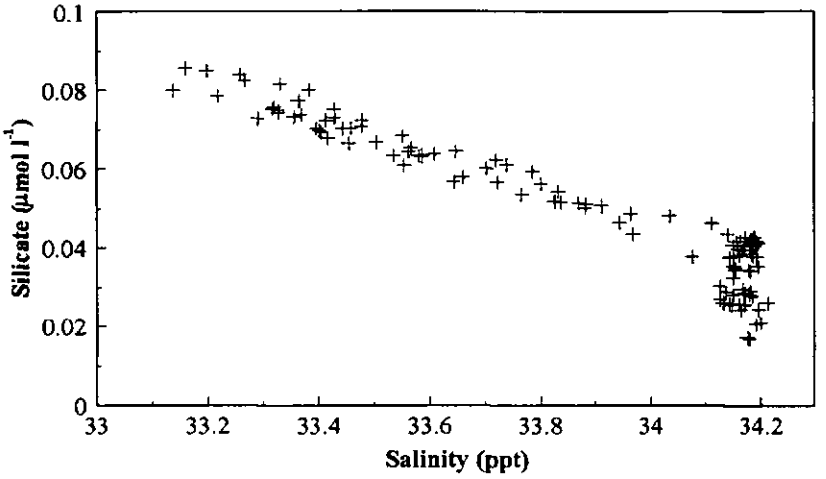

Figure 5.16. Mixing curve for silicate on track 3, on the 11th and 12th June 1995.

There was a highly linear relationship between TON and salinity, indicating conservative behaviour [17]. The mixing curves for both phosphate and silicate also illustrate conservative behaviour, although there is scattering at the high salinity range (>34 ‰) found in the coastal waters north of Spurn Head. Nutrient concentrations within the plume were lower than would be maintained solely by dilution of the Humber mouth discharge and this could be due to removal of nutrients by phytoplankton or to thorough mixing of the water column due to storm conditions one day prior to the start of sampling.

A complete record of the data obtained during each of the three cruise tracks, is given in Appendices 1, 2 and 3 respectively, logged every 5 minutes. These include latitude and longitude, temperature, salinity, fluorescence, transmittance, depth and nutrients.

5.4. CONCLUSIONS

1. The FI manifold optimised in Chapter 2 is suitable for the shipboard determination of TON in coastal waters over the range 0 - 80 µmol l^{-1} N.

2. The manifold allows frequent recalibration and therefore is likely to provide more reliable results than the AutoAnalyzer® method, particularly at low (μmol l^{-1}) levels of TON.
3. The sample presentation system is able to deal with waters having up to 100 mg l^{-1} particulate matter, providing that the membrane filter is changed every hour.
4. It is reasonable to conclude that FI is a suitable alternative to the AutoAnalyzer® for the determination of all nutrient parameters (nitrate, phosphate, silicate) and has the advantages of more robust recalibration, lower reagent consumption, more rapid response and greater flexibility.

Chapter Six
Flow Injection with Charged Coupled Device Detection for the Determination of Nitrate

6. FLOW INJECTION WITH CHARGE COUPLED DEVICE DETECTION FOR THE DETERMINATION OF NITRATE

6.1. INTRODUCTION

Technological advances have made new types of multichannel ultraviolet and visible light detectors available to the analytical chemist, offering significant improvements in performance over the photomultiplier tube (PMT). The two main classes of these detectors are photodiodes (PDs) and charge transfer devices (CTDs). Photodiodes can be used as single detectors as reviewed by Dasgupta et al. [147], or as photodiode arrays (PDAs). The single diodes provide useful, low cost, rugged portable detectors for in situ analyses. PDAs have provided an alternative technology for the measurement of ultraviolet-visible absorption spectra in short time periods and under relatively low light level conditions. The reliability inherent in a PDA spectrometer, compared with a moving mirror rapid scanning spectrometer, is a considerable advantage, especially for remote deployment, as demonstrated by Johnson et al. [64, 150].

CTDs are solid-state multichannel detectors which integrate signal information as light strikes them. An individual detector in a CTD array consists of several conductive electrodes overlying an insulating layer that forms a series of metal oxide semi-conductor (MOS) capacitors. The insulator separates the electrodes from a doped silicon region used for photogenerated charge storage. The amount of charge generated in a CTD detector is measured either by moving the charge from the detector element where it is collected to a charge sensing amplifier, as employed by charge-coupled devices (CCDs), or by moving the charge within the detector element and measuring the voltage change induced by this movement, as used by charge injection devices (CIDs).

The CCD concept was first introduced in 1970 by Boyle and Smith [211, 212], and has since been used in a variety of military, commercial and consumer imaging applications. These array type detectors are primarily silicon based devices with good spectral response characteristics from 400-1100 nm. UV coatings can be applied to extend the range down to 200 nm. For scientific operation, the CCD can be cooled with liquid nitrogen (LN) to 140 K in order to reduce the dark current to < 1 electron/pixel/hour. At this temperature, the detector can be exposed to a signal for several hours without any significant contribution from the dark current. A large body of literature exists on the operating principles and fabrication of CCD imagers, and their optimisation for scientific imaging applications [e.g. 206-221].

Figure 6.1 shows the organisation of a typical two dimensional three phase CCD array.

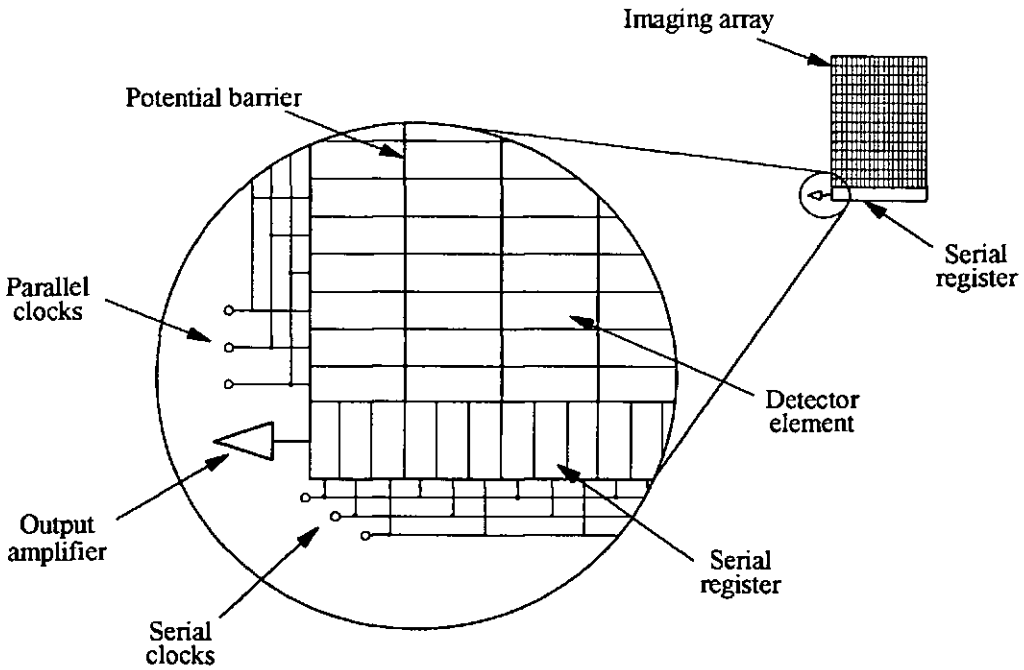

Figure 6.1. Layout of typical three-phase CCD [215].

Columns are clocked in parallel with each clock, all of the charge in the imaging array is shifted toward the serial register by one row, whereas charge from the row adjacent to the serial register is transferred into the serial register. Once the charge is there, the charge packets are shifted sequentially to the on-chip amplifier. Fixed potential barriers between

columns separate charge from adjacent columns. Extremely efficient transfer of charge from detector element to detector element is critical, because small losses accumulate and become significant after the thousands of transfers required to read large CCDs. The charge can be moved from a number of detector elements into a single element, known as binning, and then transferred from the element, or bin, to the amplifier. Charge from any number of consecutively arranged detector elements can be binned. The advantage of summing the signal on-chip is that the charge is subject to only one read operation, which reduces the noise and increases the signal to noise (S/N) ratio of a measurement.

This chapter examines the feasibility of using CCD detection for the determination of nitrate in water and coupling of CCD detection with an FI manifold using fibre-optics. Performance of an FI-CCD configuration is described and compared with the results obtained using a conventional FI method with UV/Visible spectrophotometric detection for nitrate determination as described in Chapter 2.

6.2. EXPERIMENTAL

6.2.1. Reagents and Standards

All solutions were prepared in accordance with Section 2.2.1. for all subsequent experiments unless otherwise stated.

6.2.2. Instrumentation and Procedures

A liquid nitrogen cooled (140 K) Charged-Coupled Device (256 x 1024 pixels, 27.6 x 7 mm grid of 27 μm square pixels) array with 270M imaging spectrograph (Instruments S.A.) and Spectramax Version 1.1d software (Jobin Yvon Optics and Spectroscopy) was used for the spectroscopic detection of nitrite and nitrate in water. The sampling ends of four fibre-optic

(2 x single fibre with 200 μm diameter and 2 x 18 fibre bundle with 1000 μm diameter) channels attached to the front entrance of the spectrograph and focused onto the detector surface were illuminated with a Hg lamp. The 546 nm line and 577/579 nm doublet were clearly seen on four separate areas of the array. By altering the distance between the Hg lamp and the fibre optic sampling ends, these lines were focused onto specific areas of the CCD chip without overlap between the areas. The single fibres (7 and 4) were focused at the top and bottom of the chip, with the bundled fibres (6 and 5) between them in the centre as shown in Figure 6.2 and Table 6.1. The window for fibre 5 goes from pixel 2 to pixel 1023 on the wavelength scale and from pixel 65 to 126 on the counts scale, thereby covering an area of 1022 x 61 = 62, 342 individual detectors. This area was used for all subsequent experiments.

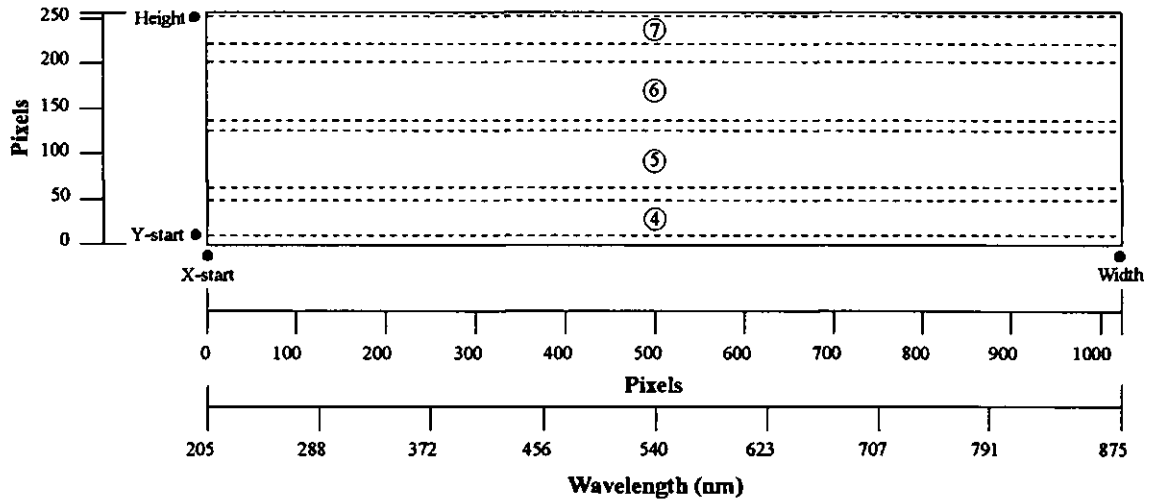

Figure 6.2. CCD array with focused areas covered by fibres 4, 5, 6 and 7.

Table 6.1. Areas on CCD covered by the fibre-optics.

FIBRE	X-START	WIDTH	Y-START	HEIGHT
7 (200 μm)	2	1023	223	28
6 (1000 μm)	2	1023	136	65
5 (1000 μm)	2	1023	65	61
4 (200 μm)	2	1023	13	33

Figure 6.3 shows the single-beam absorbance configuration used for all experiments. A tungsten halogen lamp (LS-1. Ocean Optics Inc.) was used as the light source and its spectrum is shown in Figure 6.4. The source was connected to the CCD imaging spectrograph via a cell holder as shown in Figure 6.3. Fibres 1 and 3 connected the source to the cell holder and fibre 5 made the connection between the cell holder and the imaging spectrograph. The spectrum acquired from the area on the array covered by fibre 5 was the product of binning the columns of pixels along the wavelength scale (i.e. 1022 columns, 61 pixels high). A reference spectrum through the cell was measured and stored as a file in counts per second versus wavelength. The sample spectrum was then acquired in counts per second versus wavelength and a software routine converted the two spectra to single absorbance versus wavelength spectrum in the following way;

$$\text{Absorbance} = \log (\text{Reference Spectrum}/\text{Acquired Spectrum})$$

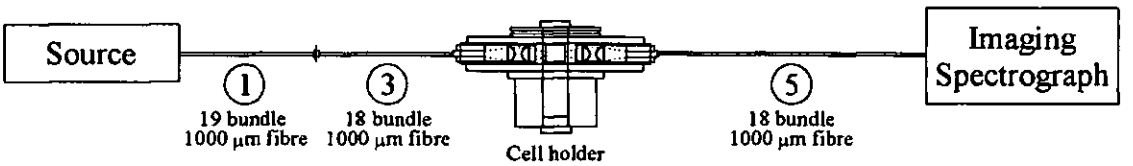

Figure 6.3. Single beam configuration for absorbance measurement.

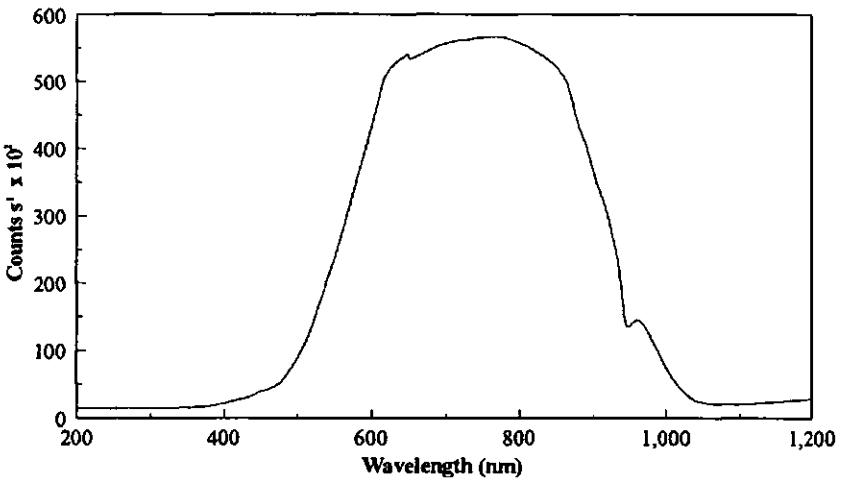

Figure 6.4. Spectrum of the tungsten source.

6.3. RESULTS AND DISCUSSION

6.3.1. Integration Time

The integration time is the amount of time allowed for the signal to be acquired for each measurement. In order to determine the optimum integration time for the system, a 0.5 mg l^{-1} NO_2-N standard (10 ml) and colour reagent (40 ml) were mixed, placed into a 1 cm quartz cuvette and the absorbance measured at various integration times (0.006-1.5 s) with 10 accumulations, e.g. for a 0.5 s integration time 10 accumulations are acquired in 5.0 s, the spectra are summed and averaged to improve the signal-to-noise ratio. Figure 6.5 shows the effect of varying integration time on the absorbance at 540 nm (λ_{max} of the product). At high integration times (> 0.5 s) the CCD chip was saturated by the unattenuated reference beam and hence the calculated absorbance was artificially low. At short integration times (< 0.1 s) the chip is exposed for such a short time that the detection system cannot respond efficiently, resulting in low calculated absorbances. The rapid movement of the shutter also resulted in higher noise and therefore poorer reproducibility. An integration time of 0.5 s was therefore used for further work.

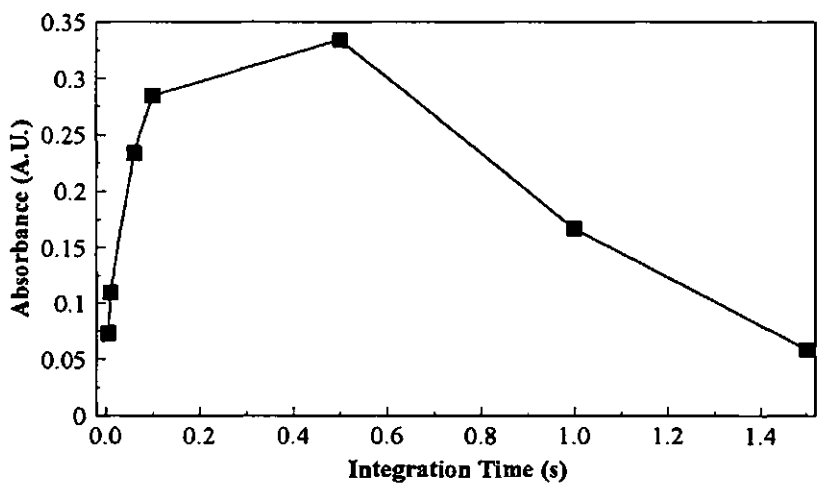

Figure 6.5. The effect on absorbance at 540 nm of varying the integration time.

6.3.2. Static Cuvette Method for Nitrite with CCD Detection

In order to examine the feasibility of using the combined FI-CCD system a static nitrite calibration was carried out. A set of calibration solutions containing 40 ml of the colour reagent and 10 ml of a nitrite standard (0-0.2 mg l^{-1} NO_2-N) were made up. Using the instrumental parameters shown in Table 6.2, the absorbance of each solution was measured by placing them sequentially into a standard 1 cm quartz cuvette in the cell holder. Figure 6.6 shows the calibration graph and absorbance spectrum of each solution and Table 6.3 presents the calibration data for the method, which achieved a LOD of 6.7×10^{-3} mg l^{-1} NO_2-N (defined as 3 times the standard deviation of 5 replicates of the blank). Although the method was not fully optimised the LOD compares well with the static method described by Grasshoff [24] which reported an LOD of 0.2×10^{-3} mg l^{-1} NO_2-N.

Table 6.2. Instrumental parameters.

PARAMETER	SPECIFICATION
Grating	150 grooves/mm at 500 nm
Axial Entrance Slit	1 mm
Integration Time	0.5 seconds
Number of Accumulations	10
Central Wavelength	540 nm
Wavelength Coverage	205-875 nm

Table 6.3. Calibration data from the static cuvette and FI methods.

PARAMETER	METHOD	CALIBRATION GRAPH	ERROR IN INTERCEPT (S_a)	ERROR IN GRADIENT (S_b)	r^2	LOD (3σ) (mg l^{-1} N)
Nitrite	Static	$y = 2.29x - 0.01$	9.76×10^{-4}	4.02×10^{-3}	0.9989	6.7×10^{-3}
Nitrite	FI	$y = 0.52x + 0.02$	1.61×10^{-3}	1.14×10^{-3}	0.9978	2.9×10^{-3}
Nitrate	FI	$y = 0.60x + 0.01$	1.43×10^{-3}	1.02×10^{-3}	0.9987	6.0×10^{-3}

y is in AU and x is in mg l^{-1} N.

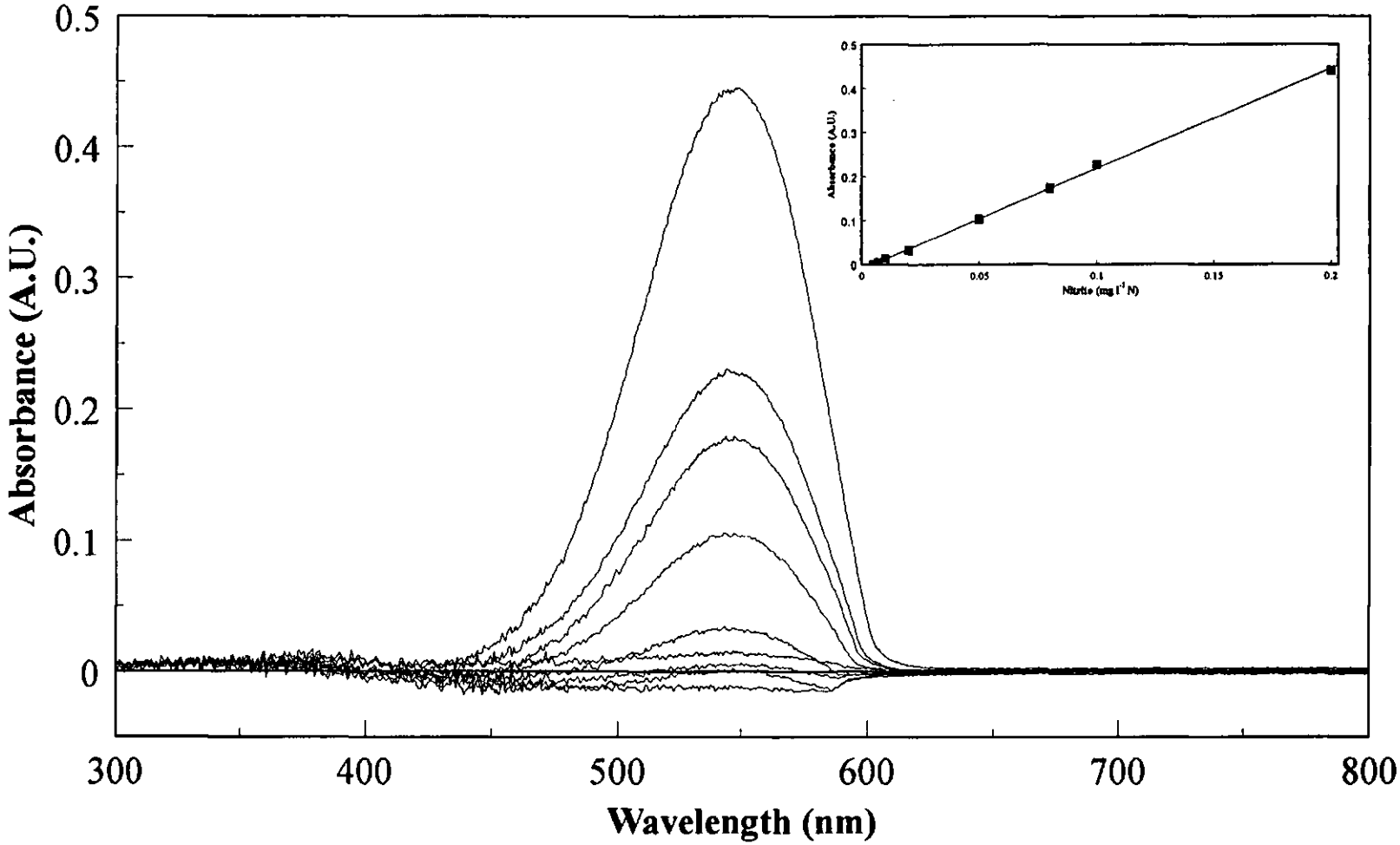

Figure 6.6. Overlaid absorbance spectra for nitrite standards (0.002, 0.005, 0.007, 0.01, 0.02, 0.05, 0.08, 0.1 and 0.2 mg $l^{-1}NO_2$-N) using the static cuvette method

6.3.3. Flow Injection Method for Nitrite with CCD Detection

The FI manifold shown in Figure 2.1, without the copperised cadmium column, was integrated with the system configuration shown in Figure 6.3 with the fibres focused on the optical path of the flow cell. Nitrite calibration standards (0-1 mg l^{-1} NO_2-N) were injected and calibration data (for absorbance at 540 nm) obtained using the CCD detection system. The instrumental parameters used were as shown in Table 6.2. The first measurement was taken 40 s after the reacted sample zone, so as to allow time for the measured product to reach the detector. Each cycle of 10 accumulations with a 0.5 s integration time was repeated 20 times with a delay between cycles of 0.5 s. Figure 6.7 shows time slices of the FI peak that was obtained for a 0.5 mg l^{-1} NO_2-N standard and Figure 6.8 shows the calibration graph (for absorbance at 540 nm) and absorbance spectra at the FI peak maximum absorbance obtained for the nitrite standards. Table 6.3 presents the calibration data and the method achieved a LOD of 2.9 x 10^{-3} mg l^{-1} NO_2-N. The detection limit is comparable with that of 2.1 x 10^{-3} mg l^{-1} NO_2-N reported by Johnson and Petty [64] for the FI determination of nitrite in sea water.

6.3.4. Flow Injection Method for Nitrate with CCD Detection

The above experiment with nitrite was repeated using nitrate standards (0-1 mg l^{-1} NO_3-N) and with the copperised cadmium column incorporated in the FI manifold (Figure 2.1). Figure 6.9 shows the resulting FI peak for a 0.5 mg l^{-1} NO_3-N standard and Figure 6.10 shows the calibration graph (for absorbance at 540 nm) and overlaid spectra at the FI peak maximum. Calibration data for the method is presented in Table 6.3, which achieved a LOD of 6 x 10^{-3} mg l^{-1} NO_3-N. The reproducibility of the FI method shown for 5 repeat injections of a 0.5 mg l^{-1} NO_3-N standard in Figure 6.11 was 1.7 %. Although not fully optimised, the analytical figures of merit for the FI-CCD method for the determination of

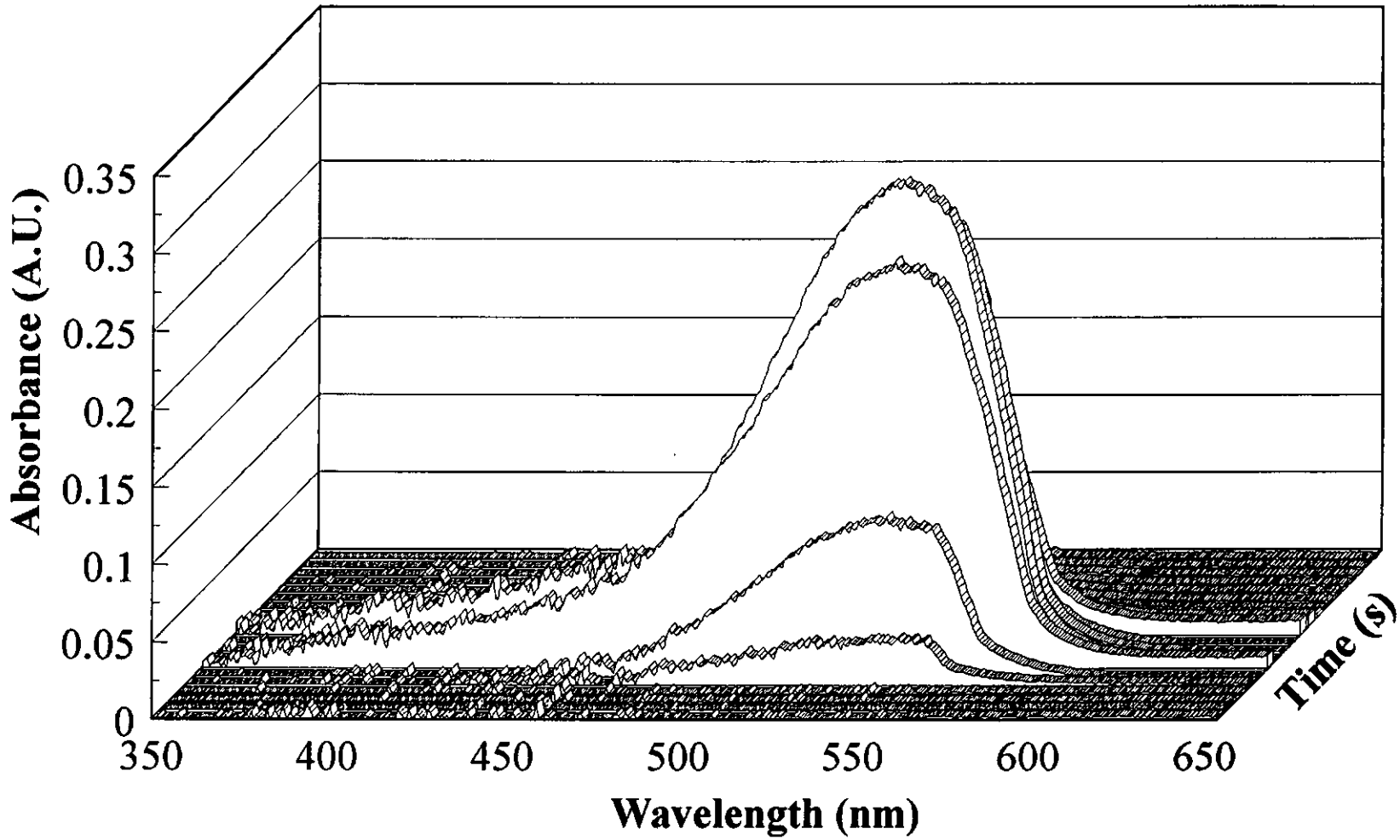

Figure 6.7. FI peak obtained for a 0.5 mg l^{-1} NO_2-N standard using CCD detection

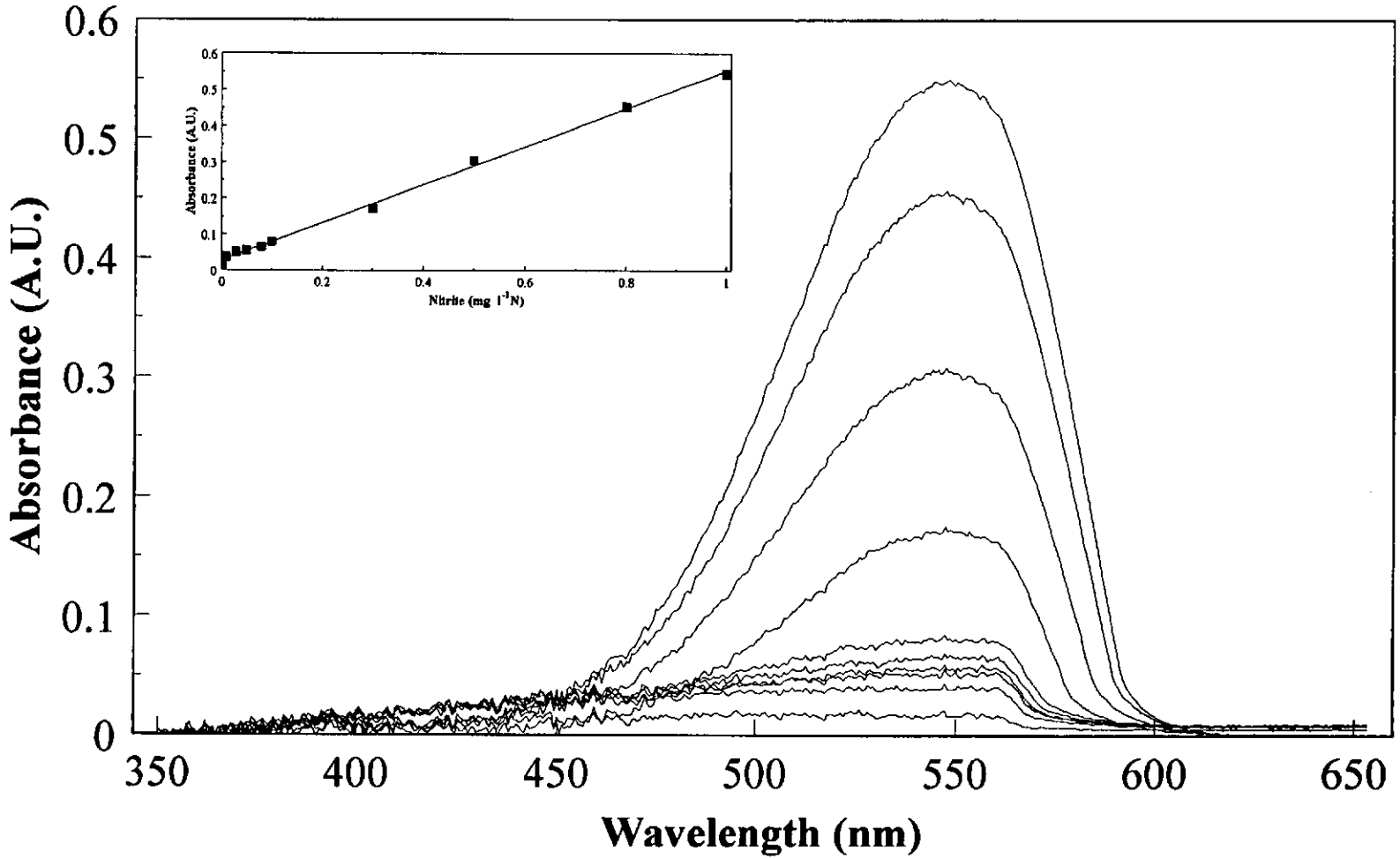

Figure 6.8. Overlaid absorbance spectra for nitrite standards (0, 0.01, 0.03, 0.05, 0.08 0.1, 0.3, 0.5, 0.8 and 1.0 mg $l^{-1}NO_2$-N) using FI

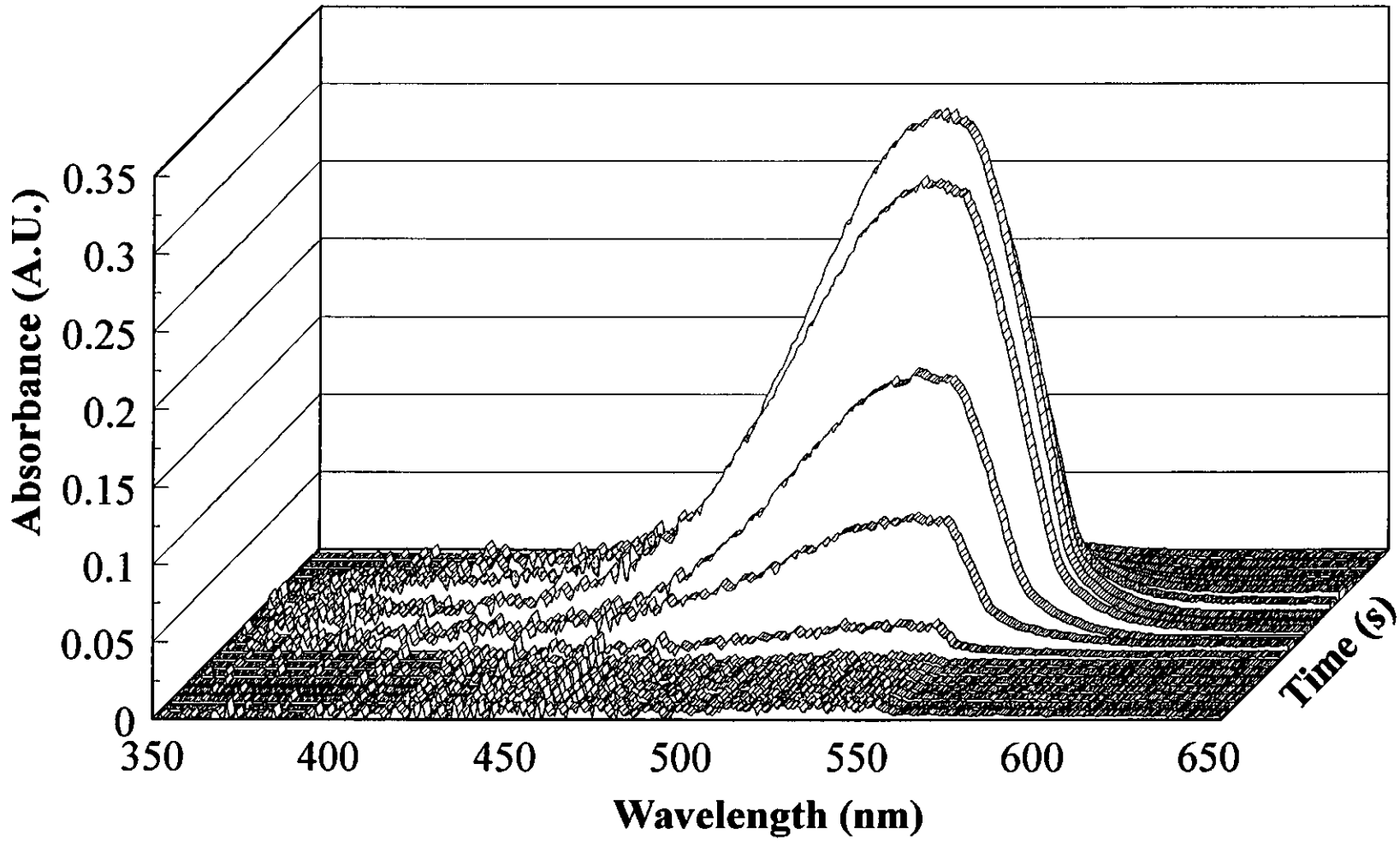

Figure 6.9. FI peak obtained for a 0.5 mg l^{-1} NO_3-N standard using CCD detection

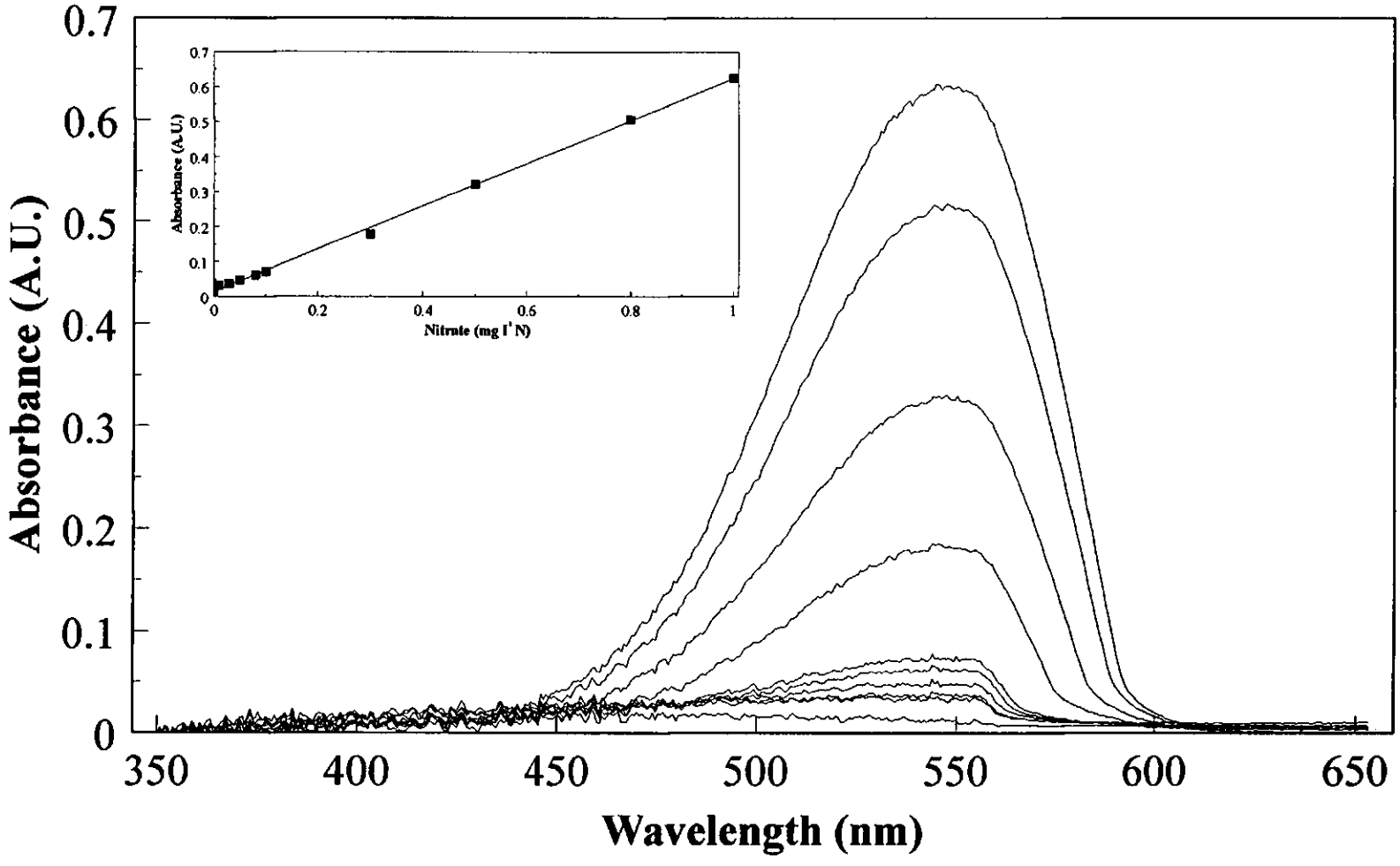

Figure 6.10. Overlaid absorbance spectra for nitrate standards (0, 0.01, 0.03, 0.05, 0.08, 0.1, 0.3, 0.5, 0.8, 1.0 mg $l^{-1}NO_3$-N) using FI

nitrate, compare favourably with the data given in Section 2.5.3 and Table 2.4 for the conventional spectroscopic method.

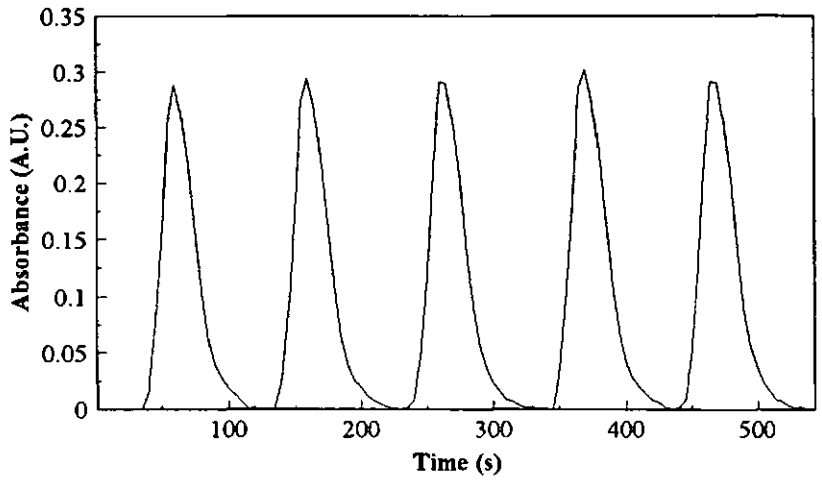

Figure 6.11. Repeat injections of a 0.5 mg l^{-1} NO_3-N standard using FI with CCD detection.

6.3.5. Attractions of CCD Detection

Recent developments in solid-state array detectors and new optical spectroscopic components have made it possible to assemble compact, rugged and power-efficient spectroscopic systems with precision rivalling that of the most sophisticated laboratory instrumentation. Scientifically operated CCDs are commercially available and give high spatial resolution, large linear dynamic ranges, high sensitivity and are able to integrate signal for long periods of time. When used in conjunction with an imaging spectrograph the two dimensional imaging capabilities of the area array CCD can be exploited by monitoring multiple fibre optic inputs. Because individual fibre channels are resolved spatially along the slit height dimension with an imaging spectrograph, spectral information from a variety of optical emission or absorbance experiments can be monitored simultaneously [222], and multiparameter determination can be performed using separate fibres. Spectroscopic systems of this type are robust, few moving parts, and are potentially useful for shipboard and in situ monitoring.

Minimum Detectable Absorbance

In order to evaluate whether the scientific CCD can achieve the necessary signal-to-noise ratio (S/N) for the determination of nitrate in sea water, the theoretical minimum detectable absorbance can be calculated in order to estimate the minimum measurable concentration. The premise is that a sample measurement can be no more certain than the measurement of the blank. The minimum detectable absorbance (A_{min}) achievable can be calculated as reported by Bilhorn et al. [217] using the following equation;

$$A_{min} \approx -\log [1-(8/Q_{sat})^{1/2}]$$

where Q_{sat} is the full well capacity of a detector element, which is the saturation level of the detector element. This equation indicates that the minimum detectable absorbance is a function of the full well capacity; the larger the full well, the smaller the minimum detectable absorbance. The full well capacity of the CCD imaging spectrograph used in this work was 65,532 counts, which gives a minimum detectable absorbance of 4.8×10^{-3} absorbance units (AU). By collecting the spectrum over several detector elements parallel to the slit dimension the precision in a single exposure can be improved by summation of the signals from multiple rows of detector elements. This is called binning, where the charge is combined from adjacent pixels to produce a 'super pixel'. Thus if an area of 1024 pixels wide by 50 pixels high is produced, the spectrum will have 1024 data points. An area of the same width but 200 pixels high, will have the same spectrum, except that the binned signal will be four times as intense and therefore have twice the signal-to-noise ratio. The minimum detectable absorbance now becomes;

$$A_{min} \approx -\log [1-(8/nQ_{sat})^{1/2}]$$

where n equals the number of elements that are summed in the plane of the entrance slit.

Theoretical Limits of Detection

Using the calculated minimum detectable absorbance, a theoretical limit of detection for N can be determined using the Beer-Lambert equation;

$$A = \varepsilon b c$$

where, A is Absorbance (AU), ε is the molar absorptivity, b is the path length and c is the molar concentration of the absorbing species of interest. For nitrite and nitrate the molar absorptivity of the diazo complex at 540 nm is 48,000 l mol^{-1} cm^{-1} and the path length is 1 cm. Table 6.4 shows the minimum detectable absorbance and theoretical LOD determined by binning 1, 61 and 256 rows in a single column at 540 nm. Even when using one pixel row for absorbance measurements the CCD detector is theoretically capable of determining the levels of nitrite and nitrate found in sea water, and summation of a number of pixel rows meets and exceeds the required limits of detection. The difference between the theoretical and actual LODs can be attributed to a number of factors: the data acquisition and the number of pixel rows summed were not optimised, and the full well capacity was not reached

Table 6.4. Theoretical values for minimum detectable absorbance and LOD.

	SINGLE ROW	61 ROWS SUMMED	256 ROWS SUMMED
Minimum detectable absorbance (AU)	4.8×10^{-3}	6.1×10^{-4}	2.9×10^{-4}
LOD (mg l^{-1} N)	1.4×10^{-3}	1.7×10^{-4}	8.7×10^{-5}

Environmental Applications of CCD Detection.

Spectroscopic systems with charge transfer device detectors can be designed to meet many of the requirements of environmental applications [223]. They are versatile, robust

spectroscopic systems capable of acquiring both sensitive and precise absorbance and fluorescence measurements, and many analytes can be analysed successfully by colorimetric and luminescent techniques [e.g. 224, 225]. Spectroscopic information can be simultaneously acquired over the entire spectral range. This ability to make multiwavelength measurements is important in a number of applications, for example;

1. *Internal referencing* can be used to compensate for erroneous absorbance readings. It requires simultaneous measurement of the analytical wavelength and of a second wavelength close to the analytical wavelength but where there is no absorption. This technique reduces the instrumental drift and is similar in principle to a double-beam spectrophotometer.
2. *Wavelength averaging* reduces noise and involves measuring an absorbance value averaged over several photo detectors in the wavelength domain. This requires the absorbance to be constant over the range used.
3. *Multicomponent analysis* measures the absorbance of two components at two wavelengths simultaneously. The absorbance at either wavelength will be the sum of the absorbances from both components, therefore the concentration of each component can be calculated using the Beer-Lambert law. More complex chemometric approaches, e.g. partial least squares algorithms can also be used in conjunction with the CCD.

Double Beam Mode.

The noise of the system comes predominantly from shot noise, source fluctuations and shutter variability. At short exposure times, the source and/or shutter instability dominate and at longer exposure times the noise is dominated by the source shot noise [223]. The read noise of the detector is negligible compared with the shot noise, source flicker and shutter variability at long exposures. Even though relative error decreases at long exposures there is still the possibility of erroneous results from the source and the

reproducibility of the shutter. To ensure the acquisition of high-precision absorbance measurements with the system, a double beam operation is desirable, as shown in Figure 6.12. The dual-beam configuration will eliminate the problems associated with shutter variability and reduce the effect of source flicker. In addition the S/N ratio should increase as a function of the exposure level. For the static cuvette method this set-up is simple but for flow injection it is more difficult because of the continuously changing background signal in the flow cell. An additional disadvantage is that this configuration uses more fibre optic input channels, therefore reducing the number of parameters that could be determined simultaneously by the detector.

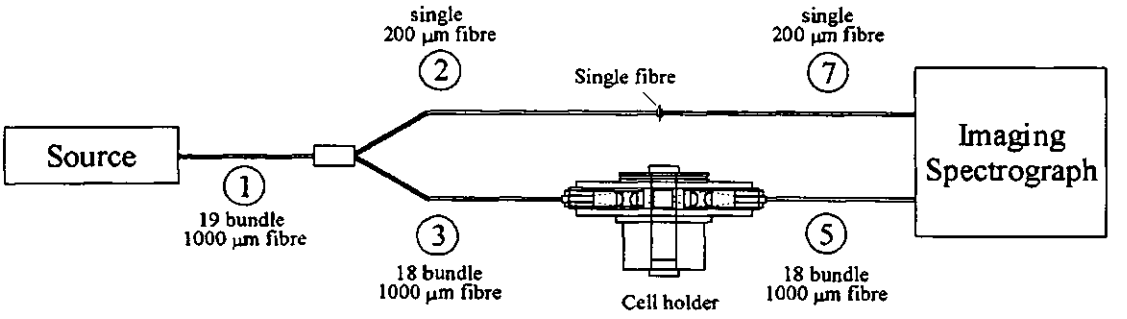

Figure 6.12. Double-beam configuration for absorbance measurement.

6.4. CONCLUSIONS

1. CCD detection can be used with spectral input via fibre optics for the spectrophotometric determination of nitrite in water using a static cuvette.
2. FI can be coupled to the CCD for the spectrophotometric determination of nitrite with an LOD of 2.9×10^{-3} mg l^{-1} NO_2-N.
3. FI can be coupled to the CCD for the spectrophotometric determination of nitrate with an LOD of 6×10^{-3} mg l^{-1} NO_3-N.
4. The theoretical LOD for nitrate, using a well capacity of 65,532 counts and occupying 61 elements is 1.7×10^{-4} NO_3-N.

Chapter Seven
Conclusions and Future Work

7. CONCLUSIONS AND FUTURE WORK

7.1. FINAL CONCLUSIONS

The following general conclusions can be drawn from the work discussed in the preceding chapters:

1. The optimised, developed and validated FI manifold for the determination of nitrate achieves a limit of detection of 0.1 μmol l^{-1} and a linear range of 0 - 73 μmol l^{-1} NO_3-N and is suitable for the analysis of samples of varying salinity (0 - 35 ‰) i.e. freshwater, estuarine, coastal and open ocean waters. The precision is good (typically less than 5 % over the above ranges of nitrate concentration and salinity) and the accuracy is acceptable (as determined by interlaboratory comparisons). The method is suitable for shipboard operation and the instrumentation is transportable, ready for use within 30 minutes and is extremely reliable. The reagents and standards are stable for at least 30 days and the method is therefore suitable for long term in situ monitoring.

2. The salinity compensation FI manifold developed for the determination of orthophosphate overcomes the 'salt error' when using tin(II) chloride as the reducing agent and gives a detection limit of 4.3 μg l^{-1} PO_4-P. This was demonstrated with shipboard operation of the FI method on the Tamar Estuary with samples of varying salinity (0 - 35 ‰). Tin chloride is the preferred reducing agent for achieving the lowest detection limit and is suitable for laboratory and short term (less than one day) shipboard deployment. The antimony-ascorbic acid method with the addition of glycerol provides greater reagent stability for longer term deployments. The use of low nutrient sea water (LNS) is essential to provide a low reagent blank signal for both reduction methods. The antimony-ascorbic

acid method with LNS achieved a limit of detection 6.3 $\mu g\ l^{-1}$ and a linear range of 0 - 0.5 $\mu g\ l^{-1}$ PO_4-P.

3. TON concentration showed an inverse correlation with salinity in the Tamar Estuary and a clear seasonal pattern with levels varying in the Sound between 0.01 - 0.39 mg l^{-1} N and at Calstock between 1.2 - 3.3 mg l^{-1} N. Orthophosphate concentration was generally invariant over the whole salinity range of the estuary (0 - 32 ‰) at a concentration of 20 $\mu g\ l^{-1}$ P due to buffering by Fe phases in the sediments and suspended solids.

The conservative behaviour of TON was also evident in Sutton Harbour as well as seasonal variability and neap/spring tide periodicity. Orthophosphate concentration was generally close or lower than the limit of detection (>0.05 mg l^{-1} P) with no inverse correlation with salinity showing either anthropogenic input or input from the sediment.

The nutrient rich low salinity riverine input from the Humber Estuary spreads southward towards the Wash dispersing into high salinity low nutrient sea water with TON within this plume showing conservative behaviour. TON concentrations varied between 0.7 - 1.6 μmol^{-1} N along the North Eastern English Coast with a maximum of 20 μmol^{-1} N in the Humber Plume.

4. Charged coupled device detection coupled with FI via fibre optics can be used for the spectrophotometric determination of nitrite and nitrate in water. The feasibility of this approach has been demonstrated and detection limits of 2.9×10^{-3} and 6.0×10^{-3} mg l^{-1} N were achieved for nitrite and nitrate respectively. The FI-CCD system has great potential for monitoring of nutrients in natural waters, particularly in terms of lower detection limits (achieved by integration of the response over several pixels in both the intensity and wavelength domains), multiple analysis with a single detector (e.g. nitrate, nitrite, phosphate and silicate) and ultimately combination with multivariate calibration procedures.

7.2. SUGGESTIONS FOR FUTURE WORK

The work described in the preceding chapters could be developed in a number of ways. Possible areas for further investigation are summarised below:

1. Integration of the FI chemistries developed for nitrate and phosphate within an automated, submersible, in situ FI monitor. This would allow detailed temporal profiles to be obtained for transient events (such as storms) by deployment of a single monitor at a particular location. By varying the depth of such a monitor spatial information i.e. depth profiles could also be obtained. Such a system would also allow more detailed information on biogeochemical cycling, e.g. within an estuary, by deploying a suite of such analysers at appropriate locations from the riverine to the sea water end-members.

2. The biogeochemical information obtained could be further enhanced by the design and deployment of FI chemistries for other nutrient parameters, e.g. silicate and, in longer term, for speciation, e.g. of organic and inorganic nitrogen. This could be achieved by the incorporation of an on-line photo-oxidation system to convert organic forms of nitrogen, e.g. urea and amino acids, into nitrate. Such a system could also be used to obtain speciation information on phosphorus and silica.

3. Further optimisation of the FI-CCD system for the determination of nitrate. This would focus on an investigation into ways of achieving lower practical limits of detection which are comparable with the theoretical LODs calculated from Bilhorn's equation. Specifically the optimal 'binning' of pixels in the intensity domain, use of different fibre optic configurations, e.g. double-beam mode, and wavelength averaging. As mentioned above the use of multivariate calibration to extract maximum information from the data is a longer term objective.

4. Deployment of the CCD system onboard ship for the determination of nutrients in natural waters. This would enable the ruggedness and analytical performance of the system to be examined under environmental conditions and allow a rigorous comparison with the FI methods presented in this thesis and the standard AutoAnalyzer® method.

References

1. T. R. Parsons *Chemical Oceanography*, J. P. Riley and G. Skirrow (Eds) Vol 2, Academic Press, London, (1975).
2. *Eutrophication Related Phenomena in the Adriatic Sea and in other Mediterranean Coastal Zones*, H. Barth and L. Fegan (Eds.) Water Pollution Research Report 16, Commission of the European Communities, Brussels, 1990.
3. *Chemistry, Agriculture and the Environment*, M. L. Richardson (Ed) Royal Society of Chemistry, Cambridge, (1991).
4. M. Meybeck., *Amer. J. Sci.*, **282**, (1982), 401.
5. UNEP/WHO *Assessment of Freshwater Quality*, London., (1988).
6. WHO/UNEP *Global Pollution and Health.*, WHO, Geneva and UNEP, Nairobi, Yale Press, London, (1987).
7. T. P. Burt, A. L. Heathwaite and S. T. Trudgill., *Nitrate, Processes, Patterns and Management*, Wiley, Chichester, (1993).
8. K. Iserman, *Fertilizer Res.*, **26**, (1990), 253.
9. *Phosphorus Cycles in Terrestrial and Aquatic Ecosystems*. Regional Workshop 1: H. Tiessen (Ed) Europe, Czerniejewo, Poland, May 1-6 1988, Saskatchewan Institute of Pedology, Canada, (1989).
10. J. P. Riley and R. Chester, *Introduction to Marine Chemistry*, Academic Press, London, (1971).
11. H. E. Allen and J. R. Kramer, *Nutrients in Natural Waters*, Wiley-Interscience, New York, (1972).
12. R. C. Dugdale and J. J. Goering, *Limnol. Oceanogr.*, **12**, (1967), 196.
13. E. J. Carpenter and D. G. Capone, *Nitrogen in the Marine Environment*, Academic Press, London, (1983).
14. T. H. Blackburn and J. Sorensen, *Nitrogen Cycling in Coastal Marine Environments*, Proceedings from a SCOPE symposium, Wiley, Chichester, (1988).
15. H. Craig and L. I. Gordon, *Geochim. Cosmochim. Acta.*, **27**, (1963), 949.
16. D. W. Pritchard, *Adv. Geophys.*, **1**, (1952), 243.
17. J. D. Burton and P. S. Liss, *Estuarine Chemistry*, Academic Press, London, (1976).
18. E. J. Griffith, A. Beeton, J. M. Spencer and D. T. Mitchell, *Environmental Phosphorus Handbook*, Wiley, Chichester, (1973).
19. *The Review of the Health of the Oceans*, / GESAMP Reports and Studies No. 15, UNESCO Paris, 1982.

20. *The State of the Marine Environment*, / GESAMP Reports and Studies No. 39, UNEP Nairobi, 1990.
21. *North Sea Quality Status Report*, North Sea Task Force, Oslo and Paris Commissions (ICES), London, 1993.
22. D. Degobbis, *Marine Pollution Bulletin*, **20**, (1989), 452.
23. J. D. H. Strickland and T. R. Parsons, *A Practical Handbook of Seawater Analysis*, Bulletin 167, 2nd Edn., Fisheries Research Board of Canada, Ottawa, (1972).
24. K. Grasshoff, M. Ehrhardt and K. Kremling, *Methods of Seawater Analysis*, Verlag Chemie, New York, (1976).
25. D. Amin, *Analyst*, **111**, (1986), 1335.
26. A. Henriksen and A.R. Selmer-Olsen, *Analyst*, **95**, (1970), 514.
27. J. P. Singh, *Plant and Soil*, **110**, (1988), 137.
28. E. K. Best, *Qld. J. Agric. Anim. Sci.*, **33**, (1976), 161.
29. A. Al-Wehaid and A. Townshend, *Anal. Chim. Acta*, **186**, (1986), 289.
30. C. D. User and G. M. Tellings, *J. Sci. Food Agric.*, **2**, (1975), 1793.
31. E Szekely, *Talanta*, **14**, (1967), 941.
32. M. B. Shinn, *Ind. Eng. Chem. Anal. Ed.*, **13**, (1941), 33.
33. K. Bendschneider and R. J. Robinson, *J. Mar. Res.*, **11**, (1952), 87.
34. G. Norwitz and P. N. Keliher, *Analyst*, **110**, (1985), 689.
35. J. B. Mullin and J. P. Riley, *Anal. Chim. Acta*, **12**, (1955), 464.
36. A. Henriksen, *Analyst*, **90**, (1965), 83.
37. M. T. Downes, *Water Res.*, **12**, (1978), 673.
38. C. E. Bower and T. Holm-Hansen, *Aquaculture*, **21**, (1980), 281.
39. B. C. Madsen, *Anal. Chim. Acta*, **124**, (1981), 437.
40. J. Hilton and E. Rigg, *Analyst*, **108**, (1983), 1026.
41. A. J. Kempers and A. G. Luft, *Analyst*, **113**, (1988), 1117.
42. T. J. Chow and M. S. Johnstone, *Anal. Chim. Acta*, **27**, (1962), 441.
43. K. Matsunaga and M. Nishimura, *Anal. Chim. Acta*, **45**, (1969), 350.
44. S. J. Bajic and B. Jaselskis, *Talanta*, **32**, (1985), 115.
45. A. Otsuki, *Anal. Chim. Acta*, **99**, (1978), 375.
46. K. Nagashima, Xue-Xin Qian and S. Suzuki, *Anal. Sci.*, **3**, (1987), 179.
47. C. Garside, *Mar. Chem.*, **44**, (1993), 25.
48. J. I. Skicko and A. Tawfik, *Analyst*, **113**, (1988), 297.

49. E. D. Wood, F. A. J. Armstrong and F. A. Richards, *J. Mar. Biol. Ass. U.K.*, **47**, (1967), 23.

50. J. J. Connors and J. Beland, *J. Am. Water Works Ass.*, (1976), 55.

51. R. F. Gaugush and R. T. Heath, *Water Res.*, **18**, (1984), 449.

52. J. H. Margeson, J. C. Suggs and M. R. Midgett, *Anal. Chem.*, **52**, (1980), 1955.

53. M. A. Kouparis, K. H. Walczak and H. V. Malmstadt, *Anal. Chim. Acta*, **142**, (1982), 119.

54. A. W. Morris and J. P. Riley, *Anal. Chim. Acta*, **29**, (1963), 272.

55. M. D. Stainton, *Anal. Chem.*, **46**, (1974), 1616.

56. D. J. Hydes and N. C. Hill, *Estuarine, Coastal and Shelf Sci.*, **21**, (1985), 127.

57. R. S. Lambert and R. J. Dubois, *Anal. Chem.*, **43**, (1971), 955.

58. C. Oudot and Y. Montel, *Mar. Chem.*, **24**, (1988), 239.

59. P. Raimbault, G. Slawyk, B. Coste and J. Fry, *Mar. Biol.*, **104**, (1990), 347.

60. L. Anderson, *Anal. Chim. Acta*, **110**, (1979), 123.

61. M. F. Gine, H. Bergamin, E. A. G. Zagatto and B. F. Reis, *Anal. Chim. Acta*, **114**, (1980), 191.

62. J. F. van Staden, *Anal. Chim. Acta*, **138**, (1982), 403.

63. M. F. Gine, B. F. Reis, E. A. G. Zagatto, F. J. Krug and A. O. Jacintho, *Anal. Chim. Acta*, **155**, (1983), 131.

64. K. S. Johnson and R. L. Petty, *Limnol. Oceanogr.*, **28**, (1983), 1260.

65. J. F. van Staden, A. E. Joubert and H. R. van Vliet, *Fres. Z. Anal Chem.*, **325**, (1986), 150.

66. B. Bermudez, A. Rios, M. D. Luque de Castro and M. Valcarcel, *Talanta*, **35**, (1988), 810.

67. K. Aikawa and R. Motohashi, *J. Flow Injection Anal.*, **6**, (1989), 137.

68. S. Devi and A. Townshend, *Anal. Chim. Acta*, **225**, (1989), 331.

69. J. Maimo, A. Cladera, F. Mas, R. Forteza, J. M. Estela and V. Cerda, *Intern. J. Environ. Anal. Chem.*, **35**, (1989), 161.

70. P. G. Brewer and J. P. Riley, *Deep Sea Res.*, **12**, (1965), 765.

71. R. B. Willis, *Anal. Chem.*, **52**, (1980), 1377.

72. J. R. Clinch, P. J. Worsfold and H. Casey, *Anal. Chim. Acta*, **200**, (1987), 523.

73. Perstorp Analytical Ltd., Application Note 136/91, (1992).

74. S. C. Pai and J. P. Riley, *Intern. J. Environ. Anal. Chem.*, **57**, (1994), 263.

75. F. Nydahl, *Talanta*, **23**, (1976), 349.

76. C. Garside, *Mar. Chem.*, **11**, (1982), 159.

77. P. van Zoonen, K. Bock, C. Gooijer, N. H. Velthorst and R. W. Frei, *Anal. Chim. Acta*, **200**, (1987), 131.

78. A. T. Pilipenko, O. V. Zuj and A. V. Terleckaja, *Khim. Tekhnol. Vody.*, **13**, (1991), 847.

79. A. T. Pilipenko and O. V. Zuj, *Khim. Tekhnol. Vody.*, **13**, (1991), 230.

80. P. Mikuska, Z. Vercera and Z. Zdrahal, *Anal. Chim. Acta*, **316**, (1995), 261.

81. A. R. Thornton, J. Pfab and R. C. Massey, *Analyst*, **114**, (1989), 747.

82. Y. Kanda and M. Taira, *Anal. Chem.*, **62**, (1990), 2084.

83. R. D. Cox, *Anal. Chem.*, **52**, (1980), 332.

84. T. Aoki, *Biomed. Chromatogr.*, **4**, (1990), 128.

85. R. S. Braman and S. A. Hendrix, *Anal. Chem.*, **61**, (1989), 2715.

86. P. A. Cawse, *Analyst*, **92**, (1967), 311.

87. L. Brown and E. G. Bellinger, *Water Res.*, **12**, (1978), 223.

88. P. Morries, *Water Treat. Exam.*, **20**, (1971), 132.

89. P. J. Rennie, A. M. Sumner and F. B. Basketter, *Analyst*, **104**, (1979), 837.

90. T. R. Crompton, *Analysis of Seawater*, Butterworths, London, 1989.

91. A. P. Doherty, R. J. Forster, M. R. Smyth and J. G. Vos, *Anal. Chim. Acta*, **225**, (1991), 45.

92. J. N. Barisci and G. G. Wallace, *Anal. Lett.*, **24**, (1991), 2059.

93. K. K. Verma and A. Verma, *Anal. Lett.*, **25**, (1992), 2083.

94. H. J. Kim and Y. K. Kim, *Anal. Chem.*, **61**, (1989), 1485.

95. M. C. Gennaro, P. L. Bertolo and A. Cordero, *Anal. Chim. Acta*, **239**, (1990), 203.

96. P. Pastore, I. Lavagnini, A. Boaretto and F. Magno, *J. Chromatogr.*, **475**, (1989), 331.

97. E. M. Burke, F. X. Suarez, D. C. Hillman and E. M. Helthmer, *Water, Res.*, **23**, (1989), 519.

98. K. Robards, I. D. McKelvie, R. L. Benson, P. J. Worsfold, N. Blundell and H. Casey, *Anal. Chim. Acta*, **287**, (1994), 143.

99. O. Broberg and K. Pettersson, *Hydrobiologia*, **170**, (1988), 45.

100. D. E. Armstrong, *Analytical Chemistry of Phosphorus Compounds*, M. Halman. (Ed.) Wiley-Interscience, New York, **37**, (1972), 744.

101. J. Murphy and J. P. Riley, *Anal. Chim. Acta.*, **27**, (1962), 31.

102. O. Broberg and G. Persson, *Hydrobiologia*, **170**, (1988), 61.

103. B. Bostrom, G. Persson and B. Broberg, *Hydrobiologia*, **170**, (1988), 133.

104. H. Holtan, L. Kamp-Nielsen and A. O. Stuanes, *Hydrobiologia*, **170**, (1988), 19.

105. M. T. Downes, *Water Res.*, **12**, (1978), 743.

106. K. S. Johnson and R. L. Petty, *Anal. Chem.*, **54**, (1982), 1185.

107. P. J. Worsfold, J. R. Clinch and H. Casey, *Anal. Chim. Acta*, **197**, (1987), 43.

108. H. Casey and S. Smith, *Trend. Anal. Chem.*, **4**, (1985), 256.

109. D. J. Malcolme-Lawes and K. H. Wong, *Analyst*, **115**, (1990), 65.

110. L. Drummond and W. Maher, *Anal. Chim. Acta*, **302**, (1995), 69.

111. J. E. Going and S. J. Eisenreich, *Anal. Chim. Acta*, **70**, (1974), 95.

112. S. Motomizu, T. Wakimoto and K. Toei, *Talanta*, **31**, (1984), 235.

113. S. Motomizu, T. Wakimoto and K. Toei, *Analyst*, **108**, (1983), 361.

114. S. A. Glazier and M. A. Arnold, *Anal. Chem.*, **60**, (1988), 2540.

115. J. Lui, Y. Masuda, E. Sekido, S. I. Wakida and K. Hiro, *Anal. Chim. Acta*, **224**, (1989), 145.

116. J. F. Coetzee and C. W. Gardner, *Anal. Chem.*, **58**, (1986), 608.

117. P. W. Alexander and J. Koopetngarm, *Anal. Chim. Acta*, **197**, (1987), 353.

118. D. E. Davey, D. E. Mulcahy and G. R. O'Connell, *Talanta*, **37**, (1990), 683.

119. A. L. Heckenberg and P. R. Haddad, *J. Chrom.*, **299**, (1984), 301.

120. P. R. Haddad and P. E. Jackson, *Ion Chromatography. Principles and Applications*, Elsevier Science Publishers BV Amsterdam, Netherlands, (1990), 776.

121. P. Jones, R. Stanley and N. Barnett, *Anal. Chim. Acta*, **249**, (1991), 539.

122. J. J. Pauer, H. R. van Vliet and J. F. van Staden, *Water, S.A.*, **14**, (1988), 125.

123. M. Aoyagi, Y. Yasumasa and A. Nishida, *Anal. Chim. Acta*, **214**, (1988), 229.

124. P. R. Freeman, I. D. McKelvie and B. T. Hart, *Anal. Chim. Acta*, **234**, (1990), 409.

125. F. Mas, J. M. Estela and V. Cerda, *Water, Air, and Soil Pollution*, **52**, (1990), 359.

126. D. Burns, D. Chimpalee, N. Chimpalee and S. Ittipornkul, *Anal. Chim. Acta*, **254**, (1991), 197.

127. Perstorp Analytical Ltd, Application Note 60-01/83 (1993).

128. T. A. H. M. Janse, P. F. A. van der Wiel and G. Kateman, *Anal. Chim. Acta*, **155**, (1993), 89.

129. J. Ruzicka and E. H. Hansen, *Flow Injection Analysis*, 2nd Edn; Wiley-Interscience, New York, (1988).

130. J. Ruzicka and E. H. Hansen, *Anal. Chim. Acta*, **78**, (1975), 145.

131. J. Ruzicka and E. H. Hansen, *Anal. Chim. Acta*, **99**, (1978), 37.

132. M. Valcarcel and M. D. Luque de Castro, *Flow Injection Analysis-Principles and Applications*, Ellis Horwood Ltd., Chichester, (1987).

133. B. Karlberg and G. E. Pacey, *Flow Injection Analysis-A Practical Guide*, Elsevier Science Publishers B. V., Amsterdam, (1989).

134. D. Betteridge, *Anal. Chem.*, **50**, (1978), 832A.

135. J. Ruzicka, *Anal. Chem.*, **55**, (1983), 1041A.

136. T. H. Maugh II, *Science.*, **224**, (1984), 45.

137. J. Ruzicka, *Analyst*, **119**, (1994), 1925.

138. G. Audunsson, *Anal. Chem.*, **58**, (1986), 2714.

139. S. Hirata, Y. Umezaki and M. Ikeda, *Anal. Chem.*, **58**, (1986), 2602.

140. W. E. van der Linden, *Anal. Chim. Acta.*, **151**, (1983), 359.

141. Y. Li and H. Ma, *Talanta*, **42**, (1995), 2033.

142. J. M. Reijn, W. E. van der Linden and H. Poppe, *Anal. Chim. Acta*, **123**, (1981), 229.

143. K. N. Andrew, N. J. Blundell, D. Price and P. J. Worsfold, *Anal. Chem.*, **66**, (1994), 916A.

144. P. J. Worsfold, J. R. Clinch and H. Casey, *Anal. Chim. Acta*, **197**, (1987), 43.

145. J. R. Clinch, P. J. Worsfold and F. Sweeting, *Anal. Chim. Acta*, **214**, (1988), 401.

146. R. L. Benson, P. J. Worsfold and F. Sweeting, *Anal. Chim. Acta*, **238**, (1990), 177.

147. P. K. Dasgupta, H. S. Bellamy, H. Liu, J. L. Lopez, J. L. Loree, K. Morris, K. Peterson and A. M. Kalam, *Talanta*, 40, (1993), 53.

148. N. J. Blundell, A. Hopkins, P. J. Worsfold and H. Casey, *J. Auto. Chem.*, **15**, (1993), 159.

149. N. J. Blundell, P. J. Worsfold and H. Casey and S. Smith, *Env. Int.*, **21**, (1995), 205.

150. K. S. Johnson, C. L. Beehler, C. M. Sakamoto-Arnold, *Anal. Chim. Acta*, **179**, (1986), 245.

151. K. S. Johnson, C. M. Sakamoto-Arnold and C. L. Beehler, *Deep-Sea Res.*, **36**, (1989), 1407.

152. A. Daniel, D. Birot, M. Lehaitre and J. Poncin, *Anal. Chim. Acta*, **308**, (1995), 413.

153. C. D. Taylor, B. L. Howes and K. W. Doherty, *MTS Journal*, **27**, (1993), 32.

154. H. W. Jannasch, K. S. Johnson and C. M. Sakamoto, *Anal. Chem.*, **66**, (1994), 3352.

155. W. Spendly, G. R. Hext and F. R. Himsworth, *Technometrics*, **4**, (1962), 441.

156. J. C. Miller and J. N. Miller, *Statistics for Analytical Chemistry*, 2nd Edn., Horwood Ltd, Chichester, (1988).

157. J. A. Nelder and R. Mead, *Computer J.*, **4**, (1965), 308.

158. S. L. Morgan and S. N. Deming, *Anal. Chem.*, **46**, (1974), 1170.

159. S. L. Morgan and S. N. Deming, *J. Chromogr.*, **112**, (1975), 267.

160. L. A. Yabro and S. N. Deming, *Anal. Chim. Acta*, **73**, (1974), 391.

161. M. W. Routh, P. A. Swartz and M. B. Denton, *Anal. Chem.*, **49**, (1977), 1422.

162. P. B. Ryan, P. L. Barr and H. D. Todd, *Anal. Chem.*, **52**, (1980), 1460.

163. G. Irons, Bsc Final Year Project, University of Hull, 1990.

164. D. Betteridge, E. L. Dagless, B. Fields and N. F. Graves, *Analyst*, **103**, (1978), 897.

165. H. Bergamin, B. F. Reis and E. A. G. Zagatto, *Anal. Chim. Acta*, **97**, (1978), 427.

166. J. Thomsen, K. S. Johnson and R. L. Petty, *Anal. Chem.*, **55**, (1983), 2378.

167. F. J. Krug, H. Bergamin, E. A. G. Zagatto and S. S. Jorgensen, *Analyst*, **102**, (1977), 503.

168. E. A. G. Zagatto, B. F. Reis, M. Martinelli, F. J. Krug, H. Bergamin and M. F. Gine, *Anal. Chim. Acta*, **198**, (1987), 153.

169. A. Daniel, D. Birot, M. Lehaitre and J. Poncin, *Anal. Chim. Acta*, (1994).

170. T. McCormack, A. R. J. David, P. J. Worsfold and R. Howland, *Anal. Proc.*, **31**, (1994), 81.

171. Ph. Quevauviller and M. Valcarcel, *The certification of the contents of nitrate in simulated freshwater*, European Commission (Community Bureau of Reference), Report EUR 16137 EN, (1995).

172. UNESCO, IOC-IAEA-UNEP, *Group of experts on standards and reference materials*, (GESREM), 2nd session, (1991), 12.

173. UNESCO, IOC-IAEA-UNEP, *Group of experts on standards and reference materials*, (GESREM), 3rd session, (1991), 16.

174. A. Aminot and R. Kerouel, *Mar. Chem.*, **49**, (1995), 221.

175. *Report on the intercalibration measurements in Copenhagen*, UNESCO Technical Papers in Marine Science, **3**, (1965), 14.

176. *Report on the intercalibration measurements*, Leningrad 24-28 May 1966, Copenhagen, September 1966, UNESCO Technical Papers in Marine Science, **9**, (1966), 114.

177. *The International Intercalibration Exercise for Nutrient Methods*, ICES Cooperative Research Report, **67**, (1977), 44.

178. *Fourth Intercomparison Exercise for Nutrients in Sea Water*, ICES Cooperative Research Report, **174**, (1991), 83.

179. L. J. Greenfield and F. A. Kalber, *Bull. Mar. Sci. Gulf. Carrib.*, **4**, (1955), 323.

180. J. Murphy and J. P. Riley, *J. Mar. Biol. Ass. U.K.*, **37**, (1958), 9.

181. L. J. Lennox, *Water Res.*, **13**, (1979), 1329.

182. K. I. Aspila, H. Agemian and A. S. Y. Chau, *Analyst*, **83**, (1976), 187.

183. R. A. Chalmers and A. G. Sinclair, *Anal. Chim. Acta*, **33**, (1965), 384.

184. S. C. Pai, C. C. Yang, and J. P. Riley, *Anal. Chim. Acta*, **229**, (1990), 115.

185. D. N. Fogg and N. T. Wilkinson, *Analyst*, **83**, (1958), 406.

186. J. E. Harwood, R. A. van Steenderen and A. L. Kuhn, *Water Res.*, **3**, (1969), 417.

187. J. T. H. Goossen and J. G. Kloosterboer, *Anal Chem.*, **50**, (1978), 707.

188. T. G. Towns, *Anal. Chem.*, **58**, (1986), 223.

189. *Standard Methods for the Examination of Water and Waste Water*, ALPHA-AWWA-WPC, L. S. Clesceri, A. E. Greenberg and R. R. Trussel (Eds) 17th edn., (1989), 4.

190. S. Blomquist, K. Hjellstrom and A. Sjosten, *Intern. J. Environ. Anal. Chem.*, **54**, (1993), 31.

191. A. G. Fogg, X. Wang and J. F. Tyson, *Analyst*, **114**, (1989), 1119.

192. H. Liu and P. K. Dasgupta, *Anal. Chim. Acta*, **289**, (1994), 347.

193. A. G. Fogg, E. Cipko, L. Farabella and J. F. Tyson, *Analyst*, **115**, (1990), 593.

194. H. W. Harvey, *J. Mar. Biol. Ass. U.K.*, **27**, (1948), 337.

195. I. M. Kolthoff and P. J. Elving (Eds) *Treatise on Analytical Chemistry II*, Interscience, New York, **3**, (1961).

196. L. H. N. Cooper, *J. Mar. Biol. Ass. U.K.*, **23**, (1938), 171.

197. R. J. Uncles and J. A. Stephens, *Estuaries*, **16**, (1993), 126.

198. J. A. Smith, *Ecological Management Strategies for Impounded Harbours*, PhD Thesis, (1995).

199. J. A. Smith, G. E. Millward and N. H. Babbedge, *Environmental International*, **21**, (1995), 197.

200. A. W. Morris, A. J. Bale and R. J. M. Howland, *Estuarine, Coastal and Shelf Science*, **12**, (1981), 205.

201. S. Knox, M. Whitfield, D. R. Turner and M. I. Liddicoat, *Estuarine, Coastal and Shelf Science*, **22**, (1986), 619.

202. A. W. Morris, R. J. M. Howland, E. M. S. Woodward, A. J. Bale and R. F. C. Mantoura, *Netherlands Journal of Sea Research*, **19**, (1985), 217.

203. J. P. Mommaerts, *J. Mar. Biol. Ass. UK.*, **49**, (1969), 749.

204. J. P. Mommaerts, *J. Mar. Biol. Ass. UK.*, **50**, (1970), 849.

205. E. I. Butler and S. Tibbitts, *J. Mar. Biol. Ass. U.K.* **52**, (1972), 681.

206. *Surveys of Harbours, Rias and Estuaries in Southern Britain*, Field Studies Council, **1**, (1986).

207. V. H. Lewin, *Water Research*, 7, (1973), 55.

208. A. W. Morris, R. J. M. Howland and A. J. Bale, *Estuarine and Coastal Marine Science*, **6**, (1978), 105.

209. E. Boyle, R. Collier, A. T. Dengler, J. M. Edmond, A. C. Ng and R. F. Stallard, *Geochim. Cosmochim. Acta*, **38**, (1974), 1719.

210. A. W. Morris, J. I. Allen, R. J. M. Howland and R. J. Wood, *Estuarine, Coastal and Shelf Science*, **40**, (1995), 387.

211. W. S. Boyle and G. E. Smith, *Bell System Technical Journal.*, **49**, (1970), 587.

212. G. T. Amelio, M. F. Tompsett and G. E. Smith, *Bell Systems Technical Journal.*, **49**, (1970), 593.

213. D. Falkin and M. Vosloo, *Spectroscopy Europe*, 5, (1993), 16.

214. R. B. Bilhorn, J. V. Sweedler, P. M. Epperson and M. B. Denton, *Appl. Spectroscopy*, **41**, (1987), 1114.

215. J. V. Sweedler, R. B. Bilhorn, P. M. Epperson, G. R. Sims and M. B. Denton, *Anal. Chem.*, **60**, (1988), 282A.

216. P. M. Epperson, J. V. Sweedler, R. B. Bilhorn, G. R. Sims and M. B. Denton, *Anal. Chem.*, **60**, (1988), 327A.

217. R. B. Bilhorn, P. M. Epperson, J. V. Sweedler and M. B. Denton, *Appl. Spectroscopy*, **41**, (1987), 1125.

218. W. E. L. Grossman, *J. Chem. Ed.*, **66**, (1989), 697.

219. M. J. Howes and D. V. Morgan (Eds) *Charge-Coupled Devices and Systems*, Wiley-Interscience Publications, New York, (1980).

220. J. D. E. Beynon and D. R. Lamb, *Charge-Coupled Devices and their applications*, McGraw-Hill Ltd., London., (1980).

221. R. Melen and D. Buss, *Charge-Coupled Devices:-Technology and Applications*, IEEE Press, New York., (1977).

222. F. Purcell, *Lazer Focus World*, May, (1993), 93.

223. R. S. Pomeroy, M. E. Baker, M. B. Denton and A. G. Dickson, *Appl. Spectroscopy*, **49**, (1995), 1729.

224. P. M. Epperson, R. D. Jalkian and M. B. Denton, *Anal. Chem.*, **61**, (1989), 282.

225. R. D. Jalkian and M. B. Denton, *Appl. Spectroscopy*, **42**, (1988), 1194.

Appendices

APPENDIX 1 CH119a Cruise Data (10/06/95)

Date	Time	LAT	LON	Tsal	Tsal	Fluor -chla	Trans	depth	Phosphate	Nitrate +	Nitrite	Silicate	PAR
	GMT	°+ve North	°+ve East	Temp °C	Sal - PSU	V or mg/m3		m	v or µM	Nitrite Vor	V or µM	V or µM	
95/06/10	10:00:00	55.7505	-1.6651	9.31	34.021	0.927	0.7319	82.37	0.08967	0	0.10033	0.0988	474.67
95/06/10	10:05:00	55.7506	-1.6887	9.347	34.017	0.927	0.72484	72.13	0.08792	0	0.09858	0.09168	395.94
95/06/10	10:10:00	55.7512	-1.7123	9.524	34.013	0.919	0.74616	74.67	0.08705	0	0.09857	0.08943	462.3
95/06/10	10:15:00	55.7514	-1.737	9.715	34.053	0.966	0.75093	66.3	0.08912	0	0.0974	0.0892	636.35
95/06/10	10:20:00	55.7519	-1.76	9.934	33.904	0.888	0.87142	61.3	0.08753	0	0.09888	0.08885	594.17
95/06/10	10:25:00	55.7522	-1.7832	10.293	33.844	0.93	1.08519	57.73	0.09773	0	0.0991	0.09397	649.08
95/06/10	10:30:00	55.7533	-1.8073	10.349	33.8	1.009	1.40204	39.23	0.10213	0	0.10042	0.10202	567.33
95/06/10	10:35:00	55.7543	-1.8293	10.433	33.815	1.083	1.37978	27.73	0.10562	0	0.10002	0.10293	460.19
95/06/10	10:40:00	55.7557	-1.853	10.461	33.811	1.199	1.62632	32.07	0.10738	0	0.10133	0.1032	433.86
95/06/10	10:45:00	55.7569	-1.8763	10.331	33.816	1.14	1.32729	32.13	0.11025	0	0.10018	0.10455	431.88
95/06/10	10:50:00	55.7579	-1.899	10.377	33.824	1.044	1.35764	33.87	0.11082	0	0.1006	0.10103	437.17
95/06/10	10:55:00	55.7578	-1.914	10.438	33.796	1.084	1.58799	31.17	0.1099	0	0.10077	0.10263	481.23
95/06/10	11:00:00	55.7579	-1.9249	10.475	33.799	1.148	1.89527	33.23	0.10958	0	0.0996	0.10443	605.44
95/06/10	11:05:00	55.7599	-1.9329	10.466	33.803	1.068	1.79841	32.77	0.1112	0	0.10055	0.10725	633.12
95/06/10	11:10:00	55.7597	-1.9329	10.47	33.819	1.181	1.82327	32.77	0.11138	0	0.1008	0.10717	674.97
95/06/10	11:15:00	55.759	-1.9332	10.498	33.819	1.316	1.91748	32.27	0.11267	0	0.10077	0.1075	741.86
95/06/10	11:20:00	55.7582	-1.9331	10.484	33.815	1.346	1.9752	32.65	0.11573	0	0.10088	0.10797	692.69
95/06/10	11:25:00	55.7572	-1.9318	10.498	33.811	1.403	1.9752	32.3	0.11597	0	0.10103	0.10775	756.71
95/06/10	11:30:00	55.7562	-1.9318	10.517	33.787	1.442	2.0141	32.07	0.11728	0	0.10125	0.10743	765.21
95/06/10	11:35:00	55.7556	-1.9315	10.498	33.795	1.394	1.9752	32	0.12378	0	0.1016	0.1101	629.28
95/06/10	11:40:00	55.7607	-1.9209	10.494	33.811	1.113	1.84815	34.77	0.11883	0	0.10097	0.07278	465.13
95/06/10	11:45:00	55.766	-1.9086	10.386	33.8	1.016	1.31641	36.53	0.11388	0	0.09968	0.07277	458.79
95/06/10	11:50:00	55.7721	-1.8945	10.349	33.792	0.975	1.18446	37.9	0.11262	0	0.10027	0.06642	498.65
95/06/10	11:55:00	55.778	-1.8802	10.279	33.808	1.013	1.07484	38.2	0.11365	0	0.10083	0.06713	461.6
95/06/10	12:00:00	55.7844	-1.8663	10.237	33.832	0.956	0.91822	47.2	0.10075	0	0.10358	0.03442	480.5
95/06/10	12:05:00	55.7908	-1.852	10.205	33.86	1.035	0.96054	55.05	0.08928	0	0.10422	0.03318	494.11
95/06/10	12:10:00	55.7972	-1.8391	10.275	33.804	0.941	1.10066	66.1	0.08617	0	0.1039	0.0326	520.92
95/06/10	12:15:00	55.8031	-1.8256	10.293	33.804	0.936	1.11364	74.65	0.08778	0	0.10123	0.06548	643.17
95/06/10	12:20:00	55.8098	-1.8105	10.293	33.772	0.897	1.10842	73.1	0.1093	0	0.10117	0.06657	612.87
95/06/10	12:25:00	55.817	-1.7943	10.307	33.772	0.895	1.16597	73.5	0.11117	0	0.10147	0.06758	465.13
95/06/10	12:30:00	55.8247	-1.7781	10.293	33.788	0.867	1.22972	74.65	0.11242	0	0.1019	0.06817	491.86
95/06/10	12:35:00	55.8322	-1.7615	10.284	33.792	0.886	1.21636	75.8	0.11498	0	0.10277	0.07145	596.89
95/06/10	12:40:00	55.8402	-1.7455	9.958	33.856	0.973	1.24312	77.45	0.11532	0	0.10257	0.07072	735.85
95/06/10	12:45:00	55.8493	-1.7289	9.664	33.981	0.84	0.82041	79.03	0.11193	0	0.10235	0.0641	981.99
95/06/10	12:50:00	55.8577	-1.7116	9.734	34.13	0.99	1.10587	74.67	0.11012	0	0.10288	0.06252	967.13
95/06/10	12:55:00	55.8665	-1.6946	9.832	34.141	1.031	1.04153	65.13	0.10073	0	0.10073	0.05967	922.97
95/06/10	13:00:00	55.8752	-1.6767	9.902	34.137	0.982	1.15551	73	0.09457	0	0.09962	0.05695	857
95/06/10	13:05:00	55.884	-1.659	9.869	34.145	0.974	0.84703	79.43	0.09157	0	0.10007	0.05708	952.02
95/06/10	13:10:00	55.8927	-1.6412	9.701	34.134	0.904	0.91822	76.93	0.08995	0	0.10058	0.05628	917.36
95/06/10	13:15:00	55.9002	-1.6214	9.59	34.15	0.945	0.93062	77.25	0.08882	0	0.10023	0.05602	762.88
95/06/10	13:20:00	55.9072	-1.602	9.506	34.155	0.936	0.89606	70.43	0.0882	0	0.10077	0.05887	621.65
95/06/10	13:25:00	55.912	-1.5877	9.468	34.163	0.955	0.74141	66.03	0.08878	0	0.10127	0.06067	513.56
95/06/10	13:30:00	55.915	-1.5804	9.482	34.171	1.039	0.77954	70.55	0.08943	0	0.10138	0.06135	435.84
95/06/10	13:35:00	55.9146	-1.5804	9.492	34.163	1.022	0.77709	69.7	0.09048	0	0.10082	0.05928	526.51
95/06/10	13:40:00	55.9141	-1.5806	9.441	34.171	1.038	0.78434	69.6	0.09047	0	0.1004	0.0587	668.49
95/06/10	13:45:00	55.9135	-1.5808	9.468	34.147	1.018	0.78434	68.67	0.09063	0	0.10005	0.05932	640.24
95/06/10	13:50:00	55.9127	-1.5799	9.468	34.171	1.019	0.77954	68.6	0.0906	0	0.09977	0.05902	742.99
95/06/10	13:55:00	55.9125	-1.5808	9.468	34.175	1.025	0.77709	68.2	0.09013	0	0.09938	0.0582	507.34
95/06/10	14:00:00	55.9124	-1.5802	9.464	34.163	1.047	0.79869	67.8	0.09022	0	0.09872	0.05787	551.7
95/06/10	14:05:00	55.9117	-1.5816	9.45	34.167	1.051	0.79633	67.27	0.09027	0	0.09858	0.05853	552.54
95/06/10	14:10:00	55.9019	-1.5799	9.445	34.184	0.994	0.76282	67.93	0.08973	0	0.0987	0.05855	445.47
95/06/10	14:15:00	55.8872	-1.5757	9.319	34.188	1.168	0.89112	70.27	0.08958	0	0.09897	0.06083	405.31
95/06/10	14:20:00	55.8726	-1.5698	#N/A	34.213	1.197	0.92076	75.15	0.09098	0	0.0985	0.06113	406.54
95/06/10	14:25:00	55.8586	-1.5657	9.543	34.175	1.077	0.81072	67.7	0.0936	0	0.09872	0.06382	561.02
95/06/10	14:30:00	55.8433	-1.5598	9.655	34.171	1.011	0.76995	70.1	0.09052	0	0.09777	0.05832	512
95/06/10	14:35:00	55.8284	-1.5546	9.692	34.13	0.976	0.77229	#N/A	0.08855	0	0.09683	0.05627	479.03
95/06/10	14:40:00	55.8134	-1.5497	9.673	34.138	0.997	0.77954	67	0.08763	0	0.09718	0.0551	490.36
95/06/10	14:45:00	55.7984	-1.5444	9.692	34.13	1.011	0.79387	57.13	0.08733	0	0.09718	0.05493	558.46
95/06/10	14:50:00	55.7837	-1.5391	9.706	34.102	1.026	0.80835	63.03	0.08792	0	0.0976	0.05533	505.02
95/06/10	14:55:00	55.7693	-1.5349	9.659	34.122	1.075	0.82279	62.73	0.0875	0	0.09852	0.05533	534.86
95/06/10	15:00:00	55.7546	-1.5308	9.455	34.114	1.11	0.86171	75.67	0.0881	0	0.09923	0.05713	595.98
95/06/10	15:05:00	55.7401	-1.5262	9.38	34.111	1.063	0.82765	73.93	0.0907	0.02	0.10245	0.06342	562.74
95/06/10	15:10:00	55.7253	-1.5221	9.329	34.123	1.029	0.79869	78.27	0.09443	0.05	0.10268	0.06638	446.83
95/06/10	15:15:00	55.7102	-1.5178	9.385	34.111	1.09	0.89849	77.9	0.09562	0	0.1032	0.06802	448.88
95/06/10	15:20:00	55.6958	-1.5143	9.837	34.001	1.288	1.10842	85.07	0.097	0	0.1016	0.06638	362.45
95/06/10	15:25:00	55.6816	-1.5107	9.543	33.965	1.109	1.011	46.93	0.0996	0	0.09942	0.06163	436.51
95/06/10	15:30:00	55.6668	-1.5155	9.748	33.937	1.033	1.12142	58.73	0.1047	0.01	0.10352	0.07025	554.22
95/06/10	15:35:00	55.6529	-1.5217	9.748	33.953	1.173	1.14497	48	0.10848	0	0.10313	0.07147	611.01
95/06/10	15:40:00	55.6386	-1.5266	9.697	33.953	0.949	0.97307	43.57	0.1077	0.02	0.10218	0.0686	554.22
95/06/10	15:45:00	55.6244	-1.5321	9.669	33.945	0.952	0.9706	48.2	0.10755	0.02	0.10255	0.06905	450.93
95/06/10	15:50:00	55.6103	-1.5367	9.566	33.957	1.008	0.9706	49.57	0.10885	0.03	0.1024	0.06805	325.11
95/06/10	15:55:00	55.5971	-1.5418	9.706	33.933	0.905	1.08519	43.33	0.1074	0.05	0.10363	0.07015	354.62
95/06/10	16:00:00	55.5828	-1.5459	9.757	33.92	0.953	1.23784	41.97	0.10768	0.07	0.10448	0.0727	443.44
95/06/10	16:05:00	55.5691	-1.5468	9.669	33.937	0.93	1.21909	39.83	0.11052	0.06	0.10498	0.07478	473.95
95/06/10	16:10:00	55.5677	-1.5491	9.757	33.896	1.057	1.14766	38.07	0.1094	0.04	0.104	0.0727	483.44
95/06/10	16:15:00	55.568	-1.5502	9.776	33.896	1.043	1.15809	38.87	0.10757	0.04	0.10442	0.07365	393.54
95/06/10	16:20:00	55.5688	-1.5505	9.753	33.908	1.021	1.17656	39.07	0.10862	0.06	0.1048	0.07445	339.11
95/06/10	16:25:00	55.5688	-1.5527	9.753	33.892	1.034	1.15809	39.27	0.10908	0.06	0.10508	0.07527	354.62
95/06/10	16:30:00	55.5698	-1.5537	9.771	33.9	1.007	1.14497	39.73	0.10868	0.06	0.10515	0.07493	465.84
95/06/10	16:35:00	55.571	-1.5543	9.776	33.904	1.028	1.1424	39.6	0.10945	0.06	0.10507	0.07595	382.69
95/06/10	16:40:00	55.5687	-1.5465	9.776	33.892	1.064	1.1951	39.07	0.10933	0.07	0.10527	0.07468	343.8
95/06/10	16:45:00	55.5651	-1.5232	9.538	33.937	1.084	1.06199	44.67	0.10987	0.03	0.10503	0.07532	364.11
95/06/10	16:50:00	55.5612	-1.5003	9.664	33.941	1.259	1.16866	42.93	0.10707	0	0.10323	0.07037	353.54
95/06/10	16:55:00	55.5577	-1.4775	9.431	33.965	1.414	1.25127	69.27	0.10525	0	0.10233	0.0692	393.54
95/06/10	17:00:00	55.5538	-1.4545	9.482	33.977	1.245	1.09546	66.3	0.10507	0.01	0.1021	0.0689	336.37
95/06/10	17:05:00	55.5496	-1.4305	9.403	33.957	1.163	0.9907	61.07	0.10428	0.01	0.10193	0.068	309.95
95/06/10	17:10:00	55.5455	-1.4073	9.45	33.957	1.293	1.1163	74.5	0.1025	0.09	0.1018	0.06695	251.04

95/06/10	17:15:00	55.5411	-1.3842	9.124	34.087	1.39	1.21636	69.6	0.10225	0.08	0.10237	0.06537	390.35
95/06/10	17:20:00	55.5381	-1.3597	9.073	34.164	1.281	1.14497	66.77	0.10978	#N/A	0.1069	0.08005	360.8
95/06/10	17:25:00	55.5361	-1.3366	9.147	34.115	1.188	1.04656	62.8	0.11393	0.12	0.10343	0.01983	391.54
95/06/10	17:30:00	55.5328	-1.3122	9.152	34.127	1.027	0.96311	74.23	0.09317	0.1	0.10272	0.01797	419.98
95/06/10	17:35:00	55.5289	-1.2892	9.129	34.111	1.182	1.11364	72.77	0.08823	0.09	0.10247	0.0174	279.72
95/06/10	17:40:00	55.5252	-1.2655	9.045	34.185	1.284	1.16597	66	0.08705	0.09	0.10232	0.01768	245.61
95/06/10	17:45:00	55.521	-1.2413	9.413	34.371	1.26	1.12666	79.63	0.08533	0.1	0.1022	0.01738	267.49
95/06/10	17:50:00	55.5174	-1.2175	9.487	34.366	1.23	1.03892	#N/A	0.08507	0.11	0.10207	0.01752	262.91
95/06/10	17:55:00	55.5139	-1.1943	9.482	34.394	1.284	1.0517	91.3	0.08478	0.1	0.10195	0.01745	253.73
95/06/10	18:00:00	55.5099	-1.1703	9.604	34.381	1.161	0.95061	95	0.0845	0.09	0.10187	0.01687	215.55

APPENDIX 2 CH119a Cruise Data (10/06/95-11/06/96)

Date	Time	LAT	LON	Tsal	Tsal	Fluor -chla	Trans	depth	Phosphate	Nitrate +	Nitrite	Silicate	PAR
	GMT	°+ve North	°+ve East	Temp °C	Sal - PSU	V or mg/m3		m	v or µM	Nitrite Vor	V or µM	V or µM	
95/06/10	23:00:00	55.3381	-1.0633	9.645	34.243	0.963	0.90344	#N/A	0.06937	0.13	-4.043	0.02373	#N/A
95/06/10	23:05:00	55.3374	-1.0631	9.645	34.251	0.981	0.88126	91.65	0.07068	0.12	-2.2146	0.02107	#N/A
95/06/10	23:10:00	55.3362	-1.0627	9.645	34.239	0.97	0.89354	92.25	0.07158	0.11	-1.8311	0.02087	#N/A
95/06/10	23:15:00	55.3348	-1.0624	9.627	34.255	0.956	0.8886	92.8	0.07198	0.1	0.16115	0.02035	#N/A
95/06/10	23:20:00	55.3333	-1.0611	9.632	34.247	0.945	0.88619	94.8	0.07193	0.09	0.1657	0.0208	#N/A
95/06/10	23:25:00	55.3317	-1.0627	9.608	34.247	0.947	0.87634	100.5	0.07223	0.09	0.1726	0.02115	#N/A
95/06/10	23:30:00	55.3293	-1.0826	9.618	34.244	0.949	0.84703	96.9	0.07198	0.09	0.15927	0.02132	#N/A
95/06/10	23:35:00	55.3268	-1.1078	9.562	34.219	0.971	0.86171	94.6	0.07177	0.08	0.16907	0.02127	#N/A
95/06/10	23:40:00	55.323	-1.1328	9.473	34.224	1.019	0.91325	91.45	0.07178	0.08	0.17442	0.02445	#N/A
95/06/10	23:45:00	55.3173	-1.1565	9.441	34.22	1.058	0.9706	83.87	0.07167	0.08	0.17675	0.0292	#N/A
95/06/10	23:50:00	55.3088	-1.1778	9.399	34.261	1.06	0.96054	80.43	0.07102	0.08	0.18015	0.02738	#N/A
95/06/10	23:55:00	55.2995	-1.1998	9.464	34.293	1.057	0.95552	77.9	0.0714	0.07	0.18208	0.02545	#N/A
95/06/11	00:00:00	55.2908	-1.2222	9.282	34.261	1.059	0.98822	73.7	0.07103	0.07	0.18293	0.02402	#N/A
95/06/11	00:05:00	55.2828	-1.2448	9.11	34.242	1.082	1.01858	70.7	0.07117	0.07	0.18512	0.02685	#N/A
95/06/11	00:10:00	55.2736	-1.2656	8.984	34.078	1.046	0.9456	68.97	0.07247	0.06	0.185	0.03338	#N/A
95/06/11	00:15:00	55.2652	-1.2876	8.994	34.09	1.077	0.95808	65.5	0.07345	0.07	0.18607	0.02527	#N/A
95/06/11	00:20:00	55.257	-1.31	9.087	34.09	1.03	0.98822	59.83	0.07327	0.07	0.18672	0.02602	#N/A
95/06/11	00:25:00	55.2485	-1.3319	9.091	34.078	1.033	1.0084	55.1	0.0727	0.06	0.18523	0.02388	#N/A
95/06/11	00:30:00	55.241	-1.3548	9.068	34.111	1.026	0.98316	54.57	0.07243	0.06	0.18412	0.02243	#N/A
95/06/11	00:35:00	55.2352	-1.3734	9.017	34.103	1.013	0.95061	56.53	0.07277	0.07	0.18308	0.02322	#N/A
95/06/11	00:40:00	55.2286	-1.3907	9.087	34.127	1.057	0.98069	54.67	0.0734	0.07	0.18087	0.02662	#N/A
95/06/11	00:45:00	55.2215	-1.4085	9.091	34.115	1.044	1.04656	52.9	0.0742	0.06	0.17743	0.02605	#N/A
95/06/11	00:50:00	55.2167	-1.4281	9.091	34.082	1.037	1.08001	49.5	0.07352	0.06	0.17417	0.02108	#N/A
95/06/11	00:55:00	55.2107	-1.4458	#N/A	#N/A	1.115	1.70396	45.67	0.07275	0.06	0.17085	0.0185	#N/A
95/06/11	01:00:00	55.2079	-1.4522	9.231	34.034	1.088	3.0746	44.1	0.07292	0.06	0.16828	0.01738	#N/A
95/06/11	01:05:00	55.2064	-1.4517	9.091	34.058	1.193	2.94505	44.17	0.07628	0.05	0.16633	0.01938	#N/A
95/06/11	01:10:00	55.2048	-1.4509	9.133	34.042	1.237	3.06817	44.73	0.07593	0.05	0.16283	0.01702	#N/A
95/06/11	01:15:00	55.2027	-1.4514	9.147	34.046	1.196	3.19967	44.3	0.07585	0.05	0.16038	0.01743	#N/A
95/06/11	01:20:00	55.201	-1.4513	9.115	34.05	1.176	3.1757	44.27	0.07657	0.04	0.15822	0.0187	#N/A
95/06/11	01:25:00	55.1996	-1.4513	9.152	34.033	1.228	3.33101	44.43	0.07645	0.04	0.15535	0.0182	#N/A
95/06/11	01:30:00	55.198	-1.4505	9.175	34.013	1.168	3.34457	45.03	0.07693	0.04	0.15318	0.01815	#N/A
95/06/11	01:35:00	55.1975	-1.4336	9.077	34.025	1.137	2.6214	46.5	0.07752	0.04	0.15223	0.01952	#N/A
95/06/11	01:40:00	55.1967	-1.409	9.124	34.115	1.077	1.20305	47.63	0.07802	0.04	0.14848	0.0178	#N/A
95/06/11	01:45:00	55.1975	-1.3833	9.045	34.115	1.028	1.01858	52.83	0.07473	0.04	0.14657	0.02045	#N/A
95/06/11	01:50:00	55.1986	-1.3576	9.073	34.164	1.008	0.97811	56.8	0.07465	0.04	0.14625	0.02358	#N/A
95/06/11	01:55:00	55.2009	-1.3316	9.017	34.152	1.087	0.98564	57.5	0.0753	0.04	0.14487	0.02992	#N/A
95/06/11	02:00:00	55.2023	-1.3072	8.966	34.103	1	0.91579	58.07	0.07547	0.04	0.14368	0.02873	#N/A
95/06/11	02:05:00	55.2027	-1.281	8.942	34.111	0.986	0.91082	64.57	0.07618	0.03	0.14238	0.02492	#N/A
95/06/11	02:10:00	55.2029	-1.2563	9.073	34.086	1.007	0.93316	67.93	0.07615	0.03	0.14112	0.02522	#N/A
95/06/11	02:15:00	55.2039	-1.2303	9.427	34.262	1.033	0.96311	72.63	0.07582	0.03	0.14037	0.02742	#N/A
95/06/11	02:20:00	55.2051	-1.2041	9.562	34.244	1.02	0.95552	82.25	0.0744	0.03	0.13783	0.02372	#N/A
95/06/11	02:25:00	55.205	-1.1792	9.599	34.232	0.988	0.90586	#N/A	0.07265	0.03	0.1376	0.0206	#N/A
95/06/11	02:30:00	55.2065	-1.1533	9.599	34.203	0.963	0.86902	#N/A	0.07198	0.03	0.13742	0.02307	#N/A
95/06/11	02:35:00	55.2073	-1.128	9.492	34.163	0.845	0.89606	91.5	0.07197	0.03	0.13693	0.02168	#N/A
95/06/11	02:40:00	55.208	-1.1029	9.524	34.155	0.803	0.89112	95.6	0.0748	0.03	0.13703	0.02328	#N/A
95/06/11	02:45:00	55.2087	-1.0766	9.576	34.175	0.808	0.83251	100.6	0.07597	0.02	0.136	0.02348	#N/A
95/06/11	02:50:00	55.208	-1.0545	9.59	34.159	0.767	0.83976	101.9	0.07625	0.03	0.13497	0.0225	#N/A
95/06/11	02:55:00	55.2078	-1.0391	9.622	34.179	0.805	0.83003	94.45	0.0763	0.03	0.1336	0.02268	0.25
95/06/11	03:00:00	55.2082	-1.0305	9.632	34.179	0.804	0.80105	#N/A	0.07577	0.03	0.13233	0.02187	0.48
95/06/11	03:05:00	55.207	-1.0299	9.641	34.179	0.827	0.80352	91	0.07528	0.02	0.1314	0.02202	0.89
95/06/11	03:10:00	55.2059	-1.0306	9.632	34.187	0.794	0.79633	91.1	0.075	0.02	0.13023	0.02112	1.34
95/06/11	03:15:00	55.2056	-1.0303	9.618	34.183	0.784	0.79869	91.1	0.07487	0.02	0.12808	0.02122	1.55
95/06/11	03:20:00	55.2045	-1.0298	9.627	34.183	0.789	0.81556	90.8	0.07488	0.02	0.12608	0.02192	1.93
95/06/11	03:25:00	55.2032	-1.0294	9.622	34.175	0.772	0.83003	90.5	0.07513	0.02	0.12353	0.02193	2.99
95/06/11	03:30:00	55.2025	-1.0288	9.608	34.183	0.763	0.82279	89.9	0.07528	0.02	0.12102	0.02163	4.66
95/06/11	03:35:00	55.2022	-1.0288	9.604	34.171	0.79	0.82279	90.5	0.07528	0.02	0.11848	0.02203	6.5
95/06/11	03:40:00	55.2003	-1.0272	9.604	34.163	0.787	0.79387	90.2	0.07535	0.02	0.11635	0.02372	7.51
95/06/11	03:45:00	55.1905	-1.0442	9.576	34.159	0.803	0.82527	101.3	0.07545	0.02	0.11448	0.0227	8.97
95/06/11	03:50:00	55.1813	-1.0647	9.613	34.159	0.795	0.83003	102.3	0.07798	0.02	0.11383	0.02437	7.42
95/06/11	03:55:00	55.1714	-1.0847	9.604	34.139	0.779	0.83003	93.67	0.07692	0.02	0.11212	0.0234	13.94
95/06/11	04:00:00	55.1628	-1.1043	9.585	34.114	0.779	0.82527	#N/A	0.07767	0.02	0.11072	0.02322	14.62
95/06/11	04:05:00	55.1526	-1.123	9.632	34.151	0.91	0.84464	#N/A	0.07533	0.01	0.10893	0.01965	15.4
95/06/11	04:10:00	55.1421	-1.1416	9.659	34.171	1.04	0.89354	#N/A	0.07585	0.02	0.10727	0.01895	16.97
95/06/11	04:15:00	55.1318	-1.1598	9.655	34.163	1.042	0.88619	86.7	0.07885	0.01	0.10695	0.01757	26.83
95/06/11	04:20:00	55.1212	-1.178	9.697	34.171	1.02	0.87885	82.67	0.0761	#N/A	0.11358	0.01835	28.79
95/06/11	04:25:00	55.1108	-1.1961	9.729	34.199	1.001	0.89354	74.47	0.08797	#N/A	0.11112	0.00725	33.26
95/06/11	04:30:00	55.1003	-1.2146	9.743	34.19	0.989	0.88619	67.93	0.07047	#N/A	0.10812	0.03127	45.99
95/06/11	04:35:00	55.0904	-1.233	9.767	34.19	0.976	0.89606	62.4	0.52065	#N/A	0.3551	0.24937	63.37
95/06/11	04:40:00	55.0804	-1.251	9.58	34.207	0.992	0.94806	56.8	0.6493	#N/A	0.5809	0.25908	80.01
95/06/11	04:45:00	55.0691	-1.2683	9.031	34.078	1.013	1.09546	54.37	1.19373	#N/A	0.60015	0.4694	85.86
95/06/11	04:50:00	55.0587	-1.286	9.007	34.082	1.041	1.16597	52.23	1.70898	#N/A	0.839	0.6833	74.47
95/06/11	04:55:00	55.0476	-1.3038	9.156	34.091	0.96	1.28371	47.1	1.73217	#N/A	1.0607	0.68663	75.24
95/06/11	05:00:00	55.0372	-1.3212	9.087	34.082	0.989	1.66196	41.43	2.24957	#N/A	1.04403	0.88652	78.52
95/06/11	05:05:00	55.0268	-1.3386	9.194	34.046	1	2.02051	36.3	0.19325	#N/A	0.10978	0.04063	89.6
95/06/11	05:10:00	55.0169	-1.3564	9.357	34.074	0.986	2.05325	21.97	0.15483	#N/A	0.45933	0.04152	91.63
95/06/11	05:15:00	55.0134	-1.365	9.38	34.074	1.005	2.06648	24	0.36967	#N/A	0.46975	0.0547	91.21
95/06/11	05:20:00	55.0136	-1.3652	9.399	34.058	0.986	2.13644	23.87	0.13868	#N/A	0.11213	0.00805	99.49
95/06/11	05:25:00	55.0136	-1.3658	9.394	34.07	1.01	2.06648	23.83	0.1008	#N/A	0.11077	0.0055	115.16
95/06/11	05:30:00	55.0143	-1.3659	9.38	34.05	0.983	2.06986	23.57	0.09188	#N/A	0.11067	0.00447	110.69
95/06/11	05:35:00	55.0148	-1.368	9.394	34.062	1.013	2.05986	22.2	0.08805	0.02	0.11147	0.00402	120.55
95/06/11	05:40:00	55.0154	-1.3682	9.403	34.062	1.043	2.0996	21.27	0.07557	0.02	0.10803	0.0168	134.39
95/06/11	05:45:00	55.0193	-1.3711	9.417	34.07	1.063	2.20078	23.53	0.08172	0.01	0.10812	0.0196	123.21
95/06/11	05:50:00	55.0239	-1.3505	9.338	34.078	1.02	2.04679	28.13	0.08283	0.01	0.10747	0.01835	123.21
95/06/11	05:55:00	55.0274	-1.3262	9.273	34.087	0.959	1.88583	39.1	0.08252	0.01	0.10712	0.01973	144.96
95/06/11	06:00:00	55.0312	-1.302	9.198	34.074	0.917	1.70989	44.53	0.08307	0.01	0.10702	0.02223	159.24
95/06/11	06:05:00	55.0346	-1.2778	9.222	34.087	0.972	1.67089	51.03	0.0837	0.02	0.10705	0.02405	92.85
95/06/11	06:10:00	55.0387	-1.2538	9.096	34.099	0.912	1.47261	53.93	0.08293	0.02	0.1072	0.02283	76.47
95/06/11	06:15:00	55.0437	-1.2302	9.343	34.184	1.042	1.25392	56.83	0.08335	0.01	0.10727	0.02613	148.16
95/06/11	06:20:00	55.0491	-1.2073	8.984	34.148	1.028	1.22172	58.23	0.08077	0.02	0.10715	0.02245	265.73
95/06/11	06:25:00	55.0538	-1.1836	#N/A	34.212	1.018	1.08773	65.45	0.08065	0.01	0.1082	0.03058	310.9
95/06/11	06:30:00	55.0594	-1.1609	9.618	34.187	1.02	0.98822	75.47	0.07782	0.01	0.10692	0.02093	369.14
95/06/11	06:35:00	55.064	-1.1386	9.659	34.178	0.951	0.95061	82.7	0.07512	0.01	0.10748	0.0162	371.58

95/06/11	06:40:00	55.0678	-1.1174	9.678	34.138	0.826	0.93062	84.8	0.07472	0.02	0.10877	0.01903	494.11
95/06/11	06:45:00	55.0731	-1.0968	9.604	34.114	0.798	0.89849	84.3	0.07738	0.02	0.10928	0.02058	616.93
95/06/11	06:50:00	55.076	-1.0776	9.627	34.122	0.768	0.85192	86.8	0.08012	0.02	0.11005	0.02038	639.26
95/06/11	06:55:00	55.0813	-1.0613	9.715	34.106	0.784	0.85441	90.3	0.08013	0.02	0.10985	0.02002	773.42
95/06/11	07:00:00	55.0846	-1.0506	9.659	34.098	0.732	0.78905	87.6	0.08035	0.01	0.10985	0.02005	712.32
95/06/11	07:05:00	55.0851	-1.0514	9.645	34.094	0.741	0.78905	88	0.07953	0.01	0.1101	0.0191	835.93
95/06/11	07:10:00	55.0858	-1.0523	9.645	34.098	0.698	0.78905	88.9	0.07903	0.02	0.1102	0.01917	1098.1
95/06/11	07:15:00	55.0862	-1.0513	9.641	34.089	0.75	0.81794	89.4	0.07918	0.02	0.11033	0.02007	1022.2
95/06/11	07:20:00	55.0883	-1.0514	9.65	34.101	0.703	0.79387	#N/A	0.07908	0.01	0.11032	0.01973	1364.1
95/06/11	07:25:00	55.0886	-1.0508	9.655	34.097	0.719	0.79869	90.7	0.07933	0.02	0.11073	0.02002	1074.37
95/06/11	07:30:00	55.0898	-1.0512	9.645	34.094	0.714	0.78905	91.3	0.07908	0.02	0.11142	0.01997	728.05
95/06/11	07:35:00	55.0911	-1.0512	9.655	34.098	0.743	0.81309	92.05	0.08077	0.02	0.11173	0.02118	472.51
95/06/11	07:40:00	55.0842	-1.0672	9.701	34.098	0.743	0.80589	89.4	0.07937	0.02	0.11182	0.01955	298.97
95/06/11	07:45:00	55.0738	-1.0845	9.697	34.102	0.795	0.88367	84.7	0.07952	0.02	0.1113	0.01907	221.32
95/06/11	07:50:00	55.0635	-1.1019	9.683	34.102	0.811	0.89849	82.67	0.07987	0.02	0.1121	0.01938	193.74
95/06/11	07:55:00	55.0529	-1.1188	9.692	34.13	#N/A	#N/A	81.77	0.07925	0.02	0.11222	0.01925	185.46
95/06/11	08:00:00	55.0432	-1.1363	9.725	34.134	#N/A	#N/A	80.9	0.07865	0.02	0.11218	0.01928	379.02
95/06/11	08:05:00	55.0327	-1.1532	9.711	34.166	0.866	1.0517	69.1	0.0781	0.02	0.11285	0.01933	352.46
95/06/11	08:10:00	55.0219	-1.1704	9.538	34.167	1.038	1.00332	61.2	0.07783	0.02	0.11277	0.01953	290.29
95/06/11	08:15:00	55.011	-1.1884	9.273	34.135	1.052	1.05684	58.2	0.07552	0.02	0.11313	0.02047	384.45
95/06/11	08:20:00	55.0002	-1.2055	9.366	34.148	0.999	1.18718	55	0.07633	0.02	0.115	0.03133	414.05
95/06/11	08:25:00	54.9894	-1.2226	9.357	34.115	0.973	1.23784	52.5	0.07797	0.03	0.11522	0.03035	459.49
95/06/11	08:30:00	54.979	-1.2392	9.52	34.119	1.041	1.25127	49.97	0.08038	0.02	0.11575	0.03095	366.34
95/06/11	08:35:00	54.9683	-1.2573	9.529	34.102	1.086	1.32179	45.8	0.07997	0.09	0.11538	0.02683	327.1
95/06/11	08:40:00	54.9577	-1.2745	9.538	34.106	1.088	1.40204	42.83	0.07918	0.03	0.11555	0.02298	369.14
95/06/11	08:45:00	54.9471	-1.2904	9.604	34.094	1.142	1.59099	36.13	0.07845	0.03	0.11572	0.02192	458.79
95/06/11	08:50:00	54.9379	-1.3049	9.678	34.058	1.132	2.17348	28.5	0.0789	0.05	0.1193	0.02172	611.94
95/06/11	08:55:00	54.9337	-1.313	9.715	34.041	1.155	2.47622	22.6	0.08155	0.06	0.12242	0.02208	753.25
95/06/11	09:00:00	54.933	-1.3148	9.725	34.017	1.168	2.54632	22.87	0.08418	0.07	0.125	0.02465	788.09
95/06/11	09:05:00	54.9331	-1.3161	9.711	34.025	1.198	2.6214	22.53	0.08678	0.07	0.12645	0.02548	917.36
95/06/11	09:10:00	54.9346	-1.2973	9.669	34.049	1.094	2.3573	29.33	0.08928	0.05	0.12602	0.0266	717.04
95/06/11	09:15:00	54.935	-1.2743	9.585	34.102	1.085	1.80461	38.9	0.08648	0.04	0.12132	0.0245	760.56
95/06/11	09:20:00	54.9355	-1.2498	9.534	34.143	1.05	1.42454	45.33	0.08382	0.03	0.11813	0.0234	726.94
95/06/11	09:25:00	54.9364	-1.2267	9.501	34.135	1.088	1.21374	47.77	0.08165	0.04	0.11657	0.02405	440.52
95/06/11	09:30:00	54.9371	-1.203	9.478	34.147	1.112	1.17926	51.03	0.07985	0.03	0.11615	0.02378	251.8
95/06/11	09:35:00	54.9376	-1.1787	9.473	34.159	1.079	1.11886	52.83	0.07915	0.03	0.11642	0.02463	476.12
95/06/11	09:40:00	54.9391	-1.1556	9.552	34.151	1.035	1.1163	55.03	0.07957	0.03	0.11647	0.0266	778.15
95/06/11	09:45:00	54.9404	-1.1316	9.715	34.106	0.857	0.84215	58.15	0.0798	0.03	0.11595	0.02553	1000.62
95/06/11	09:50:00	54.942	-1.1076	9.869	34.089	0.834	0.77229	63.73	0.08015	0.02	0.11607	0.02105	1038.42
95/06/11	09:55:00	54.943	-1.0841	10.051	34.104	0.857	0.81309	68.6	0.0792	0.03	0.11605	0.02067	981.99
95/06/11	10:00:00	54.9436	-1.0599	10.065	34.123	0.892	0.84215	76.4	0.0792	0.03	0.11573	0.01975	957.84

APPENDIX 3 CH119a Cruise Data (11/06/95-12/06/95)

Date	Time	LAT	LON	Tsal	Tsal	Fluor -chla	Trans	depth	Phosphate	Nitrate +	Nitrite	Silicate	PAR
	GMT	°+ve North	°+ve East	Temp °C	Sal - PSU	V or mg/m3		m	v or µM	Nitrite Vor	V or µM	V or µM	
95/06/11	23:00:00	54.0459	-0.047	10.27	34.134	0.833	2.79177	21.73	0.11265	0.59	0.13297	0.02612	#N/A
95/06/11	23:05:00	54.0334	-0.0312	10.209	34.138	0.767	2.36443	22.33	0.12372	0.67	0.1378	0.02887	#N/A
95/06/11	23:10:00	54.0214	-0.0169	10.153	34.127	0.76	2.16335	22.9	0.12882	0.59	0.138	0.03028	#N/A
95/06/11	23:15:00	54.0106	0.0008	10.125	34.151	0.82	2.08966	25.77	0.12848	0.46	0.13497	0.02822	#N/A
95/06/11	23:20:00	53.9995	0.0188	10.088	34.127	0.824	2.05325	28.07	0.12598	0.36	0.13097	0.027	#N/A
95/06/11	23:25:00	53.9884	0.0359	10.051	34.144	0.794	1.93027	31.93	0.12227	0.37	0.12843	0.02588	#N/A
95/06/11	23:30:00	53.9777	0.0525	10.051	34.132	0.831	1.89527	30.7	0.12313	0.34	0.12842	0.0262	#N/A
95/06/11	23:35:00	53.9664	0.0705	9.958	34.148	0.8	1.80157	30.9	0.1237	0.28	0.1271	0.02545	#N/A
95/06/11	23:40:00	53.9551	0.0883	9.892	34.165	0.789	1.70693	29.5	0.12185	0.25	0.12597	0.02438	#N/A
95/06/11	23:45:00	53.9445	0.1054	9.916	34.161	0.723	1.75241	31.43	0.1231	0.3	0.12563	0.0258	#N/A
95/06/11	23:50:00	53.9333	0.123	9.925	34.169	0.757	1.63517	32.1	0.12785	0.3	0.12735	0.02843	#N/A
95/06/11	23:55:00	53.9217	0.141	9.944	34.185	0.731	1.55884	34.47	0.12913	0.33	0.1266	0.02778	#N/A
95/06/12	00:00:00	53.9104	0.1581	10.042	34.172	0.726	1.47541	38.07	0.13008	0.39	0.12772	0.02875	#N/A
95/06/12	00:05:00	53.895	0.1686	10.153	34.167	0.729	1.69188	36.37	0.13217	0.63	0.12898	0.02962	#N/A
95/06/12	00:10:00	53.8809	0.1795	10.172	34.151	0.739	2.00105	33.67	0.13555	0.95	0.13667	0.0324	#N/A
95/06/12	00:15:00	53.8653	0.1891	10.191	34.154	0.742	2.05325	30.83	0.14122	1.1	0.14207	0.03437	#N/A
95/06/12	00:20:00	53.8503	0.2006	10.209	34.154	0.782	2.15657	29.27	0.14388	1.25	0.14448	0.035	#N/A
95/06/12	00:25:00	53.8388	0.2182	10.139	34.151	0.774	2.22476	28.3	0.14592	#N/A	0.1472	0.03545	#N/A
95/06/12	00:30:00	53.8285	0.2391	10.074	34.151	0.765	2.04679	30.85	0.1496	1.64	0.15137	0.03797	#N/A
95/06/12	00:35:00	53.8181	0.2597	10.065	34.164	0.756	1.8701	33.23	0.15383	1.65	0.15097	0.04045	#N/A
95/06/12	00:40:00	53.8094	0.2796	10.06	34.164	0.743	1.84815	34.1	0.15535	1.71	0.1522	0.04185	#N/A
95/06/12	00:45:00	53.7987	0.3018	10.004	34.172	0.758	1.77685	33.73	0.15783	1.48	0.15215	0.04277	#N/A
95/06/12	00:50:00	53.7887	0.3227	9.972	34.188	0.773	1.57638	34.1	0.15823	1.36	0.15122	0.04288	#N/A
95/06/12	00:55:00	53.7786	0.3441	9.953	34.181	0.717	1.55015	32.95	0.1575	1.31	0.15027	0.04242	#N/A
95/06/12	01:00:00	53.7684	0.3659	9.925	34.185	0.706	1.52989	32.2	0.1593	1.21	0.14957	0.04212	#N/A
95/06/12	01:05:00	53.7572	0.3858	9.883	34.181	0.725	1.62329	#N/A	0.16043	1.16	0.14765	0.04107	#N/A
95/06/12	01:10:00	53.7428	0.3982	9.892	34.189	0.723	1.5473	29.87	0.16125	1	0.14807	0.0409	#N/A
95/06/12	01:15:00	53.7255	0.4017	9.934	34.193	0.736	1.72203	28.73	0.15982	1.04	0.14695	0.03767	#N/A
95/06/12	01:20:00	53.7118	0.4133	9.939	34.185	0.767	1.64708	28.17	0.1628	0.82	0.14725	0.0385	#N/A
95/06/12	01:25:00	53.6978	0.4252	9.948	34.181	0.805	1.55884	28.57	0.15187	0.55	0.1419	0.03418	#N/A
95/06/12	01:30:00	53.6835	0.4373	9.944	34.181	0.852	1.46121	24.33	0.14182	0.35	0.13515	0.02915	#N/A
95/06/12	01:35:00	53.6673	0.4486	9.967	34.213	0.874	1.45274	20.47	0.13413	0.24	0.13108	0.02605	#N/A
95/06/12	01:40:00	53.6509	0.4599	9.986	34.197	0.96	1.50397	23	0.14058	0.09	0.12608	0.02442	#N/A
95/06/12	01:45:00	53.6341	0.4698	9.986	34.2	0.911	1.50973	22.13	0.1226	0.06	0.1198	0.02075	#N/A
95/06/12	01:50:00	53.6174	0.4744	10	34.192	0.955	1.59688	23	0.11793	0.05	0.118	0.02045	#N/A
95/06/12	01:55:00	53.6063	0.4548	10.06	34.18	1.007	1.85122	21.47	0.0983	0.05	0.11642	0.01672	#N/A
95/06/12	02:00:00	53.5938	0.4366	10.065	34.176	0.939	2.82562	21.97	0.10153	0.74	0.11998	0.017	#N/A
95/06/12	02:05:00	53.5771	0.4289	10.116	34.18	0.911	3.59785	21.13	0.11633	2.06	0.14707	0.02827	#N/A
95/06/12	02:10:00	53.5595	0.4235	10.13	34.195	0.971	2.85169	20.17	0.14447	1.68	0.15923	0.04127	#N/A
95/06/12	02:15:00	53.5429	0.4181	10.172	34.195	0.959	2.62528	19.43	0.14657	0.52	0.14325	0.03532	#N/A
95/06/12	02:20:00	53.5278	0.4136	10.228	34.171	0.921	3.10866	18.13	0.12902	1.56	0.13643	0.02552	#N/A
95/06/12	02:25:00	53.515	0.4093	10.275	34.178	0.882	3.25478	17.57	0.1391	2.49	0.15613	0.03452	#N/A
95/06/12	02:30:00	53.5034	0.4057	10.284	34.186	0.899	3.2526	17.37	0.1573	2.8	0.16528	0.0413	#N/A
95/06/12	02:35:00	53.4912	0.4023	10.363	34.189	0.914	3.24152	16.87	0.16687	2.85	0.16793	0.04268	#N/A
95/06/12	02:40:00	53.4797	0.4011	10.363	34.193	0.882	3.15826	17.23	0.16935	2.84	0.16772	0.04172	#N/A
95/06/12	02:45:00	53.4694	0.4089	10.363	34.189	0.88	2.89802	16.67	0.16962	2.74	0.16735	0.04162	0.27
95/06/12	02:50:00	53.4617	0.4205	10.377	34.189	0.891	2.84364	15.93	0.16987	2.64	0.16448	0.04047	0.49
95/06/12	02:55:00	53.4531	0.4325	10.424	34.18	0.897	2.87379	16.9	0.16895	2.7	0.16267	0.03967	0.84
95/06/12	03:00:00	53.4437	0.4407	10.47	34.184	0.903	2.85959	17.07	0.16927	2.73	0.1618	0.0385	1.5
95/06/12	03:05:00	53.4337	0.4484	10.508	34.187	0.897	2.95129	17.33	0.17013	2.75	0.16027	0.03793	2.46
95/06/12	03:10:00	53.4232	0.4561	10.629	34.162	0.862	3.14319	16	0.16985	2.85	0.15933	0.03817	4.02
95/06/12	03:15:00	53.4131	0.464	10.736	34.145	0.858	3.49279	19.4	0.17067	3.19	0.15905	0.0376	6.24
95/06/12	03:20:00	53.4032	0.4712	10.941	34.076	0.872	3.93607	#N/A	0.1726	3.82	0.16018	0.0379	9.09
95/06/12	03:25:00	53.3935	0.4785	11.091	33.968	0.878	4.1469	21.3	0.17512	5.49	0.16358	0.04358	12.67
95/06/12	03:30:00	53.3852	0.4845	11.119	33.944	0.886	4.27655	22.23	0.17958	7.23	0.17293	0.0465	16.91
95/06/12	03:35:00	53.3775	0.4905	11.189	33.881	0.905	4.64256	22.13	0.18638	7.83	0.18107	0.05018	23.03
95/06/12	03:40:00	53.3694	0.4965	11.277	33.826	0.937	4.7931	21.23	0.18908	8.77	0.18643	0.05192	29.86
95/06/12	03:45:00	53.3617	0.5028	11.357	33.767	0.938	5.59021	20.17	0.19265	10.04	0.19148	0.05355	38.56
95/06/12	03:50:00	53.3539	0.5088	11.408	33.723	0.997	6.85051	20.1	0.19708	11.33	0.19655	0.0566	48.98
95/06/12	03:55:00	53.3461	0.5121	11.455	33.739	0.96	6.97814	20.33	0.20197	11.09	0.20075	0.06105	56.78
95/06/12	04:00:00	53.3441	0.5043	11.553	33.645	1.008	8.15123	19.83	0.20182	11.38	0.1991	0.05683	68.52
95/06/12	04:05:00	53.3426	0.4957	11.534	33.661	0.992	7.94148	20.2	0.2044	12.27	0.20315	0.05792	65.63
95/06/12	04:10:00	53.3414	0.4883	11.665	33.556	0.98	8.75599	19.93	0.20758	13.31	0.20427	0.06085	65.03
95/06/12	04:15:00	53.3396	0.4798	11.725	33.506	1.029	11.01521	18.6	0.21677	15	0.21008	0.06672	66.97
95/06/12	04:20:00	53.3377	0.4713	11.8	33.46	1.102	14.89027	18.47	0.21898	16.68	0.21323	0.07038	68.42
95/06/12	04:25:00	53.3358	0.4641	11.791	33.429	1.105	14.34241	17.55	0.2233	16.38	0.2171	0.07295	81.94
95/06/12	04:30:00	53.3346	0.456	11.744	33.414	1.063	9.15296	18.23	0.2245	17.15	0.21732	0.07233	83.79
95/06/12	04:35:00	53.3328	0.4477	11.781	33.356	1.047	7.54596	19.17	0.22713	18.21	0.21882	0.07305	94.08
95/06/12	04:40:00	53.3312	0.4396	11.693	33.429	1.045	6.51332	19.27	0.22853	17.99	0.22155	0.07507	60.72
95/06/12	04:45:00	53.3295	0.4321	11.767	33.291	1.068	6.7669	20.3	0.22827	18.53	0.21973	0.07275	104.83
95/06/12	04:50:00	53.3276	0.4244	11.716	33.329	1.052	6.62244	20	0.23048	19.63	0.22352	0.07428	112.67
95/06/12	04:55:00	53.3251	0.416	11.842	33.218	1.047	7.34068	19.7	0.2351	19.6	0.22293	0.07857	104.83
95/06/12	05:00:00	53.3218	0.4136	11.856	33.138	1.068	8.34912	20.2	0.2368	22.17	0.22653	0.08002	114.52
95/06/12	05:05:00	53.3214	0.4178	11.865	33.161	1.085	8.91982	19.63	0.24338	22.43	0.2307	0.0857	161.61
95/06/12	05:10:00	53.3225	0.4205	11.791	33.199	1.083	7.37774	19.37	0.24562	22.3	0.23323	0.08497	176
95/06/12	05:15:00	53.3231	0.4219	11.735	33.26	1.053	6.89185	19.33	0.2457	21.23	0.2318	0.08405	198.32
95/06/12	05:20:00	53.3243	0.4243	11.735	33.268	1.046	6.12182	19.43	0.24427	20.77	0.22895	0.0824	201.98
95/06/12	05:25:00	53.3254	0.4258	11.665	33.333	1.06	6.17923	19.9	0.2427	20.05	0.23167	0.0816	139.33
95/06/12	05:30:00	53.3265	0.429	11.637	33.383	1.047	5.86427	20.17	0.24145	18.7	0.22553	0.08002	166.78
95/06/12	05:35:00	53.3274	0.4317	11.641	33.364	1.038	5.69498	19.67	0.23865	18.23	0.22195	0.07728	139.68
95/06/12	05:40:00	53.3276	0.4356	11.697	33.322	1.054	6.22561	19.25	0.23622	18.98	0.22143	0.0757	148.99
95/06/12	05:45:00	53.3288	0.4392	11.711	33.318	1.058	6.55877	19.47	0.23703	19.32	0.22437	0.07518	189.55
95/06/12	05:50:00	53.3303	0.4434	11.702	33.329	1.093	6.34161	19	0.23815	19.13	0.22467	0.0748	274.1
95/06/12	05:55:00	53.3311	0.447	11.641	33.368	1.071	5.5406	19.05	0.23765	18.7	0.22377	0.0737	438.51
95/06/12	06:00:00	53.3322	0.4508	11.553	33.479	1.03	4.7899	18.9	0.2367	17.81	0.22118	0.07235	369.7
95/06/12	06:05:00	53.3329	0.4539	11.571	33.479	1.058	5.17624	#N/A	0.23403	15.88	0.21672	0.07082	400.8
95/06/12	06:10:00	53.3343	0.4568	11.609	33.456	1.061	5.78198	17.33	0.22837	16.41	0.21287	0.06652	512
95/06/12	06:15:00	53.3354	0.4602	11.665	33.418	1.068	5.76115	16.4	0.22817	17.05	0.21415	0.06775	537.31
95/06/12	06:20:00	53.3363	0.464	11.665	33.406	1.042	5.93938	17.2	0.2301	17.61	0.2143	0.0693	509.66
95/06/12	06:25:00	53.3371	0.468	11.697	33.398	1.045	6.41911	15.63	0.23157	17.92	0.21447	0.07017	429.03
95/06/12	06:30:00	53.3379	0.4714	11.693	33.402	1.063	6.27718	17.47	0.23267	17.48	0.21462	0.06972	410.28
95/06/12	06:35:00	53.3381	0.4761	11.618	33.445	1.043	5.68895	17.87	0.23357	17.01	0.2139	0.07022	497.89

95/06/12	06:40:00	53.3389	0.4805	11.515	33.553	1.054	5.25256	17.7	0.23237	15.6	0.21127	0.06843	555.07
95/06/12	06:45:00	53.3397	0.4838	11.539	33.568	1.044	6.89456	18.5	0.22873	14.04	0.2048	0.06528	735.85
95/06/12	06:50:00	53.341	0.4882	11.52	33.537	1.032	7.22219	18.57	0.22492	14.32	0.20057	0.06338	752.11
95/06/12	06:55:00	53.3422	0.492	11.511	33.564	1.079	7.08667	18.53	0.22525	13.99	0.20127	0.06437	853.95
95/06/12	07:00:00	53.3431	0.4961	11.487	33.587	1.053	7.15651	18.47	0.22437	13.61	0.19833	0.06363	960.77
95/06/12	07:05:00	53.3433	0.4999	11.515	33.587	1.017	6.81269	18.47	0.22413	13.64	0.19627	0.06307	775.78
95/06/12	07:10:00	53.3449	0.5045	11.525	33.583	1.037	6.60223	17.93	0.2232	13.59	0.19565	0.06328	928.62
95/06/12	07:15:00	53.3481	0.5105	11.478	33.61	1.006	6.08104	#N/A	0.22345	13.55	0.1954	0.06368	914.57
95/06/12	07:20:00	53.3527	0.5104	11.436	33.649	1.017	5.69933	18.37	0.22423	12.72	0.19348	0.06447	917.36
95/06/12	07:25:00	53.3565	0.5081	11.366	33.72	1.007	5.39011	18.23	0.22162	11.92	0.18937	0.06227	954.93
95/06/12	07:30:00	53.3608	0.5048	11.403	33.704	1.013	5.00749	18.07	0.219	10.98	0.18605	0.06023	973.05
95/06/12	07:35:00	53.3659	0.501	11.301	33.786	0.987	4.52812	18.17	0.21572	10.29	0.18385	0.0593	1058.12
95/06/12	07:40:00	53.3706	0.4974	11.287	33.802	0.974	4.19149	18.7	0.21322	9.39	0.1792	0.05627	2028.4
95/06/12	07:45:00	53.3759	0.4937	11.296	33.833	0.972	3.65636	19.67	0.20963	8.1	0.17608	0.0542	1012.89
95/06/12	07:50:00	53.3808	0.4888	11.273	33.837	0.98	3.52109	20.97	0.20527	8.31	0.17262	0.05167	1668.92
95/06/12	07:55:00	53.3849	0.4837	11.291	33.825	0.983	3.36977	19.87	0.20417	8.19	0.17217	0.0518	1118.37
95/06/12	08:00:00	53.39	0.4795	11.254	33.869	0.942	3.07877	18.83	0.20215	7.61	0.1724	0.05147	1132.66
95/06/12	08:05:00	53.3949	0.475	11.231	33.884	0.959	2.84758	17.27	0.20152	7.38	0.17007	0.05115	2106.1
95/06/12	08:10:00	53.3991	0.4712	11.179	33.912	0.953	2.72906	17.03	0.19937	6.6	0.16957	0.05075	928.62
95/06/12	08:15:00	53.405	0.4669	11.114	33.964	0.945	2.50553	16.6	0.19745	6.17	0.16748	0.04877	538.13
95/06/12	08:20:00	53.41	0.4622	11.011	34.035	0.893	2.41809	16.5	0.19597	5.37	0.16527	0.04822	1726.7
95/06/12	08:25:00	53.4148	0.4575	10.811	34.112	0.905	2.3859	15.37	0.1938	4.12	0.16282	0.04635	1942.68
95/06/12	08:30:00	53.4203	0.4524	10.736	34.141	0.893	2.54998	13.65	0.18982	3.21	0.1593	0.04357	1587.86
95/06/12	08:35:00	53.4252	0.4482	10.708	34.157	0.906	2.59123	14.3	0.18555	2.98	0.15783	0.04155	2158.09
95/06/12	08:40:00	53.4303	0.4432	10.652	34.15	0.911	2.59123	14.2	0.184	2.86	0.15758	0.04077	880.83
95/06/12	08:45:00	53.4352	0.4383	10.592	34.186	0.911	2.58738	14.03	0.18287	2.86	0.15757	0.0407	1351.69
95/06/12	08:50:00	53.4406	0.4339	10.578	34.159	0.898	2.45442	13.5	0.18205	2.86	0.15823	0.03988	560.17
95/06/12	08:55:00	53.4463	0.4284	10.578	34.171	0.914	2.57616	12.13	0.18153	2.88	0.15912	0.03965	611.94
95/06/12	09:00:00	53.4518	0.4231	10.559	34.167	0.905	2.66716	12.37	0.18148	2.89	0.15982	0.03945	1015.98